BOOK OF ABSTRACTS

INTERNATIONAL CONFERENCE 21.-24. APRIL 2013 TARTU, ESTONIA

FUNCTIONAL MATERIALS AND NANOTECHNOLOGIES

UNIVERSITY OF TARTU
Institute of Physics
1632

FM&NT

Tartu 2013

Edited by: Toomas Plank, Rainer Pärna
Design: Vivian Klimušev

ISBN 978-9985-4-0744-8
Institute of Physics, University of Tartu
142 Riia Street, 51014, Tartu, Estonia
Phone: +372-737 4602
Fax: +372-738 3033
e-mail: dir@fi.tartu.ee
web: http://www.fi.ut.ee
Tartu, 2013

PREFACE

We warmly welcome all participants and guests attending to the international conference **Functional Materials and Nanotechnologies 2013 – FM&NT2013.**

The FM&NT conference series was started in 2006 by scientists from the Institute of Solid State Physics, University of Latvia. It is yearly conference bringing together researchers from whole world. The warm and open atmosphere of this scientific conference has turned it into event where people from rather different fields meet under the common name functional materials and nanotechnology. It is particularly important for early stage scientists who are looking for new knowledge and contacts with people from various fields. Our Latvian colleagues with their success in internationalization made us neighbouring Estonians so jealous that we could not withstand proposing organise the conference in every second year in Estonia. Actually this is in a way the continuation of idea of famous Baltic seminars which took place in last century over several decades. Due to political constraints these seminars were only opened to scientist of former Eastern Europe countries, but had a great popularity and attendance over whole Soviet Union. Much fruitful cooperation started from the initial personal contacts of scientists at these seminars hold twice per year once in Latvia and second time in Estonia.

In last FM&NT 2012 conference, the decision was made that Institute of Physics, University of Tartu will organise the event in Tartu in 2013. In a few days left to the opening of the conference, to be held first time in Tartu, we are proudly taking over the spirit of previous FM&NT. Along with traditional topics as multifunctional and nanomaterials, materials for sustainable energy applications and theory, this conference will concentrate on studies with synchrotron radiation and other novel light sources. The invited speakers from countries closer and further from Estonia will review a state of art studies in different hot topics as nanosafety, following chemical reactions in real time, ion beam technologies, secrets of fuel cells and solar elements, just to name a few. We would like to acknowledge support by Tartu University Development Fund, Estonian national projects for Materials Science, Science Internationalisation and Centre of Excellence programs based on contribution of European Structural Funds. Also graduate school on “Functional Materials and technologies” supported by European Social Fund has given generous contribution to help participation of our early stage researchers. This support is gratefully acknowledged. We hope that continuation of the tradition introduced with this conference will strengthen international cooperation of scientists from Baltic state with researchers of other countries.

Please enjoy the conference, its social program and scientific discussions.

On the behalf of organising committee

Ergo Nõmmiste
Marco Kirm
Toomas Plank

INTERNATIONAL STEERING COMMITTEE

CHAIRPERSON:

Andris Sternbergs, Institute of Solid State Physics, University of Latvia, Latvia

MEMBERS:

Juras Banys, Vilnius University, Lithuania

Gunnar Borstel, University of Osnabrueck, Germany

Niels E. Christensen, University of Aarhus, Denmark

Robert A. Evarestov, St. Petersburg State University, Russia

Claes-Goran Granqvist, Uppsala University, Sweden

Dag Høvik, The Research Council of Norway, Norway

Marco Kirm, University of Tartu, Estonia

Witold Łojkowski, Institute of High Pressure Physics, Poland

Ergo Nõmmiste, Institute of Physics, University of Tartu, Estonia

Helmut Schober, Institut Laue-Langevin, France

Ingólfur Thorbjörnsson, Icelandic Centre for Research, Iceland

Marcel H. Van de Voorde, University of Technology Delft, The Netherlands

PROGRAM COMMITTEE

CHAIRPERSON:

dr Marco Kirm

MEMBERS:

prof Ergo Nõmmiste

prof Enn Lust

prof Jaak Kikas

prof Enn Mellikov

prof Alexey Romanov

prof Mikhail Brik

LOCAL ORGANIZING COMMITTEE

CHAIRPERSON:

prof Ergo Nõmmiste

MEMBERS:

dr Marco Kirm

prof Jaak Kikas

dr Toomas Plank

prof Väino Sammelselg

dr Vambola Kisand

prof Vladimir Hižnjakov

prof Aleksandr Luštšik

dr Rainer Pärna

prof Mikhail Brik

prof Enn Lust

prof Alexey Romanov

INTERNATIONAL CONFERENCE

FUNCTIONAL MATERIALS AND NANOTECHNOLOGIES

TARTU, ESTONIA IN APRIL, 21 – 24, 2013

APRIL 21(SUNDAY)

University of Tartu; History Museum	
18:00	Registration
18:00 – 21:00	Welcome party

APRIL 22 (MONDAY)

Conference Hall "STRUVE" (Dorpat Centre)			
8:00	Registration		
9:00	Opening		
Chairman: **Prof. Ergo Nõmmiste**			
9:15	Andris Sternberg	Latvian national instruments for material science and nano-technologies within a framework of Baltic cooperation	INV-1
9:50	Anne Kahru	"Bio-nano interactions: benefits versus environmental and health risks"	INV-2
10:25	Robert Evarestov	First-principles calculations of single-walled nanotubes in sulfides AS_2 (A = Ti, Zr)	INV-3
11:00	Technical Information		
11:05 - 11:30	Coffee		
Chairman: **Prof. Mikhail Brik**			
11:30	Vladimir Makhov	VUV luminescence of wide band-gap solids studied by time-resolved spectroscopy using synchrotron radiation	INV-4
12:05	Andrzej Suchocki	Multicenter structure of cerium ions in garnet crystals studied by infrared absorption and high-pressure spectroscopies	INV-5
12:40	Miroslav D. Dramićanin	Rare earth doped sequioxide luminescent down- and up-conversion nanopowders prepared by polymer complex solution method	INV-6
13:15 – 14:15	Lunch		

APRIL 22 (MONDAY)

Conference Hall "STRUVE1"			
	Chairman: **Prof. Arvo Kikas**		
	Nanomaterials		
14:15	Dmitry Spassky	Optical spectroscopy of $Gd_3(Al_xGa_{1-x})_5O_{12}:Ce^{3+}$ epitaxial films	OR-1
14:40	Yurii Orlovskii	Fluorescence quenching in the Nd^{3+} doped Y_2O_3 nanoparticles of monoclinic phase	OR-3
15:05	Uldis Rogulis	Advances in oxyfluoride glass-ceramics	OR-4

Conference Hall "STRUVE2"			
	Chairman: **Prof. Vladimir Hizhnyakov**		
	Multifunctional materials		
14:15	Janis Teteris	Optical field-induced surface patterning of soft materials	OR-6
14:40	Andris Ozols	Effect of holographic grating period on its relaxation in amolecular glassy film	OR-7
15:05	Andrei Salak	A surface LDH structure grown on Zn-Al alloy	OR-8
15:30	Alexander Chaykin	Microscopic crystal field effects in $CsCdBr_3:Ni^{2+}$ crystals	OR-9
15:55	Veera Krasnenko	Cubic monocarbides XC (X=Ti, V, Cr, Nb, Mo, Hf) as explored by ab initio calculations	OR-10

Conference Hall "PETERSON"			
	Chairman: **Prof. Juris Purans**		
	Synchrotron radiation		
14:15	Anatoli Popov	Photostimulable storage phosphors and image-plate development for neutron imaging	OR-11
14:40	Andrei Belsky	Non-proportionality of luminescence excited in XUV photon energy range	OR-12
15:05	Alexei Kuzmin	EXAFS spectroscopy and first-principles study of $SnWO_4$	OR-13
15:30	Janis Timoshenko	Analysis of EXAFS data from copper tungstate by reverse Monte Carlo method	OR-14
15:55	Andris Anspoks	Local structure studies of $SrTi^{16}O_3$ and $SrTi^{18}O_3$	OR-15
16:20 - 17:00		Coffee & snacks	
16:20 - 19:00		**Poster Session**	

APRIL 23 (TUESDAY)

Conference Hall "STRUVE" (Dorpat Centre)			
8:00	Registration		
Chairman: **Prof. Andris Sternberg**			
9:00	Juris Purans	Synchrotron radiation X-ray absorption studies of local structure with femtometer accuracy	INV-7
9:45	Alexander Föhlisch	Direct observation of chemical dynamics: photodissociation and surface catalysis	INV-8
10:30	Peter Sushko	Revealing the character of optical absorption in complex oxides	INV-9
11:15	Technical Information		
11:20 - 11:50	Coffee		

Conference Hall "STRUVE1"			
Chairman: **Prof. Alexei Kuzmin**			
Synchrotron radiation			
11:50	Jaanus Kruusma	Electrochemical *in-situ* XPS studies of negatively polarized micromesoporous molybdenium carbide derived carbon double layer capacitor electrode	OR-16
12:15	Ilya A. Gofman	Electronic structure and inner shell excited luminescence in gadolinium molybdate crystals	OR-17
Nanomaterials			
12:40	Reinis Drunka	Synthesis and photocatalytic properties of sulfur modified TiO_2 nanopores and nanotubes	OR-18
13:05	Urmas Joost	Synthesis of nanoparticles using wet chemistry methods	OR-19
13:30	Mikk Antsov	Static friction of CuO nanowires on substrates with varying roughness	OR-20

APRIL 23 (TUESDAY)

Conference Hall "STRUVE2"			
	Chairman: **Prof. Vladimir Makhov**		
	Multifunctional materials		
11:50	Mikhail G. Brik	Ab-initio studies of the structural, electronic, optical and elastic properties of $ZnWO_4$ and $CdWO_4$ single crystals	OR-21
12:15	Chong-Geng Ma	A hybrid computational-experimental spectroscopic analysis of Eu^{3+} ions doped in hexagonal wurtzite ZnS	OR-22
12:40	Vladimir Hizhnyakov	Theory and MD simulations of intrinsic localized modes and defect formation in solids	OR-23
13:05	Anatolijs Sarakovskis	Oxygen related defects and their impact on upconversion processes in $NaLaF_4:Er^{3+}$	OR-24
13:30	Eduard Aleksanyan	Luminescence properties of hafnia and zirconia nano-powders prepared by solution combustion synthesis	OR-25

Conference Hall "PETERSON"			
	Chairman: **Prof. Toomas Plank**		
	Commercial		
11:50	Suzy Lidström Physica Scripta	This is the way it is	INV-11
12:15	Martin Kirchner Raith GmbH	Raith	OR-50
12:35	Pete Lander Xradia	4D X-ray microscopy(XRM), *in situ* imaging of practical volume samples	OR-51
12:55	Raimon Zoetemelk Park Systems	Polymer Pen Lithography: Massive parallel fabrication of repetitive nanostructures	OR-52
13:15	David Vardanjan SIA Armgate	Introduction to free liquid surface technology as developed by Elmarco s.r.o.	OR-53
13:35	Andrei Izvolski Bruker Baltic	Bruker	OR-54
13:55 - 15:00		Lunch	
15:00 - 18:00 Excursion walking tour in Tartu centre and visit to Institutes of Physics and Chemistry			
18:15 Conference photo at Science Centre "AHHAA" (Sadama 1, Tartu)			
18:30-24:00 Conference Dinner at Science Centre "AHHAA" (Sadama 1, Tartu)			

APRIL 24 (WEDNESDAY)

Conference Hall "STRUVE" (Dorpat Centre)			
Chairman: **Prof. Aleksandr Lushchik**			
9:00	Kurt Schwartz	Ion tracks and nanotechnology	INV-12
9:35	Marina Popova	Far infrared studies of multiferroic iron borates	INV-13
10:10	Vladimir Trepakov	Heavily manganese doped strontium titanate nano-particles: synthesis, structure and properties	INV-14
10:45 - 11:15		Coffee	

Conference Hall "STRUVE1"			
Chairman: **Prof. Jaan Aarik**			
Nanomaterials			
11:15	Maido Merisalu	Development of effective atomic layer deposited corrosion resistant coatings for Al 2024-T3	OR-26
11:40	Vambola Kisand	Heat treatment effects in case of metal containing titania sol-gel films	OR-27
12:05	Yuri Shunin	Electromagnetic properties of interconnects in nanodevices based on CNT, GNR and graphene aerogels	OR-28
12:30	Guntars Zvejnieks	Cellular automata modelling of void latice selforganization in CaF_2 under irradiation	OR-29
13:00 - 14:00		Lunch	
Chairman: **Prof. Väino Sammelselg**			
14:00	Linas Ardaravicius	High frequency noise in epitaxial graphene on SiC	OR-38
14:25	Mikhail Shuba	The influence of finite-size effect on the electromagnetic response of carbon nanotubes	OR-39
14:55	Polina Kuzhir	Multi-layered graphene in microwaves	OR-40
15:15	Andris Sutka	Photocatalytic activity of $ZnFe_2O_4$ nanoparticle clusters under visble light irradiation	OR-41

APRIL 24 (WEDNESDAY)

Conference Hall "STRUVE2"			
	Chairman: **Prof. Marina Popova**		
	Multifunctional materials		
11:15	Urmas Nagel	Terahertz spectroscopy of the cycloid in multiferroic $BiFeO_3$ in high magnetic fields	OR-30
11:40	Toomas Rõõm	Spin waves and directional dichroism in the multiferroic $Ba_2CoGe_2O_7$ probed by THz spectroscopy	OR-31
12:05	Boris Hudec	Resistive switching vs. charge trapping in TiO_2-based metal-insulator-metal structures with Al_2O_3 barrier	OR-33
12.30	Peter Sushko	Embedded clusters for ion-covalent crystals	OR-32
13:00-14:00		*Lunch*	
	Chairman: **Prof. Nina Mironova-Ulmane**		
14:00	Ekaterina Politova	Dielectric relaxation in bismuth-containing ceramics	OR-42
14:25	Kelli Hanschmidt	Structure and properties of nanocolloidal SnO_2 watersols applied in preparation of optical quality micro- and nanospheres	OR-43
14:55	Eriks Klotins	Electron-phonon interactions: spatial localization	OR-44
15:15	Mikhail G. Brik	Ab-initio analysis of the (001) surface in cubic $CaZrO_3$	OR-45

Conference Hall "PETERSON"			
	Chairman: **Prof. Guntars Vaivars**		
	Sustainable energetics		
11:15	Liga Grinberga	Gravimetric and spectroscopic studies on reversible hydrogen adsorption on nanoporous clinoptilolite	OR-34
11:40	Yuri F. Zhukovskii	Modeling of Y-O precipitation in α-Fe and γ-Fe lattices	OR-35
12:05	Eugene A. Kotomin	Prediction of structural stability of complex perovskites for solid oxide fuel cells from first principles	OR-36
12:30	Gunnar Nurk	Redox behaviour of sulphur at Ni/GDC SOFC anode at midand low-range temperatures: S K-edge XANES study	OR-37
13:00-14.00		*Lunch*	
	Chairman: **Prof. Vambola Kisand**		
14:00	Maarja Grossberg	Photoluminescence studies of solar cell absorber material Cu_2ZnSnS_4	OR-46
14:30	Marit Kauk-Kuusik	Investigation of quaternary compounds for monograin layer solar cells	OR-47
15:00	Teolan Tomson	Formal and technological solar resource in Estonia	OR-49

Conference Hall "STRUVE"		
Closing		
15:50 - 17:00	*Goodbye refreshments*	

SPONSORS

Raith

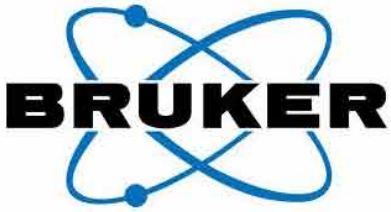
BRUKER

Vistec
Lithography

S.A.I.N.T
Tech
Security Analytics Industry Nano Technics

Doma
Group

ARMGATE

AMERICAN
ELEMENTS
®
America's Leading Manufacturer of Engineered and Advanced Material Products

Invited speakers

Andris STERNBERG

Andris Sternberg, Full member of Latvian Academy of Science, graduated University of Latvia, Faculty of Physics and Mathematics in 1970. He obtained his PhD in 1978 on „The features of phase transitions and electrooptic properties of La-doped lead zirconate-titanate and lead scandate-niobate ferroelectric ceramics" and in 1999 Dr. Hab. phys. on „The effects of structure ordering and radiation defects on phase transition dynamics in ferroelectric relaxors".
In period 1988 - 1995 he time period worked at Atomic Institute of Austrian Universities, Vienna, Siemens AG, Munich, Shonan Institute of Technology and Kyoto University and Universität des Saarlandes, Saarbrücken. Since 1999 Director of the Institute of Solid State Physics, University of Latvia.
His research interests cover nanoscience and nanotechnologies, particularly, processing of ferroelectric materials (PLD, sol-gel, magnetron sputtering), structure ordering and phase transitions, application of thin films and hetero-structures, radiation effects in ferroelectrics, plasma physics and design of materials for tentative application in International thermonuclear experimental reactor (ITER). His publication list includes over 230 published works in scientific journals and proceedings of conferences.
He is Latvian representative at EC COST Domain „Materials , physics and nanoscience", Latvian representative in EC High level group in Nanotechnologies, Head of Research Unit of Association EURATOM-University of Latvia (AEUL), Latvia representative in EURATOM Committees (CCE-FU, EFDA- SC), Governing Board member from Latvia in ELE Fusion for Energy (F4E), Editorial board member of journal „ Ferroelectrics".

LATVIAN NATIONAL INSTRUMENTS FOR MATERIAL SCIENCE AND NANOTECHNOLOGIES WITHIN A FRAMEWORK OF BALTIC COOPERATION

Andris Sternberg, Līga Grīnberga and Mārtiņš Rutkis
Institute of Solid State Physics, University of Latvia, Latvia
e-mail: stern@latnet.lv

Further progress of material science in Latvia is generally maintained by two instruments – National Research Program "Development of Innovative Multifunctional Materials, Signal Processing and Information Technologies for Competitive Science Intensive Products" (further ***Program***) and by build-up of "National Center for Research of Nanostructured and Multifunctional Materials, Constructions and Related Technologies" (***Center***). Both of these national instruments are in close relation. The ***Program***, as a framework for research projects, supposed to be supported by an establishment of ***Center*** as a new advanced research infrastructure. Institute of Solid State Physics University of Latvia have been chosen as coordinator for both national activities. At current situation ***Program*** consist of six projects. Material science and nanotechnology is an important part at four of them.

The ***Center*** should be established by ERDF supported project. According to this project enhanced material research supporting infrastructure will be created by refurbishing existing and building new laboratory facilities as well as by modernization of existing and purchase of new scientific equipment. It is planned to establish Latvian nanostructured material research center "LATNANO-C" with 632 m^2 clean room facility. The functional structure of LATNANO-C will involve five complementary and mutually reinforcing parts: (i)Technologies and Processing; (ii) Morphology and Structuring; (iii) Composition and Structure Control; (iv) Properties and Characterization; (v) Application Assessment.

Within our presentation we would like discuss potential impact of ***Program*** and ***Center*** on Baltic cooperation within field of material science and nanotechnology and talk over further Baltic joint activities for infrastructure development under initiative "Baltic Infrastructure of Research, Technology and Innovation" (**BIRTI**) – platform for research and innovation.

Anne KAHRU

Anne Kahru is a leading research scientist of National Institute of Chemical Physics and Biophysics (NICPB) and Head of the Laboratory of Environmental Toxicology of NICPB, Tallinn, Estonia. Her group was among the first ones in conducting research into the nanoecotoxicology of metal oxide nanoparticles. She has 80 articles in ISI WoS cited 1560 times and she belongs to the top 1% most cited scientists in area Environment/Ecology. She is also the first Estonian scientist ever interviewed by Thomson Reuters Science Watch (2009) for her fast breaking paper in nanoecotoxicology.

In 2011, she received the Estonian State Science Award for her research „Ecotoxicology of synthetic nanoparticles and their toxicity mechanisms". She has been awarded several FP6 and FP7 research grants.

Her current research focuses on the mechanisms of (eco) toxicicity and bioavailability of synthetic nanoparticles. Research in her laboratory combines molecular techniques, in vitro and ecotoxicological systems and analytical chemistry. She is also a founder (1997) and the President of the Estonian Society of Toxicology.

BIO-NANO INTERACTIONS: BENEFITS *VERSUS* ENVIRONMENTAL AND HEALTH RISKS

Anne Kahru, Angela Ivask, Kaja Kasemets, Irina Blinova
National Institute of Chemical Physics and Biophysics, Tallinn, Estonia
e-mail: anne.kahru@kbfi.ee

Nanotechnology has been considered the next industrial revolution, and consumer products and a variety of industries increasingly use engineered nanoparticles (eNPs). eNPs, i.e., particles with at least one dimension < 100 nm can be metals and metal oxides (e.g., nAg, nAu, TiO_2, ZnO, CeO_2), metal salts like CdS or CdSe (quantum dots) or carbon-based (e.g., C60-fullerenes, single- and multi-wall carbon nanotubes, dendrimers). Currently, the greatest impact of nanotechnologies to the society is from the materials and manufacturing sector, e.g., coatings and composites for cars and buildings, followed by electronics, e.g., displays and batteries and, finally, healthcare, driven by pharmaceutical applications [1].

At nanoscale the materials have different properties compared with the same ones at larger size. The changed physico-chemical properties, however, may lead to increased bioavailability and toxicity, mostly due to greater number of reactive groups on the particle surface [2]. The processes taking place at the nano-bio interface can be used for the design of novel biocidal nanomaterials such as antimicrobial surface coatings. However, if toxicity is undesirable side effect of a specific nanomaterial, the safe-by-design strategy should be applied. The latter means the synthesis of nanomaterials that possess the desired properties but where the unwanted toxic side-effects are minimised. For the balanced development of nanotechnology, cooperation among industry, scientists, and regulatory agencies is crucial for addressing the "benefits *versus* risks" assessment of nanotechnologies. In this presentation, the state of the art of the respective research in the world [3] but also in Estonia [4] will be presented.

References

1. Lux Research. Boston 2008; https://portal.luxresearchinc.com/research/document_excerpt/3735.

2. A. Nel, T. Xia, L. Mädler, N. Li, *Science*, 2006, Vol. 311, 622–627.

3. A. Kahru, A. Ivask, *Acc Chem Res*., 2012 [Epub ahead of print] DOI: 10.1021/ar3000212

4. A. Kahru, A. Ivask, K. Kasemets, I. Blinova. In: Research in Estonia. Present and future. 2011, p. 346-367. http://www.akadeemia.ee/_repository/file/publikatsioonid/2011/Recearch_in_Estonia.pdf

Robert EVARESTOV

Robert A. Evarestov graduated St. Petersburg State University as theoretical physicsist in 1960. He obtained his PhD in the Department of Theoretical Physics at St. Petersburg State University in 1964 (supervisor Prof. Marija Petrashen), Habilitation degree -in the same Department in 1977 „ Molecular models in the electronic structure theory of crystals“. From 1968 he works at the Department of Quantum Chemistry of St.Petersburg State University (Professor – from 1979). In 1990-1994 he was Director of the Chemistry Institute of St.Petersburg State University, in 1994-1998 he was First Vice Rector of St.Petersburg State University. Since 1999 till present time he is Head of Department of Quantum Chemistry of St.Petersburg State University.

His research interest cover symmetry of crystalline solids (the monograph „Site Symmetry in crystals” has been published by Springer in 1993 , second edition in 1997). He is interested also by the application of quantum chemistry methods to perfect and defective crystals (the monograph „ Quantum Chemistry of Solids” has been published by Springer in 2007 , second edition in 2013). Now his interests cover symmetry and quantum chemical study of monoperiodic nanostructures (nanotubes, nanowires). He is Foreign Member of Latvian Academy of Science (from 2005), Humboldt Foundation Awardee (1998). His publication list includes over 250 papers cited more than 2600 times, his Hirsh index is 23 (Web of Science data, April 2013).

FIRST-PRINCIPLES CALCULATIONS OF SINGLE-WALLED NANOTUBES IN SULFIDES AS_2 (A = Ti, Zr)

Robert Evarestov, Andrei Bandura

Department of Chemistry, Quantum Chemistry Division, St. Petersburg State University, Russia

e-mail: re1973@re1973.spb.edu

The first-principles study is performed for the first time of the structure and stability of TiS_2 and ZrS_2 nanotubes (NTs) in comparison to each other and to similar oxide nanotubes. The hybrid HF-KS PBE0 calculations are made within the scope of the LCAO approximation by means of the CRYSTAL-2009 computer code. To the best of our knowledge, all previous theoretical modelling of tubular disulfides is based on the semiempirical DFTB technique.

Transition metal disulfides are known to exist in two modifications 1 T and 2 H with octahedral and trigonal prismatic coordination of metal atoms, respectively. The applied method allows us to reproduce the experimental properties of the stable 1 T phase in good quality. The 3-plane (O-A-O) hexagonal (001) layers from both phases have been used to construct the tubular structures. The possibility of folding the layers from the other presumptive phases with different (cubic, tetragonal and orthorhombic) morphology has also been analysed. The full optimization of all atomic positions has been performed to determine the most favourable nanostructures.

Our calculations on single-walled TiS_2 and ZrS_2 nanotubes confirmed that the NTs obtained by rolling of the hexagonal crystalline layers with octahedral 1T coordination are the most stable. Besides of the NTs with hexagonal morphology, it is possible to obtain the relatively stable NTs with lepidocrocite morphology by rolling up layers of the metastable marcasite-like orthorhombic phase. The strain energy of 1 T NTs is almost the same for titanium and zirconium disulfides and obeys the classical $1/R^2$ law. In spite of the fact that the strain energy of sulfide NTs is greater than that of the similar oxide NTs, the formation energy of the formers is considerably less than the formation energy of latters. Both TiS_2 and ZrS_2 NTs exhibit properties of the narrow gap semiconductors with the calculated band gap between 1.5 and 2.5 eV.

Acknowledgements

The authors are grateful for the support to RBRF (Grant 11-03-00466a).

Vladimir MAKHOV

After graduation from Moscow Physical Engineering Institute in 1973 Vladimir Makhov worked at Lebedev Physical Institute in Moscow as junior, senior, leading and from 2008 as principal researcher.
He obtained his PhD in 1984 „Luminescence excitation and defect creation in ionic crystals under irradiation by synchrotron radiation (5-30 eV)“, which was supervised by Dr. Yu.M. Aleksandrov and Prof. Ch.B. Lushchik. In 1998 he got his degree of Doctor of Science in Physics (habilitation) „Time-resolved luminescence spectroscopy of wide band-gap crystals using synchrotron radiation“. His research interests cover luminescence of wide band-gap solids studied by synchrotron radiation excitation. His publication list includes over 160 papers cited more than 1000 times. He was awarded many times by iternational (ISF, INTAS, DAAD, NATO, University Paris-Sud) and national (RFBR) Grants and Fellowships.

VUV LUMINESCENCE OF WIDE BAND-GAP SOLIDS STUDIED BY TIME-RESOLVED SPECTROSCOPY USING SYNCHROTRON RADIATION

Vladimir Makhov

P.N. Lebedev Physical Institute, Moscow, Russia

e-mail: makhov@sci.lebedev.ru

Some highlights and historical aspects of time-resolved VUV luminescence spectroscopy of solids using synchrotron radiation (SR) are outlined, including studies of such unique phenomenon as crossluminescence (CL) and contribution of VUV spectroscopy to understanding of d-f transitions of rare earth (RE) ions in solids.

The key experiment for the explanation of the nature of CL (for BaF_2 crystals as an example) has been made using time-resolved spectroscopy technique under excitation by SR from S-60 synchrotron at Lebedev Physical Institute [1]. Thereafter the detailed studies of CL properties were performed at different SR sources, including SRS (Daresbury) [2] and DORIS (Hamburg). The first observation of the fast and slow components of VUV luminescence due to 5d-4f transitions in heavy RE ions was carried out at the Superlumi set-up at DORIS [3]. Later, 5d-4f luminescence in deep VUV region (near 10 eV) of Gd^{3+} and Lu^{3+} ions incorporated into some wide band-gap fluoride hosts has been discovered [4]. Using the unique opportunities for time-resolved spectroscopy at the Superlumi set-up the high-resolution ($\Delta\lambda \sim 0.5$ Å) 5d-4f emission and 4f-5d excitation spectra were obtained for Gd^{3+} and Lu^{3+} ions in various fluoride hosts [5,6] allowing the detailed analysis of the electron-phonon coupling in these systems.

The results of recent studies of some CL-active nanosize materials will be presented. The possible future developments in time-resolved luminescence spectroscopy of solids, in particular, with free electron laser (FEL), will be discussed.

References

1. Yu. M. Aleksandrov, V. N. Makhov, P. A. Rodnyi, T. I. Syrejshchikova, M. N. Yakimenko, *Sov. Phys. – Solid State*, 1984, 26, 1734 -1735.

2. V. N. Makhov, M. A. Terekhin, I. H. Munro, C. Mythen, D. A. Shaw, *J. Lumin.*, 1997, 72-74, 114-115 .

3. J. Becker, J. Y. Gesland, N. Yu. Kirikova, et al., *J. Lumin.*, 1998, 78, 91-98.

4. M. Kirm, J. C. Krupa, V. N. Makhov, et al., *Phys. Rev. B*, 2004, 70, 241101(R).

5. M. Kirm, G. Stryganyuk, S. Vielhauer, et al., *Phys. Rev. B*, 2007, 75, 075111.

6. V. N. Makhov, M. Kirm, G. Stryganyuk, et al., *J. Lumin.*, 2012, 132, 418-424.

Andrzej SUCHOCKI

Andrzej Suchocki graduated from Physics Department of Warsaw University (Poland) in 1978. He obtained Ph.D. degree from the Institute of Physics of the Polish Academy of Sciences in 1984, presenting theis entitled The Energy Structure and Recombination Processes of Mn Dopants in CdF_2 Crystals. He had a post-doctoral research associate position at Oklahoma State University in Stillwater, OK, USA in 1985-1987. Afterwards he was employed in the Institute of Physics of the Polish Academy of Sciences in Warsaw, where currently he held a professor position from 2002. From 2007 he works also for the Institute of Physics of Kazimierz Wielki University in Bydgoszcz, Poland. His research interests cover the field of optical spectroscopy of condensed matter, spectroscopy under high-pressures, nonlinear optics, nanomaterials, and materials for water-splitting. He is a coauthor of over 190 publications cited around 1400 times.

Multicenter structure of cerium ions in garnet crystals studied by infrared absorption and high-pressure spectroscopies

A. Kamińska[1], H. Przybylińska[1],Chong-Geng Ma[2], M.G. Brik[2] , J. Szczepkowski[1], P. Sybilski[1], A. Wittlin[1,3], M. Berkowski[1], W. Jastrzębski[1], Yu. Zorenko[4], and A. Suchocki[1,4]

[1] *Institute of Physics, Polish Academy of Sciences, Al. Lotników 32/46, 02-668 Warsaw, Poland*

[2] *Institute of Physics, University of Tartu, Riia 142, Tartu 51014, Estonia*

[3] *Cardinal Stefan Wyszyński University in Warsaw, ul. Dewajtis 5, 01-815 Warsaw, Poland*

[4] *Institute of Physics, Kazimierz Wielki University, Weyssenhoffa 11, 85-072 Bydgoszcz, Poland*

e-mail of presenting author: suchy@ifpan.edu.pl

Cerium doped materials are the subject of numerous studies for solid state laser materials, phosphors, and scintillators. Ce^{3+} has the simplest of the $4f^n$ ground state configurations ($n = 1$) and in many compounds it exhibits broadband emission originating from parity allowed inter-configurational $4f\,^0 5d\,^1 \rightarrow 4f\,^1 5d\,^0$ transitions. It is also studied for better understanding of $d \leftrightarrow f$ absorption and luminescence processes, both experimentally, and theoretically.

Low temperature, infrared absorption spectra of gadolinium gallium garnet crystals doped with Ce will be discussed. In the region of intra-configurational $4f - 4f$ transitions the spectra exhibit existence of at least two different, major Ce^{3+} related centers in the GGG crystals and also some other centers at lower concentration. The spectrum of $4f$-$4f$ intrashell transitions of Ce^{3+} ions extends up to about 3700 cm^{-1} due to the large splitting of the $^2F_{7/2}$ excited state. In the visible region the absorption spectrum shows influence of symmetry-related selection rules. The absorption coefficient changes in region of $4f^1 - 5d^1$ transitions due to thermal population of the second level, belonging to the $^2F_{5/2}$ ground state. This suggests that the symmetry of the site occupied by Ce^{3+} ions, which substitute Gd^{3+}, is higher than D_2 expected for garnet hosts. [1]

In spite of strong inter-shell $4f \rightarrow 5d$ absorption bands at ambient pressure the cerium luminescence in $Gd_3Ga_5O_{12}$ is entirely quenched even at low temperatures. It has been shown that applying pressure allows for recovering the $5d \rightarrow 4f$ radiative transitions. Further increase of pressure improves the emission efficiency. This effect is analyzed in terms of two possibilities: (i) by pressure induced electronic crossover of the excited $5d$ energy level of the Ce^{3+} with the conduction-band bottom of host crystal, and (ii) by decrease of electron-lattice coupling with increasing pressure, resulting in reducing of Stokes shift and non-radiative transitions between the low vibrational levels of the $5d$ state and high vibrational levels of the ground $4f$ state.[2]

Multicenters of Ce^{3+} ions have been also studied in bulk YAG:Ce, a very important scintillator material. The multicenters are associated with the so called cation anisities, i.e. Ce ions substituting aluminum octahedral sites in YAG host. The theoretical calculations with use of crystal-field theory confirm this assumption.The results of measurements of epitaxially-grown YAG:Ce layers, which do not contain rare-earth multisities due to low temperature epitaxial growth allow to distinguish the energy structure of regular Ce^{3+} ions in YAG crystal and Ce^{3+} ions in octahedral antisities.

It will be shown that YAG:Nd crystals can also serve as a p ressure sensor for high-pressure spectroscopy in diamond-anvil cell in the infrared spectral region.[3]

Acknowledgements:

The cooperation program between Estonian and Polish Academies of Sciences for the years 2009–2012 is kindly acknowledged. This work was partially supported by the European Union within the European Regional Development Fund through the Innovative Economy grant MIME (POIG.01.01.02-00-108/09)

References:

1. H. Przybylińska, et al. , Phys. Rev. B **87**, 045114 (2013).
2. A. Kamińska, et al. Phys. Rev. B **85**, 155111 (2012)
3. S. Kobyakov, et al. Appl. Phys. Lett. **88**, 234102 (2006)

Miroslav DRAMIĆANIN

Miroslav Dramićanin, born 1966, graduated at Faculty of Electrical Engineering, University of Belgrade in engineering physics in 1992. He obtained his PhD in the Faculty of Electrical Engineering at University of Belgrade in 1998. From 1994 until 1995 he worked at Center for Multidisciplinary Studies in Belgrade University. From 1995 until present time he works in the Vinča Institute of Nuclear Sciences, University of Belgrade. From 2006 he is Director of the Laboratory for Radiation Chemistry and Physics in Vinča Institute. He is also full time professor in the Department for Applied Physics at Faculty of Physics, Belgrade University. He is co-chairperson of the International Conference on the Physics of Optical Materials and Devices (ICOM). His research interest covers spectroscopy, fluorescence spectroscopy and luminescent materials.

His publication list includes about 115 papers in international journals from the SCI list, and his papers are cited more than 1090 times according to Google Scholar.

RARE EARTH DOPED SEQUIOXIDE LUMINESCENT DOWN- AND UP-CONVERSION NANOPOWDERS PREPARED BY POLYMER COMPLEX SOLUTION METHOD

Miroslav D. Dramićanin

Vinča Institute of Nuclear Sciences, University of Belgrade, Belgrade, Serbia

e-mail of presenting author: dramican@vinca.rs

Rare-earth luminescent materials have attracted much attention because of their down-conversion applications (for: artificial lights, X-ray medical radiography, lamps and display devices and high-power solid-state lasers, etc) and up-conversion (for: infrared quantum counter detectors, three-dimensional displays, temperature sensors, bio-imaging, sensitive luminescent bio-labels, GaAs-coated highly efficient light emitting diodes, etc). Among them, rare-earth (RE) sesquioxides are well recognized host materials due to good chemical stability, adequate thermal conductivity and high light output. In this lecture synthesis of rare earth doped sesquioxide nanopowders by polymer complex solution method (PCS) as well as structure, morphology and luminescent properties of these nanopowders are reviewed.

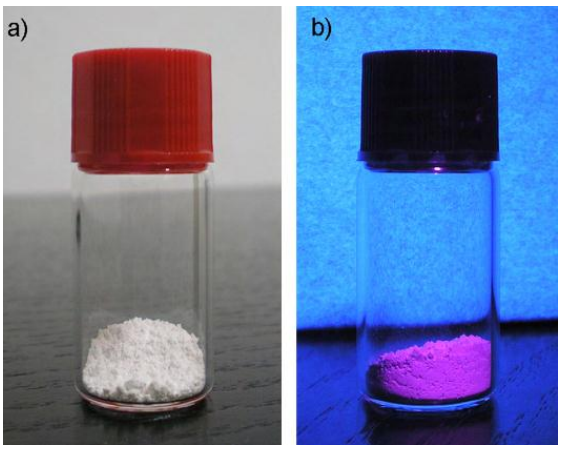

Fig.1 Photo of $Lu_2O_3:Sm^{3+}$ nanopowder (a) as-synthesized, (b) emitting strong red light under UV excitation.

Polymer complex solution method is a modified combustion method where instead of classical fuel (urea, glycine, carbohydrazide) organic water-soluble polymer (in our case polyethylene glycol – PEG) is used. The utility of this polymeric approach comes from the coordination of metal cations on the polymer chains during gelation process, resulting in very low cation mobility. Polymer precursor works both as a chelating agent and as an organic fuel to provide combustion heat for the calcination process. In this way PCS provides mixing of constituting elements at the atomic level and allows homogeneous control of very small dopant concentration.

Juris PURANS

Juris Purans received his PhD from the University of Latvia (UL) in 1980 "EPR of disordered solid state materials" and his habilitation from the ISSP UL in 1993 "XAFS Spectroscopy of Transition Metal Oxides". Since 1993, he is a head of the EXAFS laboratory at the ISSP in Riga (www.dragon.lv/exafs). J. Purans was qualified to the list of Professors of Universities of France “MILIEUX DENSES ET MATERIAUX” and “CHIMIE DES MATERIAUX”. He worked for many times at the synchrotron radiation facilities ADONE/DAFNA (ITALY), LURE-SOLEIL (France) as a beam-line scientist, as well as invited professor - Universities of France, Italy and Switzerland. J. Purans has 30 years of experience and published more than 200 papers on studies of functional materials using synchrotron radiation at the ESRF (Grenoble), LURE-SOLEIL (Orsay), HASYLAB (Hamburg), ADONE/DAFNA - ELLETRA (ITALY). He is the author/coauthor of 270 papers and 2 review articles on synchrotron radiation EXAFS studies, as well as RAMAN, EPR and XRD. His H-index is 23, with 1400 citations. His laboratory has recently developed EXAFS experiments with unprecedented (femtometer 10-5 Å) accuracy and nanometer scale (50 nm) lateral resolution (FP6 STRP project “X-TIP”). 2013-2016 - head of Latvian National grant "XAFS studies of functional materials with femtometer accuracy" Latvian Council of Science; 2010-2013 - Head of Latvian EU regional development grant ERAF-088 "Innovative glass coatings" VIAA.

SYNCHROTRON RADIATION X-RAY ABSORPTION STUDIES OF LOCAL STRUCTURE WITH FEMTOMETER ACCURACY

Juris Purans[1] (presenting author)

[1]*Institute of solid State Physics, University of Latvia*

e-mail of presenting author: purans@cfi.lu.lv

In the last years, the XAFS experimental techniques have undergo remarkable developments: (i) experiments with unprecedented accuracy and under extreme conditions of high pressure and temperature [1], (ii) experiments with nanoscale lateral resolution [2], that were not even conceivable just a few years ago, can nowadays be performed. New applications, stimulated by accurate experimental temperature-dependent XAFS measurements on Ge, ReO_3 and $SrFe_xTi_{1-x}O_3$, can be carried out. In parallel with the experimental techniques, XAFS theory and data analysis have made considerable progress. Femtometer accuracy in the determination of interatomic distances is now attainable [1,2]. Therefore, new effects can be studied with femtometer accuracy, for example:

- isotopic effect on EXAFS and isotopic effect on the lattice dynamics and anharmonic properties of Ge^{70} and Ge^{76} (see [1] and Highlight ESRF 2008);
- materials with negative thermal expansion as ReO_3, AgO_2, etc. (see Highlight ESRF 2006);
- materials with Jahn-Teller (JT) effect as $SrFe_xTi_{1-x}O_3$, with small radium polaron (WO_3) or with charge disproportionation as $CaFe_xTi_{1-x}O_3$;
- Solid solutions as $SrFe_xTi_{1-x}O_3$, $Th_{1-x}U_xO_2$ etc. ([3,4], Highlight ESRF 2007).

References

1. J.Purans, N. D.Afify, G.Dalba, R.Grisenti, S.De Panfilis, A.Kuzmin, V.I.Ozhogin, F.Rocca, A.Sanson, S. I. Tiutiunnikov, P.Fornasini, *Phys.Rev.Lett.*, 100, 00055901 (2008)

2. S. Larcheri, F. Rocca, F. Jandard, D. Pailharey, R. Graziola, A. Kuzmin and J. Purans, *Rev. Sci. Instrum.* 79, 013702 (2008)

3. M. Vračar, A. Kuzmin, R. Merkle, J. Purans, E. A. Kotomin, J. Maier and O. Mathon, Phys. Rev. B 76, 174107 (2007)

4. J.Purans, S.Hubert, G.Heisbourg, N.Dacheux, Ph.Moisy, Inorg. Chem. 45, 3887 (2006)

Alexander FÖHLISCH

Alexander Föhlisch obtained his education Physics at Tübingen, Stony Brook, Hamburg, LBNL and Uppsala University. His research focuses on the investigation of the electronic structure and the ultrafast dynamics on the atomic scale with innovative X-ray methods. He has contributed in the development and the application of time resolved femtosecond X-ray methods, with research on the nature of surface chemical bonding and the associated femtosecond and attosecond charge transfer at interfaces, phase transition dynamics and magnetisation dynamics. With innovative X-ray methods he explores functionality from molecular dynamics in the gas and liquid phase and phase transition behaviour in condensed matter. Since 2009 he is Professor at the University of Potsdam and the Director of the Institute of Synchrotron Radiation Methods and Instrumentation at the Helmholtz-Zentrum Berlin für Materialien und Energie. He continues to push the frontiers in synchrotron radiation research towards highest energy, momentum and time resolution to see how electronic structure and ultrafast dynamics on the atomic scaleinterplay.

Direct observation of chemical dynamics: Photodissociation and Surface Catalysis

Alexander Föhlisch
Institute for Methods and Instrumentation in Synchrotron Radiation Research (G-ISRR),
Helmholtz-Zentrum, Berlin
and
Institute of Physics and Astronomy, Potsdam University,
Potsdam, Germany
alexander.foehlisch@helmholtz-berlin.de

Changes in chemical bonding, in particular bond breaking and bond creation seem conceptually simple, but as a result of coherent wave packet motion it is difficult to catch the dynamic pathways in a multidimensional potential energy landscape. In this contribution the quenching of sequential dissociation through ultrafast solvent capture is explored in the prototypical metal carbonyl Iron pentacarbonyl ($Fe(CO)_5$) in gas phase and solution.

On the catalytically active Ruthenium surface, we determined that in the desorption of CO from the Ru(0001) surface roughly one third of the molecules doesn't move away from the surface directly but instead becomes trapped near it in a kind of "transition state." This weak chemical bonding ensures that the molecules are unable to detach yet remain mobile parallel to the surface. The researchers suspect that these types of weakly bonded, activated states might play an important role in catalytic processes.transiently existing precursor state of CO/Ru(0001) has been also investigatd.

An outlook is given to the Variable Pulse Length Storage Ring BESSY ^{VSR}. With this innovative up grade initiative of the Helmholtz-Zentrum Berlin für Materialien und Energie we aime at a MHz repetition rate picosecond and sub-picosencond Synchrotron Radiation facility ideally suited to observe chemical dynamics for functional materials.

1. **Transient states of photo excited $Fe(CO)_5$ and the solvent induced quenching of ultrafast sequential dissociation**, Ph. Wernet, K. Kunnus, M. Odelius, I. Josefsson, I. Rajkovic, S. Schreck, W. Quevedo, M. Beye, S. Grübel, M. Scholz, D. Nordlund, W. Zhang, R. Hartsock, K. Gaffney, W. F. Schlotter, J. J. Turner, B. Kennedy, F. Hennies, F. de Groot, S. Techert and A. Föhlisch, *Submitted.*

2. **Real-Time Observation of Surface Bond Breaking with an X-ray Laser**, M. Dell'Angela, T. Anniyev, M. Beye, R. Coffee, A. Föhlisch, J. Gladh, T. Katayama, S. Kaya, O. Krupin, J. LaRue, A. Møgelhøj, D. Nordlund, J. K. Nørskov, H. Öberg, H. Ogasawara, H. Öström, L. G. M. Pettersson, W. F. Schlotter, J. A. Sellberg, F. Sorgenfrei, J. Turner, M. Wolf, W. Wurth and A. Nilsson, ***Science**, 2013; DOI: 10.1126/science.1231711.*

3. **Selective ultrafast probing of transient hot chemisorbed and precursor states of CO on Ru(0001)**, M. Beye[1,2], T. Anniyev[1], R. Coffee[3], M. Dell'Angela[4], A. Föhlisch[2,5], J. Gladh[6], T. Katayama[1], S. Kaya[1], O. Krupin[3,7], A. Møgelhøj[8,9], A. Nilsson[1,6,8,10], D. Nordlund[10], J. K. Nørskov[8,11], H. Öberg[6], H. Ogasawara[10], L.G.M. Pettersson[6], W. F. Schlotter[3], J. A. Sellberg[1,6], F. Sorgenfrei[4], J. J. Turner[3], M. Wolf[12], W. Wurth[4] and H. Öström[6,*] ***Phys. Rev. Lett.** In press 2013.*

Peter SUSHKO

Peter Sushko graduated with MSc degree in Physics from St. Petersburg State University in 1996. He was working on his PhD Thesis at the Royal Institution of Great Britain and University College London (UCL) under the supervision of Profs. Alexander Shluger and Richard Catlow and obtained his PhD in Physics from the University of London in 2000. Following this, he worked as a post-doctoral researcher at UCL and the London Centre for Nano-technology.

In 2008 he was awarded a Royal Society University Research Fellowship, which he brought to the Department of Physics and Astronomy at UCL, where he was appointed as a Lecturer (2008) and then a Reader (2012).

His research interests are in the area of computational modelling of materials with an emphasis on defects in oxides and oxide interfaces. He is a co-author of over 100 papers.

REVEALING THE CHARACTER OF OPTICAL ABSORPTION IN COMPLEX OXIDES

Peter V. Sushko

Department of Physics and Astronomy and London Centre for Nanotechnology, University College London, Gower Street, London, WC1E 6BT, UK

e-mail: p.sushko@ucl.ac.uk

Harvesting solar energy is a promising way of addressing global energy needs. However, greater efficiency in capturing sunlight needs to be achieved for the technology to become sustainable. Accordingly, a great deal of experimental and theoretical research efforts are directed to finding materials and structures with novel optical properties and specific electronic structure features. To advance on this path, fundamental insight into the character of the optical transitions is required.

We explore how optical properties of complex oxides can be modified in order to provide greater absorption in a desirable spectral region. To this end, we investigate theoretically optical absorption in strained epitaxial $LaCrO_3$ films deposited on various substrates [1] and in solid solutions of α-Fe_2O_3 and α-Cr_2O_3 [2]. We use an embedded cluster method, together with an accurate electrostatic embedding potential [3] and hybrid density functionals, which provide a reliable description of band gaps in insulators and wide band gap semiconductors.

Our results show that $LaCrO_3$ optical absorption spectrum contains distinct contributions associated with two types of the intra-Cr $t_{2g} \rightarrow e_g$ (2.7, 3.6 eV), inter-Cr $t_{2g} \rightarrow t_{2g}$ (4.4 eV), and O 2*p* $\rightarrow$ Cr 3*d* transitions. The onset of the O 2*p* – Cr 3*d* charge transfer gap is between 4.6 and 5.0 eV, in contrast to earlier reports, which put it at ~3.4 eV. Finally, the magnitude of the charge-transfer gap depends on the lattice strain and can be varied by ~0.2 eV by the judicious choice of the substrate. On the contrary, the energies of the Cr *d*–*d* transitions are strain insensitive. In the case of the α-$Cr_xFe_{2-x}O_3$ solid solutions, the dependence of the optical absorption spectra on the Fe:Cr ratio is driven not by the lattice strain but by the dramatic difference in the electronic structures of pure α-Fe_2O_3 and α-Cr_2O_3 as well as by their incommensurate spin structures.

We propose that combining cation intermixing with the substrate-induced strain effects can provide a powerful method for tuning optical absorption properties of complex oxides.

[1] P. V. Sushko, L. Qiao, M. Bowden, T. Varga, G. J. Exarhos, F. K. Urban III, D. Barton, S. A. Chambers, *Phys. Rev. Lett.* **110**, 077401 (2013).

[2] Y. Wang, N. Govind, S. A. Chambers, P. V. Sushko (*submitted*).

[3] I. V. Abarenkov, *Phys. Rev. B* **76**, 165127 (2007). P. V. Sushko, I. V. Abarenkov, *J. Chem. Theory Comput.* **6**, 1323 (2010).

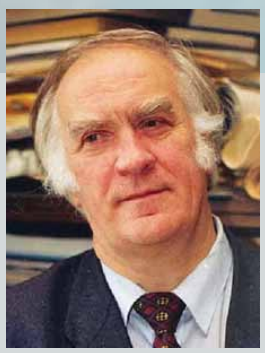

Vitaly MIKHAILIN

Professor V.V. Mikhailin is working as a head of Division of physical problems of quantum electronics at the Skobeltsyn Institute of Nuclear Physics, Lomonosov Moscow State University. His reserach interest cover study and search for new scintillation materials using advanced theoretical and experimental methods. He is one of pioneers in applying short wavelength synchrotron radiation in studies of optical properties of solids using various methods. He written several monographs and publisher numerous papers in world leading scientific journals.

SYNCHROTRON RADIATION IN SCINTILLATOR INVESTIGATIONS

Vitaly V. Mikhailin

Faculty of Physics of M.V.Lomonosov Moscow State University, Russia

e-mail: vvm@srd.sinp.msu.ru

A historical review of the usage of synchrotron radiation in scintillator investigation is presented. Unique properties of synchrotron radiation allow to separately investigate elementary excitations in scintillators and their interactions and transformations. Excitations in solids are well classified by corresponding spectral ranges of dielectric functions: e.g. defect excitation region, defect ionization region, Urbach tail, exciton creation region, fundamental absorption region with production of separated electron-hole pairs, core exciton region and core ionization regions. Therefore separate excitation by monochromatized synchrotron radiation is useful to prepare different initial states in scintillators. The examples of such investigations in different types of crystals (BaF_2, scintillators with charge transfer luminescence, tungstates, molybdates, fluorides, MgO, etc.) are presented.

Suzy LIDSTRÖM

Suzy Lidström is editor-in-chief of Physica Scripta, the broad-based physics journal owned by the Royal Swedish Academy of Sciences. Although she was born and brought up in England, a chance conversation with a Swedish professor in a corridor at Sussex University opened up the opportunity to participate in an exchange programme in Sweden. Without hesitation, she raced off to Uppsala, finishing her first degree in the Engineering Department and signing up for a PhD in the Physics Department, where she studied the diffusion of hydrogen and muons in amorphous and crystalline materials. She has worked as a scientific editor and proofreader in the Netherlands and France.
She lives in northern France with too many children, cats, horses and other four-legged dependents.

This is the way it is

Suzy Lidström, *Physica Scripta*, Royal Swedish Academy of Sciences, Stockholm, Sweden

E-mail: suzy.lidstrom@kva.se

Writing for a broad-band peer-reviewed journal necessitates the adoption of a somewhat different approach to that employed when targeting a specialist journal. Those aspects of greatest importance to the publication of the proceedings from this conference will be discussed with a view to smoothing the path to acceptance and publication for all authors and assisting the guest editors with the task ahead of them.

Given the pace with which the world of academic publishing is evolving, there has probably never been a better opportunity to consider the alternatives to conventional peer-reviewed publication. Although it has adversaries who are ready to enumerate and expound upon its many flaws, the proponents of peer review believe that the considered opinion of experts in the relevant field offers the best means of ensuring the scientific validity of publications. No balanced debate can fail to consider both the pros and the cons, for, despite its deficiencies, peer review can also contribute by reducing the volume of work that reaches the public domain.

With a view to stimulating a debate on the future of peer review, multiple factors leading to the rejection of an article will be considered. One of these, of potential interest to many delegates, is the role of language and, more specifically, the implication that having to write in a non-native tongue can have on the likelihood of a manuscript being accepted. In this day and age, it is inevitable that the publication of the papers ensuing from this meeting will be in English to guarantee that the advances discussed reach the international community. Given that this is a non-native language to the majority of those attending the meeting, advice will be given on counteracting the disadvantage of writing in a foreign tongue, because, in the words of Gannon, at least in this era and on this occasion, “This is the way it is.”

Gannon, F., 2008. Language barriers. *European Molecular Biology Organization Reports* 9:207.
Keywords:

Peer review, publishing, second language, English, broad-band journal, rejection,

Kurt SCHWARTZ

Kurt Schwartz, born 27.04.1930 in Riga, Latvia. From 1949 to 1954 physic s studies at the Latvian State University. Ph.D. 1969 at the University of Tartu (Luminescence efficiency of doped alkali halides). Habilitation in 1970 at the P. Lebedev Physical Institute (FIAN) of the Academy of Sciences, Moscow (Radio-luminescence and radiation damage of alkali halides). Member of Latvian Academy of Sciences (1991; Award of the Latvian Academy of Sciences for radiation damage studies - 2010).

Scientific and pedagogical activities:

From 1957 to 1961 assistant professor at the Department of Physics, Latvian State University. From 1961 to 1991 head of the Radiation Physics Labor, Institute of Physics, Latvian Academy of Sciences. From 1974 to 1985 also professor at the Department of Physics at the Technical University (Riga).

From 1992 up to now in Germany, German citizenship. From 1992 to 1994 visiting professor at the University of Heidelberg. From 1994 up to now senior scientist at the Gesellschaft für Schwerionenforschung, Department Material Science. From 2005 up to now Consultant for ion research at the ion cyclotron DC 60 (Institute of Nuclear Physics, Astana, Kazakhstan).

Publications: more than 250 including 5 monographs (for the last years see Supplement “Publications on radiation damage”).

Research Interest: solid state physics, optical spectroscopy, radiation damage in dielectric materials, applications in radiation dosimetry and nanotechnology.

Ion tracks and nanotechnology

K. Schwartz

GSI Helmholtz Zentrum für Schwerionen Forschung (GSI), Planckstr. 1, 64201, Darmstadt, Germany

e-mail: k.schwartz@gsi.de

Swift heavy ions (SHI) with energies (E_{ion}) higher than 1 MeV per nucleon (MeV/u) and masses higher than 20 nucleons can produce structure and phase transformations in solids in nanometric vicinities of their trajectories. The damage structure of SHI tracks in various solids depends on chemical binding, the ion energy E_{ion} and dE/dx, as well as on the irradiation temperature [1, 2].

SHI effects in solids open new possibilities for nanotechnology due to the nanometric damage scales, the extremely high ratio of the track diameter (10 nm) to the length (100 nm),, and specific structure modifications along the ion path. Developed applications are conductive nanochannels in solids and nanopores in polymers for molecular biology and nanowire technology [3, 4]. New tunable electronic devices are developed for information processing [5]. Damage creation and possible applications are discussed.

References

[1] N. Itoh, D. N. Dufly, S. Khadshouri, A. M. Stoneham, J. Phys.: Condens. Matter, "Making Tracks: electronic excitation roles in forming swift heavy ion tracks", **21**, 474205 (2009).

[2] K. Schwartz, A. E.Volkov, M. V. Sorokin, C. Trautmann, K.-O.Voss, R. Neumann, M. Lang, "Effect of electronic energy loss and irradiation temperature on color-center creation in LiF and NaC crystals irradiated with swift heavy ions", Phys. Rev. B **78**, 024120 (2008).

[3] A. Rudin, Ph. Choi, *"Elements of Polymer Science & Engineering"* Elsevier, 2012.

[4] M. A. White,"*Physical Properties of Materials"* CRC PRESS, 2011.

[5] D. Fink, A. Saad, S. Dhamodaran, A. Chandra, W. R. Fahner, K. Hoppe, L. T. Chadderton, , Rad. Measurements **43**, S546 (2008)

Marina POPOVA

Marina Popova has graduated from the Moscow Institute of Physics and Technology (MIPT) in 1964. She worked as PhD student in the Laboratory of Luminescence of the Lebedev Physical Institute, USSR Academy of Sciences, under the supervision of Prof. M.D. Galanin and Dr. A.M. Leontovich, creators of the first laser in the USSR. She received her PhD from the Lebedev Physical Institute in 1968, after defending her PhD thesis "Dynamics of ruby laser". During 1968-1975 she worked as researcher in the Problem Laboratory of Semiconductor Physics of the Latvian State University in Riga. She has made a ruby laser there (the first one in Baltic states) and studied multiphoton absorption in crystals. Since 1975 she is with the Institute of Spectroscopy, Russian Academy of Sciences, were she also got her Doctor of physical and mathematical sciences degree (1992) after defending her second thesis: "High-resolution Fourier-transform spectroscopy of rare earth containing crystals". In 2001 the title of professor in optics was conferred on her. At present, she is head of the Laboratory of Fourier Spectroscopy in the Department of Solid State Spectroscopy in the Institute of Spectroscopy, Russian Academy of Sciences. She is expert in physics of impurity centers in crystals, Fourier-transform spectroscopy, spectra of rare-earth ions, solid-state lasers, spectroscopy of magnetic insulators. Her laboratory concentrates on studies of new functional materials for quantum and optoelectronics, quantum informatics.

FAR INFRARED STUDIES OF MULTIFERROIC IRON BORATES

Marina Popova
[1]*Institute of Spectroscopy, Russian Academy of Sciences*
e-mail: popova@isan.troitsk.ru

Iron borates with general formula $RFe_3(BO_3)_4$ (R stands for a rare earth or yttrium) crystallize in a trigonal noncentrosymmetric structure of the natural mineral huntite. These materials exhibit long range antiferroelectric and antiferromagnetic orders and, thus, are multiferroics. Some of iron borates demonstrate considerable magnetoelectric and magnetodielectric effects which promises device applications because magnetic properties can be governed by an electric field and vice versa.

My group carries on systematic optical studies of rare earth (RE) iron borates. In this talk, I'll consider recent results obtained by the method of far infrared (FIR) spectroscopy on europium [1] and praseodymium iron borates. Temperature-dependent FIR absorption and reflection were studied at the facilities of the Institute of Spectroscopy. Several \ellipsometry measurements were performed at the Brookhaven National Laboratory synchrotron FIR line. The FIR spectra of $EuFe_3(BO_3)_4$ present a clear evidence of a first-order structural phase transition at $T_S = 58$ K. This transition manifests itself by sharp shifts of phonon frequencies and by a sudden appearance of new vibrational modes of the lower symmetry low-temperature structure. Similarity between the temperature dependences describing the phonon frequency shift $\omega(T)$ and the splitting of the electronic doublet of Eu^{3+} in $EuFe_3(BO_3)_4$ below the temperature T_S points to lattice distortions as a dominant mechanism affecting phonon frequencies. Peculiarities at the temperature T_N of the magnetic ordering observed in the $\omega(T)$ curves manifest a spin-lattice coupling. The mechanism of this coupling is, most probably, connected with atomic displacements stimulated by the internal magnetic field arising in the magnetically ordered state below T_N. Similar peculiarities at T_N were observed for phonon frequencies of $PrFe_3(BO_3)_4$. FIR spectra of $PrFe_3(BO_3)_4$ also clearly demonstrate an interaction between the 58 cm^{-1} phonon and the crystal-field level of Pr^{3+}.

I am grateful to my coauthors of Ref. 1. A financial support of the Russian Academy of Sciences under the Programs for basic research is acknowledged.

References

1. K.N. Boldyrev, T.N. Stanislavchuk, S.A. Klimin, M.N. Popova, L.N. Bezmaternykh, *Phys. Lett. A* **376** (2012) 2562.

Vladimir TREPAKOV

Vladimir Trepakov graduated from St.-Peteresburg Polytechnical Institute (State Polytechnical University) in 1972. He obtained his PhD physics degree in physics at A.F. Ioffe Physical-Technical Institute in 1980 ("Optical and Photoinduced Phenomena in Ferroelectrics with Diffuse Phase Transitions" supervised by Professor G.A. Smolensky). From 1972 – he has been working in AF Ioffe Physical-Technical Institute, St-Petersburg, Russia; during 2001 - 2003 – Professor C-III in Osnabrueck University, Germany; from 2003 he joined the Institute of Physics AS CR, Prague, Czech Republic.

Belonging to the Scientific School of Professor GA Smolensky, V .Trepakov is a well known distinguished specialist in physics of perovskite-like oxides, ferroelectrics, quantum paraelectric crystals, ceramics, thin films, nano-powders, structures.

V. Trepakov's research activities has included investigations of the phase transitions, multiscale ordering and photoinduced phenomena; zero and low-T phase transitions, incipient ferroelectrics and related highly polarizable advanced oxides; structural and spectroscopic active impurities in highly polarizable materials; confine geometry and nano-size effects; strongly correlated Mott-Hubbard systems, localized to itinerant electronic transitions, multiferroics.

He is the author or co-author of more than 200 papers. V. Trepakov is also the co-author of the several very important fundamental pioneer results.

HEAVILY MANGANESE DOPED STRONTIUM TITANATE NANOPARTICLES: SYNTHESIS, STRUCTURE AND PROPERTIES.

Vladimir Trepakov[1,2] (presenting author), Marina Makarova[1,3], Olexandr Stupakov[1], Alexander Dejneka[1], Fedir Borodavka[1], Jan Drahokoupil[1], Ales Jäger[1] and Lubomir Jastrabik[1]

[1]Institute of Physics ASCR, Praha, Czech Republic, [2]Ioffe Physical-Technical Institute RAS, St-Petersburg Russia, [3]NIMS, 1-1 Namiki, Tsukuba, Ibaraki, 305-0044 Japan

e-mail of presenting author: trevl@fzu.cz

Cubic perovskite $SrTi_{1-x}Mn_xO_3$ nanopowders with x = 0 – 0.5 - that is much higher than the conventionally believed Mn incorporation limit – and particles size 10 – 80 nm have been successfully synthesized by citrate sol-gel method. The crystalline structure, morphology, chemical composition and lattice constant behaviour versus annealing temperature and Mn concentration have been characterized by X-ray diffraction, scanning electron microscopy and proton-induced X-ray emission techniques.

Studies of Raman light scattering and magnetic properties revealed activation of TO2 polar phonon mode and magnetic ordering effects at low temperatures. Such features are treated as evidences of non-d^0 Mn-driven transition to a polar phase and multiferroicity in heavily Mn concentrated perovskite $SrTi_{1-x}Mn_xO_3$ nanoparticles.

Oral presentations

OPTICAL SPECTROSCOPY OF $Gd_3(Al_xGa_{1-x})_5O_{12}:Ce^{3+}$ EPITAXIAL FILMS

N.V. Vasil'eva[1], D.A. Spassky[2,3], I.V. Randoshkin[1], E.M. Aleksanyan[3], S. Vielhauer[3], V.O. Sokolov[4], V.G. Plotnichenko[4], V.N. Kolobanov[5], A.V. Khakhalin[5]

[1]Prokhorov General Physics Institute, Russian Academy of Sciences, Moscow, Russia, [2]Skobeltsyn Institute of Nuclear Physics, Lomonosov Moscow State University, Russia, [3]Institute of Physics, University of Tartu, Estonia, [4]Fiber Optics Research Center, Russian Academy of Sciences, Moscow, Russia, [5]Physics Department, Lomonosov Moscow State University, Russia

e-mail: dmitry.spasskiy@ut.ee

Yttrium and lutetium garnet single crystals doped with Ce^{3+} are known as fast scintillators with high light yield. The band-gap engineering with Ga-doping and the partial or complete substitution of Lu and Y cations with Gd resulted in significant improvement of their scintillation properties [1,2]. However, the presence of antisite defects in garnets is an inevitable consequence of the high growth temperature of the bulk crystals. The growth of single crystalline films using the liquid phase epitaxy method avoids the creation of antisite defects in the garnets structure, obtaining films with scintillation performance not worse than that for the single crystals [3]. Here we report on the growth, optical and luminescence characterization of Ce^{3+} – doped $Gd_3(Al_xGa_{1-x})_5O_{12}$ (x=0.00, 0.22, 0.31, 0.38) single crystalline films.

The quantitative chemical analyses of films were performed using electron-ion scanning microscope «QUANTA 3 D FEG» and scanning electron microscope Quanta 600 FEG. Transmission spectra were measured using Perkin Elmer Lambda 900 spectrophotometer. The luminescence characteristics as well as the reflectivity were measured using synchrotron radiation at the beamlines I (SUPERLUMI station) and BW3 at DESY (Hamburg) and at the branch-line FINEST at MAX-lab, Lund. Ce^{3+} - related luminescence has been observed in the case of partial substitution of Ga with Al ions. The effect is connected with the shift of 5d Ce levels to the bandgap. Experimental evidence of the bandgap increase with the introduction of Al^{3+} ions into gadolinium gallium garnet is presented as well. This work was supported in part by M.V. Lomonosov Moscow State University Program of Development.

References

1. M. Fasoli, A. Vedda, M. Nikl, et al., *Phys.Rev.* 2011, v. 84 , 081102(R), 21-23.
2. K. Kamada, T. Yanagida, J. Pejchal, et al., *J. Phys. D: Appl. Phys*., 2011, v. 44, 505104.
3. J. Tous, K. Blazek, M. Kucera, et al., *Rad. Meas.*, 2012, v. 47, 311-314.

FLUORESCENCE QUENCHING IN THE Nd^{3+} DOPED Y_2O_3 NANOPARTICLES OF MONOCLINIC PHASE

Yurii Orlovskii[1,2], Alexandr Popov[1,2], Stanislav Fedorenko[3], Ilmo Sildos[1]

[1] *Institute of Physics,University of Tartu, 142 Riia str., 51014 Tartu, Estonia,* [2]*General Physics Institute RAS, 38 Vavilov str., 119991, Moscow, Russia,* [3]*Institute of Chemical Kinetics and Combustion SB RAS, Novosibirsk, 630090, Russia*

e-mail of presenting author: yury.orlovskiy@ut.ee

This work was supported by European Social Fund (MTT50 and MJD167) and RFBR #11-02-0248.

We study the fluorescence quenching kinetics $I(t)$ from the $^4F_{3/2}$ laser level in the Nd^{3+} doped Y_2O_3 spherical nanoparticles (NPs) of monoclinic phase synthesized by laser ablation of solid targets with subsequent recondensation in flow of air at atmospheric pressure [1]. We show that the fluorescence quenching in the NPs is determined by two processes: static dipole-dipole quenching by vibrations of OH^- molecular groups associated with the oxygen vacancies and Nd^{3+} - Nd^{3+} dipole-dipole energy migration with subsequent Nd^{3+} - OH^- quenching. We find that at 0.1 at.% of Nd^{3+} concentration the process of static quenching by the OH^- acceptors dominates for two types of optical centers detected. In the 1.0 at.% Nd^{3+}:Y_2O_3 spherical NPs the first time in a solid-state impurity laser medium we observe non-stationary kinetics on the entire length of a time-dependent luminescence quenching (Fig. 1), starting from static decay and ending with fluctuation kinetics of fluorescence hopping quenching. We discuss the kinetics at 3 & 8% of Nd^{3+}.

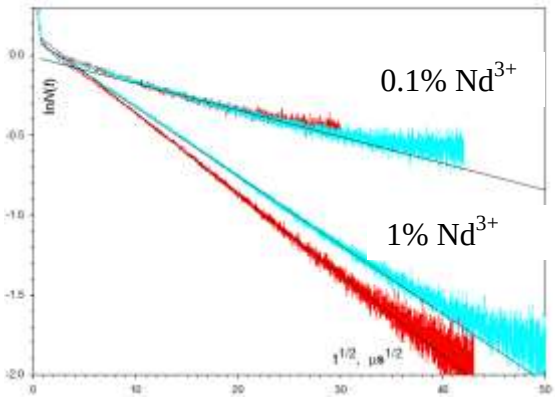

Fig.1 Fluctuation kinetics of fluorescence hopping quenching $N(t)=I(t)/exp(-t/\tau_R)$, where τ_R spontaneous emission lifetime, on vibrations of OH^- acceptors for two different types of optical centers (red and blue) in the 1.0 at.% Nd^{3+}:Y_2O_3 crystalline spherical NPs - two lower curves. The increase in the Nd^{3+} donor concentration enhances the migration of excitations over them, and accelerates their quenching on the acceptors. Excitation decay in the regions depleted in donors and acceptors is determined by the kinetics of the Förster type $N(t)=exp(-\gamma t^{1/2})$ with the increased decay decrement $\gamma=\gamma_A+\gamma_D$ comparing to static Förster kinetics $\gamma=\gamma_A$ in the 0.1 at.% Nd^{3+}:Y_2O_3 sample – upper curves.

References

V.V. Osipov, Yu.A. Kotov, M.G. Ivanov, et al., *Laser Phys.*, **2006**, 16, 116-125.

ADVANCES IN OXYFLUORIDE GLASS-CERAMICS

Uldis Rogulis, Anatolijs Sarakovskis, Edgars Elsts, Andris Fedotovs, Inga Brice
Institute of solid State Physics, University of Latvia,
e-mail of presenting author: rogulis@latnet.lv

Besides being a good medium for up-conversion displays [1], oxyfluoride glass-ceramics have shown several new prospective application directions. For investigations of the up-conversion mechanisms, the comparison of the optical spectra of the glass-ceramics and corresponding fluoride macrocrystals has been fruitful [2]. Pan et al showed that terbium-doped glasses and glass-ceramics of composition SiO_2-Al_2O_3-Li_2O-LaF_3 have high scintillation efficiency [3]; this efficiency is the highest for glass-ceramics samples. We compared cathodoluminescence decay times for terbium-, cerium- and europium-doped oxyfluoride glass-ceramics [4] and obtained that cerium-doped glass-ceramics have shortest decay times. Formation of fluoride crystallites in the oxyfluoride glass-ceramics could be tracked by the EPR hyperfine structure of impurity ions [5]. Activator ions in the oxyfluoride glass-ceramics could be embedded in the oxide glass as well as in the fluoride crystal parts of the ceramics, revealing new possibilities of the construction of the spectral shape for solid state lighting [6]. These and other new possibilities for applications of oxyfluoride glass-ceramics will be discussed.

References

1. M.J. Dejneka, *MRS Bull.,* 1998, vol. 23, 57.

2. A. Sarakovskis, J. Grube, G. Doke, M. Springis, *J. Lumin*. 2010, vol. 30, 805.

3. Z. Pan, K. James, Y. Cui, A. Burger, N. Cherepy, S.A. Payne, R. Mu, S.H. Morgan, *Nucl. Instr. and Meth. in Phys. Res. A* , 2008, vol. 594, 215.

4. U. Rogulis, E. Elsts, J. Jansons, A. Sarakovskis, G. Doke, A. Stunda, K. Kundzins, *IEEE Transact. Nucl. Sci.*, 2012, vol. 59, 2201.

5. A. Fedotovs, Dz. Berzins, O. Kiselova, A. Sarakovskis, U. Rogulis, *IOP Conf. Ser.: Mater. Sci. Eng.*, 2011, vol. 23, 012018.

6. I. Brice, U. Rogulis, E. Elsts, J. Grūbe, *Latv. J. Phys. Techn. Sci*., 2012, No. 6, 44.

Support by the ERAF project 2010/0204/2DP/2.1.1.2.0/10/APIA/VIAA/010 is gratefully acknowledged.

OPTICAL FIELD-INDUCED SURFACE PATTERNING OF SOFT MATERIALS

Janis Teteris
Institute of Solid State Physics, University of Latvia
teteris@latnet.lv

An interaction between laser light beam with high intensity gradient and soft materials (amorphous chalcogenide and organic polymer films) was studied. The single light beam focusing and two coherent beam interference were used for high light intensity gradient formation. Under intensive illumination the formation of relief structures on the surface of amorphous films due to lateral mass transport regarding the light propagation direction has been observed.

The amorphous films of chalcogenides (As-S, As-S-Se, As-Se and Ge-Se systems), azo-dye containing organic polymers and low molecular organic glasses were used for the studies. The influence of the amorphous film thickness, recording laser wavelength in the spectral range of (248 nm - 671 nm), grating period, light intensity and polarization state on the relief formation process in amorphous inorganic and organic films was studied. It was shown that the efficiency of the surface-relief formation strongly depends on the recording light polarization state [1]. The best surface relief grating (SRG) formation was observed with ($+45^0$, -45^0) and (RCP, LCP) combinations, which involve primarily variation in polarization state across the film [2,3]. The relief grating profile on amorphous films was analyzed by means of atomic force microscope (AFM).

The correlation between the exciting light field and the resulting surface deformation was studied. The resulting surface deformation is determined by photoinduced birefringence in film material.

The mechanism of the direct recording of surface-relief on amorphous films based on the photo-induced softening of the matrix, formation of defects with enhanced polarizability, and their drift under the optical field gradient force has been discussed.

References

1. J. Teteris, U. Gertners, M. Reinfelde, *Phys.St.Sol.(*c), **8** (2011) 2780.
2. J.Teteris, U.Gertners, *IOP Conf. Series:Materials Science and Engineering,* **38** (2012) 012012.
3. M.Reinfelde, R.Grants, J.Teteris, *Phys.Stat.Sol*.C, 9, No.12 (2012) 2586-9.

EFFECT OF HOLOGRAPHIC GRATING PERIOD ON ITS RELAXATION IN A MOLECULAR GLASSY FILM

Andris Ozols , Peteris Augustovs, Valdis Kokars, Kaspars Traskovskis, Dmitry Saharov
Faculty of Material Science and Applied Chemistry, Riga Technical University, Latvia
e-mail : aozols@latnet.lv

Disordered materials are thermodynamically unstable and this instability manifests itself by the relaxation of their structure. Relaxation phenomena in glasses and polymers have been studied for a long time [1]. Holographic gratings (HG) recorded in relaxing photosensitive materials are useful tools for relaxation studies [2]. Recently we have studied the effect of recording light polarization on the HG relaxation [3].

In this paper, we report on the HG relaxation studies in 5,5,5-triphenylpentyl 4-((4-(bis(5,5,5-triphenylpentyl)amino) phenyl) diazenyl) benzoate molecular glassy film. The thickness of the film was about 2 μm. Transmission HG with the periods (L) of 0.50, 2.0 and 8.6 μm were recorded with two symmetrically incident 532 nm laser beams until the maximum 633 nm readout light transmission diffraction efficiency (DE_t) was reached. After that DE_t and reflection diffraction efficiency (DE_r) were monitored during about 20 minutes. Further, DE_t and DE_r measurements were repeated during three months.

Completely different DE_t temporal dependences were observed for different periods. DE_t was monotonically decaying in the case of L=0.50 μm, nonmonotonically changing (small maxima, deep minima) in the case of L=2.0 μm and it was relatively stable at L = 8.6 μm. DE_r was nonmonotonically increasing in the case of both L=2.0 μm and L = 8.6 μm. No significant relaxational self-enhancement was observed as in the case of a-As_2S_3 films [2]. The obtained results will be discussed in terms of thermal movement of large molecules bound by weak van der Waals forces.

Acknowledgment: Thanks to Latvian State Research Program in material sciences for financial support.

References

1. D.Sanditov and T.M.Bartenev, *Physical Properties of Disordered Structures* (Nauka, Novosibirsk, 1982) (in Russian).
2. A.Ozols, O.Salminen and M.Reinfelde, J.Appl.Phys. **75** , 7, 3326 (1994).
3. A.Ozols, V. Kokars, P.Augustovs, K.Kenins, E.Zarins, Abstracts of the 28th Scientific Conference, Instititute of Solid State Physics, University of Latvia, February 8-10, 2012, Riga, p.35.

A SURFACE LDH STRUCTURE GROWN ON Zn-Al ALLOY

A.N. Salak, A.D. Lisenkov, M.L. Zheludkevich, M.G.S. Ferreira
Department of Materials and Ceramic Engineering/CICECO, University of Aveiro, Portugal
e-mail: salak@ua.pt

Layered double hydroxides (LDHs) are composed of positively charged (host) layers of mixed metal hydroxide and charge-compensating (inter)layers of anions and water molecules. It has been reported that an LDH is the main phase in a corrosion product on Zn-Al alloy (50-55% aluminium). It was observed that regardless of a type of the main corrosion-active anion (Cl^-, SO_4^{2-}) in the environment, the interlayer height value of such LDH is equal to the double oxygen van der Waals radius. Then the LDH composition was accepted to be a Zn-Al-carbonate with a 'flat' arrangement of CO_3^{2-} anions in the interlayer.

In this work, a natural Zn-Al LDH structure was grown on a surface of Zn50Al alloy (Al ~50%, Zn ~40%, Si ~10%) in decarbonized water (Figure 1). Parameters of the hexagonal crystal lattice were measured to be a = 0.305 nm, c = 2.253 nm, where the latter corresponds to the interlayer height of 0.274 nm. Based on the data of both chemical analysis and XRD, the Zn/Al ratio in the host hydroxide layers was found to be about 1. This is rather unusual since the most stable LDHs are those with the bivalent-to-trivalent metal ratio between 2 and 3.

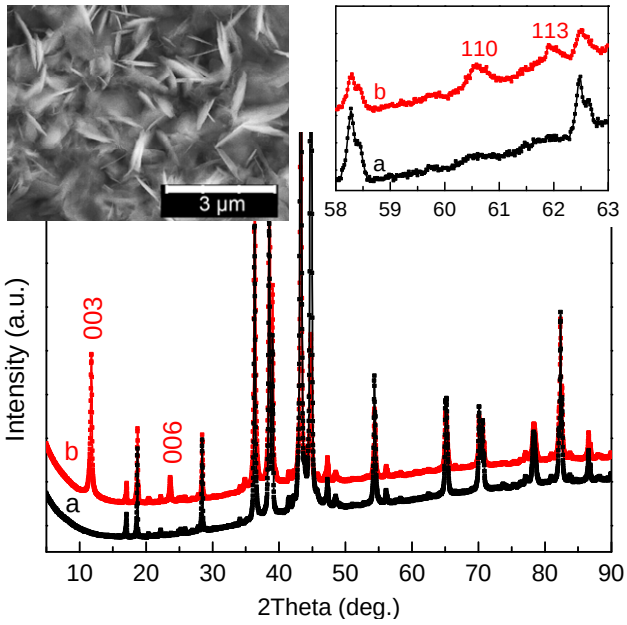

Fig.1 XRD patterns of a Zn50Al alloy surface before (a) and after (b) formation of the LDH phase. Inset: SEM image of the LDH structure.

It was revealed that the main intercalated anion in the obtained LDH is OH^-. The arrangement of hydroxide anions and crystal water molecules in the interlayer was suggested and simulated. Mechanism of the LDH phase formation and methods to control its composition and crystal structure were proposed. It is expected that a modified surface LDH structure can provide efficient corrosion protection of Zn-Al alloys.

MICROSCOPIC CRYSTAL FIELD EFFECTS IN $CsCdBr_3:Ni^{2+}$ CRYSTALS

A.A. Chaykin, M.G. Brik

Institute of Physics, University of Tartu, Riia 142, Tartu 51014, Estonia

E-mail of presenting author: sanchaikin@rambler.ru

$CsCdBr_3:Ni^{2+}$ is known as one of a few borate systems to exhibit luminescence from various Ni^{2+} levels [1]. Ni^{2+} ions substitute for the Cd^{2+} ions at slightly distorted octahedral positions. Using the experimental spectra from Ref. [1], we have calculated the Ni^{2+} energy levels in the framework of the exchange charge model of crystal field [2]; good correspondence to the experimental results was demonstrated, including the trigonal splitting of the orbital triplet states (Fig. 1). Besides, the effect of changing interatomic separation on the overall behavior of the nickel energy levels was studied by calculating the corresponding energy level schemes for 21 different Ni-Br distances R (Fig. 1). In this way we determined the power dependence of the crystal field strength $10Dq$ on R as $10Dq = 3.57804 \times 10^6 / R^{6.15423}$, where R is expressed in Å and $10Dq$ in cm^{-1}. Knowledge of the $10Dq(R)$ function allows for further estimations of the parameters of the electron-vibrational interaction, Huang-Rhys factors and Stokes shifts. In particular, with the above given $10Dq(R)$ dependence we calculated the Stokes shift for the $^3A_{2g}$-$^3T_{2g}$ absorption and the $^3T_{2g}$-$^3A_{2g}$ emission to be about 1700 cm^{-1}, in reasonable agreement with the values of 1900 cm^{-1} and 1400 cm^{-1}, as reported in Refs. [1] and [3], respectively.

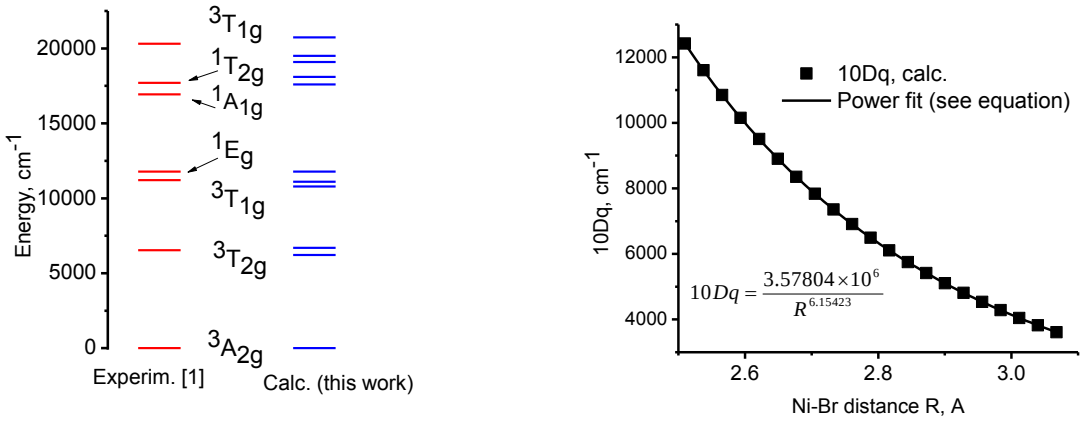

Fig.1. Comparison between the calculated (this work) and experimental [1] energy level schemes of Ni^{2+} in $CsCdBr_3$ (left) and dependence of the crystal field strength 10Dq on distance R (right).

References

1. O.S. Wenger, S. Benard, H. U. Güdel, *Inorg. Chem.*, 2002, 41, 5968-5977.
2. B.Z. Malkin, in: A.A.Kaplyanskii, B.M. Macfarlane (Eds.), Spectroscopy of solids containing rare-earth ions, North-Holland, Amsterdam, 1987, p. 13.
3. D. De Viry, N. Tercier, J.P. Denis, B. Blanzat, F. Pelle, *J. Chem. Phys.*, 1992, 97, 2263.

Cubic monocarbides *X*C (*X*=Ti, V, Cr, Nb, Mo, Hf) as explored by *ab initio* calculations

V. Krasnenko*, M.G. Brik

Institute of Physics, University of Tartu, Riia 142, Tartu 51014, Estonia

*Corresponding author, e-mail: veera.krasnenko@ut.ee

Carbides of the transition metals are extensively studied both theoretically and experimentally, since they are very important technological materials due to a unique combination of their remarkable physical properties such as chemical stability, hardness, high melting temperature and thermal conductivity, corrosion and wear resistance, which allows for their wide use in the wear-resistant parts of various mechanisms operating at extreme conditions.

In the present work six transition metal monocarbides (TiC, VC, CrC, NbC, MoC, HfC) with the rock-salt structure were selected for a detailed comparative *ab initio* study of their structural, electronic, elastic, and thermodynamic properties at ambient and elevated up to 50 GPa hydrostatic pressures. The CASTEP module of the Materials Studio package was used for calculations.

The relation between the elastic and bonding properties and the number of valence electrons in each compound was considered. A certain correlation between the elastic parameters and "metal-carbon" effective charge difference, on one side, and a number of the valence electrons, on the other side, was found. The calculated values of the elastic constants were used for further estimations of the Debye temperatures, Grüneisen parameters, specific heat capacities and linear coefficients of thermal expansion. For CrC and MoC the Debye temperature and Grüneisen parameter were estimated for the first time; reliability of those estimations is based on good agreement between those parameters for TiC, VC, NbC, HfC obtained in the present work with the experimental data.

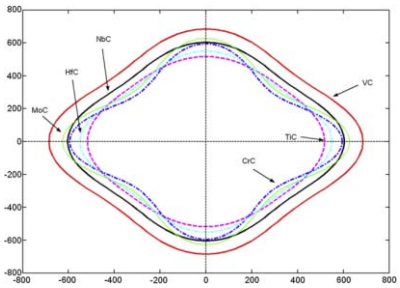

Fig. 1. Cross-sections of the Young's moduli surfaces in the ab plane. The axes units are GPa.

The elastic anisotropy of the considered carbides was studied to identify those directions in the crystal lattice, which correspond to the greatest and smallest Young's moduli values (Fig. 1) [1].

We believe that several "property-property" and "structure-property" relations uncovered in the present study can be helpful for the analysis and predictions of properties of similar compounds.

References

[1] V. Krasnenko, M.G. Brik, *Solid State Sci*., 2012, 14, 1431-1444.

PHOTOSTIMULABLE STORAGE PHOSPHORS AND IMAGE-PLATE DEVELOPMENT FOR NEUTRON IMAGING

A.I. Popov[1,2] and G.J. McIntyre[3]

[1] *Institute of Solid StatePhysics, University of Latvia, LV-1063 Riga, Latvia*
[2] *Institut Laue-Langevin, BP156, 38042 Grenoble Cedex 9, France*
[3] *Australian Nuclear Science and Technology Organisation, Lucas Heights, NSW, Australia*
e-mail: popov@ill.fr, popov@latnet.lv

The neutron-sensitive image plates (NIP's) [1,2] used on the LADI [3] and VIVALDI [4] Laue diffractometers at the Ins titute of Laue-Langevin offer se veral advantages as cold- and thermal-neutron detectors, notably excellent re solution, wide dynam ic range, and easy incorporation in large-solid angle detectors. They consist of a fil m of finely dispersed storage phosphor (e.g. BaFBr:Eu^{2+}) in an organic binder on a thin plastic support. In general, a storage phosphor functions as f ollows: ionizing radiation generates metastable electron and hole trap centers, whose concentration is proportional to the incident dose. T he centres with trapped electrons are photostimulable, so upon photostimu lation each electron recom bines with a hole center to produce photostim ulated luminescence (PSL), which is proportiona l to the density of the locally trapped electron and hole pairs and thus proportional to the locally absorbed dose of incident ionizing radiation. These storage phosphor s are made sensitive to neutrons by adding a neutron converter. Scanning the NIP with a fo cused laser and a photomultiplier faced by an optical filter allows simultaneous excitation and detection of lum inescence from the co lour centres so that stored information is read out spot-by-spot.

In this presentation we will:

1. Summarize the current status of research in the field of neutron storage phosphors with emphasis on the specific requirements for both phosphor and converter.
2. Report the luminescence properties – emission and stimulation characteristics – and the temperature dependence, of current popular NIP's as well as their characterization with different γ-ray sources.
3. Give an ov erview of recent re sults of com parative measurements of PSL record ed after neutron irradiation of a num ber of new combinations of converter/storage phosphors, namely Eu^{2+}-doped BaSrFBr, CsBr etc, c ontaining various quantities of Gd_2O_3, B_2O_3, LiF or $Li_2B_4O_7$ neutron converter.
4. Demonstrate the preparation of large unifo rm prototype NIP's by layering a BaSrF Br:Eu^{2+} phosphor (obtained from P.Leblans, Agfa) alternately with Gd_2O_3 converter (with D.A.A. Myles).
5. Report new results of luminescence characterization of some novel neutron storage phosphor (jointly with TU Delft, TU Darmstadt, and Lviv University, Ukraine)
6. Suggest some possibilities to improve current instruments.

References

[1] - C. Rausch, T. Bücherl, R. Gähler, H.V. Seggern & A. Winnacker, SPIE **1737**, 255, (1992).
[2] - N. Niimura, Y. Karasawa, I. Tanaka, J. Miyahara, K. Takahashi, H. Saito, S. Koizumi & M.Hidaka, Nucl. Instr. Meth. Phys. Res. A**349**, 521, (1994)
[3] - F. Cipriani, J.-C. Castagna, L. Claustre, C. Wilkinson & M. S. Lehmann. Nucl. Instr. Methods A **392**, 471 (1997)
[4] - C. Wilkinson, J.A. Cowan, D.A.A. Myles, F. Cipriani & G.J. McIntyre, Neutron News **13**, 37, (2002) ; G.J. McIntyre, M.-H.. Lemée-Cailleau & C. Wilkinson, Physica B, **385-386**, 1055, (2006)

OR-12

NON-PROPORTIONALITY OF LUMINESCENCE EXCITATED IN XUV PHOTON ENERGY RANGE

A. Belsky[1], A. N. Vasil'ev[2], A. Giglia[3], E. Meltchakov[4], F. Moretti[1], C. Dujardin[1], A. Gektin[5], S. Nanaronne[3]

[1]*Institut Lumière Matière, CNRS-Université Lyon 1, F-696222 Villeurbanne, France*

[2]*Skobeltsyn Institute of Nuclear Physics, Lomonosov Moscow State University, Moscow, 119991, Russia*

[3] *INFM-CNR, TASC Laboratory, Trieste, Italy*

[4]*Institut Optique, 91127 Palaiseau, France*

[5]*Institute for Scintillation Materials, 60 Lenin Avenue, 61001 Kharkov, Ukraine*

e-mail of presenting author: andrei.belsky@univ-lyon1.fr

The measuring of luminescence excitation spectra of insulators in extra wide region of spectra from UV to soft x-rays is a difficult but very informative problem. This spectral region covers most peculiarities of electron structure of insulators, starting from fundamental absorption region up to most core levels. Therefore the luminescence excitation spectroscopy provides information about relaxation channels of most excitations produced as intermediate ones in scintillation process. Some semi-phenomenological processes are influenced on the excitation spectra, namely, surface losses and photoemission. However, a lot ofexperiments in the soft X-ray range showed the contribution of other mechanisms [1]. X-ray edges displays not only dips in excitation spectra (which is typical for surface losses), but also positive steps [2]. This enhance of efficiency of several channels of relaxation, as well as nonproportional yield in regions far from core levels demonstrate the role of non-uniform spatial distribution of secondary excitations, which depends strongly on the energy and a nature of the primary ones [3].

To study the EEs relaxation process in spatially non-uniform regions of electronic excitations, we have selected a series of the wide bandgap crystals possessing different emission mechanisms: $La_xCe_{1-x}F_3$, CsI (pure and doped by Tl, In, or Na), BaF_2 and cerium doped trioxides. The experimental data were taken at BEAR beamline of Elettra synchrotron light source. This machine is operated in multibunch mode using the stabilization system for beam position and current. The large spectral range from 5 to 1600 eV is covered by using the plane-grating monochromator supplied with three interchangeable gratings. The emission spectra of crystals were recorded by using ANDOR Newton CCD coupled with small ANDOR spectrograph.

This work is supported by 7th FP INCO.2010-6.1 grant agreement No 266531 (project SUCCESS).

References

[1] A.N.Belsky et al, NIMA 361, (1995) 384–387,.

[2] A.N.Belsky, et al, J. of Lum. **72-74** (1997) 93-95

[3] A.Belsky et al, in: Proc. of SCINT2005, Kharkov, Ukraine, 2006, pp.22–25.

EXAFS spectroscopy and first-principles study of $SnWO_4$

A. Kuzmin, A. Anspoks, A. Kalinko, J. Timoshenko, R. Kalendarev
Institute of Solid State Physics, University of Latvia, Latvia
e-mail: a.kuzmin@cfi.lu.lv

Stannous tungstate $SnWO_4$ is very interesting compound, rarely studied in the past. It has two stable phases: the low-temperature orthorhombic α-phase and high-temperature cubic β-phase, which transform into each other by a diffusion-controlled phase transition mechanism at 670°C [1]. The crystalline structure of α-$SnWO_4$ is composed of distorted SnO_6 and WO_6 octahedra, which are joined by vertices into 2D-sheets held together by Sn^{2+} ions [2]. In high-temperature β-phase, which is metastable at room temperature, the structure is built up of slightly deformed WO_4 tetrahedra interconnected with four strongly distorted SnO_6 octahedra [2]. A distortion of metal-oxygen octahedra is caused by the second-order Jahn-Teller effect (SOJT) [3] and has been of interest in the present study.

We will report recent results of synchrotron radiation W L_3-edge x-ray absorption spectroscopy study of the local atomic structure in α-$SnWO_4$ and β-$SnWO_4$ phases and compare them with the results of the first-principles linear combination of atomic orbital (LCAO) calculations based on the hybrid exchange-correlation density functional (DFT)/Hartree-Fock (HF) scheme [4].

References

[1] W. Jeitschko and A. W. Sleight, Acta Cryst. B **28**, 3174 (1972); **30**, 2088 (1974)
[2] J. L. Solis, et al., Phys. Rev. B **57**, 13491 (1998)
[3] M.W. Stoltzfus, et al., Inorg. Chem. **46**, 3839 (2007)
[4] A. Kuzmin, A. Kalinko, and R.A. Evarestov, Acta Mater. **61**, 371 (2013)

ANALYSIS OF EXAFS DATA FROM COPPER TUNGSTATE BY REVERSE MONTE CARLO METHOD

Janis Timoshenko, Andris Anspoks, Aleksandr Kalinko, Alexei Kuzmin

Institute of Solid State Physics, University of Latvia, Latvia

e-mail: janis.timoshenko@gmail.com

Transition-metal tungstates are important materials with interesting optical, magnetic and ferroelectric properties, which make them suitable for many practical applications [1,2]. However, a relation between properties of tungstates and their structure and lattice dynamics is still debatable. X-ray absorption spectroscopy is a proper tool to address this question due to its local sensitivity and element selectivity. A complex structure of tungstates makes an interpretation of the extended x-ray absorption fine structure (EXAFS) using conventional methods very challenging. Therefore, in this study we analyze the Cu K- and W L_3- edges EXAFS data for $CuWO_4$ using the reverse Monte Carlo (RMC) method.

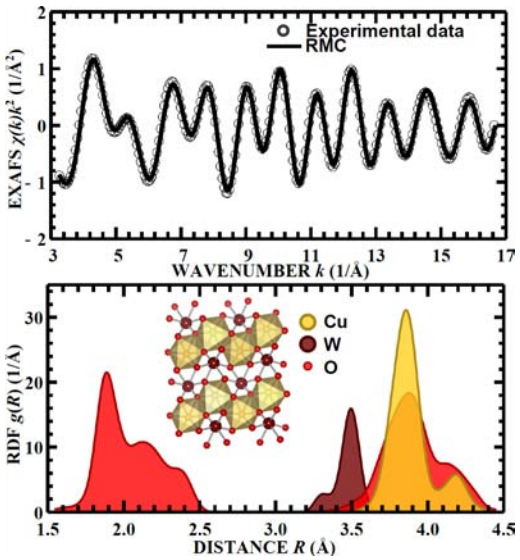

Fig.1. Upper panel: experimental (T =10 K) and calculated by the RMC method W L_3-edge EXAFS spectrum for $CuWO_4$. Lower panel: the radial distribution function (RDF) around tungsten, calculated from the RMC results.

RMC method is a numerical technique for reconstruction of 3D atomic structure of material by minimizing the difference between theoretically calculated and experimental structure-related data. Recently we have demonstrated that the RMC-EXAFS analysis can be successfully used to investigate relatively simple crystalline structures such as germanium and rhenium trioxide [3]. Here we apply the RMC technique to simultaneously interpret Cu K- and W L_3- edges EXAFS data for significantly more complex system as $CuWO_4$ with the aim to reconstruct the local environment around copper and tungsten atoms.

References

[1] R. Lacomba-Perales et al., EPL 83, 37002 (2008)

[2] A. Kuzmin, A. Kalinko, R.A. Evarestov, Acta Mater. 61, 371 (2013)

[3] J.Timoshenko, A. Kuzmin, J. Purans, Comp. Phys. Commun. 183, 1237 (2012)

LOCAL STRUCTURE STUDIES OF $SrTi^{16}O_3$ AND $SrTi^{18}O_3$

Andris Anspoks[1] (presenting author), Dimitry Bocharov[1], Juris Purans[1], Francesco Rocca[2], Anatolijs Sarakovskis[1], Vladimir Trepakov[3,4], Alexander Dejneka[3] and Mutsuru Itoh[5]

[1]Institute of Solid State Physics, University of Latvia, [2] IFN-CNR, Institute for Photonics and Nanotechnologies, Unit 'FBK-Photonics' of Trento, Povo (Trento), Italy, [3]Institute of Physics, AS CR, Prague, Czech Republic, [4]Ioffe Physical-Technical Institute RAS, St-Petersburg, Russia, [5] Tokyo Institute of Technology, Japan

e-mail of presenting author: andris.anspoks@cfi.lu.lv

$SrTiO_3$ is a model quantum paraelectric in which in the region of dominating quantum statistics the ferroelectric (FE) instability is inhibited due to nearly complete compensation of the harmonic contribution into FE soft mode frequeancy by the zero-point motion. The enhancement of atomic masses by the substitution of ^{18}O for ^{16}O decreases the zero-point atomic motion and low-T ferroelectricity in $SrTi^{18}O_3$ realizes [1,2].

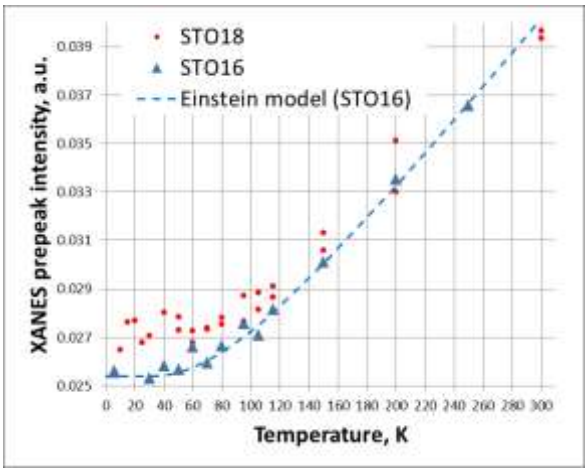

Fig.1 Thermal dependence of the XANES pre-peak intensity for STO18 (red dots) and STO16 (blue triangles) compared with the Einstein model.

We report on local structure studies of Ti in $SrTi^{16}O_3$ (STO16) and $SrTi^{18}O_3$ (STO18) by extended x-ray absorption fine structure (EXAFS) and x-ray absorption near edge structure (XANES) spectroscopy supplemented by optical second harmonic generation (SHG) at low temperature (6 – 300 K). By comparing EXAFS and XANES we have identified the isotopic effect which produces at $T < 50$ K a strong deviation of mean square relative displacement of Ti-O bonds from the Einstein model.

References

1. O. W. Kvyatkovskii, Sol. State. Comm. 117 (2001) 455

2. M. Itoh, R. Wang, Y. Inaguma, et.al., *Phys. Rev Letters*., 1999, No.17, Vol.82, 3540-3543.

ELECTROCHEMICAL *IN-SITU* XPS STUDIES OF NEGATIVELY POLARIZED MICROMESOPOROUS MOLYBDENIUM CARBIDE DERIVED CARBON DOUBLE LAYER CAPACITOR ELECTRODE

Arvo Tõnisoo[1], Jaanus Kruusma[2], Rainer Pärna[1], Arvo Kikas[1], Ergo Nõmmiste[1], Enn Lust[2].

[1] *Institute of Physics, University of Tartu, Riia 142, 51014 Tartu, Estonia,* [2] *Institute of Chemistry University of Tartu, Ravila 14A, 50411 Tartu, Estonia*

e-mail: arvo.tonisoo@ut.ee and/or jaanus.kruusma@ut.ee

Electrochemical double-layer capacitors (EDLC) are modern energy storage devices applied for high power pulse systems. Two- and three-electrode cells were prepared for the *in-situ* synchrotron radiation initiated X-ray photoelectron spectroscopy (XPS) investigations of the electrochemical faradic processes at the electrode surface. 1-ethyl-3-methylimidazolium tetrafluoroborate ($EMImBF_4$) as a room-temperature ionic liquid (RTIL) electrolyte and molybdenum carbide derived carbon ($C(Mo_2C)$) electrodes were used to construct a supercapacitor cell, where the region of electrodes polarizability was scaled up to $\Delta E = 3.5$ V (T = 25 °C).

While at cell potentials $\Delta E \geq 2.9$ V some faradic processes take place at the electrode | ionic liquid interface, XPS measurements were applied for the investigation of the elemental composition, and the binding energies (BE) of B, C, F and N 1s electrons under real applied EDLC cell potential conditions. Due to the very thin electrode | RTIL interface the changes in the monitored elements 1s electronic structure, located at the working electrode surface, were analysed.

XPS data for the negatively polarised micromesoporous $C(Mo_2C)$ electrode indicate, that the changes in C atom 1s BE spectra at $\Delta E > 3.0$ V are initiated by the reduction of the carbon atoms, located between two N atoms in the hetero-aromatic imidazolium ($EMIm^+$) ring. As a result of a faradic process, the aromaticity of the EMIm heterocyclic ring has been lost and in the XPS spectra the intensity of the signal generated by aliphatic C 1s photoelectrons increased.

At the cell potentials $\Delta E \geq 3.2$ V (measured for the negatively polarised $C(Mo_2C)$), a shoulder in the lower BE value side starts to form on the N 1s BE peak. The reduction of the intensity of the main N 1s BE peak (BE = 403.9 eV) accompanies with this. The appearance of this shoulder indicates noticeable changes in the electronic state of the nitrogen(s) 1s electrons in the $EMIm^+$ cation, probably as a result of the start of the $N\text{-}CH_3$ and/or $N\text{-}C_2H_5$ bonds cleavage.

ELECTRONIC STRUCTURE AND INNER SHELL EXCITED LUMINESCENCE IN GADOLINIUM MOLYBDATE CRYSTALS

Ilya A. Gofman (presenting author)[1], Vladimir A. Pustovarov[1], Mikhail V. Kuznetsov[2]

[1]*Institute of Physics and Technology, Ural Federal University, Yekaterinburg, Russia*

[2]*Institute of Solid State Chemistry, Ural Branch of RAS, Yekaterinburg, Russia*

e-mail: ilya.gofman87@gmail.com

Luminescence excitation in the inner shells was studied at BW3 beamline (HASYLAB, DESY), was used to study electronic structure of gadolinium molybdate $Gd_2(MoO_4)_3$ (GMO). It is characterized by the pronounced decays in luminescence excitation spectra in the regions of the core excitations of the atoms of the solid. X-ray photoelectron spectroscopy (XPS) and XUV excited luminescence were shown to be mutually complementary. While XPS reveals the electronic structure in the hole region and depicts its rearrangement after removing an electron from the shell, luminescence excitation spectra show the density of unfilled states, which can sometimes be correlated with the structure of the conduction band.

By comparing the results of XPS and inner shell excited luminescence, the position of Fermi level in GMO was estimated at E_F=2.7 eV above the top of the valence band. This also allowed for Gd 4f level location, which was calculated at E_{Gd4f}= -5.8 eV relative to the top of the valence band. This data was compared with appropriate estimations in the literature and found to be in general agreement with them.

Luminescence of Gd^{3+} ions was registered under inner-shell excitation in contrast to the VUV excitation range, where even at E_{exc}=25 eV no gadolinium emission was found. Moreover, intensive Gd^{3+} lines were registered in the excitation spectrum of intrinsic emission of GMO at T=8 K and in absorption spectra at T=300 K. There are several possible explanations, how Gd^{3+} emission could leave the crystal without reabsorption. The absorption might have intensity just enough for the lines to be registered but not enough to absorb all emission. However, our estimates show that excitation density at the BW3 beamline could be enough to excite a substantial part of Gd^{3+} ions in the small near-surface area of the crystal, leading to decrease of absorption in this spectral region. Some results of luminescent studies are presented more in detail in Ref. [1].

References

1. I.A.Gofman, V.A.Pustovarov, N.I.Lobachevskaya, V.D.Zhuravlev. *Radiation Measurements*, 2013 (in press).

SYNTHESIS AND PHOTOCATALYTIC PROPERTIES OF SULFUR MODIFIED TiO_2 NANOPORES AND NANOTUBES

R. Drunka[1], J. Grabis[1], A. Patmalnieks[2]

[1]*Riga Technical University Institute of Inorganic Chemistry,*

[2]*University of Latvia Institute of Microbiology and Biotechnology*

Email: reinis_drunka@inbox.lv

Titanium diokside is very promissing material for photocatalysts, degradation of organic compounds, splitting of water, for manifacturine self-cleaning materials and dye- sensitized solar cells. It is generally concluded that the photocatalytic activity depends on the specific surface area, degree of crystalization of the titania particles, phase composion and presence of dopants, witch promotes absorbtion of visible light.

Self-organized TiO_2 nanotube-layers were formed by electrochemical anodization of titania foil in a $(NH_4)_2SO_4$/HF electrolyte. Doped with sulfur nanopores were prepared by using method of micro arc oxidation in sulfur containing electrolyte. Doped with sulfur nanotubes were prepared by using their treatment at 380^{o}C in H_2S flow.

The catalytic activity was determined by degradation of MB solution under UV and visible light illumination. The photocatalytic activity of the prepared TiO_2 nanotubes and nanopores depends on the preparation conditions and the presence of sulfur. During illumination the degradation of MB reaches 85–90%. The prepared modifed photocatalysts have higher activity with respect to pure TiO_2 nanotubes. Sulfur doped nanotubes have higher activity with respect to sulfur doped nanopores.

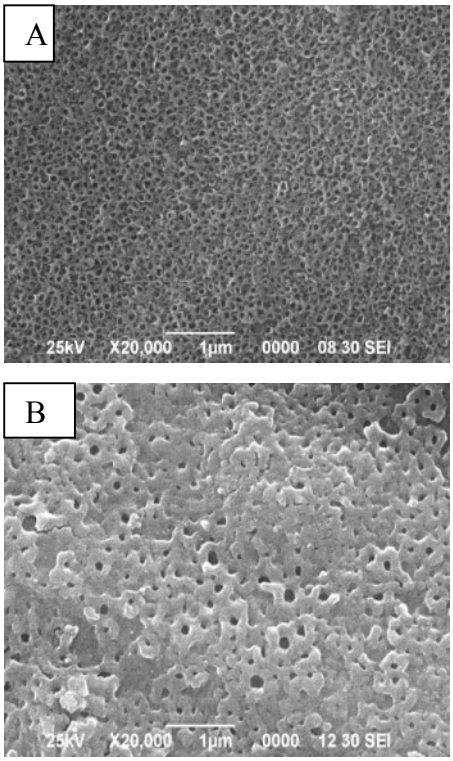

Fig.1 A) SEM micrograph of sulfur doped TiO_2 nanotubes B) SEM micrograph of sulfur doped TiO_2 nanopores.

References:

Jianfeng Li, Li Wan, Jiayou Feng *J. Mat. Proc. Tech* 2009, No.209, 762–766.

Drunka R., Grabis J., Jankoviča Dz., Patmalnieks A. *Latvian J.Chem.* 2011, No.3/4, 250-255.

SYNTHESIS OF NANOPARTICLES USING WET CHEMISTRY METHODS

Urmas Joost[1,2], Rando Saar[1,2], Kathriin Utt[1], Vambola Kisand[1,2]

[1] *Institute of Physics, University of Tartu, Estonia*

[2] *Estonian Nanotechnology Competence Centre, Tartu, Estonia*

e-mail of presenting author: urmas.joost@ut.ee

For huge amount of applications it is essential to control shape, structure and composition of nanoparticles (NP). One of the ways to obtain NP with controlled parameters is to perform synthesis of NP and then to separate NP with necessary parameters from synthesized material (using centrifugation and/or other methods). However, such a way has extremely small efficiency, since most of the synthesized material goes to the waste.

Another and challenging way is direct synthesis of NP with controlled morphology, size and crystalline structure in large quantities.

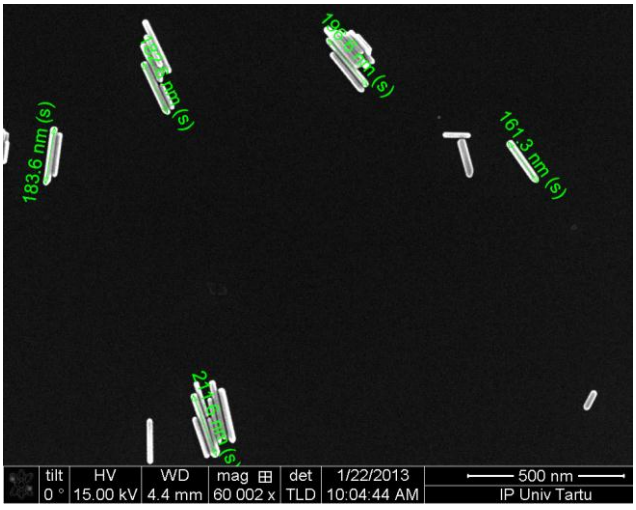

Fig. 1. SEM image of ZnO nanorods.

In this context wet chemistry methods are very interesting, since these methods offer the possibility to produce NP in large quantities [1]. Also wet chemistry methods allow to control the shape, size [1] and crystalline structure [2] of the synthesized particles.

As example of synthesis of NP with controlled morphology, we present ZnO nanorods with homogeneous parameters (see Fig.1). One of the potential applications for such ZnO nanorods is switchable IR reflecting “smart glass”.

References

1. O. Harnack, C. Pacholski, H. Weller, A.Yasuda, J. M. Wessels, *Nano Lett.*, 2003, No8, 1097-1101.
2. A. Vioux, *Chem. Mater.*, 1997, No 9, 2292-2299.

Static friction of CuO nanowires on substrates with varying roughness

Mikk Antsov[1,3], Boris Polyakov[1,2], Leonid Dorogin[1,3], Sergei Vlassov[1,3], Mikk Vahtrus[1], Sven Oras[1], Ilmar Kink[1,3], Rünno Lõhmus[1,3]

[1]Institute of Physics, University of Tartu, Estonia
[2]Institute of Solid State Physics, University of Latvia, Latvia
[3]Estonian Nanotechnology Competence Centre, Riia 142, 51014 Tartu, Estonia
e-mail: mikk.antsov@ut.ee

Nanowires (NWs) have many unique properties and are promising material class in many various applications as parts of MEMS/NEMS devices. From this point of view it is evident, that a greater understanding of adhesion and friction phenomena at the nanoscale is necessary to engineer improved high performance devices. The manifestation of friction laws at the nanoscale is completely different from their counterparts at the macroscale and the need to determine, how friction depends on the contact area is one of the most important issues in nanotribology.

We used nanomanipulation techniques, which have great potential in both fundamental and practical aspects of nanotribology research. Copper oxide NWs were deposited on silicon wafer coated with amorphous silicon and used as a basis to determine static friction force. The substrate was chemically etched to achieve different levels of surface roughness. Friction experiments were performed inside a scanning electron microscope (SEM), where the NW lying on the substrate was manipulated by atomic force microscope (AFM) tip attached to a nanomanipulation device. The NW was pushed by one end until complete displacement of NW was reached. The bending profile of NW before complete displacement was used to calculate the ultimate static friction force acting on the NW. As a result, different average ultimate static friction forces for the varying roughness were measured, meaning that a strong correlation between roughness and static friction exists. To estimate the real contact area and interfacial strength, a multiple elastic asperity model was implemented based on the Derjaguin–Muller–Toporov (DMT) contact mechanics.

References

[4] B. Polyakov, S. Vlassov, L. M. Dorogin, P.Kulis, I. Kink, R. Lõhmus, Surf. Sci. **606**, 1393-1399 (2012)

AB-INITIO STUDIES OF THE STRUCTURAL, ELECTRONIC, OPTICAL AND ELASTIC PROPERTIES OF $ZnWO_4$ AND $CdWO_4$ SINGLE CRYSTALS

M.G. Brik, V. Nagirnyi, M. Kirm

Institute of Physics, University of Tartu, Riia 142, Tartu 51014, Estonia

E-mail of presenting author: brik@fi.tartu.ee

Two important scintillator materials, cadmium and zinc tungstate ($CdWO_4$ and $ZnWO_4$), were studied in details using the plane wave based first principles calculations [1]. The theoretical results were in good agreement with the experimental X-ray photoelectron spectra and reflectivity data available in the literature (Fig.1), and allowed us to explain the main experimental features, including those induced by differences in the Cd 4d and Zn 3d states. Variations in the electron density distributions due to crystallographically non-equivalent oxygen positions were revealed. The influence of elevated hydrostatic pressure on the structural, electronic and elastic properties of both compounds was studied theoretically. It was shown that the band gaps in both tungstates, direct at ambient pressure, turn into indirect ones in the pressure range from 5 to 10 GPa. Linear approximations of all characteristic chemical bond lengths on pressure and the complete set of elastic tensor constants were calculated for both materials for the first time. We believe that the present approach successfully tested on two selected tungstates can be applied to other compounds to reveal "property-property" relations important for understanding fundamental material properties.

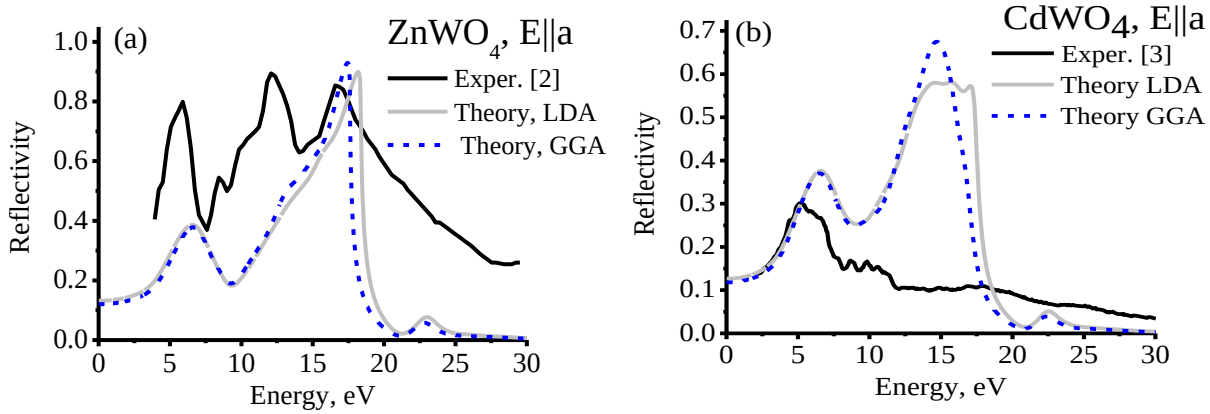

Fig.1. Comparison between the calculated (this work) and experimental [2, 3] reflectivity spectra for $ZnWO_4$ (a) and $CdWO_4$ (b) in the E||a polarization.

References

1. M.G. Brik, V. Nagirnyi, M. Kirm, *Mater. Chem. Phys.*, 2012, 134, 1113-1120; *Ibid.*, 2013, 137, 977-983.
2. V. Nagirnyi, E. Feldbach, L. Jönsson, M. Kirm, A. Kotlov, A. Lushchik,V.A. Nefedov, B.I. Zadneprovski, *Nucl. Instrum. Meth. Phys. Res. A*, 2002, 486, 395-398.
3. M. Fujita, M. Itoh, T. Katagiri, D. Iri, M. Kitaura, V.B. Mikhailik, *Phys. Rev. B*, 2008, 77, 155118.

A HYBRID COMPUTATIONAL-EXPERIMENTAL SPECTROSCOPIC ANALYSIS OF Eu^{3+} IONS DOPED IN HEXAGONAL WURTZITE ZnS

C.-G. Ma[1], R.M. Krsmanović[2], D. Jovanović[2], M.D. Dramičanin[2], M.G. Brik[1]

[1]*Institute of Physics, University of Tartu, Riia 142, Tartu 51014, Estonia*

[2]*Vinča Institute of Nuclear Sciences, University of Belgrade, P.O. Box 522, 11001 Belgrade, Serbia*

E-mail: chonggeng.ma@ut.ee

Rare earth-doped semiconductors, like ZnS:Eu^{3+}, have attracted significant interest because of their potential applications in electroluminescence. The luminescent properties of Eu^{3+} ions in cubic ZnS were investigated and the crystal-field (CF) analysis was performed in the cubic field approximation by Mao and Yuen *et al.* [1]. However, such a CF calculation is very rough and cannot be used to explain the three-fold splitting of the $^7F_1$ multiplet due to the site symmetry descent induced by the charge compensation effect. Therefore, in the present work, we propose a hybrid computational-experimental approach to reproduce the true coordination environment of Eu^{3+} impurities with charge compensating mechanism in its application to the spectroscopic analysis of Eu^{3+} ions in hexagonal wurtzite ZnS.

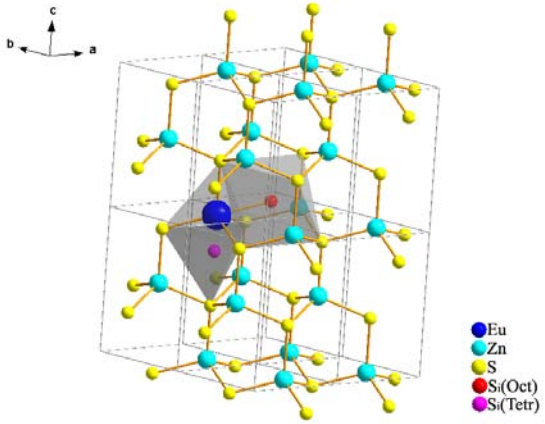

Fig.1 *Schematic representation of the local coordination structure of Eu^{3+} impurity ion in hexagonal wurtzite ZnS. The symbol "S_i" represents the introduced S^{2-} ion occupying the possible interstitial sites due to the charge compensation effect.*

The true coordination structure of Eu^{3+} ion in the studied host can be understood as four original sulfur ligands plus an addition charge compensating sulfur ion (termed as S_i(Oct), see Fig. 1). On the basis of the proposed local cluster of Eu^{3+} ion embedded in the host environment, the CF fitting calculations were carried out by employing the exchange charge model [2]. The reasonable standard root-mean-square deviation (~24 cm^{-1}) indicates good agreement between the experimental and theoretical results. To the best of our knowledge, this is the first time the luminescent properties of the Eu^{3+}-doped hexagonal wurtzite ZnS were reported along with the CF studies.

References:

1. S.-L. Hou, Y.-Y. Yuen, H.-B. Mao, J.-Q. Wang, Z.-Q. Zhu, J. Phys. D: Appl. Phys., 42 (2009) 215105(5pp).
2. B.Z. Malkin, K.K. Pukhov, S.K. Saikin, E.I. Baibekov, A.R. Zakirov, J. Mol. Struct. 838 (2007) 170.

THEORY AND MD SIMULATIONS OF INTRINSIC LOCALIZED MODES AND DEFECT FORMATION IN SOLIDS

V. Hizhnyakov[1], M. Haas[1], A. Pishtshev[1], A. Shelkan[1], M. Klopov[2]

[1]*Institute of Physics, University of Tartu, Riia 142, 51014 Tartu, Estonia*

[2]*Tallinn University of Technology, Ehitaja tee 5, 19086 Tallinn, Estonia*

e-mail: hizh@fi.tartu.ee

Modelling of nonlinear dynamics of solids presents a serious problem in material science. Here we present an analytical theory and a new MD method which include: 1) long-range linear interatomic forces described by means of phonon Greens functions and 2) short-range non-linear (anharmonic) forces considered explicitly [1,2]. The methods allow one to take into account the effects of the macroscopic field on the intrinsic localized modes (ILMs) in insulators. We also predicted that ILMs can cause the appearance of the linear local modes (LLMs) which cause modulation of their amplitudes [3]. Conducted by us calculations of intrinsic localized modes with the frequencies in the gap of the phonon spectrum in NaI are in good agreement with experiment. Recently the existence of LLMs has been also confirmed experimentally.

We also performed MD simulations of recoil processes in alkali halide crystals following the scattering of X-rays or neutrons taking into account the long-range linear interactions. At small energies (<10 eV) the recoil can induce ILMs and associated with them LLMs. In metals, as a result of the screening of the atomic interactions by free electrons, the odd anharmonicities may be essentially reduced. Due to this reduction the frequencies of ILMs and LLMs can be positioned above the phonon spectrum [4]. The MD simulations of the atomic motion in metallic Ni, Nb and Fe (iron) confirm this prediction. If the recoil energy exceeds several tens of eV vacancies and interstitials can be formed, in a strong dependence on the direction of the recoil momentum. In fcc lattices the recoil momentum in (110) direction can produce a vacancy and a crowdion while in case of recoil momentum in (100) and in (111) directions a bi-vacancy and a crowdion can be formed.

The research was supported by the project IUT2-27 and by the European Union through the European Regional Development Fund (project 3.2.0101.11-0029).

References

1. V. Hizhnyakov, A. Shelkan, M. Klopov, *Phys. Lett. A* **357** (2006) 393.

2. A. Shelkan, V. Hizhnyakov, M. Klopov, *Phys. Rev. B* **75** (2007) 134304.

3. V. Hizhnyakov et al, *Phys. Rev. B* **73** (2006) 224302.

4. M. Haas, et al, *Phys. Rev. B* **84** 280 (2011) 144303.

OXYGEN RELATED DEFECTS AND THEIR IMPACT ON UP-CONVERSION PROCESSES IN $NaLaF_4:Er^{3+}$

Anatolijs Sarakovskis, Guna Doke, Jurgis Grube, Maris Springis
Institute of Solid State Physics, University of Latvia
e-mail of presenting author: anatolijs.sarakovskis@cfi.lu.lv

Due to their relatively small effective phonon energy that suppresses the rate of nonradiative transitions numerous rare-earth doped fluoride and complex fluoride materials are considered to be promising materials for various up-conversion luminescence applications.

The fluorides however suffer from oxygen-related defects [1, 2] emerging if no precautions are taken during the synthesis of these materials. The presence of oxygen defects in fluorides may disturb the energy-transfer processes which are particularly important in the case of up-conversion because energy transfer is one of the most effective up-conversion mechanisms.

In this work $NaLaF_4$: Er^{3+} has been synthesized in different atmospheres (air and fluorine). The samples have been characterized by both stationary and time-resolved up-conversion luminescence spectra. Excitation spectra for the dominant luminescence bands have also been measured and analyzed. The analysis of the obtained data shows that the synthesis atmosphere is crucial for obtaining of high quality efficient up-conversion phosphor. Additionally it has been found that the prevailing mechanism of the "green" up-conversion luminescence of Er^{3+} in $NaLaF_4$ depends on the synthesis conditions: in the sample synthesized in fluorine atmosphere the dominant up-conversion mechanism is energy-transfer between Er^{3+}, while the up-conversion luminescence in the sample synthesized in the air atmosphere is governed by excited-state-absorption process.

The financial support of ERDF project Nr. 2010/0204/2DP/2.1.1.2.0/10/APIA/VIAA/010 and VPP IMIS is greatly acknowledged.

References

1. M. Karbowiak, A. Mech, A. Bednarkiewicz, W. Strek, *Journal of Alloys and Compounds*, 2004, 380, 321–326
2. A. Mech, M. Karbowiak ,L.Kepinski, A. Bednarkiewicz, W. Strek, *Journal of Alloys and Compounds*, 2004, 380, 315–320

LUMINESCENCE PROPERTIES OF HAFNIA AND ZIRCONIA NANOPOWDERS PREPARED BY SOLUTION COMBUSTION SYNTHESIS

Eduard Aleksanyan[1,2], Marco Kirm[1], Eduard Feldbach[1], Vitali Nagirnyi[1], Aarne Maaroos[1], Hugo Mändar[1]

[1]*Institute of Physics, University of Tartu, Estonia,*

[2]*A.Alikhanyan National Scientific Laboratory, Yerevan, Armenia*

e-mail: aeduard@fi.tartu.ee

Hafnia and zirconia are famous materials for such properties as high thermo-mechanical resistance, low optical losses and transparency in wide spectral range from UV to near IR and are suitable for various applications including scintillators [1], gas sensors [2,3] and protective coatings. Previous studies on HfO_2 and ZrO_2 thin films showed that intense emission of self-trapped excitons (STEs) at 4.2-4.4 eV can be observed at low temperatures with potential for scintillators [1]. Nano-powders of the same compounds have some advantages over single crystals and thin films because of their easy fabrication and lower cost. In [2,3], a low-energy emission was revealed near 2-3 eV in ZrO_2 nano-powders and attributed to oxygen vacancies and related defects. Less attention was paid to the excitonic emission and its behavior at low temperatures. From this point of view the study of spectroscopic properties of nano-sized hafnia and zirconia is of great importance.

The samples studied were prepared by solution combustion synthesis using different fuels (urea or glycine). Annealing of samples at 700°C for 2 hours in air was performed to crystallize powders. XRD measurements showed that as-synthesized hafnia was amorphous, while annealing resulted in a monoclinic structure. Zirconia powders were a mixture of tetragonal and monoclinic phases. According to the SEM study (in agreement with XRD) the average particle size varied from 4 to 20 nm. Synchrotron radiation at SUPERLUMI beamline (HASYLAB at DESY) along with laboratory setups (cathodo- and photoluminescence) at our home institute were used in luminescence experiments on hafnia and zirconia nanopowders at T=8-300 K.

Along with the STE emission at 4.4 eV the defect emission bands in visible range near 3 eV were observed at 8 K in the annealed hafnia. Zirconia possessed stronger luminescence bands near 2.6-3.2 eV range due to defects. Excitation and relaxation mechanisms for both excitonic and defect emissions in nano-size hafnia and zirconia powders will be discussed.

References

1. M. Kirm, J. Aarik, M. Jürgens, I. Sildos, *NIM A*, 2005, 537, 251-255.

2. L. Grigorjeva, D. Millers, A. Kalinko, V . Pankratov, K. Smits, *J of Eur. Ceramic Society***,** 2009, 29, 255-259.

3. S. Mochizuki, T. Saito, *Physica B*, 2012, 407, 2911-2914.

DEVELOPMENT OF EFFECTIVE ATOMIC LAYER DEPOSITED CORROSION RESISTANT COATINGS FOR AL 2024-T3

Maido Merisalu[1,2], Lauri Aarik[1], Jekaterina Kozlova[1], Jelena Asari[1], Leonard Matisen[1], Väino Sammelselg[1,2]

[1]*Institute of Physics, University of Tartu, Estonia* [2]*Institute of Chemistry, University of Tartu, Estonia*

e-mail: maido.merisalu@ut.ee

In this study a new excellent thin corrosion resistant coating for Al 2024-T3 is demonstrated. The coating is obtained by first applying anodizing process on aluminium alloy substrates and then sealing all open pores by atomic layer deposited Al_2O_3/TiO_2 nanolaminates with the thickness range of 100 nm. Previously the laminates alone were used for protecting surfaces of steel [1].Solutions used in conventional anodizing processes were tested in electrochemical pretreatments of Al 2024-T3 samples for better compatibility with ALD films. The surface of bare Al alloy samples and coatings prepared on them were characterized with HR-SEM, having also FIB, X-ray microanalysis using EDXS spectrometer, and with XPS. Corrosion testing was done with cyclic voltammetry, electrochemical impedance spectroscopy and by immersion in neutral salt solution following microscopical studies. ALD laminate uniformly covered the alloy surface and sealed the pores and defects in it, thus, greatly improving the corrosion resistance of the anodized samples compared to unsealed anodized ones.

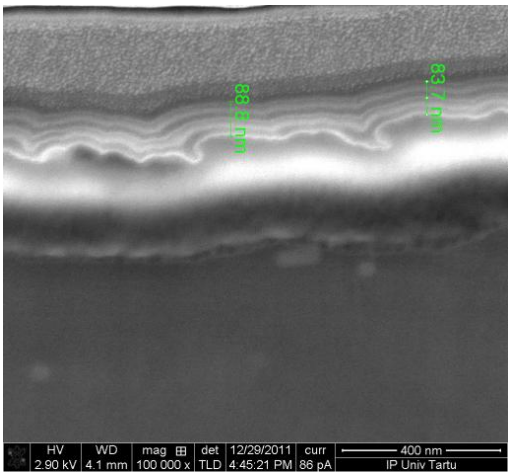

Fig.1 FIB made cross section SEM image of sub-micrometer coating on Al 2024-T3.

Reference

[1] Harkonen, E ; Diaz, B ; Swiatowska, J ; Maurice, V ; Seyeux, A ; Vehkamaki, M ; Sajavaara, T [3]; Fenker, M ; Marcus, P [2]; Ritala, M . J. Elechtrochem. Soc. 158 (2011) C369-C378.

HEAT TREATMENT EFFECTS IN CASE OF METAL CONTAINING TITANIA SOL-GEL FILMS

Vambola Kisand[1,2], Urmas Joost[1,2], Rainer Pärna[1,2], Ilmar Kink[1,2]

[1] *Institute of Physics, University of Tartu, Estonia*

[2] *Estonian Nanotechnology Competence Centre, Tartu, Estonia*

e-mail of presenting author: vambola.kisand@ut.ee

Titania (TiO_2) has attracted attention as a perspective material for many advanced applications using sunlight. Unfortunately, TiO_2 absorbs only a fraction of sunlight, which reduces efficiency of its use in solar based applications. One way proposed to enhance the absorption properties of titania is to dope it with cations [1]. The key idea here is that the added impurities modify the electronic structure, which would effectively shrink the band gap.

One method which allows introducing impurities in large concentrations into the samples is sol-gel method. This method includes preparation of precursor films, aging and heat treatment. It is well known that the morphological and structural properties of pure titania films depend strongly on the heating temperature.

However, less is known about influence of heating temperature on the metal impurities containing TiO_2 samples [2-4]. Exactly this is in focus of the present work: influence of the heating temperature on the crystallite growth, crystal structure, formation of impurity rich regions etc. In the present work it is used nickel, cobalt and copper impurities, since these metals are reported in the literature as promising impurities for TiO_2 solar based applications.

References

1. O. Carp, C. L. Huisman, A. Reller, *Prog. Solid State Chem*. **32**, 33-177 (2004).
2. U. Joost, R. Pärna, M. Lembinen, K. Utt, I. Kink, M. Visnapuu, V. Kisand, *Phys. Status Solidi (A)*, (2013, in press), DOI 10.1002/pssa.201228751
3. R. Pärna, U. Joost, E. Nõmmiste, T. Käämbre, A. Kikas, I. Kuusik, M. Hirsimäki, I. Kink, and V. Kisand, *Phys. Status Solidi (A)*, (2012), DOI 10.1002/pssa.201127641
4. R.Pärna, U. Joost, E. Nõmmiste, T. Käämbre, A. Kikas, I. Kuusik, M. Hirsimäki, I. Kink, and V. Kisand, *Applied Surface Science*, **257** (2011) 6897, DOI: 10.1016/j.apsusc.2011.03.026.

ELECTROMAGNETIC PROPERTIES OF INTERCONNECTS IN NANODEVICES BASED ON CNT, GNR AND GRAPHENE AEROGELS

Yuri Shunin[1,2] (presenting author), Yuri Zhukovskii[1], Victor Gopejenko[2], Nataly Burlutskaya[2], Tamara Lobanova-Shunina[2] and Stefano Bellucci[3]

[1]*Institute of Solid State Physics, University of Latvia, Riga, Latvia* [2]*Information Systems Management Institute, Riga, Latvia,* [3]*INFN - Laboratori Nazionali di Frascati, Frascati-Rome, Italy*

e-mail of presenting author: shunin@isma.lv

Electromagnetic properties of carbon-based nanosystems are essential for creation of various nanoelectronic devices. We pay main attention to CNT, graphene nanoribbons and nanofibers (*i.e.*, GNR and GNF) and graphene-based aerogels (GBA), consisting of graphene nanoflakes, metallic nanowires and nanopores, as the basis for the high-speed nanoelectronics and potential nanosensors. Special attention is paid to fundamental properties of CNTs, GNRs as well as various CNT-Me, GNR-Me, CNT-graphene interconnects. 3D GBA nanosystems are considered as complicated system of basic nanocarbon interconnected elements. The developed cluster approach based on the multiple scattering theory formalism as well as effective medium approximation is used for nanosized systems modeling including calculations of dispersion law, electronic density of states, conductivity, *etc*. [1]. Technological interest to contacts of CNTs or GNRs with other conducting elements in nanocircuits, FET-type nanodevices and GBA is the reason to estimate various interconnect resistances, which depend on chirality effects in nanotubes and nanoribbons. Simulations of electromagnetic properties in interconnects for the evaluation of integral resistances, capacitances and impedances of various topologies of nanodevices (1D, 2D and 3D), including frequency properties (GHz&THz), have been performed. Parametric calculations of *dc*- and *ac*-conductivities for CNT- and GNR-based elements (pure and doped) with various chiralities, which provide important information for nanotechnology, are principal for nanosensoring devices. On the other hand, both CNT-Me and GNR-Me based nanostructures can be considered as perspective nanosensor structures, due to the active dangling atomic bonds within the interconnect area [1,2].

References

1. Yu. N. Shunin, Yu. F. Zhukovskii, V. I. Gopejenko, N. Burlutskaya, S. Bellucci. In: *Nanodevices and Nanomaterials for Ecological Security*, Yu. Shunin and A. Kiv, Eds. *Series: Nato Science for Peace Series B - Physics and Biophysics*, Springer Verlag, 2012, 237-262

2. Yu. N. Shunin, Yu. F. Zhukovskii, V. I. Gopejenko, N. Burlutskaya, T. Lobanova-Shunina and S. Bellucci, *Journal of Nanophotonics* , 2012, Vol. 6, No.1, 061706-1-16. doi:10.1117/1.JNP.6.061706.

CELLULAR AUTOMATA MODELLING OF VOID LATICE SELF-ORGANIZATION IN CAF_2 UNDER IRRADIATION

G. Zvejnieks, P. Merzlyakov, V.N. Kuzovkov and E.A. Kotomin
Institute of Solid State Physics, University of Latvia,
e-mail: guntars@latnet.lv

Irradiation of many insulating solids with energetic particles may lead to a formation of ordered long-range structures, e.g., void lattices [1]. They arise in open dissipative systems far from equilibrium as a result of self-organization process. Despite numerous experiments, the void lattice formation in CaF_2 under electron irradiation still possesses open questions regarding the microscopic processes that govern the self-organization phenomenon [2].

In this work we propose a microscopic model that allows us to obtain a macroscopic ordering of void lattice in accordance with experimental data. Electron irradiation leaves Ca atoms intact. Therefore we model only F-atom sublattice, where irradiation can produce uncorrelated F-atom vacancy and interstitial pairs. Interstitial and vacancy recombination is allowed when they are in nearest neighbor (NN) positions. Further slow vacancy diffusion is accompanied with their NN attractive interaction leading to the formation of vacancy clusters, i.e., voids. The driving forces for the long-range void ordering are interstitial planes. They are formed from quickly diffusing interstitial atoms that experience three atoms in a line (trio) attractive interaction.

Our cellular automata simulations demonstrate that global void lattice self-organization occurs in a narrow parameter interval where void cluster and interstitial formed plane average spacing is balanced. Moreover we can follow the kinetics of ordered void lattice emergence starting from initial unordered stage according to experimental data.

G.Z. and P.M. greatly acknowledge the financial support of ERAF project 2010/0204/2DP/2.1.1.2.0/10/APIA/VIAA/010.

References

1. T.H. Ding, S. Zhu, and L.M. Wang, Microsc. Microanal. 11, 2064 (2005).
2. M. Stoneham, Rep. Prog. Phys. 70, 1055 (2007)

TERAHERTZ SPECTROSCOPY OF THE CYCLOID IN MULTIFERROIC $BiFeO_3$ IN HIGH MAGNETIC FIELDS

U. Nagel (presenting author) [1], T. Katuwal [1], H. Engelkamp [2], D. Talbayev [3], Hee Taek Yi [4], S.-W. Cheong [4], T. Rõõm [1]

[1] *National Institute of Chemical Physics and Biophysics, Akadeemia tee 23, 12618 Tallinn,*

[2] *High Field Magnet Laboratory, Radboud University Nijmegen, The Netherlands,*

[3] *Department of Physics, Tulane University, 5032 Percival Stern Hall, New Orleans,*

[4] *Rutgers Center for Emergent Materials, Rutgers University, Piscataway, USA*

e-mail of presenting author: urmas.nagel@kbfi.ee

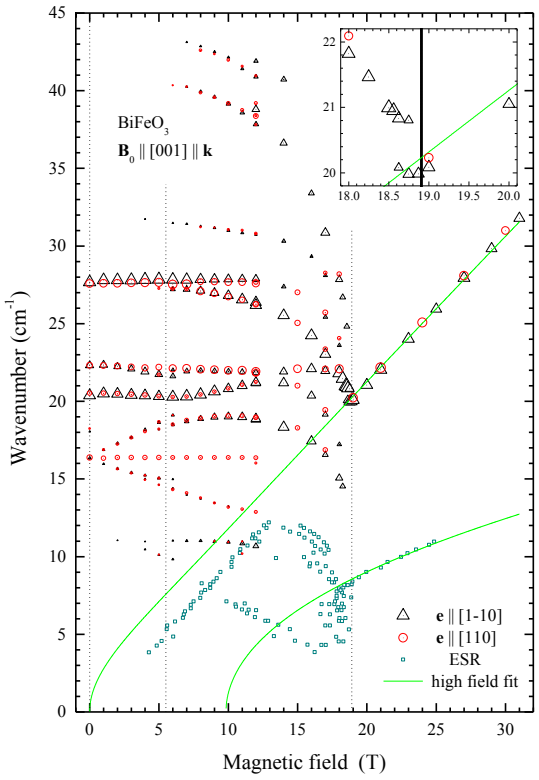

Magnetic field dependence of magnon modes in the THz spectrum of $BiFeO_3$ at low temperature.The areas of triangles and circles is proportional to the absorption line areas. Vertical dashed lines mark the metamagnetic transition at B_c = 18.8 T and another critical field B_a = 5.5 T. Solid lines are the fit of our data and ESR data [1] (squares) above 19T.

$BiFeO_3$ is both antiferromagnetic and ferroelectric with high Néel and Curie temperatures, about 640K and 110 K, respectively. In low magnetic field Fe^{3+} spins order cycloidally, inducing an additional electric polarization, which interacts with the ferroelectric polarization of the lattice and produces a magneto-electric term in the total energy. We have measured the magnetic field dependence of infrared active magnon modes in an untwinned $BiFeO_3$ single crystal at 4K. The magnon modes soften close to the critical field of about 18.8T along the [001] cubic axis, where the cycloid is destroyed and the low field magnon modes disappear. A new strong mode with linear magnetic field dependence appears above 19T and persists at least up to 31T. This allows us to assign all the low field modes as excitations of the cycloid.

References

1. B. Ruette, S. Zvyagin, A. P. Pyatakov, A. Bush, J. F. Li, V. I. Belotelov, A. K. Zvezdin, and D. Viehland, Phys. Rev. B 69, 064114 (2004).

Spin waves and directional dichroism in the multiferroic $Ba_2CoGe_2O_7$ probed by THz spectroscopy

Toomas Rõõm[1] , U.Nagel[1], K.Penc[2], J. Romhanyi[2], D.Szaller[3], S.Bordacs[3], I.Kezsmarki[3], L.Demko[3], A.Antal[3], T.Feher[3], A.Janossy[3], H.Engelkamp[4], N.Kida[5], H.Murakawa[5], Y.Onose[5], R.Shimano[5], S.Miyahara[5], N.Furukawa[5], Y.Tokura[5]

[1]NICPB, Tallinn, Estonia, [2]Institute for Solid State Physics and Optics, Hungarian Academy of Sciences, Budapest, [3]Department of Physics, Budapest University of Technology and Economics, [4]Institute for Molecules and Materials, Radboud University and High Field Magnet Laboratory, Nijmegen, [5]Multiferroics Project, ERATO, University of Tokyo, Japan

e-mail: toomas.room@kbfi.ee

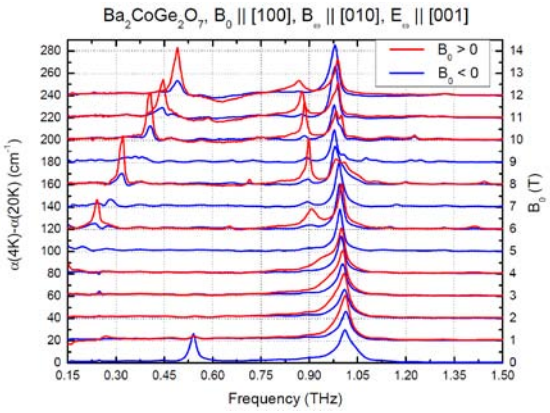

Fig.1 Dependence of THz light absorption on the direction of applied field B_0 relative to the light propagation, **k**||[100].

$Ba_2CoGe_2O_7$ is a multiferroic where there is an entanglement between the magnetic moments of Co and the electronic charge on Co-O bond. By applying external magnetic field this square-lattice antiferromagnet can be transformed to a chiral form, evidenced by large optical activity when the light is in resonance with spin excitations at sub-terahertz frequencies. We found that the directional dichroism, the absorption difference for the light beams propagating parallel and anti-parallel to the applied magnetic field, has an exceptionally large amplitude close to 100% and persists to fields up to 30T. The chirality-induced directional dichroism is ascribed to the magnetoelectric nature of spin excitations as they interact with both, the electric and magnetic components of light [1]. In the ESR and THz absorption spectra we found several spin excitations beyond the two conventional magnon modes expected for such a two-sublattice antiferromagnet. A multiboson spin-wave theory describes these unconventional modes, including spin-stretching modes, characterized by an oscillating magnetic dipole and quadrupole moment. The lack of inversion symmetry allows each mode to become electric dipole active. We observe a spin flop at 16 T, that is consistent with our theoretical calculations[2].

References

1. S. Bordacs et al., Nature Physics **8**, 734 (2012)
2. K. Penc et al., Phys. Rev. Lett. **108**, 257203 (2012)

RESISTIVE SWITCHING VS. CHARGE TRAPPING IN TiO_2-BASED METAL-INSULATOR-METAL STRUCTURES WITH Al_2O_3 BARRIER

Boris Hudec[1] (presenting author), M. Ťapajna[1], A. Paskaleva[2], A. Rosová[1], E. Dobročka[1], J. Dérer[1], and K. Fröhlich[1]

[1]*Institute of Electrical Engineering, SAS, Dúbravská cesta 9, 841 04 Bratislava, Slovakia,*

[2]*Institute of Solid State Physics, BAS, 72 Tzarigradsko Chaussee, 1784 Sofia, Bulgaria*

e-mail of presenting author: boris.hudec@savba.sk

TiO_2-based MIM structures and their application in future non-volatile Redox resistive RAMs were subject of intense studies in last period. Incorporation of thin Al_2O_3 barrier was recently proposed [1] to reduce high operating currents of such structures. In this contribution we investigate resistive switching properties of TiO_2 thin films equipped with thin Al_2O_3 barriers of different thickness prepared by PEALD sandwiched in between of Pt electrodes. As the Al-oxide barrier gets thinner, the hysteretic resistive switching behaviour changes from rather unpredictable, scattered switching loops typical for Al-oxide to rather uniform hysteretic I-V loops (left Fig.) with improved controllability and promising endurance characteristics (right Fig.). We attribute this transition to charge trapping phenomenon and we investigate its effect on the switching properties with respect to their potential application in non-volatile ReRAMs.

References

1. M.J. Kim et al., IEDM 2010, 19.3.1.

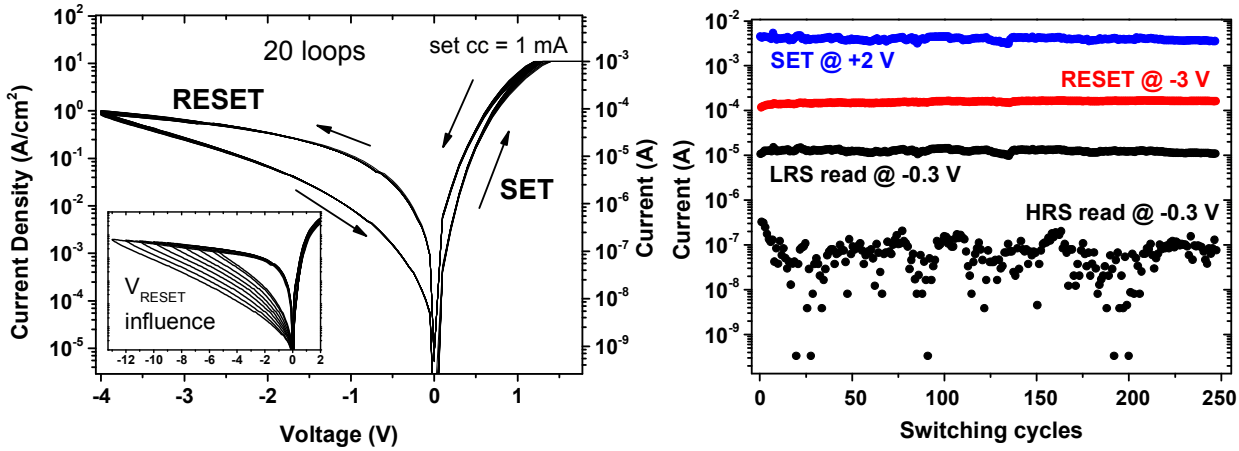

Left fig.: Twenty hysteretic resistive switching loops with the reset voltage influence (inset). Right fig: Endurance characteristics obtained by SET-read-RESET-read pulsing scheme.

GRAVIMETRIC AND SPECTROSCOPIC STUDIES ON REVERSIBLE HYDROGEN ADSORPTION ON NANOPOROUS CLINOPTILOLITE

Liga Grinberga, Peteris Lesnicenoks, Andris Sivars, Janis Kleperis
Institute of solid State Physics, University of Latvia,
kleperis@latnet.lv

Detailed understanding of hydrogen-solid interactions is important not only for practical applications in hydrogen storage tanks but also for fundamental research. Clinoptilolite is one of 40 naturally occurring zeolite frameworks currently known. However there are almost 3 million theoretically possible structural combinations reported of synthetic zeolites. Economical aspect is a good reason to seek simple, common and cheap materials for hydrogen storage; therefore natural materials are especially favourable.

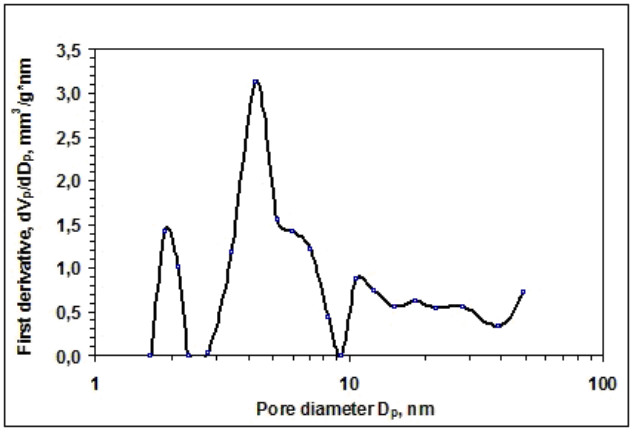

Fig.1 Pore volume of clinoptilolite.

There are several theories about hydrogen bonding process with zeolite, such as Langmuir equations, that explains hydrogen adsorption basic filling of pores, and spillover effect, where catalyst presence allows manipulating hydrogen gas as well as atomic hydrogen; nevertheless the results are not always consistent. That is concluded in experiments using different methods to precise the mechanism of adsorption and measuring efficiency.

In our work the various experiments using natural zeolite (clinoptilolite) are performed - Mass spectroscopy, volumetric and thermogravimetric sorption experiment of clinoptilolite are performed. FTIR spectroscopic studies are used to confirm adsorption of hydrogen molecules in the vicinity of light metal ions introduced in zeolite by repeated ion-exchange procedures. Effects of air humidity and temperature on hydrogen adsorption efficiency are investigated.

Acknowledgement: Authors acknowledge ERDF project Nr. 2010/0188/2DP/2.1.1.1.0/10/APIA/VIAA/031 for financial support of scientific experiments and ERDF project Nr. 2010/0204/2DP/2.1.1.2.0/10/APIA/VIAA/010 for financial support of travel expenses.

MODELING OF Y-O PRECIPITATION IN α-Fe AND γ-Fe LATTICES

Yuri F. Zhukovskii[1], Aleksejs Gopejenko[1], Yuri A. Mastrikov[1], Eugene A. Kotomin[1], Pavel V. Vladimirov[2], Anton Möslang[2]

[1]*Institute of Solid State Physics, University of Latvia,*

[2]*Institut für Angewandte Materialien, Karlsruhe Institut für Technologie, Germany*

e-mail: quantzh@latnet.lv

Reduced activation ferritic-martensitic steels (RAFM) strengthened by yttria precipitates are promising structure materials for future fission and fusion reactors. Implementation of these materials allows increasing the operation temperature of blanket structures by ~100°C. The mechanism and kinetics of Y_2O_3 nanoparticle formation in the steel matrix are required to be clarified to develop the oxide dispersed strengthened (ODS) steels. A number of Y and O atoms are decomposed from yttria clusters in Fe matrix with concentrations above their equilibrium solubility.

Ab initio calculations performed using the method of plane-wave density functional theory (PW-DFT) within the generalized gradient approximation (GGA) evidently show that the iron vacancies influence on a bonding between the impurity defects (O and Y atoms) in lattices of *bcc* and *fcc* iron phases existing at operation temperatures.

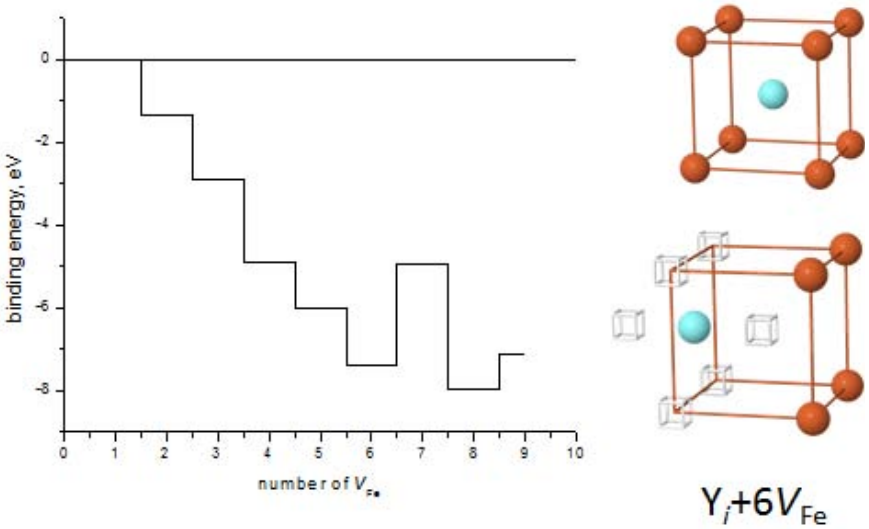

Fig.1 Energetic stabilization of Y atom surrounded by different number of V_{Fe} vacancies in bcc iron lattice

If oxygen impurity atoms can reside in both vacancies (V_{Fe}) and lattice interstitials of α- and γ-iron phases, with comparatively small migration barrier inside the lattice (1.1 eV in the case of interstitial transition), the yttrium atoms can substitute iron atoms only and Y migration is possible in presence of V_{Fe} vacancies [1]. Stabilization of solute Y atoms by vacancies increases the binding energy between them up to six nearest V_{Fe} neighbors (Fig. 1) and reduces the migration barrier.

References

1. A. Gopejenko, Yu.F. Zhukovskii, P.V. Vladimirov, E.A. Kotomin, A. Möslang, *J. Nucl. Mater.*, 2010, **406**, 345-350.

PREDICTION OF STRUCTURAL STABILITY OF COMPLEX PEROVSKITES FOR SOLID OXIDE FUEL CELLS FROM FIRST PRINCIPLES

E.A. Kotomin[1,2], M.M. Kuklja[3], Yu. A. Mastrikov[2], O.Sharia[3], D. Fuks[4], J. Maier[1]

[1]Max Planck Institute for Solid State Research, Heisenbergstr., 1, Stuttgart, Germany
[2]Institute for Solid State Physics, University of Latvia, Kengaraga str. 8,, Latvia
[3]Materials Science and Engineering Department, University of Maryland, MD, USA
[4]Dept Materials Engineering, Ben Gurion University of the Negev, Beer Sheva, Israel

Among advanced materials for clean energy, non-stoichiometric $Ba_xSr_{1-x}Co_{1-y}Fe_yO_{3-\delta}$ (BSCF) and $La_xSr_{1-x}Co_{1-y}Fe_yO_{3-\delta}$ (LSCF) are considered as promising materials for cathodes in solid oxide fuel cells (SOFC) and oxygen permeation membranes [1,2]. BSCF exhibits the best oxygen exchange performance amongst similar materials, mixed ionic and electronic conductivity, high oxygen vacancy concentration, and low diffusion activation barrier, which largely define the oxygen reduction kinetics. However, it exhibits a trend to decompose at low temperatures into a mixture of cubic and hexagonal perovskite phases, which strongly affects its use.

To understand the mechanism(s) of this undesirable process, the first principles quantum mechanical calculations of BSCF and LSCF crystals with different non-stoichiometry were performed and possible decomposition scenarios were studied. It is shown [3] that formation energies of oxygen vacancies in the cubic and hexagonal phases of BSCF differ considerably and also behave in quite different ways depending on non-stoichiometry; in fact, it is the oxygen non-stoichiometry that makes the cubic phase more stable than the hexagonal phase. In comparison, LSCF is shown to be much more stable with respect to both the phase transformation and phase decomposition. The first principles calculations are accompanied by a thermodynamic analysis of the conditions under which a cubic phase is stable, in a good agreement with experimental data.

This work is supported by the GIF project # 1-1025-5-10/2009, EC COST project CM 1104, and US National Science Foundation (NSF, grant CMMI-1132451).

[1] L. Wang et al, J. Mater.Res. 27, 2000 (2012); R. Merkle et al, JECS **159**, B219 (2012)
M.M. Kukla et al, Phys Chem Chem Phys (a review article), 2013 in press
[2] Yu.A. Mastrikov et al, PCCP, **15**, 911 (2013)
[3] M.M. Kukla et al, J Phys Chem **C 116**, 18605 (2012).

REDOX BEHAVIOUR OF SULPHUR AT NI/GDC SOFC ANODE AT MID- AND LOW-RANGE TEMPERATURES: S K-EDGE XANES STUDY

G. Nurk[a], T. Huthwelker[c], A. Braun[b], Chr. Ludwig[d],[e], E. Lust[a] and R. P. W. J. Struis[d]

a Institute of Chemistry, University of Tartu, 14A Ravila Str., 50411 Tartu, Estonia

b Laboratory for High Performance Ceramics, Empa-Swiss Federal Laboratories for Materials Science and Technology, CH-8600 Dübendorf, Switzerland

c Swiss Light Source (SLS) & Laboratory for Catalysis and Sustainable Chemistry (LSK), Paul Scherrer Institut, CH-5232 Villigen PSI, Switzerland

d Laboratory for Bioenergy and Catalysis (LBK), Paul Scherrer Institut, CH-5232 Villigen PSI, Switzerland

e École Polytechnique Fédérale de Lausanne (EPFL-ENAC-IIE), 1015 Lausanne, Switzerland

e-mail of presenting author: gunnar.nurk@ut.ee

Sulphur poisoning of nickel–cermet solid oxide fuel cell (SOFC) anode catalysts working at mid- and low temperatures is widely studied but not completely understood. Here we demonstrate novel experimental approach to obtain Sulphur K-shell X-ray absorption near edge spectroscopic information at operando conditions, thus, at working fuel cell with the flux of O^{2-} from cathode to anode. Spectroscopic information was collected at different temperatures from T=550°C to 250 °C, at 5 ppm H_2S/H_2 reacting with the Ni-gadolinium doped ceria anode. Several sulphur species in different oxidation states (6+, 4+, 0, -2) were observed. According sulphur speciation analysis, the species could either relate to $–SO_4^{2-}$ or SO_3(g), $–SO_3^{2-}$ or SO_2(g), S_2(g) or surface-adsorbed S atoms, and, Ni or Ce sulphides, respectively. The appearance of different sulphur oxidation states as a function of temperature was analysed and compared with thermodynamic calculations. Deviations between experimental data and calculations were observed. Differences are most likely caused by fact that calculations are equilibrial but at working fuel cell steady state conditions are prevailing. Differences between stoichiometric CeO_2 used in calculations and partially reduced $Ce_{0.9}Gd_{0.1}O_{2-\delta}$ in the working fuel cell could also cause deviations from theoretical preictions.

HIGH FREQUENCY NOISE IN EPITAXIAL GRAPHENE ON SiC

L. Ardaravičius[1], J. Liberis[1], A. Matulionis[1],
S. Shivaraman[2], L. F. Eastman[2], M. G. Spencer[2]
[1]*Fluctuation Research Laboratory, Center for Physical Sciences and Technology, Lithuania,* [2]*Cornell University, USA*
e-mail of presenting author: : linas.ardaravicius@ftmc.lt

Graphene, a single layer of carbon atoms arranged in a honeycomb lattice, seems to be a very promising material. The combination of perfect charge-carrier confinement with very high carrier mobility in a two-dimensional structure makes it an ideal material for highly scaled electronics [1, 2]. Various methods such as mechanical exfoliation, laser irradiation, chemical vapor deposition, and thermal decomposition (sublimation) are used for graphene preparation/growth.

Microwave noise technique is applied to study in-plane electronic properties of epitaxial graphene layers grown on semi-insulating SiC in a cold wall ultra high vacuum chamber by thermal decomposition method. The layers were subjected to high electric field applied in the plain. The noise spectrum is measured in the field direction at room temperature. While an $1/f^{\alpha}$-type dependence is found in 200 MHz – 2.5 GHz band, a shot noise contribution dominates at 10 GHz. The high-frequency noise of graphene on silicon carbide is compared with the noise of graphene on sapphire grown by chemical vapor deposition [3]: the $1/f$ noise is stronger in the graphene layers on silicon carbide. The shot noise is possibly associated with electron jumps across the potential barriers located between the graphene crystallite domains.

References

1. T. Palacios, *Nature Nanotechnology*, 2011, **6**, No. 8, 464-465.
2. Y. Wu, K. A. Jenkins, A. Valdes-Garcia, D. B. Farmer, Y. Zhu, A. A. Bol, C. Dimitrakopoulos, W. Zhu, F. Xia, P. Avouris and Yu-Ming Lin, *Nano Letters*, 2012, **12,** No. 6, 3062 -3067.
3. J. Hwang, M. Kim, D. Campbell, H. A. Alsalman, J. Y. Kwak, S. Shivaraman, A. R. Woll, A. K. Singh, R. G. Hennig, S. Gorantla, M. H. Rummeli, and M. G. Spencer, *ACS Nano*, 2013, **7**, No. 1, 385-395.

THE INFLUENCE OF FINITE-SIZE EFFECT ON THE ELECTROMAGNETIC RESPONSE OF CARBON NANOTUBES

Mikhail Shuba, Alexander Melnikov
Institute for Nuclear Problems, Belarus State University, Minsk, Belarus
e-mail: mikhail.shuba@gmail.com

Multiwall carbon nanotube (MWCNT) based composites are under intensive investigations due to their remarkable electromagnetic (EM) shielding properties realizing at small volume fraction of the inclusions [1]. Nowadays the main efforts in the development of composite production technology are directed to increase effective permittivity of MWCNTs-based composite by means of homogenous nanotube dispersion in the dielectric matrix. However, much less attention has been paid to the possibility of EM response enhancement of MWCNT-based composite by appropriate choice of nanotube geometry - length and diameter.

In the present report the electromagnetic response of finite length multiwall carbon nanotubes was theoretically studied in the terahertz and sub-terahertz regimes, by solving electromagnetic boundary-value problem [2]. The polarizability of the MWCNTs has peak in the sub-terahertz regime. The peak frequency depends on the length and diameter of MWCNTs. Two regimes (quasi-static and dynamical) of nanotube interaction with EM radiation have been established. In quasi-static regime a strong depolarizing field creates a shielding effect: the penetration depth of the axial component of incident field depends on the frequency, the length, and the electron relaxation time. The screening effect makes MWNTs suitable as interconnects.

The shielding efficiency and effective permittivity of MWCNT-based composite material were calculated at different nanotube diameters and lengths. The main features of the gigahertz spectra of the effective parameters of MWCNTs composite, previously observed in experiments have been systematized and theoretically described. The optimization of MWCNT geometry has been done in order to get the maximal effective permittivity of MWCNT-base composite in terahertz and sub-terahertz frequency regimes.

References

1. P. Kuzhir, *et.al.*, *Thin Solid Films*, 2011, Vol. 519, No.12, 4114-4118.

2. M.V. Shuba, G.Ya. Slepyan, S.A. Maksimenko, C. Thomsen, A. Lakhtakia, *Phys. Rev. B*, 2009, Vol. 79, 155403.

MULTI-LAYERD GRAPHENE IN MICROWAVES

Polina Kuzhir [1](presenting author), Nadeya Valynets[1], Alesya Paddubskaya[1], Sophia Voronovich[1], Konstantin Batrakov[1], Sergey Maksimenko[1], Tommi Kaplas[2] and Yuri Svirko[2]

[1]*Research Institute for Nuclear Problems, Belarusian State University,*

[2]*Department of Physics and Mathematics, University of Eastern*

e-mail of presenting author: polina.kuzhir@gmail.com

We report on the experimental study of electromagnetic (EM) properties of multilayered graphene in K_a-band synthesized by chemical vapor deposition (CVD) process in between nanometrically thin Cu catalyst film and dielectric (SiO_2) substrate. The quality of the produced graphene samples was monitored by Raman spectroscopy. The thickness of graphene films was controlled by atomic force microscopy (AFM) and was found to be a few nanometers (up to 5 nm). The microwave measurements were provided by scalar network analyzer R2-40 8R (ELMIKA, Vilnius, Lithuania). The reflective ability of investigated sample (approx. 25% of incident power) is mostly due to substrate, whereas absorption losses are due to the presence of the multilayered graphene. EM absorption of graphene film is found to be as high as 35-43% and in the frequency range from 27 to 29 GHz it is in the level of 40% and almost frequency independent. Theoretical modeling using Fresnel's formulae taking into account boundary conditions in the rectangular waveguide demonstrates good correspondence to the experimental data collected for graphene film on silica substrate in K_a-band.

To conclude, we discovered, that the fabricated graphene, being only some thousandth of skin depth, provided remarkably high EM shielding efficiency caused by absorption losses at the level of 40% of incident power. Being highly conductive at room temperature, multilayer graphene emerge as a promising material for manufacturing ultrathin microwave coatings to be used in aerospace applications.

This work was partially supported by EU FP7 projects FP7-266529 BY-NanoERA and FP7-247007 CACOMEL.

PHOTOCATALYTIC ACTIVITY OF $ZnFe_2O_4$ NANOPARTICLE CLUSTERS UNDER VISBLE LIGHT IRRADIATION

Andris Sutka[1], Gundars Mezinskis[1], Janis Kleperis[2], Kaspars Malnieks[1], Liga Grinberga[2]

[1] *Institute of Silicate Materials, Riga Technical University,* [2]*Institute of solid State Physics, University of Latvia*

e-mail of presenting author: andris.sutka@rtu.lv

Porous zinc ferrite ($ZnFe_2O_4$) nanoparticle clusters have been synthesized by the sol-gel auto-combustion method and the effect of excess iron on structural and visible light photocatalytic activity have been studied. X-ray diffraction (XRD), BET, scanning electron microscopy (SEM) and diffuse reflectance spectroscopy are used to investigate characteristics of synthesized $ZnFe_2O_4$ nanomaterials. The XRD patterns show that samples consist of single phase spinel structure with crystallite sizes below 50 nm. SEM analysis indicate that nanosized particles are grown together in clusters with size of several microns. The photocatalytic activity of synthesized ferrite nanomaterials to methylene blue (MB) under visible light irradiation is investigated. Results show that stoichiometric zinc ferrite exhibited higher photocatalytic activity (40%) than excess-iron sample (6%) under visible light irradiation by 3 hours. Lower photocatalytic activity of iron excess samples could be related to oxygen vacancies, which are created by restoring overall charge balance in the material and can behave as recombination centres.

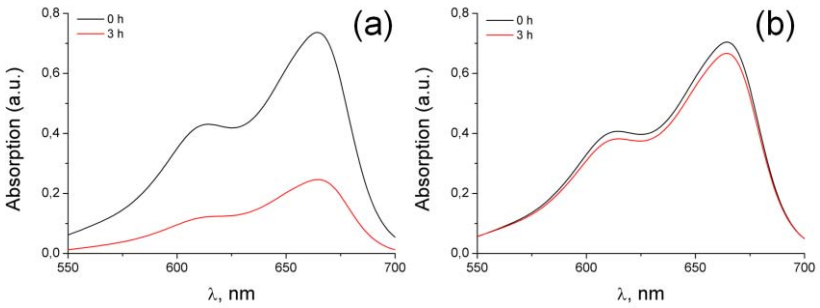

Fig.1 Photodegradation of MB over stoichiometric (a) and excess iron (b) $ZnFe_2O_4$ nanoparticle clusters under visible light irradiation

Acknowledgement

Authors acknowledge National Research Program in material sciences IMIS for financial support of scientific experiments and ERDF project Nr. 2010/0204/2DP/2.1.1.2.0/10/APIA/VIAA/010 for financial support of travel expenses.

Dielectric relaxation in bismuth-containing ceramics

E. D. Politova[1], G. M. Kaleva[1], A. V. Mosunov[1], and A. H. Segalla[2]
[1] *Karpov Institute of Physical Chemistry, 105064, Obukha s-str., 3-1/12, b.6, Moscow, Russia*
[2] *ELPA Company, Panfilovsky pr. 10, Zelenograd, 124460, Moscow, Russia*
E-mail: politova@cc.nifhi.ac.ru

Modification of composition is widely used for development of ceramic oxide materials with improved functional properties. However, effects of dielectric relaxation are often observed in compositionally disordered complex oxides. In this work dielectric properties of Bi -containing solid solutions on the base of perovskite-like compounds promising for the development of piezoelectric ceramics for high-temperature applications were studied.

Layered structure $Ca(Bi,Nd)_4(Ti,B)_4O_{15}$ (B - Cr, Ta – 10 at. %) and perovskite structure solid solutions $(Bi,Pb,A)(Sc,M)O_3$ (A – Nd – 10 at. %; M – Ti, Ga, Lu, Yb, Er, Y – 10 at. %) were prepared by the conventional solid state reaction method. The compositions were additionally modified by additives (Bi_2O_3, MnO_2, Ni_2O_3, Cr_2O_3, and LiF) in amounts less than 5 w. % in order to improve density of ceramics and their dielectric properties. Ceramics on the base of composition $0.36BiScO_3$ - $0.64PbTiO_3$ (BSPT) were modified by the powdered $Bi_4Ti_3O_{12}$ and $Bi_{0.75}Sr_{0.25}O_{1.36}$ single crystals additives (5 - 10 w. %) to stimulate the texture formation.

Structure parameters, phase transitions, dielectric and ferroelectric properties of ceramics were studied using the X-Ray diffraction and dielectric spectroscopy method, piezoelectric coefficients of some ceramics were measured as well.

The 1st order ferroelectric-paraelectric phase transitions were observed for all samples at temperatures 700 – 1000 K. Besides the dielectric anomalies corresponding to phase transitions, broad dielectric anomalies of relaxation nature were also revealed, with temperature position of peaks in dielectric permittivity curves depending on measuring frequency. These effects are pronounced in the samples obtained at higher sintering temperatures, so a microscopic mechanism of the relaxor behaviour may be related to the motion of dipoles formed by oxygen vacancies. Decrease of the total conductivity value to more than one order in modified samples sintered at lower temperatures supports this conclusion.

High values of piezoelectric coefficients d_{33} ~500 pC/N and of electromechanical coupling coefficient k_t ~0.50 were measured for some BSPT ceramics. The improvement of properties observed is obviously related to the optimization of crystal structure parameters and decrease of concentration of oxygen vacancies favoring to the enhancement of the domain walls movement and to improvement of piezoelectric properties.

The work was supported by the Russian Fund for Basic Research (Grant 12-03-00388).

STRUCTURE AND PROPERTIES OF NANOCOLLOIDAL SNO_2 WATERSOLS APPLIED IN PREPARATION OF OPTICAL QUALITY MICRO- AND NANOSPHERES

Glen Kelp[1,2], Tanel Tätte[1], Siim Pikker[1], Rünno Lõhmus[1], Hugo Mändar[1], Alex Rozhin[3], Kelli Hanschmidt[1], Uno Mäeorg[4], Marco Natali[5], Ingmar Persson[6]

[1]Institute of Physics, University of Tartu, Estonia, [2]Department of Physics, The University of Texas at Austin, USA, [3]Aston University, UK, [4]Institute of Chemistry, University of Tartu, Estonia, [5]ICIS-CNR, Italy, [6]Department of Chemistry, Swedish University of Agricultural, Sweden

The problems related to wet preparation of advanced ceramic materials often arise from initial point of processing – the precursor. SnO_2 in particular is difficult to prepare without contamination originating from precursors. In current work a novel kind of sol precursor is proposed for solving the problems related to preparation of nanocrystalline SnO_2 with desired geometrical shape. The proposed process for precursor preparation is very robust, involving simple mixing of tin alkoxides ($Sn(OR)_4$) with large excess of water at room temperature [1]. The precursor, a water based SnO_2 colloidal system, is set out as separate liquid phase. The stability of the system, based on cassiterite phase nano-crystallites 2-3 nm in diameter could be explained by strong interaction between -OH groups on the surface of the particles and surrounding water molecules. Exact size, structure and shape of precursor particles is revealed by XRD, SAXS, EXAFS, HRTEM imaging and IR spectroscopic analyses. Chemical mechanism for explanation of formation and nature of colloidal particles is proposed. The applicability of the precursor is proved in preparation of optically homogeneous microspheres. As great advantage of the precursor, obtained xerogel particles can be heat treated rapidly just by putting the sample directly into pre-heated oven or flame. The crystallization of materials caused by thermal treatment is studied with micro Raman spectroscopy and SEM imaging. The proposed method is simple and safe and should be applicable in industrial processing of technologically important SnO_2 materials in defined geometrical forms.

References

1. Invention: Method of preparation of nanocolloidal SnO_2 watersols; Owner: University of Tartu; Authors: Tanel Tätte, Uno Mäeorg, Siim Pikker, Aile Tamm, Madis Paalo, Glen Kelp; Priority number: P201000096; Priority date: 31.12.2010

ELECTRON-PHONON INTERACTIONS: SPATIAL LOCALIZATION

Eriks Klotins[1] , Guntars Zvejnieks[2]
[1,2] Institute of Solid State Physics, University of Latvia
e-mail of presenting author: klotins@cfi.lu.lv

We present a first-principles technique for electrons in a cloud of their lattice distortion with emphasis on local description of polarons associated with the lattice sites.

The scientific background is lattice Hamiltonians with electron-phonon interaction in a momentum space representation missing position space properties of polarons as a disadvantage.

Milestones to avoid this disadvantage include transition from the Bloch momentum space representation to appropriate localized functions in position space and successive Baker–Hausdorf canonical transformation applied to the position space Hamiltonian with mixed electron and phonon states.

This transformation yields the expected position space property, transition of a polaron between lattice sites.

In more detail, the approach starts with the single electron energy in the Blochs representation. The primary quantities needed to choose are position space basis functions corresponding to criteria of localization and gauge invariance [1]. The subsequent momentum space – position space transformation results in effective Hamiltonian with electron and phonon birth/annihilation operators assigned to a lattice site.

At variance with the conventional Baker-Hausdorf canonical transformation applied for the decoupling of the mixed electron and phonon states in momentum space, some care is required for generator of the transformation [2] to construct the effective Hamiltonian with the standard renormalized electron-electron and phonon terms as well as, as an entity of special interest, the effective interaction of polarons.

References

1. N. Marzari , A.A. Mostofi , J.R. Yates, I. Souza, D.Vanderbilt 2012 *Rev.Mod.Phys.* 2012, 84, 1419
2. O. Madelung , *Introduction to Solid-State Theory* (Springer – Verlag Berlin, Heidelberg, New York) (1978) pp.493

AB-INITIO ANALYSIS OF THE (001) SURFACE IN CUBIC $CaZrO_3$

M.G. Brik, C.-G. Ma, V. Krasnenko

Institute of Physics, University of Tartu, Riia 142, Tartu 51014, Estonia

E-mail of presenting author: brik@fi.tartu.ee

The (001) surface of cubic perovskite $CaZrO_3$ has been modelled by the DFT-based calculations as implemented in the CASTEP module of Materials Studio package using both local density and generalized gradient approximations (LDA and GGA, respectively). The surface energies, electronic band structure, density of states, effective Mulliken charges and electron density difference were calculated for both possible CaO and ZrO_2 terminations [1]. It was shown that the surface rumpling is more pronounced in the case of the CaO terminated surface (11.3 % in terms of the bulk lattice constant, as compared to 1.15 % for the ZrO_2 termination, see Fig. 1). The surface energy of the CaO termination (0.558/0.130 eV, LDA/GGA) was found to be lower than the surface energy of the ZrO_2 termination (0.829/0.291 eV), thus showing the former surface to be energetically favorable.

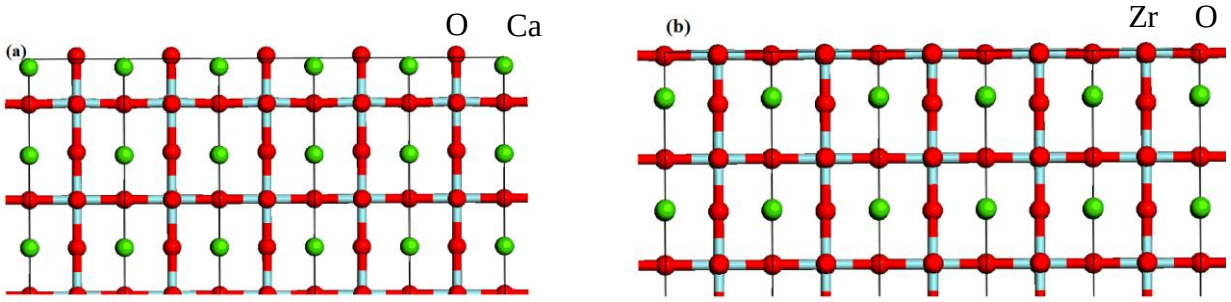

Fig.1. The optimized CaO (a) and ZrO_2 (b) terminated (001) surfaces in $CaZrO_3$. Difference in the uppermost layers is clearly seen. The Zr atoms in Fig. 1b are located behind the O atoms.

The differences in the electronic properties of both slabs were revealed, e.g. the calculated band gap of the CaO-terminated slab was found to be 2.913/3.106 eV (LDA/GGA), whereas the ZrO_2-terminated slab has the band gap of 2.827/2.967 eV (LDA/GGA). An analysis of the density of states diagrams for ions from various layers allowed for highlighting remarkable difference between the surface and deep layers. The calculated surface energies were compared with other theoretical data for the isostructural cubic perovskites available in the literature.

References

1. M.G. Brik, C.-G. Ma, V. Krasnenko, *Surf. Sci.*, 2013, 608, 146-153.

PHOTOLUMINESCENCE STUDIES OF SOLAR CELL ABSORBER MATERIAL CU_2ZNSNS_4

Maarja Grossberg[1], Taavi Raadik, Pille Salu, Jaan Raudoja, Jüri Krustok.
[1]*Department of Materials Science, Tallinn University of Technology, Estonia*
e-mail: maarja.grossberg@ttu.ee

Photoluminescence studies of Cu_2ZnSnS_4 (CZTS) polycrystals with varying chemical composition were performed. Temperature and excitation power dependent measurements revealed the following results. In the low-temperature (T = 10 K) PL spectrum of slightly Cu-rich CZTS polycrystals two PL bands were detected at 1.27 eV and 1.35 eV arising from the band-to-impurity (BI) recombination involving deep acceptor defect with the ionisation energy of around 280 meV but different CZTS phase with different bandgap energy. In the low-temperature PL spectrum of nearly stoichiometric CZTS polycrystals a deep PL band at 0.66 eV and another band at 1.35 eV were observed. These PL bands are proposed to be related to the presence of $\left(Cu^{-}_{Zn} + Sn^{2+}_{Zn}\right)$ and $\left(2Cu^{-}_{Zn} + Sn^{2+}_{Zn}\right)$ defect clusters in nearly stoichiometric CZTS. Room-temperature micro-photoluminescence study of CZTS polycrystals with different chemical composition allowed us to observe band-to-tail (BT) and band-to-band (BB) recombination at 1.39 eV and 1.53 eV, respectively. These results show that the model of heavily doped semiconductors applies to CZTS and that on the contrast to the ternary analogues, ternary chalcopyrites, BT band has very low intensity in CZTS.

INVESTIGATION OF QUATERNARY COMPOUNDS FOR MONOGRAIN LAYER SOLAR CELLS

Marit Kauk-Kuusik, Kristi Timmo, Katri Muska, Mare Altosaar, Maris Pilvet, Tiit Varema, Jaan Raudoja, Maarja Grossberg, Enn Mellikov, Olga Volobujeva

Department of Material Sciences, Tallinn University of Technology

e-mail: marit.kauk-kuusik@ttu.ee

$Cu_2ZnSn(S_{1-x}Se_x)_4$ (CZTS) are promising absorber materials for solar cells due to their optimal direct band gap, high absorption ability and due to their abundant and non-toxic constituent elements. Best efficiency achieved with kesterite absorber materials is 11.1% [1]. Solar cell results depend strongly on the material composition, therefore a tight control of the composition and the structure of CZTS is important for achieving high efficiency solar cells. Solar cell characteristics can also be improved by post-treatments, but during high temperature post-treatments, the decomposition of CZTS can occur. The volatile products of CZTS decomposition are SnS_2 or $SnSe_2$ and sulfur or selenium. By applying vapor pressure of these volatile components in post growth heat treatments the composition of kesterite absorber material can be controlled.

In current study, $Cu_2ZnSn(S_{1-x}Se_x)_4$ materials with x= 0 - 1 were synthesized in monograin form in the liquid phase of KI as flux material with different Cu/(Zn+Sn) and Zn/Sn concentration ratios. Synthesized monograins were post-treated in different atmospheres at various temperatures using either isothermal or two-temperature zone arrangement. Heat-treated monograins were used as absorber layers in monograin layer (MGL) solar cells. The elemental composition, phase composition, and electrical and morphological properties of as-grown and post-treated monograin powders were studied using EDX, SEM, Raman spectroscopy, XRD and hot probe measurements. The MGL solar cells were characterized by current-voltage (*I-V*) and *QE* measurements.

It was found that the bulk and phase composition of the synthesized monograins could be controlled by initial precursor composition. Experiments showed that Cu and Zn are to some extent interchangeable in the crystal lattice. The best conversion efficiency 7.4% were achieved with Cu-poor and Zn-rich Cu_2ZnSnS_4 monograins post-treated in SnS_2 vapor.

References

1. T. K. Todorov, J. Tang, S. Bag, O. Gunawan, T. Gokmen, Y. Zhu and D. B. Mitzi, *Advanced Energy Materials, 2013, Vol.3, Issue 1, 34-38.*

Formal and technological solar resource in Estonia

Teolan Tomson

Department of Materials Science, Tallinn University of Technology,

Ehitajate tee 5, 19086, Tallinn, Estonia, e-mail: Teolan.Tomson@ttu.ee

Northern Europe: Scotland, Scandinavia, the Baltic States and North-west Russia are highly influenced by (Atlantic) cyclones. Due to corresponding cloudiness Fig. 1 there is high share of diffuse fraction of solar radiation. Regular actinometrical measurements (Tartu Observatory: since 1955) record beam radiation from the sun's position and diffuse radiation from horizontal surfaces [1]

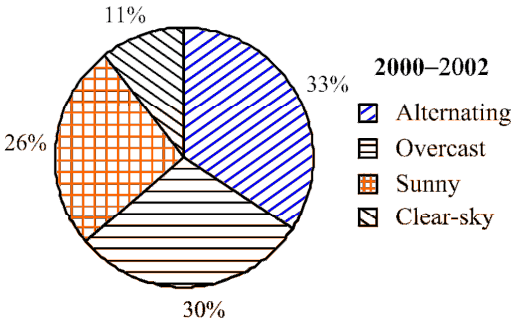

Fig. 1 Prevailing sky conditions in Estonia; summer seasons (Apr. – Sep.) 2000 – 2002

These continuous recordings are the basis for the prognosis of energy production (thermal, electrical), and for the comparison of different technological solutions. As real solar collectors operate in different positions, the recorded (average) data have to be recalculated for corresponding azimuths and tilt angles. Calculations of the beam fraction are trustworthy, but calculations of the diffuse fraction contain uncertainties due to different approximation models. The most popular of these is the isotropic model, but we will show that it this different in overcast conditions and with alternating (*Cumulus*) clouds. In the latter case, the well-known approximation model has to be corrected, and in this study, a new empirical approximation model is created. To increase the energy yield, different exposition strategies can be used and we will evaluate them: optimal fixed exposition, continuous tracking and discrete tracking in two different expositions for AM and PM performance correspondingly.

Keywords: *diffuse radiation, clouds, tilted surfaces, exposition strategies*

References

1. H. Tooming (Ed), Handbook of Estonian solar radiation climate. 2003, EMHI

Commercial

About Raith:

Raith is a leading provider and manufacturer of electron and ion beam lithography systems for nanofabrication. Founded in 1980 and headquartered in Dortmund, Germany, the company offers solutions for researchers and engineers in both academic and industry settings. With approximately 120 employees supporting customers in Europe, the Americas, Asia and the Pacific region, Raith provides a professional support infrastructure that delivers added value to customers. Raith includes high level universities, academic institutions as well as companies from high technology business among its clientele. For more information please visit www.raith.com.

Effective February 15, 2013 Raith and Vistec Lithography announce that they unite their worldwide activities for electron and ion beam lithography and nanofabrication instruments to form one solution provider. Raith has agreed to acquire Vistec Lithography from private equity firm Golden Gate Capital.

Raith GmbH

Konrad-Adenauer-Allee 8

44263 Dortmund, Germany

Telefon: +49 (0)231 / 95004 - 0

Telefax: +49 (0)231 / 95004 - 460

Email: sales@raith.com

Web: http://www.raith.com/

Conference contact:

Martin Kichner

Email. kichner@raith.de

4D X-ray microscopy(XRM), In Situ imaging of practical volume samples

S H Lau, Jeff Gelb, Pete Lander Xradia, Inc., Pleasanton, CA, USA

Abstract

In situ, 4D microscopy using X Ray microscopy is evolving as a valuable scientific technique. In order to develop this further it is important to develop the technique using realistic representative volumes in a wide range of materials. It is also important to evaluate the efficacy of the application against more traditional methods by employing correlative imaging.

Conventional electron and optical microscopy techniques require the sample to be sectioned, polished or etched to expose the internal surfaces for imaging. However, such sample preparation techniques have traditionally prevented the observation of the same sample over time, under realistic three-dimensional geometries and in an environment representative of real-world operating conditions. X-ray microscopy (XRM) is a rapidly emerging technique that enables non-destructive evaluation of buried structures within hard to soft materials in 3D, requiring little to no sample preparation. Furthermore in situ and 4D quantification of microstructural evolution under controlled environment as a function of time, temperature, chemistry or stress can be performed repeatably on the same sample, using practical specimen sizes ranging from tens of microns to several cm diameter, with achievable spatial imaging resolution from submicron to 50 nm. Many of these studies were reported using XRM in synchrotron beamlines. These include crack propagation on composite materials; corrosion studies; microstructural changes in battery electrodes during charge-discharge or during the setting of cement; stress in bones under load; flow studies within porous media to mention but a few. While synchrotron-based XRM has the advantage of high flux and energy tunability, in this study we present several similar in situ and ex situ studies using lab-based XRM utilizing conventional x-ray sources, at resolutions and contrast comparable to those obtained at synchrotron micro and nano beam lines. Crack propagation and compression-tension studies in both hard and soft materials, featuring Alumina based refractory, TiSiC and polymer foam will be discussed. Others include corrosion studies on intergranular corrosion pitting of aluminium alloys used in aircraft, the formation of tin whiskers in medical and aerospace electronics; fluid flow studies and CO2 sequestration in geomaterials and biomechanical studies of animal tissue and organs will also be discussed. Unlike electron microscopy, XRM has much less limitations in sample size and can image both surface or internal structures. Therefore, it is a powerful technique to model materials, structures and whole systems for thermal-mechanical or transport properties more accurately and is capable of doing it across multi lengthscale in 3D. System can be used as a standalone technique or can be combined with optical, FIB-SEM, electron tomography and spectroscopy as part of a correlative microscopy investigation, with XRM providing the 3D Hierarchical Framework for the multiscale model. Examples will be illustrated with pore network modeling of reservoir rock which is currently being increasingly being employed in enhanced oil recovery in the oil and gas industry.

References

1. Chawla,N, Williams, JJ, Deng,X., Climon,C., Hunter,L., Lau, S H.," 3D characterization and modelling of Porosity in Power Metturlurgical Steel," IJPM Vol 45, Issue 2 (2009)

2. Dudek,M.A., Hunter,L., Kranz,S., William,JJ,. Lau,S H., Chawla,N. "3D modelling of reflow porosity and modelling of Pb free Solder, Material Characterization" 61 (2010), p 433-43.
3. SP Knight, M Salagaras, AR Trueman, "The Study of Intergranular Corrosion in Aircraft Aluminium Alloys Using X-ray Tomography," Corrosion Science 53 (2011) 727-734.
4. G Muralidharan, K Kurumaddali, AK Kercher, SG Leslie, "Reliability of Sn-3.5Ag Joints in High Temperature Packaging Applications," 2010 Electronic Components and Technology Conference.
5. BM Patterson, K Henderson, Z Smith, D Zhang, P Giguere, "Applications of Micro-CT to In-Situ Foam Compression and Numerical Modeling," Microscopy and Analysis 26 (2012)
6. M Zhang, Y He, G Ye, DA Lange, K van Breugel, "Computational Investigation on Mass Diffusivity in Portland Cement Paste Based on X-ray Computed Tomography," Construction and Building Materials 27 (2012): 472-481.
7. F Awaja, B Arhatari, K Wiesauer, E Leiss, D Stifter, "An investigation of the accelerated thermal degradation of different epoxy resin composites using X-ray microcomputed tomography and optical coherence tomography," Polymer Degradation and Stability (2009) 1814-1824.

Polymer Pen Lithography

Massive parallel fabrication of repetitive nanostructures

Raimon Zoetemelk, Park Systems

Nanofabrication strategies are becoming increasingly expensive and equipment-intensive, and thus less accessible to researchers. As an alternative, scanning probe lithography has become a popular technique for preparing nanoscale structures, in part owing to its relatively low cost and high resolution, and a registration accuracy that exceeds most existing technologies. However, increasing the throughput of cantilever-based scanning probe systems, while maintaining their resolution and registration advantages, has been a significant challenge. Even with impressive recent advances in cantilever array design, such arrays tend to be highly specialized for a given application, expensive, and often difficult to implement. It is therefore difficult to imagine commercially available production methods based on scanning probe systems that rely on conventional cantilevers. We implemented a low-cost, high throughput scanning probe lithography method that uses a soft elastomeric tip array to deliver inks to a surface in a 'direct writing' manner. This, so called Polymer pen lithography combines the large-area capability of contact printing with the feature size control of dip-pen lithography. The method allows forming features on the nanometer, micrometer, and macroscopic length scale with the same tip array and in the same writing step. Polymer Pen Lithography is a direct printing method with parallel replicating functionality. As it uses direct contact of an elastic polymer for each pattern, the controllability of the pattern size is increased and so is the uniformity of the pattern.

Introduction to free liquid surface technology as developed by Elmarco s.r.o.

One of the classical methods of polymer nanofiber electrospinning, known for decades, involves passing a polymer solution through a metallic nozzle. An electrode is placed at a certain distance from the nozzle, with the nozzle itself acting as the second electrode. Using a high-voltage power source, a potential difference is created between the two electrodes, and the static charge causes the polymer solution to form a Taylor cone and elongate, forming nanofibers, which are then deposited to form a layer.

Elmarco, s.r.o. has developed a novel, nozzle-free method for nanofiber electrospinning, using either a polymer solution-covered metallic roller or wire in place of the nozzle. Therefore the formation of Taylor cones is governed by the forces of electrostatic repulsion and surface tension, instead of being imposed by the structure and placement of polymer nozzles. This approach has several distinct advantages. Firstly, unlike nozzle electrospinning methods, the number and distribution of Taylor cones can be controlled simply by changing process parameters (roller rotation speed, voltage, etc.), with no change in hardware required. Secondly, the simple mechanical construction of the electrodes and the polymer solution supply allows for a simple and fast cleaning procedure – in nozzle-type system, depending on the scale of the system, the cleaning process can take hours or even days. Thirdly, the nozzle-free design allows for an easy upscaling of the method to industrial scale units – with nozzle electrospinning, hundreds or even thousands of nozzles can be needed to achieve sufficient productivity, making it economically unfeasible in most cases.

The range of materials that can be spun covers many organic polymers (PA6, PAI, PUR, PVA, etc.), non-organic materials (TiO2, SiO2, Li4Ti5O12, Pt, Cu, Mn, etc.), as well as biopolymers (Gelatine, Chitosan, Collagen, PAA, etc.). Advice and assistance is available with the development of recipes using previously untested materials, and proposals for new applications are very welcome.

Elmarco s.r.o. offers systems in all scales – from lab-scale systems for development work to industrial-scale systems that have been specifically designed to integrate with textile production lines. Nanofiber production techniques can be easily upscaled. Recipes for many common polymers are supplied along with the system, allowing for a rapid start of production or development process.

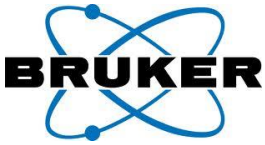

How Bruker's innovative and reliable material science solutions support industries and organizations in delivering high-quality products and materials.

Materials such as semiconductors, metals, composites, nanotech materials, carbons or high-tech ceramics make our lives easier. They are sources of industrial growth and technological changes. Thus, material science is an interdisciplinary field incorporating elements of applied physics and chemistry.

Bruker offers advanced productive and profitable solutions for material testing and research. They enable companies and organizations to reliably identify the components of finished goods, characterize irregularities or trace impurities. We provide our clients with a wide range of analytic devices and systems for semiconductors, material research & nanotech, mining and metals & automotive.

Nanotechnology builds the bridge across research fields as biology, chemistry, physics, and engineering. Thus, various well established analytical methods are applied in order to study, or modify the nano-cosmos, or finally to generate usable products.

Atomic force microscopy provides detailed information about sample surfaces at the nanoscale, and has become an important technology for research of nanomaterials, biomaterials, inorganics and composites, electonic materials and many more. Bruker's industry-leading atomic force microscopes (AFMs) incorporate the very latest advances in AFM techniques to enable the widest array of nanoscale materials research.

Quantitative nanomechanical analysis in conjunction with high-fidelity topographic measurements is one of Bruker's methods of unraveling the function of complex materials. From modulus measurements in the mega- to gigapascal range, adhesion and frictional maps, calorimetric and electrical data, correlated nanoscale AFM, and Raman spectroscopy to three-dimensional morphological plots with sub-nanometer accuracy, Bruker has the AFM solution for your problem.

In addition, methods such as electron microscopy, IR-, UV-, or FTIR-spectroscopy, NMR, EPR, or MS, X-ray diffraction and scattering are considered important due to two essential reasons: X-ray diffraction is virtually non-destructive, and X-ray photons with a wavelength in the nanometer range are the ideal sensor for the nanocosmos.

X-ray diffraction offers a number of different dedicated methods to investigate nano-structures: X-ray Reflectometry (XRR) determines layer thickness, roughness, and density; High-Resolution X-ray Diffraction (HRXRD) helps to verify layer thickness, roughness, chemical composition, lattice spacing and mismatches, relaxation, etc.; X-ray diffuse scattering to determine lateral and transversal correlations, distortions, density, and porosity; in-plane grazing incidence diffraction (IP-GID) to study lateral correlations of thinnest organic and inorganic layers, and depth profiling; Small Angle X-ray Scattering (SAXS) in transmission or grazing incidence SAXS (GISAXS) in reflection to determine the size, the shape, the distribution, orientation, and correlation of nano-particles present in solids or solutions.

INTERNATIONAL CONFERENCE

FUNCTIONAL MATERIALS AND NANOTECHNOLOGIES

TARTU, ESTONIA IN APRIL, 21 – 24, 2013

POSTER SESSION

APRIL, 22 at 16:20– 19:00

Poster Session: Nanomaterials		
A. Zhyshkovych	The luminescence of $CaF_2:Eu^{3+}$ nanoparticles	PO-1
Vladimir I. Kondratiev	Sol-gel technics for processing transparent and conductive Al-doped zinc oxide films	PO-2
Viesturs Sints	Nanoparticle transfer under magnetic field in a nonisothermal porous layer saturated with a ferrofluid	PO-3
Vera Serga	Catalytic activity of novel ceria supported nano-sized platinum catalyst synthesized by extractive-pyrolytic method for low-temperature WGS reaction	PO-4
Vera Serga	Production of mono- and bimetallic nanoparticles of noble metals by pyrolysis of organic extracts on silicon dioxide	PO-5
Valdis Kampars	Synthesis and thermal deoxygenation of graphite oxide	PO-6
Veera Krasnenko	Conjoined structures of carbon nanotubes and graphene ribbons	PO-7
Triinu Taaber	Novel anti-wear lubricant based on nanoparticles/ionic liquid combination	PO-8
Jana Grigorjeva	Spectral characterization of AlGaN nanomaterials with tunable bandgap	OR-2
Toomas Plank	Technet_nano – the cooperation network of clean rooms in baltic sea region	PO-9
Tõnis Arroval	Atomic layer deposition of nanostructural TiO_2 films on Si, α-Al_2O_3 and RuO_2	PO-10
Tauno Kahro	Temperature induced reversal of oxygen response in CVD graphene on SiO_2	PO-11
Tatjana Dedova	Growth of zinc oxide nanostructured layers on SnO_2 electrodes by spray pyrolysis	PO-12
Tatjana Dedova	Nanostructured layers of zinc sulfide obtained by spray pyrolysis	PO-13
Tanel Käämbre	Iron oxide nanoparticles by precipitation from ferrous source: structural phase transformation dependence on synthesis parameters and annealing	PO-14
Taivo Jõgiaas	Atomic layer deposition of aluminium oxide on silicon carbide nanopowder	PO-15
Svetlana Vihodceva	Improvement of UV protection properties of the textile from natural fibres by the sol-gel method	PO-17
Silver Leinberg	Aligning nano-wires for anisotropic spectral properties	PO-18
Siim Heinsalu	Core-shell silica-gold nanoparticles for control of fluorescence in the sol-gel films activated by rare earth	PO-19
Sergey Tsarenko	Generation of metal nanoparticles in cathode spots of pulsed discharges	PO-20
Sergey Plotnikov	Segregation on the surface of titanium steel 12Cr18Ni10Ti exposed electron beam	PO-21
Šarunas Svirskas	Dielectric and ultrasonic investigations on polyurea elastomers with embedded inorganic nanotubes	PO-22
Šarunas Svirskas	Broadband dielectric spectroscopy of PVDF polymers embedded with ferrite nanoparticles	PO-23

Santa Stepina	Ethylene vinylacetate copolymer and nanographite composite as chemical vapour sensor	PO-24
Sanja Ćulubrk	Synthesis of Eu and Sm doped Y_2O_3 nanophosphors by room temperature self-propagating reaction	PO-25
R. Zabels	Structural and micromechanical changes in MgO after high-dose irradiation with swift heavy ions	PO-26
Raul Rammula	Atomic layer deposition of aluminum oxide films on graphene	PO-27
Rainer Pärna	Influence of iodine doping and annealing on the properties of sol-gel prepared thin titania films	PO-28
R. Mackevičiūtė	Dielectric properties of nanograin BSPT caramics	PO-29
Pavel Merzlyakov	Statistical analysis of void lattice formation in CaF_2	PO-30
Olga Malyshkina	Conoscopic study of strontium-barium niobate single crystals	PO-31
O.M. Morozov	Deuterium desorption temperature from Mg-Ti composites prepared by method of atom-by-atom mixing of components	PO-32
Nina Mironova-Ulmane	Neutron scattering study of structural and magnetic size effects in NiO	PO-33
Nadzeya Valynets	Exfoliated graphite composites: microwave applications	PO-34
Mikk Vahtrus	Two point electrical measurements of 1D nanostructures	PO-35
Meeri Visnapuu	Dissolution-dependent antibacterial effects of silver nanowires	PO-36
Maksim S. Shashkov	Examination of dielectric dispersion of complex oxides on the basis of bismuth-containing titanates	PO-37
Madis Umalas	Elaboration of alumina nanofibers reinforced yttria stabilized zirconia nanocomposites by sol-gel method	PO-38
Madis Paalo	Preparation and characterization of electrically conductive metal oxide CNT-composites by sol-gel method	PO-39
Lauri Aarik	Titanium dioxide thin films grown from titanium chloride and ozone by atomic layer deposition	PO-40
Larisa Grigorjeva	Characterization of hydroxiapatite by time-resolved luminescence and FTIR spectroscopy	PO-41
L.Kuznecova	Spark plasma sintering (SPS) of nanosized zirconia powders, obtained by azeotopic distillation	PO-42
Krisjanis Smits	Rare earth doped zirconia nanostructured transparent ceramics	PO-43
Konstantins Dubencovs	Novel fine-disperse bimetallic Pt-Pd/Al_2O_3 catalysts for glycerol oxidation with molecular oxygen	PO-44
Kaspar Roosalu	Investigation of Ti doping effect on stabilization of R'-plane oriented epitaxial Cr_2O_3 thin films on R-plane sapphire	PO-45
Kaido Siimon	Development of nanofibrous 3D collagen/polyaniline composites as tissue engineering scaffolds	PO-46
Kaarel Piip	Influence of He/ D_2 plasma fluxes on tungsten coatings morphology and crystallinity	PO-47

Juris Katkevics	Impedance and admittance characteristics of Bi_2S_3 nanowire arrays	PO-48
Jekaterina Kozlova	Characterization of graphene prepared by chemical vapour deposition on nickel	PO-49
Janis Timoshenko	Two limits of electron capture in a dynamic quantum dot	PO-50
Janis Maniks	Structure, micromechanical and magnetic properties of polycarbonate nanocomposites	PO-51
Janis Maniks	Modification of LiF structure by irradiation with swift heavy ions under oblique incidence	PO-52
Janis Kleperis	Electrodeposition of nanoporous nickel layers using inductive voltage pulses	PO-53
J.Kalnacs	Chemical vapor deposited graphene adsorbtion ability	PO-54
Janis Grabis	Characteristics of stabilizied zirconia nanoparticles prepared by molten salts and microwave synthesis	PO-55
Jan Macutkevic	Electrical percoliation in onion like carbon composites	PO-56
Jan Macutkevic	Influence of preparation technology on the dielectric properties of carbon nanotubes polymer composites	PO-57
Ivan Zakharchuk	Magnetic moment of single vortices in YBCO nanosuperconducting particles: eilenberger approach	PO-58
Ivan Netšipailo	Corrosion protection of metals using multilayer thin films based on TiO_2 and Al_2O_3 grown by ALD	PO-59
Indrek Tallo	Hydrogen chloride as a possible reactant for synthesis of titanium carbide derived carbon powders for high-technology devices	PO-60
Ieva Kranauskaite	Dielectric spectroscopy of graphite loaded epoxy resin composites	PO-61
Guntis Japins	Manufacturing, structure and properties of recycled polyethylene terepthalate/liquid crystal/montmorillonite clay nanocomposites	PO-62
Erkki Lähderanta	Transport properties of indium antimonide with magnetic nanoprecipitates	PO-63
Dziugas Jablonskas	Dielectric and ultrasonic investigations of composites of poly(ε-caprolactone) and $Mo_6S_3I_6$ nanowires	PO-64
Dmitry Kuruch	Nanotubes folded from cubic and orthorhombic $SrZrO_3$: first-principles study	PO-65
Dmitry Zablotsky	Numerical investigation of arrays of concentration microstructures in dispersions of magnetic nanoparticles	PO-66
Daulet Sergeyev	The influence of external weak magnetic field on anharmonic nanocontacts of Josephson type	PO-67
A. Vīksna	Preparation of short range ordered nanodot arrays and analysis of particle optical properties	PO-68
Andrei Bandura	Force-field choice for the simulation of TiO_2- and ZrO_2-based nanotubes	PO-69
Anastasija Ivanova	Near-infrared sensitive organic solar cell	PO-70
Alexandr Popov	Spectroscopy of the $5d^1$-$4f^1$ transitions of Ce^{3+} in nanocrystalline xenotime- and rhabdophane-type yttrium phosphates	PO-71

Alexander Vanetsev	Microwave-hydrothermal synthesis of nanocrystalline xenotime- and rhabdophane-type yttrium phosphates doped with Ce^{3+} ions	PO-72
Alar Jänes	Surface analysis of supercapacitor electrodes after long-lasting constant current tests	PO-75
Aile Tamm	Atomic layer deposition of hafnium and zirconium oxides on carbon nanoparticles	PO-76
Agnese Grigalovica	Explotitation and structural properties of modified polyacetal nanocomposites	PO-77
A.I. Popov	Cathodoluminescence study of Al-doped ZnO nanofilms	PO-78
Patrick Martin	Femtosecond excitonic dynamic and relaxation in solid ZnO: dependence of the luminescence decay time on nano particles size and excitation mode	OR-5
Poster Session: Multifunctional materials		
A.M. Pashaev	On the Possibilities for Improving the Efficiency of Radiation in Heterostructures Based on the IV-VI Semiconductors	PO-79
Włodzimierz Śmiga	Investigation of Mechanical and Electrical Properties of Li Doped Sodium Niobate Ceramic System	PO-80
Vladimir Lisitsin	Dielectric and Pyroelectric Properties of Calcium-Barium Niobate Single Crystals	PO-81
Vladimir Ivanov	Luminescence of $LaBr_3$:Ce,Hf Scintillation Crystals under UV-VUV-XUV and X-Ray Excitation	PO-82
Virginija Liepina	Investigation of Luminescence Mechanism of Persistent Strontium Aluminate Phosphor	PO-84
V.Dimza	The Effect of Cu Admixture on Relaxor Properties of The PLT8/65/35 Electrooptical Ceramics	PO-85
Vera Skvortsova	Optical Properties of Natural Topaz	PO-86
V.S. Levushkina	Luminescent Properties and Energy Transfer in $Y_xLu_{1-x}PO_4:Re^{3+}$ (Re = Eu, Ce) Solid Solutions	PO-87
Ugis Gertners	Optical-Field Induced Surface-Relief Formation Phenomenon in Thin Films of Vitreous Chalcogenide Semiconducors	PO-88
Triin Kangur	Cell Growth on Patterned Surfaces Prepared by a Novel Sol-Gel Phase Separation Method	PO-89
Svetlana Zazubovich	Electron and Hole Centers in X-Ray- or UV-Irradiated Oxyorthosilicate Crystals	PO-90
Sergey Nikoghosyan	The Effect of Aging on the Superconducting Transition Temperature And Resistivity Of Y-Ba-Cu-O Ceramics After High Temperature Treatment	PO-91
Santa Popova	Optical and Electroluminescence Properties of Tercbutil Group Containing Piraniliden Derivatives	PO-92
Rimas Janeliukstis	Improvement of CdS Film Optical Properties by Laser Radiation for Application in Solar Cells	PO-94
Reinis Ignatans	Structure and Dielectric Properties of $Na_{1/2}Bi_{1/2}TiO_3$-$BaTiO_3$ Solid Solutions in the Phase Transition Region	PO-95

Raul Välbe	Modification of Carbon Nanotubes and Cellulose Cotton Fibers Using Hybrid Ionic Liquid – Sol-Gel Approach	PO-96
Raul Laasner	Band Tail Absorption Saturation In $CdWO_4$ with 80-fs Laser Pulses	PO-97
Rasmus Talviste	Atmospheric Pressure Plasma Jet in Microtubes	PO-98
R.M. Grechishkin	Laser Conoscopy of Large-Sized Optical Crystals	PO-99
R. Mackevičiūtė	Dielectric and Impedance Spectroscopy of Fe Doped $0.94(Na_{0.5}Bi_{0.5}TiO_3)$-$0.06BaTiO_3$ Ceramics	PO-100
R. Mackevičiūtė	High-Frequency Dielectric Properties of $Pb(Fe_{1/2}Nb_{1/2})O_3$ Ceramics and Single Crystal	PO-101
Peet Konsin	Semi-Microscopic Vibronic Theory of Quantum Paraelectricity and Ferroelectricity	PO-102
Nurgul Zhanturina	The Influence of Elastic Stress on the Surface of Adiabatic Potential of KI Crystal at Fixed Temperatures	PO-103
Nikolajs Ponomarenko	The Study of Correlation Between Microstructure of Ferrites and their Complex Permeability Spectra	PO-104
Gunta Kizane	Tritium retention studies in W coated JET divertor CFC tiles	PO-105
M.Narels	Influence of Temperature on Photoisomerisation Process of Polymer Films Doped by Azobenzene Derivatives	PO-106
Marko Part	ZrO_2 Microtubes As Substrates in ALD Processes	PO-107
Maris Springis	Green Luminescence Decay Kinetics Analysis in $NaLaF_4:Er^{3+}$	PO-108
Marija Dunce	Phase Transitions and Physical Properties in Ca Modified $Na_{1/2}Bi_{1/2}TiO_3$-$SrTiO_3$-$PbTiO_3$ Solid Solutions	PO-109
Margarita Baitimirova	Characterization of Functional Groups of Airborne Particulate Matter	PO-110
M. Reinfelde	Influence of Grating Period on Surface Relief Hologram Recording Efficiency in Amorphous AS_2S_3 and $AS_{40}S_{15}SE_{45}$ films	PO-111
Maksims Polakovs	Influence of Radiation on EPR and Optical Spectroscopy of Human Blood	PO-112
M. Zubkins	Hall-Effect Studies in Doped ZnO Thin Films	PO-113
M. Kinka	Dielectric Properties of $Ba_2NdFeNb_{3,7}Ta_{0,3}O_{15}$ Solid Solution	PO-114
Liga Freivalde	Hemp Fiber Non-Wovens Properties Analysis	PO-115
Liga Avotina	Analysis of Fullerene C_{60} Possible Formed in the Divertor Area of a Tokamak Like Devices	PO-116
Laurits Puust	Afterglow and Thermoluminescence of ZrO_2 Nanopowders	PO-118
Kuanyshbek Shunkeyev	Exciton-Phonon Interaction in Alkali Halide Crystals at Low Temperature Uniaxial Elastic Stress	PO-119
Kuanyshbek Shunkeyev	Specificity of Stabilization of H^- Centers in Crystal KBr at Low Temperature Deformation	PO-120
Kristel Möldre	Real-Time Optical Characterization of Atomic Layer Deposition of Dielectrics on Graphene	PO-121

K. Klismeta	Photoinduced Mass Transport in Azo-Benzene Containing Compounds	PO-122
Kirils Surovovs	Modelling of Crust Thickness for Silicon Purifying Process with Electron Beam	PO-123
Kaspars Traskovskis	Triphenylpentane Substituents Containing Molecular Glasses with Nonlinear Optical Activity	PO-124
Kaspars Pudzs	Charge Carrier Mobility in Thin Films of Glass Forming Low Molecular Organic Compounds	PO-125
Kaiva Luse	Reflectance and Multispectral Evaluation of Color Vision Asessment Plates	PO-126
Kairi Otto	Effect of Titanium(IV)Isopropoxide and Acetylacetone Molar Ratio in the Solution on Spray Deposited TiO_2 Films	PO-127
K.Konieczny	Influence of Compressive Stress on Dielectric and Ferroelectric Properties of the $(Na_{0.5}Bi_{0.5})_{0.7}Sr_{0.3}TiO_3$ Ceramic	PO-128
K. Chernenko	The Effect of Annealing on Spectra and Decay Time of X-Ray Luminescence of Zinc Oxide Powders	PO-129
K. Bormanis	Photorefractive Light Scattering In $LiNbO_3$:B, $LiNbO_3$:Y, $LiNbO_3$:Y:Mg, and $LiNbO_3$:Ta:Mg Crystals	PO-130
K. Bormanis	Ferroelectric Lead Nickel-Niobium Titanate Ceramics: Phase Transition Studies	PO-131
M. Antonova	Effects of Illumination on the Dielectric Response of Barium-Strontium Niobate Ceramics	PO-132
Jurgis Grube	Up-Conversion Luminescence of $NaLaF_4$ Doped With Tm^{3+} And Yb^{3+}	PO-133
Janis Latvels	Photoelectrical Properties of DMAB Derivatives as Materials For Solar Cells	PO-134
Jakob Jõgi	Role of Diffusion in Formation and Properties of Sol-gel Micro-Structures	PO-135
J.Gabrusenoks	Lattice dynamics of $CdWO_4$	PO-136
Ivo Romet	Thermally and optically stimulated luminescence in $Li_2B_4O_7$ doped with metal ions	PO-137
Ingars Reinholds	The effect of radiation modification on properties of poly(ethylene-1-octene) magnetic nanocomposites	PO-138
Ieva Kranauskaitė	Broadband dielectric investigation of $(Sr_{1-1.5x}Bi_x)TiO$ (x=0.15, 0.1, 0.05)	PO-139
Irina Kudryavtseva	Electronic excitations and self-trapping of electrons in $CaSO_4$	PO-140
I. Smeltere	Features of lithium niobate single crystals modified by rare earth admixtures	PO-141
Harijs Cerins	Improvement of sol-gel deposited ZnO:Al thin films by laser radiation	PO-142
Guna Doke	Synthesis and photoluminescence in Eu^{3+} doped $NaLaF_4$ material	PO-143
George Chikvaidze	Raman scattering analyses of defects in SiC	PO-144
Galyna Dovbeshko	Strong secondary emission of opal-based photonic crystal: light localization and defect luminescence	PO-145

Fatima U. Abuova	First-principles calculations of defects in MgF_2	PO-146
Elina Potanina	Photo-induced formation of surface relief in amorphous AS_2S_3 films	PO-147
Edvins Dauksta	Improvement of CdZnTe detector properties by laser	PO-148
E.V. Barabanova	Effect of porosity on the electrical properties of PZT ceramics	PO-149
Dorota Sitko	Dielectric properties of $BaTiO_3$ based materials with addition of transition metal ions with variable valence	PO-150
Dmitry V. Azamat	Fourier transform-EPR spectroscopy of transition metal ions in ZnO	PO-151
Barbara Garbarz-Glos	Structural, microstructural and dielectric spectroscopy study of functional ferroelectric ceramic materials based on barium titanate	PO-152
Aurimas Sakanas	Broadband dielectric investigation of barium titanate and nickel-zinc ferrite composite ceramics	PO-153
Arturs Zarins	Influence of Li_2TiO_3 on chemical reactivity of Li_4SiO_4 pebbles	PO-154
Ansis Mezulis	Application of sedimentation experiments with suspended nanoparticles	PO-155
Annika Pille	Investigation of iodine implanted C12A7 ceramics	PO-156
Anna Putnina	Multifunctional materials from hemp fibers treated with steam explosion technology	PO-157
Andris Lescinskis	Experimental setup for analysis of sorption and desorption of tritium in liquid lithium under different external conditions	PO-159
Andrejs Lusis	Investigation of carbonized layer on surface of NaAlSi glass fibers	PO-160
Andrejs Gerbreders	Photosensitive properties of composite films based on copper chloride in polymer matrix	PO-161
R. Kassymkanova	Pecularities of defect creation in LiF-WO_3, LiF- TiO_2 and LiF-Fe_2O_3 crystals under pulsed electron irradiation	PO-162
A. Zolotarjovs	TSL equipment development and application for crystalline silicon dioxide study	PO-164
Jelena Aleksejeva	Surface relief grating recording in AZO polymer films	PO-165
Aleksandr Pishtshev	A comparative DFT study of structural energetics and chemical bonding features in crystalline lithium borates	PO-166
Aivars Vembris	Energy structure and photoelectrical properties of glass forming pyranyliden derivatives in thin films	PO-167
A. Usseinov	First principles calculations of ZnO crystals doped with hydrogen	PO-168
A. V. Sorokine	First-principles calculations of electronic structure and phonon properties of Al- and H-doped ZnO	PO-169
A.S. Kuprin	Nanocrystalline tin films after deuterium ions irradiation	PO-170
A.I. Ivanova	Engineering aspects of multilayer piezoceramic actuators	PO-171
A. N.Trukhin	Luminescence of stishovite	PO-172
Andrius Dziaugys	Dielectric and electric properties of $CuFeP_2S_6$ crystal	PO-173

Dmiri Azamat	Pulse-EPR studies of transition metal impurities in $SrTiO_3$	OR-32
Poster Session: Synchrotron radiation		
A.I. Popov	VUV synchrotron radiation spectroscopy of PLZT ceramics	PO-176
Eduard Aleksanyan	X-ray excited emission of YAG and YAG:Nd^{3+} single crystals	PO-177
N.R. Krutyak	Temperature dependence of energy transfer to the luminescence centers in $ZnWO_4$ and $ZnWO_4$:Mo	PO-178
Mika Lastusaari	Local structures and valences of dopants in persistent luminescence materials	PO-179
Marek Oja	Luminescence studies of ultra-porous alumina nanopowders	PO-180
Lucas C.V. Rodrigues	Persistent luminescence of cadmium silicates	PO-181
Ivar Kuusik	X-ray spectroscopy of $Li_6YB_3O_9$ and $Li_6GdB_3O_9$ single crystals	PO-182
V. Pankratov	Ionic liquid-based synthesis and ultraviolet excitation spectroscopy of luminescent nanocrystals	PO-183
V. Pankratov	Origins of room temperature ferromagnetism and photoluminescence in co-concentrated $CO_XZn_{1-X}O$ films	PO-184
Tero Laihinen	Probing the local structure of ZrO_2:Yb^{3+},Er^{3+} up-conversion luminescence materials by X-ray absorption spectroscopy	PO-185
Tetiana Shalapska	Spectroscopic properties of Pr^{3+} -based polyphosphates doped with Ce^{3+} ions upon VUV-UV and X-ray excitation	PO-186
Sebastian Vielhauer	VUV photoluminescence spectroscopy setup at MAX III	PO-187
Poster Session: Sustainable Energetics		
A.N. Salak	Crystal structure of Cu-deficient phases in the(1-x)Cu_2S-xGa_2S_3 system	PO-188
Valery Garaev	Modification of nafion® membrane with 2-hydroxyethylammonium ionic liquids	PO-189
Teoman Taskesen	$Cu_2ZnGeSe_4$ monograin powder as absorber material for solar cells	PO-190
Tauno Tooming	Carbon materials for supercapacitor application by hydrotehrmal carbonization of D-glucose	PO-191
Natalia Maticiuc	Comparative study of CdS thin film properties on glass and ITO substrates	PO-192
Maris Pilvet	Synthesis of Cu_2ZnSnS_4 monograin powders in liquid phase of cadmium iodide for photovoltaic applications	PO-193
Liga Lasmane	Acidic ionic liquids as composite forming additives for ion-conducting materials	PO-194
A. Kainarbay	Luminescent materials based on nanoparticles of oxide silicon for solar cells	PO-195
Julija Pervenecka	Laser crystallization effects in amorphous silicon layers for solar cells	PO-196

Ineta Liepina	Preparation and characterization of nanostructured Fe-TiO_2 thin films	PO-197
Heisi Kurig	The effect of the properties of carbon materials on the hydrogen up-take	PO-198
Gunita Kolosovska	Quantication of impurities in solar silicon	PO-199
Karina Bikova	Preparation and electrochemical properties of $LiFePO_4$/C/graphene nanocomposite cathode for lithium ion batteries	PO-200
Einars Sprugis	Composite speek polymer membranes with acidic ionic liquids for high temperature pem fuel cells	PO-201
Guntars Vaivars	Glucose oxidase as a biocatalytic enzyme-based biofuel cell using nafion membrane limiting crossover	PO-203
Ainars Knoks	Optical, structural and photoelectric properties of multilayer TiO_2/$CoFe_2O_4$ thin films	PO-204

Nanomaterials

THE LUMINESCENCE OF $CaF_2:Eu^{3+}$ NANOPARTICLES

A. Zhyshkovych[1], V. Vistovskyy[1], N. Mitina[2], A. Zaichenko[2], T. Shalapska[3], A. Gektin[4], A. Voloshinovskii[1]

[1]Ivan Franko National University of Lviv, Ukraine, [2]Lviv Polytechnic National University, Ukraine, [3]Institute of Physics, University of Tartu, Estonia, [4]Institute for Scintillation Materials NAS of Ukraine, Kharkiv, Ukraine

e-mail: andrew-lviv@i.ua

The CaF_2 nanoparticles doped with Eu^{3+} ions attract attention as luminescent biomarkers which can be excited by optical and X-ray quanta. High penetration ability of X-rays and coinciding of $CaF_2:Eu^{3+}$ nanoparticles emission range with transparency region of biotissue may allow the visualization of processes deeply inside of biological tissue. In this work the dependence of luminescence parameters on the size of CaF_2-Eu^{3+} nanoparticles (20 – 135 nm) have been analyzed for different energies of excitation light in the range of 9 – 40 eV. Measurements were performed at SUPERLUMI station of HASYLAB in DESY, Hamburg. The $CaF_2:Eu^{3+}$ nanoparticles were synthesized by the low-temperature chemical methods.

The structure of the 4f-4f luminescence spectrum of Eu^{3+}-centers strongly depends on its local symmetry. This circumstance allows revealing the different sites of Eu^{3+}-centers in the crystal lattice. In the CaF_2-Eu^{3+} nanoparticles of $a > 40$ nm size one can observe two different Eu^{3+}-centers. In the transparency range of the CaF_2 matrix the Eu^{3+}-centers with dominating band at 590 nm ($^5D_0 \rightarrow {}^7F_1$) are mainly excited in the band of charge-transfer from F^- ions located in interstitial positions (6.8eV) [1]. Meanwhile, the Eu^{3+}-centers with 620 nm ($^5D_0 \rightarrow {}^7F_2$) dominating band are excited both in the band peaked at 6.8 eV and in the band of charge-transfer from F^- ions located in regular lattice sites (8.1 eV). The band peaked at 590 nm dominates in the emission spectra under excitation in the fundamental absorption range of the CaF_2 matrix. The small nanoparticles ($a < 40$ nm) reveal only one type of Eu^{3+}-centers. In the excitation spectra for small nanoparticles in the matrix transparency range only the band at 6.8eV is present. As the size of the CaF_2-Eu^{3+} decrease the efficiency of luminescence excitation in the fundamental absorption range of matrix strongly decreases.

References

1. E. Radzhabov, *Solid State Communications*, 2008**, 146**, 376.

SOL-GEL TECHNICS FOR PROCESSING TRANSPARENT AND CONDUCTIVE AL-DOPED ZINC OXIDE FILMS

Vladimir I. Kondratiev[1], Alexey E. Romanov[1,2], Ilmar Kink[1]

[1]*Institute of Physics, University of Tartu, Estonia*

[2]*Ioffe Physical-Technical Institute RAS, Russia*

e-mail: kondraty@ut.ee

Transparent conductive oxides (TCO) are optically transparent and electrically conductive thin layers. They are important components in the modern optoelectronic devices such as light-emitting diodes, solar cells, flat panel displays, optical switchers etc. To date, the industry standard in TCO is tin-doped indium-oxide (ITO). ZnO-based TCOs are promising to replace ITO for transparent electrode applications in terms of their electrical and optical properties [1-2]. They can be readily produced by the sol–gel process, which is preferential for large-scale coatings. Desirable properties of the films: transmittance > 85% in visible spectrum, low resistivity, cheap precursors and reproducible results.

Highly transparent films of aluminum doped zinc oxide (AZO) have been prepared. Optical transparency was over 90% at 550 nm for a thickness of 152 - 550 nm. AZO films from various metal-organic precursors were deposited by sol-gel method on different substrates and then characterized. Resistivity of ZnO films was measured by using 4-probe method; film transparency was measured using by Spectrophotometer; thickness was measured using by SEM. Element analysis was performed using by energy-dispersive X-ray spectroscopy. Dependence of resistivity and transmittance from aluminum content, temperature of annealing were studied. After varying several process parameters it was noticed that annealing in Ar decreases the resistivity greater then annealing in air. Longer exposition in Ar provides better results. Current research focuses on optimization of the technology for processing and characterization of transparent electrode materials based on AZO.

References

1. M.J. Alam, D.C. Cameron, *J. Vac. Sci. Technol. A.*, 2001, No.19, 1642-1646.

2. H. Wang, M.H. Xu, J.W. Xu, M.F. Ren, L. Yang, *J. Mater. Sci.: Mater. Electron*, 2010, No.21, 589-594.

NANOPARTICLE TRANSFER UNDER MAGNETIC FIELD IN A NONISOTHERMAL POROUS LAYER SATURATED WITH A FERROFLUID

Viesturs Sints, Elmars Blums, Michail Maiorov, Gunars Kronkalns
Institute of Physics, University of Latvia
e-mail of presenting author: viesturs.shints@gmail.com

Experimental investigation of magnetic nanoparticle distribution and transfer in a porous environment is conducted. While transfer of nanoparticles under influence of temperature gradient has been the subject of previous investigations [1], the current series of experiments and related theoretical investigation are aimed at a deeper understanding of nanoparticle redistribution in a porous environment subjected to both temperature gradient and a magnetic field. Under such conditions, particle redistribution from the initial uniform distribution is a result of osmotic and thermoosmotic forces, magnetic field-driven interactions between particles and, possibly, convective instabilities in particle flow.

The physical system is that of a porous environment made of ten layers, with total thickness of 1.3 mm, pressed between two plates of definite temperature, and, optionally, subjected to a magnetic field. Particle characteristics in each of the ten layers are measured at the end of a 24-hour experiment. Employed experimental technique of magnetometry allows us to learn not only particle concentration, but also their size distribution in each layer. Two ferrofluid samples of different ordinary Soret coefficient values are investigated. Measurements are performed at various temperature gradients applied across the layer in the presence of a magnetic field oriented parallel or transversal to the temperature gradient. The measurement results are interpreted taking into account the particle magnetophoretic slip velocity accompanied by thermoosmosis.

The work is supported by European Regional Development Foundation, Project 2011/0001/2DP/2.1.1.1.0/10/APIA/VIAA/007

References

1. E.Blums, G.Kronkalns, M.M.Maiorov, A.Mezulis, *Journal of Magnetism and Magnetic Materials*, 2005, No.289, 275-277.

CATALYTIC ACTIVITY OF NOVEL CERIA SUPPORTED NANO-SIZED PLATINUM CATALYST SYNTHESIZED BY EXTRACTIVE-PYROLYTIC METHOD FOR LOW-TEMPERATURE WGS REACTION

Vera Serga[1], Lidija Kulikova[1], Vladimir Georgiev[2], Todor Batakliev[2], Slavcho Rakovsky[2]

[1]*Institute of Inorganic Chemistry, Riga Technical University, Latvia,* [2]*Institute of catalysis, Bulgarian Academy of Science, Bulgaria*

e-mail: vera_serga@inbox.lv

Ceria (CeO_2) supported metal catalysts are of great interest in the modern catalytic industry because of its important applications, particularly in CO oxidation and water-gas-shift reaction (WGS), which recently seemed to be of most importance. The hydrogen produced from reformed gas, obtained through steam reforming of natural gas, for example, contains up to 12% CO [1], which can be poison for polymer fuel cells membranes. Thereby, WGS is preferred reaction for CO removal. Ceria-supported platinum catalysts were prepared by extractive-pyrolytic method [2] and were characterized by several methods as X-ray diffraction, TPR, TEM and EPR. The catalytic activity of the samples with different platinum loading, measured in the temperature range 140–350° C is represented in Fig. 1.

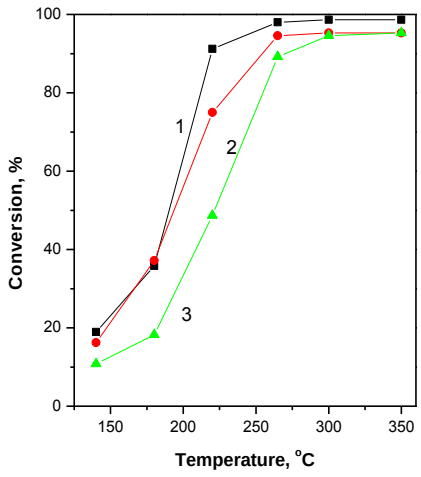

Fig.1. Effect of platinum loading on the WGS activity: (1) 1,2Pt/CeO_2; (2) 2,4Pt/CeO_2; (3) 4,8Pt/CeO_2.

References

1. R. Hwang, S. Shore, L. Ruettinger, W. Lampert, J. Giroux, T. Liu, Y. Ilinich, *Annual Review of Materials Research*, 2003, **33**, 1-27.
2. V.Serga, L.Kulikova, A.Cvetkov, A.Krumina, *IOP Conf. Series: Materials Science and Engineering*, 2012, No. 38, 012062.

PRODUCTION OF MONO- AND BIMETALLIC NANOPARTICLES OF NOBLE METALS BY PYROLYSIS OF ORGANIC EXTRACTS ON SILICON DIOXIDE

Vera Serga[1], Lidija Kulikova[1], Anton Cvetkov[1], Aija Krumina[1], Maris Kodols[1], Svetlana Chornaja[2], Konstantins Dubencovs[2], Elina Sproge[2]

[1]*Institute of Inorganic Chemistry, Riga Technical University, Latvia,* [2]*Faculty of Material Science and Applied Chemistry, Riga Technical University, Latvia*

e-mail: vera_serga@inbox.lv

The extractive-pyrolytic method was applied in [1] to produce Pt/SiO_2 nanocomposites by thermal decomposition of the tri-n-octylammonium salt ($[Oct_3NH]_2PtCl_6$) on SiO_2. The aim of this investigation is, first, to study the influence of salt Oct_3NH^+ anion ($PtCl_6^{2-}$, $PdCl_4^{2-}$, $AuCl_4^-$) nature on the phase composition and mean size of crystallites of the extract pyrolysis products on the SiO_2 nanopowder at the production of monometallic composites and, second, to prepare the bimetallic particles by thermal decomposition of two-component mixtures of extracts on the carrier.

The XRD phase analysis of the monometallic composites, produced under the same conditions, at the pyrolysis of Pt- and Au-containing extracts has shown the formation of nanoparticles of Pt (d_{Pt} = 15 nm) and Au (d_{Au} = 33 nm), respectively. The end product of the thermal decomposition of the Pd-containing extract has an admixture phase of palladium oxide along with the main metal phase (d_{Pd} = 21 nm). In order to produce bimetallic composites, the pyrolysis of mixtures of metallic extracts on the carrier was performed, and it has been found that the nanoparticles of PtPd alloy and PdO, as the admixture phase, are the products of the thermal decomposition of a mixture of Pt- and Pd-containing extracts; a mixture of Pt- and Au-containing extracts gives Pt and Au nanoparticles; a mixture of Pd and Au-containing extracts provides nanoparticles of Pd, Au and PdO.

The catalytic properties of the produced composites were studied in the reaction of glycerol oxidation by molecular oxygen in alkaline aqueous solutions, and it has been shown that the monometallic gold- and palladium-containing composites are practically non-active in contrast to the platinum-containing composites. At the same time, all bimetallic composites exhibit catalytic activity, moreover, the platinum-containing nano-composites are much more active.

Acknowledgments

This work was supported by the ERAF project No. 2010/0304/2DP/2.1.1.1.0/10/APIA/VIAA/087.

Reference

1. V.Serga, L.Kulikova, A.Cvetkov, A.Krumina, *IOP Conf. Series: Materials Science and Engineering*, 2012, No. 38, 012062.

SYNTHESIS AND THERMAL DEOXYGENATION OF GRAPHITE OXIDE

Valdis Kampars (presenting author), Kristīne Lazdoviča, Kristaps Māliņš (example co-authors)
Riga Technical University, LV 1048 Riga, Latvia
e-mail of presenting author: kampars@ktf.rtu.lv

The thermal or solvothermal exfoliation and deoxygenation of graphene oxide is less complicated and more easily controllable method than the chemical reduction and thus could give a more effective way for production of well-defined graphene sheets. In order to obtain preliminary information about the thermal characteristics of graphite oxide we have synthesised the graphene oxide accordingly to the modified Hummer's method [1] and after the treating with organic solvent and draying under vacuum made the thermogravimetric analysis and microwave assisted deoxygenation of the obtained product. The FTIR spectra with characteristic absorption of OH, C=O, C=C, C-O and C-O-C group and XRD patterns with intensive peak at $2\theta \sim 10.5^{o}$ corresponding to a layered structure with an interlayer distance higher than 0.8 nm corroborate the graphite oxide structure of the sample before the heating. The TG investigation shows, than the heating rates exceeding 1 ^{o}C/min set off an explosion like mass loss at 130 ^{o}C indicating the near to full deoxygenation and spontaneous defoliation of graphite oxide.

The FTIR spectra of products throw out from the sample pan during the TG experiments as well as the spectra of the products obtained by microwave treatment do not show the presence of oxygen atom containing bond absorption. The deoxygenation temperature for obtained product is remarkably lower than characteristic temperatures of graphene deoxygenation [2].

Acknowledgement

The financial support from the Program "IMIS" is gratefully acknowledged.

References

[1] X.Wang, W.Dou. *Thermochimica Acta*, 2012, Vol.529, 25-28.

[2] No: K.Yin, H.Li, Y.Xia, H.Bi, J.Sun, Z.Liu, L.Sun. *Nano-Micro Lett*., 2011, Vol.3, No.1, 51-55.

CONJOINED STRUCTURES OF CARBON NANOTUBES AND GRAPHENE RIBBONS

V. Krasnenko[1], V. Boltrushko[1], V. Hizhnyakov[1], M. Klopov[2]

[1]*Institute of Physics, University of Tartu, Riia 142, 51014 Tartu, Estonia*

[2]*Tallinn University of Technology, Ehitajate tee 5, 19086 Tallinn, Estonia*

e-mail: veera.krasnenko@ut.ee

In the last few years the hybrid materials built from combined structures of carbon nanotubes (CNT) and graphene ribbons (GNR) have attracted considerable attention. It is expected that these materials may have new important mechanic, electric and catalytic properties, and can act as energy and hydrogen storage. In this communication we have performed a numerical study of some CNTs and GNR structures. A series of MD simulations of GNRs and CNTs have been performed by using LAMMPS, Material Studio and VASP software packages.

The typical total number of carbon atoms included in our MD simulations when using a LAMMPS package was several thousands. The diameter of nanotubes was varying from 1.5 nm up to to 0.4 nm. It was found that all nanotubes, except the smallest ones (with diameter less than 0.5 nm) may be entirely wrapped over by GNR. The distance between the wrapped ribbon and the nanotube is 0.34 nm - the typical distance between graphene sheets. If the length of the nanotube is smaller than the width of the ribbon then, depending on the difference of the width of CNT and GNR, the latter may be wrapped around the CNT (narrow ribbon) or bent to an angle. In case the CNT was initially situated at the end of the long GNR with a fixed position of its end, the nanotube was revolving upon the GNR.

To check the results, we have also performed the calculations of GNRs and CNTs, using a CASTEP module of Material Studio and a VASP package, allowing one to include into calculations the exchange correlation functional. In these calculations, to optimize the geometry, one calculates electronic densities, electronic energies and the corresponding forces to the atoms by using a super-cell technique. As compared to LAMPS, this algorithm is rather time-consuming. Therefore, the calculations were made for relatively small super-cells which include several hundreds of atoms. We have found that the CNT with GNR wrapped around it at a distance 0.34 nm indeed form a static structure.

The research was supported by the project IUT2-27 and by the European Union through the European Regional Development Fund (project 3.2.0101.11-0029).

NOVEL ANTI-WEAR LUBRICANT BASED ON NANOPARTICLES/IONIC LIQUID COMBINATION

Triinu Taaber[1,2], Kaija Põhako-Esko[1,2], Kristjan Saal[2], Rünno Lõhmus[2], Uno Mäeorg[1], Ilmar Kink[2]

[a] *University of Tartu, Institute of Chemistry, 14a Ravila St.,50411, Tartu, Estonia*
[b] *University of Tartu, Institute of Physics and Estonian Nanotechnology Competence Center,142 Riia St., 51014, Tartu, Estonia*
email: triinu.taaber@ut.ee

Nowadays the production and development of lubricating oils is a vast technological sphere which is continuously growing because of the ongoing needs for reducing energy and material losses in mechanical devices. The lubricant performance is usually enhanced by various additives that improve its chemical durability, lubricating efficiency and contaminant binding ability.

The aim of the present study is to investigate the applicability of nanoparticles/ionic liquid composites as novel protective lubricating films for metal wear parts. Either nanoparticles or ionic liquids independently have been shown to exhibit exceptional lubricating qualities[1,2]. However, the combinations of the two have not been demonstrated before.

Ionic liquids have remarkable lubrication and anti-wear capabilities as compared with lubrication oils in general use. Ionic liquids are suitable at harsh friction conditions that require high thermal stability and chemical inertness[3]. There is a very wide range of different ionic liquids and their properties can be modified by selection of suitable cation and anion.

In current study different imidazolium and bis-imidazolium ionic liquids with TFSI (bis(trifluoromethane)sulfonimide) and FAP (trifluorotris(pentafluoroethyl)phosphate) anions were investigated. To obtain better adhesion with lubricated surface polar functional groups were added to ionic liquid cation structure. Ionic liquids were combined with differently functionalized carbon nanotubes and obtained mixtures were tested with standard tribological tests. The combination of nanoparticles/ionic liquid can significantly reduce the long-term instability and clustering of the particles in suspensions (e.g. oil suspensions), as it is well known that ionic liquids are highly effective stabilizer for nanoparticles[4]. In addition, the novel type lubricant has many advantages and can also widen the range of applications, e.g. wider temperature range and preserved functionality at harsh conditions where oil-based lubricants fail.

---

[1] M.-D. Bermúdez, A.-E. Jiménez, J. Sanes, F.-J. Carrión, *Molecules* **2009**, *14*, 2888-2908.

[2] V.N. Bakunin, A.Yu. Suslov, G.N. Kuzmina, O.P. Parenago. *J. Nanopart. Res*., **2004**, 6, 273–284.

[3] I. Minami, *Molecules* **2009**, *14*, 2286-2305.

[4] J. Dupont, J. D. Scholten, *Chem. Soc. Rev.*, **2010**, 39, 1780–1804.

SPECTRAL CHARACTERIZATION OF AlGaN NANOMATERIALS WITH TUNABLE BANDGAP

J. Grigorjeva[1], B. Berzina[1] L.Trinkler[1], V.Korsaks[1], Li-Chyong Chen[2], Kuei-Hsien Chen[2], and K. Jarasiunas[3]

[1]*Institute of Solid State Physics, University of Latvia, 8 Kengaraga, 1063 Riga, Latvia*

[2]*Center for Condensed Matter Sciences, National Taiwan University, Taipei 106, Taiwan*

[3]*Institute of Applied Research, Vilnius University, Vilnius 10222, Lithuania*

e-mail: baiber@latnet.lv

Ternary AlGaN is a wide band gap semiconductor with the variable energy band gap within a large energy range between 6,1 eV a nd 3,4 eV depending on ratio of Al and Ga content in material affecting exciton luminescence, which also demonstrates a tunable spectral position within a deep ultr aviolet (UV) spectral region as it is shown in research of Nepal et al [1].

The present report is devoted to investigation of lum inescence properties of ternary $Al_xGa_{1-x}N$ nanostructures – nanorods and thin layers synthesized in National Taiwan University using th ermo chemical evaporation (T-CVD) and metalo rganic chemical evaporation (MOCVD) m ethods. The obtained m aterials were characterized using X-ray structure analysis (XRD) and m icroscopy methods (SEM). The photolum inescence (PL) spectra were st udied for $Al_xGa_{1-x}N$ nanostructures when x var ies within a small range: $0{,}015<x<0{,}12$.

The $Al_xGa_{1-x}N$ materials were irradiated with 263 nm laser light and photolum inescence spectra were stud ied within a tem perature range 17 - 300 K. The observed luminescence forms a single band around 360 nm which is related to the bound excitons. Increase of sample temperature results in a decrease of the lum inescence intensity and in the “read shift” of the luminescence band peak position ($\Delta\lambda$=6 nm). The results observe d can be r elated to the temperature-induced destruction of the bound exc itons and an influence of the tem perature on the band gap.

References

1. N.Nepal, J.Li, L.Nakarmi, J.Y.Lin, H.X.Jiang, Appl. Phys. Letters **88** (2006) 062103.

TECHNET_NANO – THE COOPERATION NETWORK OF CLEAN ROOMS IN BALTIC SEA REGION

Toomas Plank, Margus Kodu, Raul Rammula
Institute Physics, University of Tartu, Estonia
e-mail: Toomas.Plank@ut.ee

The network of Baltic Sea Region (BSR) clean rooms, Technet_nano [1], offers to small and medium sized enterprises (SME) the access to clean room facilities. It is a BSR project [2], financed by European Union (Fig. 1). Seven partners – SDU in Denmark, KTH and Acreo AB in Sweden, CAU and WTSH in Germany, University of Latvia in Latvia, Kaunas University of Technology in Lithuania - own the clean room.

Sometimes the suitable clean room is not even in the same but in neighbouring country. All Technet_nano partners are the access points to the network partners. They help to get access to clean rooms and other research facilities at partners labs.

Tartu University builds his own clean room in a new building of Institute of Physics, which will be ready in year 2014. At the moment, a working clean room (see Fig 2) in Tartu is at premises of Tartu Science Park [3].

Fig.1 Technet_nano is a BSR project, financed by European Union.

Fig.2 The clean room in Tartu Science Parks Nanolab, operated by Estonian Nanotechnology Competence Center.

References

1. Technet_nano http://www.technet-nano.eu
2. The Baltic Sea Region Programme 2007-2013 http://eu.baltic.net/
3. Tartu Science Park http://www.teaduspark.ee/en

ATOMIC LAYER DEPOSITION OF NANOSTRUCTURAL TiO_2 FILMS ON Si, α-Al_2O_3 AND RuO_2

Tõnis Arroval[1], Kristel Möldre[1], Aivar Tarre[1], Ahti Niilisk[1], Hugo Mändar[1], Boris Hudec[2], Kristina Hušekova[2], Karol Fröhlich[2], Jaan Aarik[1]

[1]*Institute of Physics, University of Tartu, Estonia*

[2]*Institute of Electrical Engineering, Slovak Academy of Sciences, Bratislava, Slovakia*

e-mail: tonis.arroval@ut.ee

Rutile-type TiO_2 films with thicknesses below 10–15 nm have attracted great interest as very prospective high-κ dielectric layers of DRAM structures. In this application, local epitaxy of TiO_2 on RuO_2 bottom electrodes plays crucial role in determination of required dielectric properties. Therefore we investigated atomic layer deposition (ALD) of TiO_2 from $TiCl_4$ and H_2O on RuO_2/Si as well as on Si(100) and α-Al_2O_3 substrates at various growth temperatures (T_G), concentrating on structure development in films with thicknesses of 12–25 nm. According to the results obtained, amorphous to crystalline (anatase) growth transition takes place and density increases close to the bulk anatase value (3,7 g/cm^3) with the increase of T_G to 200–225°C in case of all substrates. Anatase to rutile transition together with the increase of density up to 4.2 g/cm^3 can be seen on r-sapphire and RuO_2/Si at 225–250°C. Structure analysis of films deposited on c-sapphire substrates at T_G > 425°C revealed rutile and orthorhombic (TiO_2-II) phases.

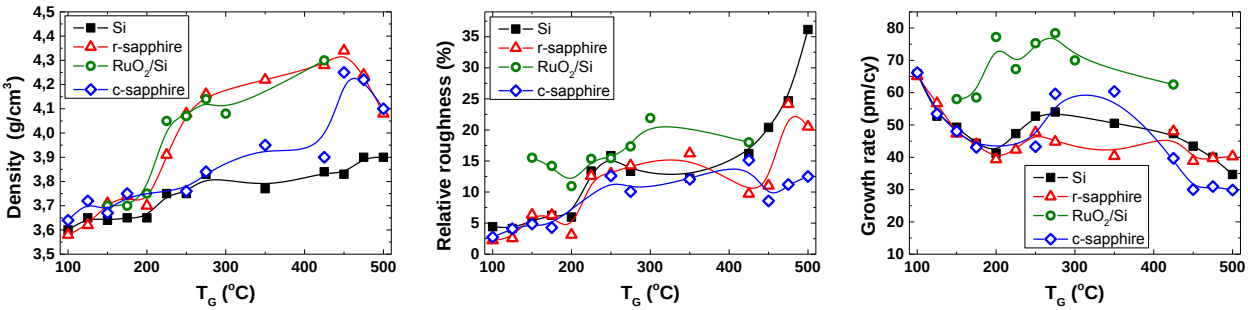

Fig.1 Parameters determined from XRR measurements.

Crystallization caused rapid increase of surface roughness at T_G = 200–225°C. Another region of surface roughening was observed for films deposited on r-sapphire at 475–500°C. Increase of roughness along with a decrease of density at these temperatures could be explained by Stranski-Krastanov type of growth. TiO_2 on RuO_2/Si showed the highest growth rate values at all temperatures used. This was related to surface roughness of RuO_2 and much shorter incubation period in the beginning of film growth on these substrates compared with the other substrates used.

TEMPERATURE INDUCED REVERSAL OF OXYGEN RESPONSE IN CVD GRAPHENE ON SiO_2

Tauno Kahro[1], Jekaterina Kozlova[1], Jaan Aarik[1], Lauri Aarik[1], Harry Alles[1], Aare Floren[1], Alar Gerst[1], Raivo Jaaniso[1], Aarne Kasikov[1], Ahti Niilisk[1] and Väino Sammelselg[1,2]

[1]Institute of Physics, University of Tartu, [2]Institute of Physical Chemistry, University of Tartu

e-mail of presenting author: tauno.kahro@ut.ee

Graphene as a two-dimensional material has every atom at its surface and possesses thus a great potential for the use in chemical sensors. In this work we prepared graphene samples on polycrystalline Cu foil using chemical vapour deposition (CVD) method. Next, graphene was transferred from copper onto the top of Si/SiO_2 substrate with Ti/Au electrodes that had been deposited trough the shadow mask by electron beam evaporation.

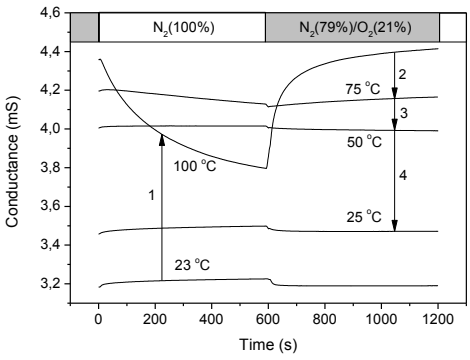

Fig.1 Temperature dependence of gas sensor response to changes of gas composition (nitrogen and synthetic air). The arrows (marked with 1 to 4) show the order in time how the temperature was changed.

A resistive graphene-based gas sensor prepared in this way revealed n-type oxygen response at room temperature and we have fitted the data obtained with varying oxygen levels using a Langmuir model. p-Type oxygen response of our sensor was observed after the temperature was rise to 100 °C, with a reversible transition to n-type behaviour when the temperature was lowered back to room temperature.

Such change in the response type was interpreted as a result of balance inversion between the change of charge carrier density and mobility at oxygen adsorption with temperature.

GROWTH OF ZINC OXIDE NANOSTRUCTURED LAYERS ON SNO2 ELECTRODES BY SPRAY PYROLYSIS

Tatjana Dedova[1], Olga Volobujeva[1], Inga Gromõko[1], Valdek Mikli[2], , Arvo Mere[1], Malle Krunks[1]

[1]Department of Materials Science, Tallinn University of Technology, Estonia, [2]Centre of Materials Research, Tallinn University of Technology, Estonia,

e-mail: tatjana.dedova@ttu.ee

ZnO nanostructured layers comprizing nanorods were deposited by spray pyrolysis method on series of different SnO2/glass substrates. ZnO layers were deposited by chemical spray pyrolysis (CSP) using zinc chloride aqueous solutions at growth temperatures of 550° C. SnO_2/glass substrates were purchased from different supplies and differ by morphology, grain size and roughness of SnO_2 electrode. The SnO2/glass substrates and ZnO layers grown on it were characterised with the help of XRD, AFM, high resolution SEM, EDX methods. The relationship between nanorod formation and substrate properties was studied. It was found that substrate morphology, crystal structure, and roughness influence the ZnO nanorods formation. Deposition of nanorods (d=200 nm, L=1 μm) was successful on the SnO_2 layers with grain sizes around 50-70 nm, whereas large-grained SnO_2 (grain size > 150 nm) resulted in thick, low-aspect ratio crystals with diameter around 400 nm and length of about 400 nm.

NANOSTRUCTURED LAYERS OF ZINC SULFIDE OBTAINED BY SPRAY PYROLYSIS

Tatjana Dedova[1], Inga Gromõko[1], Valdek Mikli[2], Olga Volobujeva[1], Ilmo Sildos[3], Kathriin Utt[3], Arvo Mere[1], Malle Krunks[1]

[1]Department of Materials Science, Tallinn University of Technology, Estonia, [2]Centre of Materials Research, Tallinn University of Technology, Estonia, [3]Institute of Physics, University of Tartu, Estonia

e-mail: tatjana.dedova@ttu.ee

The ZnS nanostructured layers formation, composition, structure, morphology, dimensionality and orientation of the ZnS crystals as well as optical properties were investigated with respect to the growth temperature, precursors (zinc chloride and thiocarbamide) molar ratio, substrate type (glass, glass/TCO) and solvent type. The films were grown at different temperatures in the range of 350–550 ˚C at precursors molar ratios of 1:1, 1:2 and 1:3. SEM, XRD, EDS, UV-VIS and PL spectroscopy were applied to characterize the properties of ZnS layers.

Dense ZnS thin films formed at temperatures around 400 ºC were transformed to structured layers if grown at temperatures around 450 ºC or above. Structured ZnS layers comprising rod-like crystals with preferred c-axis orientation could be grown at temperatures around 500-550 °C using $ZnCl_2$ and thiocarbamide at molar ratios of Zn:S at 1:2 and 1:3. According to XRD analysis, additional ZnO phase was detected in 1:1 ZnS layers deposited at T_S=550ºC while this phase was not detected for the layers obtained from the 1:2 and 1:3 solution at this temperature. According to UV-VIS spectroscopy the Eg of ZnS layers obtained from 1:2 and 1:3 solution are 3.7 eV, which corresponds to ZnS of wurzite structure. Dimensions of the ZnS layers can be controlled by deposition temperature, precursor concentration, and solvent type. PL measurements reveal near band-gap emission centered at 3.8 eV and broad trap-state emission at ~2.70 eV in all studied samples. Relative intensity of trap-state emission to band-gap emission depends on the deposition temperature and precursors molar ratio in the spraying solution. In general, it was found that trap-state emission decreases with increase of sulphur content.

IRON OXIDE NANOPARTICLES BY PRECIPITATION FROM FERROUS SOURCE: STRUCTURAL PHASE TRANSFORMATION DEPENDENCE ON SYNTHESIS PARAMETERS AND ANNEALING

A. Sutka[1], S. Lagzdina[1], T. Käämbre[1*], R. Pärna[2], V. Kisand[2,3], G. Mezinskis[1], J. Kleperis[3], M. Maiorov[4], I. Kuusik[1], A. Kikas[1], D. Jakovlev[5]

[1]*Institute of Silicate Materials, Riga Technical University, Azenes 14/24, Riga 1048, Latvia,*

[2]*Institute of Physics, University of Tartu, Riia 142, 51014 Tartu, Estonia*

[3]*Institute of Solid State Physics, University of Latvia, Kengaraga 8, Riga, LV-1063, Latvia*

[4]*Institute of Physics, University of Latvia, Miera 32, Salaspils, LV-2169, Latvia*

[5]*Estonian Nanotechnology Competence Center, Riia 142, 51014 Tartu, Estonia*

[6]*Riga Biomaterials Innovation and Development Centre, Riga Technical Univ., Riga, Latvia*

*e-mail: tanel.kaambre@ut.ee

Magnetite (Fe_3O_4) nanoparticles have found extensive scientific and technological applications, such as ferrofluids, data storage materials, photocatalysts, for water splitting under visible light, nanoparticle adsorbents for detoxication of biological fluids or removal of the heavy metals.

Monophasic magnetite monodisperse nanoparticles ~30 nm in diameter were precipitated by NaOH from ferrous salt aqueous solution in air atmosphere. The influence of the solution molarity, precipitator agent drop rate and stirring time on the powder morphology, phase purity and magnetic properties was studied by using SEM, XRD, DTG, XPS, VSM and (FY)XAS analysis. Remarkable influence on grain size, morphology and phase purity was observed. XRD analysis and the comparison of Fe 2p fluorescence yield X-ray absorption spectra to reference compounds[1] shows that it is possible to obtain monophasic Fe_3O_4 or mixture of γ-Fe_2O_3, α-Fe_2O_3 and FeOOH with FeOOH dominance by regulating synthesis parameters. Magnetite nanoparticles shown high saturation magnetization (85.84 emu/g) and composition mainly of magnetite with little or no maghemite phase.

References

1. D. H. Kim, H. J. Lee, G. Kim, Y. S. Koo, J. H. Jung, H. J. Shin, J.-Y. Kim, and J.-S. Kang , Phys. Rev. B 79 (2009) 033402.

ATOMIC LAYER DEPOSITION OF ALUMINIUM OXIDE ON SILICON CARBIDE NANOPOWDER

Taivo Jõgiaas[1], Lauri Kollo[2], Jekaterina Kozlova[1], Aile Tamm[1], Irina Hussainova[2] Kaupo Kukli[1,3]

[1] University of Tartu, Institute of Physics, Department of Materials Science, Riia 142, EE-51014 Tartu, Estonia, [2] Tallinn University of Technology, Department of Materials Engineering, Ehitajate tee 5, EE-19086 Tallinn, Estonia, [3] University of Helsinki, Department of Chemistry, P.O. Box 55, FI-00014, Univ. Helsinki, Finland

e-mail: taivo.jogiaas@ut.ee

Atomic layer deposition (ALD) is one of the most applicable methods for the conformal growth over three-dimensional substrates [1]; therefore it can be used for deposition of films onto porous objects [2]. In the present work the ALD routine was explored for treatment of consolidated to green body SiC powder with avarage particle size of 40 nm.

SiC tablets were pressed in a 20x20 mm die at 96 MPa. Avarage tablet densities were 1.3 g/cm^3. Consolidated porous green bodies were coated by about 10 nm thick Al_2O_3 at 300 ^{0}C, using $Al(CH_3)_3$-H_2O based ALD process. A pre-treatment of 10 cycles of only $Al(CH_3)_3$ (10 s pulse and 20 s purge) was used to eliminate water in pores. Then, 100 cycles (10s/10s/10s/30s pulse times of $Al(CH_3)_3$, N_2, H_2O, N_2, respectively) of alumina deposition was conducted. Phase composition, coating conformality and residual porosity of coated SiC was analyzed. Gained information is considered for designing of nanocomposites using ALD as a possible route.

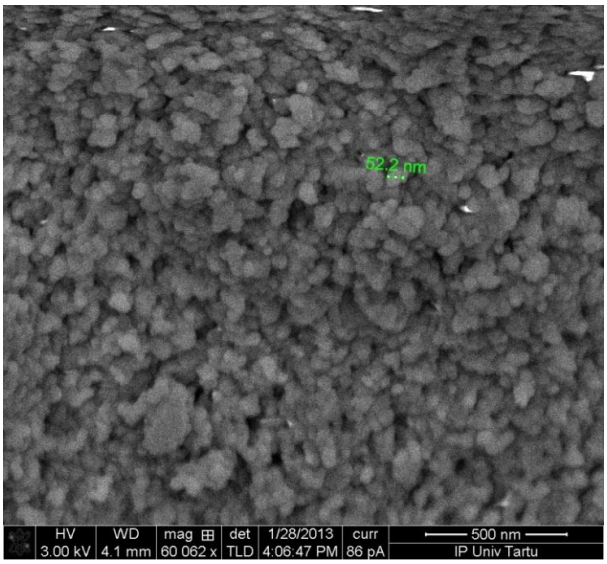

Fig. 1. Scanning electron microscopy image of alumina coated SiC nanoparticles. Carbide particles initial mean size 40 nm.

References:

1. V. Miikkulainen, M. Leskelä, M. Ritala, R. L. Puurunen. Crystallinity of Inorganic Films Grown by Atomic Layer Deposition: Overview And General Trends. J. Appl. Phys. 113, (2013), 021301.

2. Oliver J. Kilbury. Atomic layer deposition of solid lubricating coatings on particles. Powder Technology 221 (2012) 26-35.

IMPROVEMENT OF UV PROTECTION PROPERTIES OF THE TEXTILE FROM NATURAL FIBRES BY THE SOL-GEL METHOD

Svetlana Vihodceva[1], Silvija Kukle[2]

[1]*Institute of Textile Materials technology and Design, Riga technical University*

e-mail of presenting author: Svetlana.Vihodceva@rtu.lv

In this research pure cotton textile has been modified by the sol-gel technology to implement zinc oxide nano-level coating on textile surface to ensure ultraviolet (UV) radiation protection.

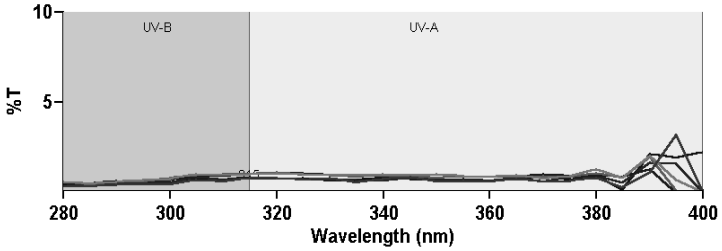

Fig.1 UVA and UVB transmission graphic after sample treatment.

One of the advantages of this method is the possibility to obtain thin layers on various materials, as well as the sol-gel layers can cover all fibres with enough high adhesion. Comparison of coatings of samples prepared using different concentrations of TEOS in nano-sols and thermal post-treatment of samples was made. Scanning electron microscopy (SEM) has been used to examine the nature of the surface modification after textile coating and laundering tests. Before and after laundering UV protective properties of the fabric samples were determined according to the standard, results show that textiles after treatment with nano-sol have excellent UV protection properties (UPF rating 50+ according to the standard - excellent protection). Analyses based on the SEM and spectrophotometer measurements show that obtained textile coatings are distributed evenly, not only on surface of yarns but in the depth of textile material as well, and are resistant to exploitation processes. After 50 drying-washing cycles defects of coatings not observed, the UPF ratings are still 50+ UPF that testify that treated fabric after exploitation simulation still provide excellent UV protection.

This work has been supported by the European Social Fund within the project «Support for the implementation of doctoral studies at Riga Technical University».

ALIGNING NANO-WIRES FOR ANISOTROPIC SPECTRAL PROPERTIES

Silver Leinberg[1,2], Martin Timusk[1,2], Vambola Kisand[1,2], Ergo Nõmmiste[1], Rünno Lõhmus[1,2], Kristjan Saal[1,2]

[1]*Institute of Physics, University of Tartu, Estonia*

[2]*Estonian Nanotechnology Competence Center, Estonia*

e-mail: silver.leinberg@ut.ee

Raising demand for energy efficient buildings has led to various thermal isolation techniques for windows. In addition to using multiple layers of glass in glazing unit, it is also possible to cover a glass with low emission film. These kinds of films can be made to reflect infra-red radiation and therefore reduce the amount of thermal energy passing through. It is possible to use films which reflect either in near infra-red (Solar radiation) or far infra-red (radiation from household), but their spectral properties are static, without the way to change their infra-red blocking properties. For example in the spring and autumn the Solar radiation which passes through windows would be useful for heating, yet in summer it would raise room temperature to uncomfortably high level and so would be unwanted.

This work investigates possibilities to develop glazing unit with changeable infra-red blocking properties. For this purpose it was studied different metallic nano-wires suspended in optically transparent polymerizable viscous media. After applying external magnetic- (for magnetic nano-wires) or electric field, nano-wires become aligned and exhibiting anisotropic spectral properties. Spectroscopic measurements of aligned nickel nano-wires in polymer showed anisotropic properties when incident light was directed collinear or perpendicular to nanowires. For example transparency for radiation with wavelength 2000 nm is 55 % in parallel, compared to 30 % in direction perpendicular to nano-wires.

This work was supported by Estonian Ministry of Defence.

Core-shell silica-gold nanoparticles for control of fluorescence in the sol-gel films activated by rare earth

Siim Heinsalu[1], Leonid Dolgov[1], Sergii Mamykin[2], Siim Pikker[1], Kathriin Utt[1], Ilmo Sildos[1]

[1]*Institute of Physics, University of Tartu,* [2]*V. Lashkaryov Institute of Semiconductor Physics of National Academy of Sciences of Ukraine*

e-mail of presenting author: gepard92@ut.ee

Development of metal enhanced fluorescence is stipulated by needs of sensitive optical detection and microscopy [1]. This method implies the placement of fluorophore near the noble metal film or nanoparticle. Spectral overlapping of the light induced plasmon resonance from such metal objects with the absorption or emission bands of the fluorophore can result in increase of local fluorescence intensity, changes in polarization and direction of the emitted light. At the same time, up to our knowledge, using of plasmonic dopants in the active fluorescent sol-gel films and waveguides is quite rare [2]. It is probably caused by non-trivial procedure of incorporation and stabilization of nanoparticles in sol-gel materials. Small particles of metal have non-uniform size and shape, which complicates tuning of spectral position for the surface plasmon resonance.

Inequality in nanoparticles' sizes can be overcome by initial preparation of uniform dielectric cores and further their covering by metal shell [3]. We propose silica-gold core-shell nanoparticles as plasmonic dopant for enhancement and control of fluorescence in TiO_2:Sm^{3+} sol-gel films. Water solutions of small gold particles 15-20 nm were prepared. These particles were attached to the surface of uniform spherical silica cores 180-200 nm. Solutions demonstrated plasmonic resonance absorption band near 550 nm. Silica-gold particles were redispersed in the butanol and added to the TiO_2:Sm^{3+} sol precursor. This precursor was spincoated on the glass substrates and annealed at 500°C. As a result TiO_2:Sm^{3+} films doped by minute amount of gold nanoparticles were obtained. Distribution of gold nanoparticles inside the films was visualized by dark field microscopy method. Greenish-yellowish color of light dots in the film can be associated this plasmonic light scattering by gold nanoparticles. Preliminary measurements of Sm^{3+} fluorescence testifies about 1.5 times increased emission detected from the samples doped with gold nanoparticles in comparison with undoped ones.

References

1. K.Ray et al., *Adv. Biochem. Eng. Biot.*, 2010 Vol. 116, 29-72.
2. A.C.Marques, R.M. Almeida, *J. Non-Cryst. Solids*, 2007, Vol. 353, 2613–2618.
3. Tan Pham et al., *Langmuir*, 2002, Vol. 18, 4915-4920.

GENERATION OF METAL NANOPARTICLES IN CATHODE SPOTS OF PULSED DISCHARGES

Sergey Tsarenko, Aleksandr Lissovski, Evgeni Shulga, Sander Mirme, Janek Uin, Eduard Tamm, Aleksei Treshchalov

Institute of Physics, University of Tartu, Estonia

e-mail of presenting author: tsarenko@fi.tartu.ee

Pulsed (~10 ns) discharge in abnormal glow or spark regimes has been organized in the flowing inert gas (He, Ar) at atmospheric pressure. Cathode is a thin metal wire inserted into an alumina tube with the inner diameter of 1 mm, the grounded anode ring is placed at the end of the tube, the length of the discharge is 2-10 mm. Simultaneous ignition of many microscopic cathode spots has been observed at the peak of the discharge current pulse. The local breakdown of the cathode layer in cathode spots is caused by a field-enhanced thermionic emission of electrons from microprotrusions, rapidly switched to the explosive emission. A dense metallic vapor cloud released from the spot is rapidly cooled by adiabatic expansion to the gas, followed by the supersaturation/nucleation of vapors leading to the formation of metal nanoparticles. In the glow discharge, short-lived cathode spot as a powerful microscopic (~10 μm) reactor, allows reaching superior small sizes and narrow size distribution of synthesized nanoparticles compared with the spark regime. Fe, Cu, Au, W-nanoparticles were successfully produced during this work.

Time-resolved spontaneous emission VUV-VIS spectra have been measured to clarify kinetics of excitation and recombination for neutral and ionic excited species in plasma.

Size distributions of positively and negatively charged as well as neutral nanoparticles were analysed by two different electrical aerosol spectrometers: 0.8-40 nm for charged, and 2-40 nm for neutral particles. Aerosol from the reactor output was diluted 40-fold by filtered air to suppress coagulation (agglomeration) and to decrease concentrations for particle distribution measurement. By controlling the inert gas flow rate (2-0.02 l/min), the mean particle size (mobility equivalent diameter d) can be varied from as small as 2 nm up to 20 nm and above. For example, for Fe particles with d = 3 nm, the total concentration of neutral particles before dilution was 6.3×10^{8} cm^{-3}, the concentration of charged particles was 2.2×10^{7} cm^{-3} that corresponds to 3.3% for both polarities. Particle size distribution can be approximated by lognormal function with $\sigma_g \approx 1.3$.

Produced nanoparticles were precipitated on the Si substrate and analyzed by SEM and EDX techniques. Due to poor resolution, the small primary particles (~1-5 nm) were not visible; however their agglomerates (~10-30 nm) were clearly detected.

SEGREGATION ON THE SURFACE OF TITANIUM STEEL 12CR18NI10TI EXPOSED ELECTRON BEAM

Sergey Plotnikov, Nazgul Yerdibayeva
East Kazakhstan State Technical University, 69 Protozanov, Ust-Kamenogorsk, the Republic of Kazakhstan
e-mail of presenting author: plotsv@ektu.kz

To support the research program in Kazakhstan material TOKAMAK KTM the stand of simulation tests was designed (FIC). The installation working on the beam-plasma discharge is used to generate plasma. The irradiation of samples by continuous electron beam was carried out in this installation. The aim of the work on the simulation stand is to obtain data of the degradation degree of construction materials samples surface under the influence of the electron beam exposure and plasma discharge.The work objective is to study the structural and phase changes of the surface under the influence of the continuous electron beam on construction steel 12Cr18Ni10Ti.

Experiment

Study of the structural and phase changes of the samples surface after exposure by continuous electron beam is performed on a scanning electron microscope JEOL JSM-6390LV with energy dispersive microanalysis attachment INSA Energy.

Four heat-affected zones are clearly distinguished on the Plates of titanium precipitates are clearly visible in the central zone. The experiment shows that islet thin films of Ti is formed in the scopes of electron beam.

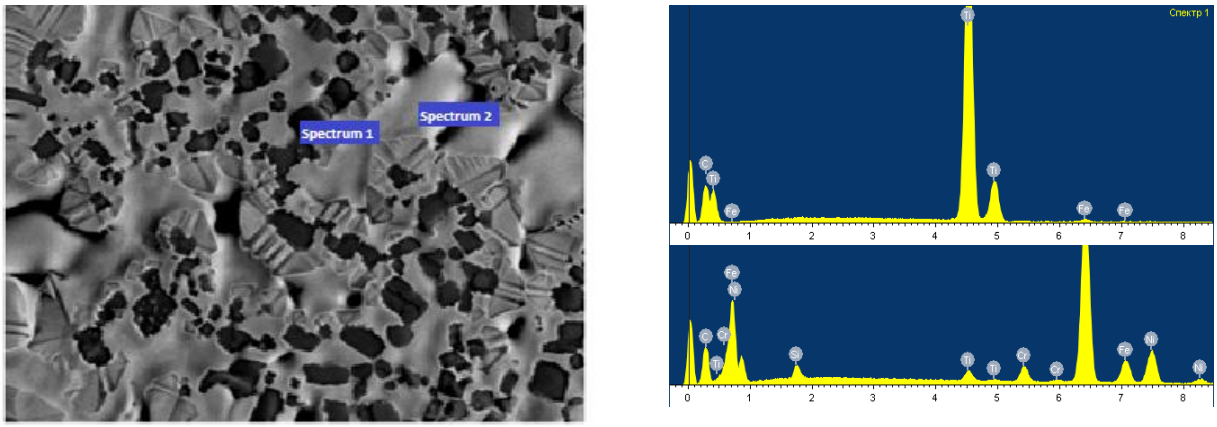

Figure 1 - Photomicrograph of the 1st one (center) x1500

Table 1 - Elemental analysis in%

Spectrum	Si	Ti	Cr	Fe	Ni	Total
Spectrum **1**		98.49		1.51		100.00
Spectrum **2**	2.29	2.13	4.02	70.56	21.00	100.00

The segregation of Ti alloy core is on the border of the 2nd and 3rd zones also, but in the form of cubic precipitates on the surface as shown by the mapping of the zone.

Result and Discussion

Structural and phase changes in the sample surface is the result of thermal effects of the electron beam. In this regard, temperature distribution was calculated.

Isolation of impurities can be explained by the presence of point defects gradients near the border.

Excess of thermodynamic equilibrium vacancies occurs due to intense heat after turning off the electron beam.

DIELECTRIC AND ULTRASONIC INVESTIGATIONS ON POLYUREA ELASTOMERS WITH EMBEDDED INORGANIC NANOTUBES

Š. Svirskas[1], V. Samulionis[1], J. Banys[1], A. Sanchez-Ferrer[2], R. Mezzenga[2]

[1]*Vilnius University, Faculty of physics, Saulėtekio av. 9, III b., LT-10222 Vilnius, Lithuania,*

[2] *Institute of Food Science and Nutrition, D-HEST, ETH Zurich, Switzerland*

e-mail of presenting author: sarunas.svirskas@ff.vu.lt

Elastomers are crosslinked polymer melts which show viscoelastic properties due to the flexibility of their polymer chains and friction between them. Such materials are the combination of amorphous or semi-crystalline polymers and crosslinkers which keep the chains into a single macromolecule. Inorganic nanotubes are believed to enhance various thermal, electrical and mechanical properties of elastomers. Such nanocomposites are promising materials for various applications like in the automotive industry, constructing chemistry, or in the development of optical and electronic devices.

In this work, some polyurea elastomers with different concentration of molybdenum sulfide (MoS_2) nanotubes were investigated by means of dielectric and ultrasonic spectroscopy. The temperature-dependent behavior of the dielectric permittivity revealed a phase transition above room temperature from the semi-crystalline to the amorphous phase which is also visible in temperature-dependent experiments of the longitudinal ultrasonic velocity (Fig. 1).

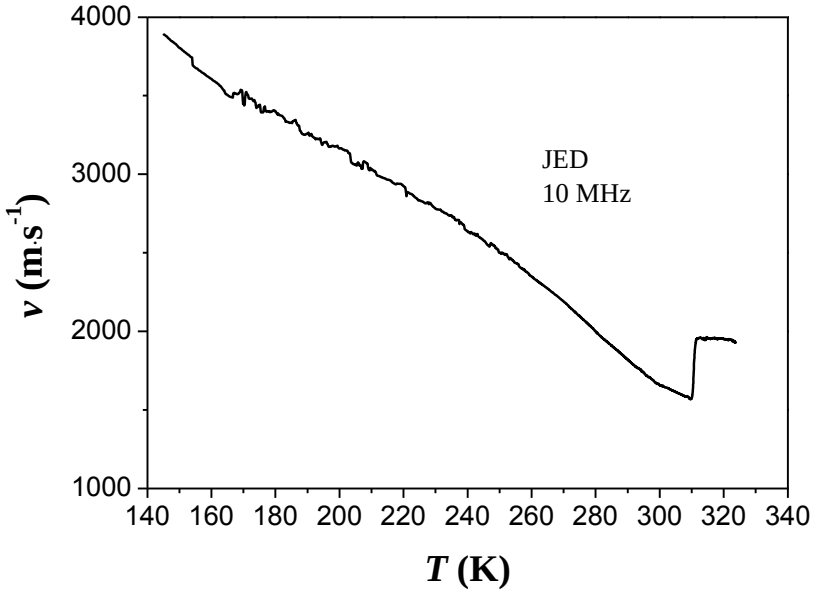

Figure 1. Longitudinal ultrasonic velocity as function of temperature for a semi-crystalline elastomer (JED) without nanotubes

BROADBAND DIELECTRIC SPECTROSCOPY OF PVDF POLYMERS EMBEDDED WITH FERRITE NANOPARTICLES

Š. Svirskas[1], M. Šeputis[1], J. Banys[1], P. Martins[2,3] and S. Lanceros-Mendez[2,3]

[1]*Vilnius University, Faculty of physics, Saulėtekio av. 9, III b., LT-10222 Vilnius, Lithuania*

[2]*Centro/Departamento de Física, Universidade do Minho, 4710-057, Braga, Portugal*

[3]*INL-International Iberian Nanotechnology Laboratory, 4715-330 Braga, Portugal*

e-mail of presenting author: sarunas.svirskas@ff.vu.lt

Polyvinylidene fluoride is well known for its high piezoelectric response compared to other polymers. PVDF has several phases of which polar β phase is of huge interest for various applications [1]. Several comprehensive studies of PVDF composites with various ferroelectric materials such as barium titanate or PZT [2,3] were performed in order to further increase the electromechanical properties of PVDF. Moreover, inclusions of ferrites in the PVDF might give rise to a multiferroic state [4]. Coupled ferroelectric and ferromagnetic phenomena would be attractive for multifunctional devices.

In this work we present dielectric spectroscopy results for PVDF with inclusions of $CoFe_2O_4$(0.01, 1 ,10 wt.%), $NiZnFe_2O_4$ (10 wt.%) and $NiFe_2O_4$ (10 wt.%). Dielectric properties were measured in 20 Hz – 1 GHz frequency range and 100 K - 380K temperature range.

References

1. V. Sencadas et al. J. MACROMOL. SCIE. B-Pysics Vol. 48 (3) pp. 514-525 (2009)
2. B. Hilczer et. al. J. Non-Cryst. Solids vol.305(1-3), pp. 167-173 (2002).
3. S. F. Mendes, C. M. Costa, C. Caparros, V. Sencadas, S. Lanceros-Mendez, J. Mat. Sci. Vol. 47(3), pp. 1378-1388 (2012);
4. P. Martins, C. M. Costa, G. Botelho, S. Lanceros-Mendez, J. M. Barandiaran, J. Gutierrez, Mat. Chem. and Phys., Vol. 131(3), pp. 698-705 (2012)

ETHYLENE VINYLACETATE COPOLYMER AND NANOGRAPHITE COMPOSITE AS CHEMICAL VAPOUR SENSOR

Santa Stepina, Gita Sakale, Maris Knite
Riga Technical University

e-mail of presenting author: Santa.Stepina@rtu.lv

Previous studies of polymer-nanostructured carbon composite (P-NCC) have shown that polyethylene glycol (PEG) can be used as ethanol sensor in dry air. Therefore it is necessary to investigate more composites and estimate their capability to sense volatile organic compounds (VOCs) at elevated relative humidity.

We had chosen ethylene vinylacetate copolymer (EVA) as matrix for P-NCC. EVA (Fig.1) consist of two repeating parts - ethylene (non-polar) and vinylacetate (polar) which gave an opportunity to detect both polar and non-polar VOC. It is incompatible with water as well.

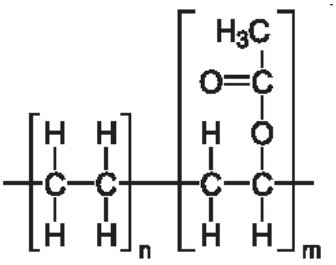

Fig.1 Structure of EVA.

As conductive filler we use graphitized carbon black nanoparticles PRINTEX XE-2 with mean size of particle 30nm.

Previous experiments showed that thickness of the composite layer, concentration of VOC, as well as polarity of VOC and relative humidity can affect P-NCC VOC sensoreffect.

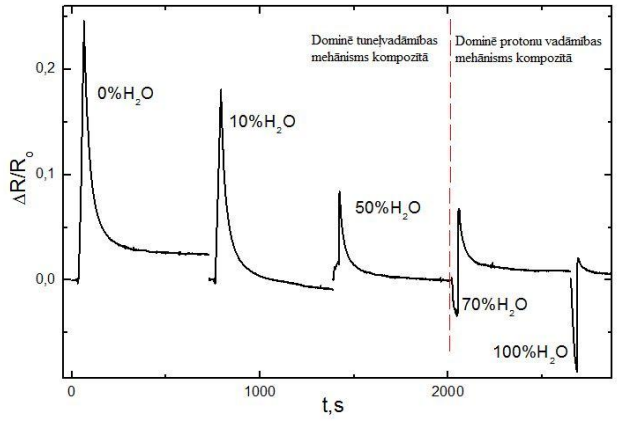

Fig.2 Electrical resistance change versus periodical exposition time in different water-ethanol vapour concentration

Experimental data (Fig.2) shows that EVA-NCC is able to detect VOCs at elevated relative humidity. It was found that at the water-ethanol mixture of 70:30 ratio changes the composite response mechanism to vapour: the contribution of proton conductivity overcomes the contribution of tunneling currents.

EVA-NCC shows good sensoreffect on different kind fuels vapour. It is explainable with ethanol and methanol molecules presence in fuel vapour. There has been found the sensitivity on both petrol and diesel vapours.

SYNTHESIS OF Eu AND Sm DOPED Y_2O_3 NANOPHOSPHORS BY ROOM TEMPERATURE SELF-PROPAGATING REACTION

Sanja Ćulubrk, Marko Nikolić, Vesna Lojpur and Miroslav D. Dramićanin
Vinča Institute of Nuclear Sciences, University of Belgrade, Belgrade, Serbia
e-mail of presenting author: sanjaculubrk@gmail.com

In this report we present simple, cost and time effective method for synthesis of $Y_2O_3:Sm^{3+}$ and $Y_2O_3:Er^{3+}$ nanoparticles based on self-propagating room temperature reaction between metal nitrates and sodium hydroxide.

In brief, appropriate amounts of yttrium nitrate hexahydrate, europium nitrate hexahydrate or samarium nitrate hexahydrate are mixed with sodium hydroxide. Reaction proceeds at room temperature after the mixture of reactants is mechanically activated by hand mixing in alumina mortar. After being exposed to air for 3h the mixture is washed in centrifuge with distilled water and ethanol and dried for 12h at 70°C. Series of samples are prepared by annealing of powder on different temperatures. Crystallite size of powders obtained at different calcinations temperatures are evaluated through X-ray diffraction analysis. Photoluminescence measurements are performed to analyze emission and emission decay characteristics of nanophosphors.

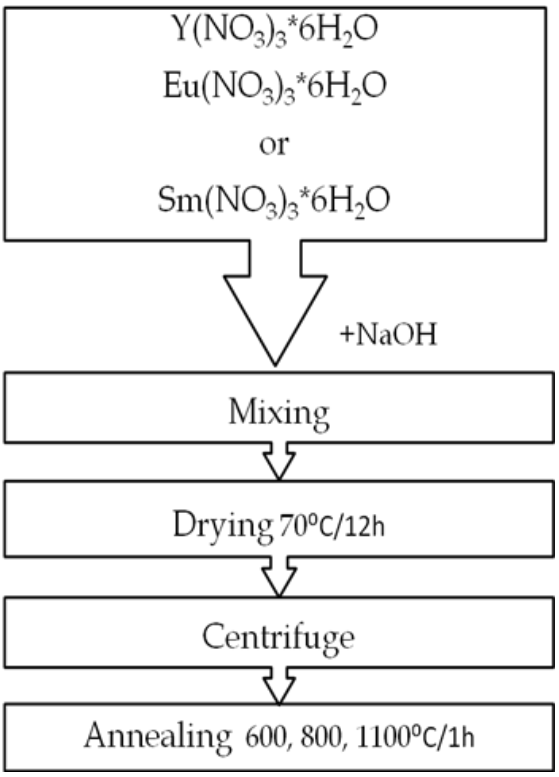

Fig.1 Schematics of Self-propagating room temperature reaction method for nanophosphor synthesis.

STRUCTURAL AND MICROMECHANICAL CHANGES IN MgO AFTER HIGH-DOSE IRRADIATION WITH SWIFT HEAVY IONS

R. Zabels[1], I. Manika[1], K. Schwartz[2], J. Maniks[1], R. Grants[1]

[1]*Institute of Solid State Physics, University of Latvia, Riga, Latvia,*

[2] *GSI Helmholtzzentrum für Schwerionenforschung, Darmstadt, Germany,*

e-mail: rzabels@gmail.com

MgO in known to have potential applications in nuclear waste management and in nuclear energetics as a part of nuclear fuel containment matrix, thus its structural damage and mechanical behavior after high-fluence irradiation is of importance.

The presented study is oriented on investigation of structural and micromechanical changes in MgO single crystals after irradiation with high energy (GeV) and high dose Au and U ions (fluences up to 7×10^{13} ions·cm^{-2}). The irradiated samples were investigated by XRD, atomic force microscopy (after chemical etching), instrumented nanoindentation, and optical absorption spectroscopy. In irradiated samples XRD shows a single crystalline state with radiation induced disordering. Irradiation causes a slight coloring of samples and optical absorption spectroscopy shows an intensive absorption band around 252 nm which is related to F^+ centers. Besides, AFM measurements reveal ion-induced dislocations. The structural damage leads to substantial hardening. Instrumented indentation as a structure sensitive method shows an increase of hardness at fluences above 10^{10} ions·cm^{-2}. The hardening at the highest fluence of 7×10^{13} ions·cm^{-2} reaches 56% against virgin MgO. The hardening of irradiated samples is accompanied by slight decrease in indentation plasticity. The analysis of deformation zone around indents reveals a reduction in indentation induced dislocation mobility with increasing the fluence.

Overall, MgO has proved to be highly radiation resistant material, it maintains a single crystalline state, structural integrity, high hardness and reasonable plasticity even after high doses (up to 950 MGy) of swift heavy ions.

ATOMIC LAYER DEPOSITION OF ALUMINUM OXIDE FILMS ON GRAPHENE

Raul Rammula[1], Lauri Aarik[1], Arne Kasikov[1], Jekaterina Kozlova[1,2], Tauno Kahro[1], Ahti Niilisk[1], Harry Alles[1] and Jaan Aarik[1]

[1]*Institute of Physics, University of Tartu, Tartu, 51014, Estonia*

[2]*Institute of Chemistry, University of Tartu, Tartu, 50011, Estonia*

e-mail: raulr@ut.ee

High quality dielectric films on graphene are of great interest due to the versatile field of applications, especially in nanoelectronics and spintronics. In the latter case only few nanometers of film material are often needed. For this reason, thickness uniformity and coverage provided by atomic layer deposition (ALD) is essential. ALD of thin films on graphene is, however, not a straightforward task because graphene remains chemically inert allowing thin film nucleation mainly on surface defects or atomic steps. These defects or any C–C bond interruption degrade graphene quality. Therefore it is important to find combination of process parameters allowing uniform dielectric coverage as well as maintaining electrical properties of graphene.

In this work, exfoliated and chemical vapor deposited (CVD) graphene was used to examine nucleation, coverage and uniformity of ALD dielectrics. To investigate initiation of Al_2O_3 growth we used three basic approaches, (i) direct deposition onto graphene without any functionalization, (ii) deposition on 0.3–0.5 nm thick Al_2O_3 seed layers prepared by electron beam evaporation (EBE) and (iii) application of two temperature sequence for ALD. Atomic force microscopy studies showed that the nucleation of Al_2O_3 films directly on bare graphene surface was non-uniform. More uniform films were obtained when the ALD process was started at relatively low substrate temperatures while the fastest growth and the smoothest dielectrics were obtained when a seed layer was used (Fig .1).

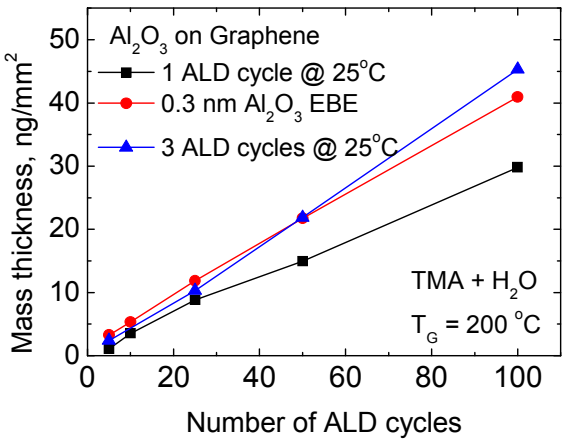

Fig.1 Dependence of Al_2O_3 mass thickness on number of ALD cycles applied for growing Al_2O_3 on different seed layers deposited on CVD graphene. Mass thickness was measured by X-ray fluorescence .

INFLUENCE OF IODINE DOPING AND ANNEALING ON THE PROPERTIES OF SOL-GEL PREPARED THIN TITANIA FILMS

R. Pärna[1], U. Joost[1,2], A. Värva[1], M. Visnapuu[1], M. Lembinen[1], I. Kink[1,2], V. Kisand[1,2]

[1]Institute of Physics, University of Tartu, Riia 142, 51014 Tartu, Estonia

[2]Estonian Nanotechnology Competence Center, Riia 142, 51014 Tartu, Estonia

e-mail of presenting author: rainer.parna@ut.ee

TiO_2 attract great attention for photocatalytic and self-cleaning applications [1,2]. However in these applications, an effective electron-hole pair generation and a long lifetime of electron-hole pairs are required. Unfortunately titania absorbs only a fraction of sunlight. Its band gap depends on crystal structure and is typically 3.2 eV in case of anatase and 3.0 eV in case of rutile. Therefore it would be technologically and economically advantageous to shrink the titania bandgap.

One possibility to enhance absorption of sunlight in TiO_2 is introducing impurities to the structure of titania (doping). It has been reported, that doping TiO_2 with iodine has shifted its absorption edge towards the visible light maximum of solar radiation [3].

In this study 4.2 and 20.8 at.% iodine-doped TiO_2 thin films have been prepared on silicon monocrystal and quartz substrates by using sol–gel deposition and subsequent annealing in air at 200 to 900 °C. Several experimental techniques (x-ray photoelectron spectroscopy, Raman spectroscopy, atomic force microscopy, UV-VIS spectroscopy, and hydrophilicity measurements) have been applied to characterize these films.

It was demonstrated that films morphology, evolution of crystalline structure, surface composition depend on the iodine concentration in the films and on annealing temperature. Furthermore, iodine doping leads to appear of additional absorption band in UV-VIS spectra and the surface hydrophilic properties depend up on the initial iodine concentration in the films.

References

1. M. Keshmiri, M. Mohseni, T. Troczynski, *Appl. Catal. B Environ.* 53 (2004) 209-219.

2. R. Wang, K. Hashimoto, A. Fujishiama, M. Chikuni, E. Kojima, A. Kitamura, M. Shimohigoshi, T. Watanabe, *Adv. Mater.* 10 (1998) 135-138.

3. X. Hong, Z. Wang, W. Cai, F. Lu, J. Zhang, Y. Yang, N. Ma, Y. Liu**.**, *Chem. Mater.* 17, 1548–1552, (2005**).**

DIELECTRIC PROPERTIES OF NANOGRAIN BSPT CARAMICS

S. Balčiūnas[1], R. Mackevičiūtė[1], M. Ivanov[1], H.Amorín[2], A. Castro[2], M. Algueró[2], J. Banys[1]

[1]*Faculty of Physics, Vilnius University, Sauletekio 9/3 817k., LT10222 Vilnius, Lithuania*

[2]*Instituto de Ciencia de Materiales de Madrid, CSIC, Cantoblanco, 28049 Madrid, Spain*

e-mail: sergejus.balciunas@gmail.com

Ferroelectric materials are of high interest for both researchers and engineers due to their remarkable properties. Their switchable electric polarization [1] is ideal for use in devices for memory storage and integrated microelectronics. Advanced devices tend to nanoscale, that raises necessity to research new cheaper and more durable materials.

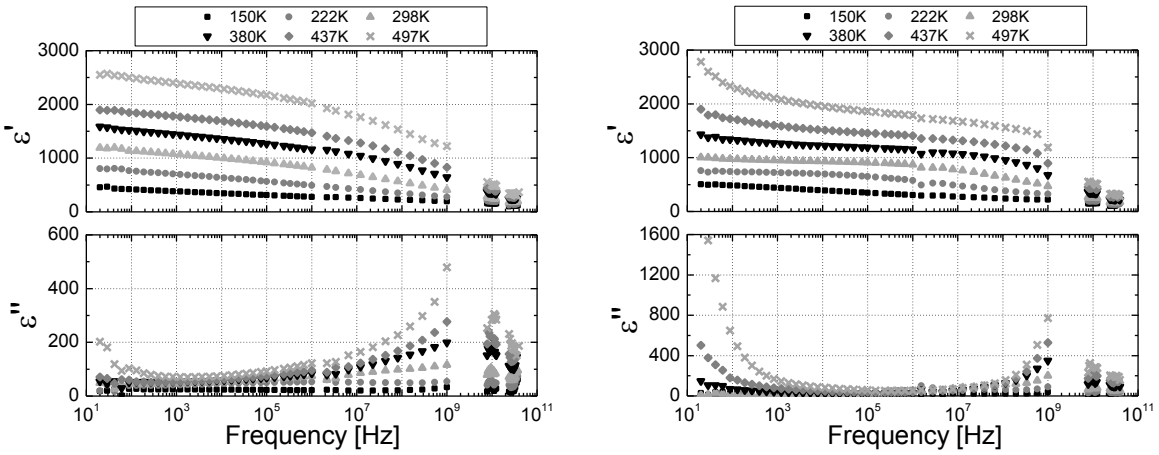

Fig.1 Frequency dependence of real (top) and imaginary (bottom) parts if dielectric permittivity for BSPT 1.6 μm grain size ceramics produced in WC milling media (left) and Stainless steel milling media (right).

BSPT ($xBiScO_3$-(1-x) $PbTiO_3$) x=0.36 and 0.375 ceramics with micron, submicron and nanoscale grains were produced from nanocrystalline powders obtained by mechanosynthesis [2] in different milling media. In figure 1 we can see that ceramics made with stainless steel milling media have higher dielectric permittivity at low frequencies compared to ones produced with WC milling media. WC-milled ceramics also exhibit a more narrow dispersion region, however dielectric permittivity decreases more rapidly at high frequencies (10^6-10^9 Hz) in this case. Both ceramics have similar dielectric properties in microwave region (10 – 40 GHz).

References

1. C. H. Ahn, K. M. Rabe, J.M. Triscone, *Science 23 January*, 2004, Vol. 303 No. 5657 pp. 488-491

2. T. Hungrı´a, H. Amorı´n, M. Alguero, A. Castro, *Scripta Materialia*, 2011, No.64, 97-100

STATISTICAL ANALYSIS OF VOID LATTICE FORMATION IN CaF_2

P. Merzlyakov, G. Zvejnieks, V.N. Kuzovkov, E.A. Kotomin
Institute of Solid State Physics, University of Latvia, Latvia
e-mail: pavel.merzlyakov@gmail.com

Calcium fluoride CaF_2 is widely used both in microlithography and as UV and deep UV (DUV) window material. It is also known that electron beam irradiation by displacing F atoms can produce highly ordered F-vacancy cluster lattice, i.e., void lattice [1]. We perform a quantitative analysis of experimental data demonstrating void lattice formation under electron irradiation of CaF_2.

We develop two distinct image filters. The first filter is based on analysis of difference between two Gaussian convolutions with image intensity function that allows us effectively remove a noisy background from an image. The following application of a step function, leads to a binary matrix where unity corresponds to the presence of a void.

The second filter is based on a grouping of image points with similar intensity. Next, the connected clusters of these points are detected. This is followed by a neighboring intensity cluster analysis starting from the maximal intensity. We identify the presence of void clusters if information in the corresponding neighboring layers is consistent.

From the filtered experimental data images we can easily calculate concentration, cluster distribution function as well as average distance between clusters (void lattice spacing). In particular analysis of consecutive experimental snapshots at increased irradiation doses, allows us quantitatively follow to the void lattice formation processes. Results from both filters coincide and demonstrate that void cluster growth is accompanied with the slight void lattice spacing increase.

P.M. and G.Z. greatly acknowledge the financial support of ERAF project 2010/0204/2DP/2.1.1.2.0/10/APIA/VIAA/010.

References

1. T.H.Ding, S.Zhu, L.M.Wang, *Microsc.Microanal.*, 2005, Vol.11, 2064-2065.

CONOSCOPIC STUDY OF STRONTIUM-BARIUM NIOBATE SINGLE CRYSTALS

Aleksander Kolesnikov[1], Rostislav Grechishkin[1], Olga Malyshkina[1], Yury Malyshkin[1], Jan Dec[2], Tadeusz Łukasiewicz[3]

[1]Tver State University, Tver, Russia

[2]University of Silesia, Institute of Materials Science, Katowice.

[3]Institute of Electronic Materials Technology, Warsaw

e-mail: Olga.Malyshkina@mail.ru

Strontium-barium niobate, $Sr_xBa_{1-x}Nb_2O_6$ (SBN), single crystals with the structure of tetragonal tungsten bronze are of significant interest for many important electrooptic, piezoelectric and pyroelectric applications. In the present work we studied an optic anisotropy of uniaxial (polar class 4mm) SBN single crystals with nominal concentrations of strontium in the solution 26, 35, 50, 61 and 70% with the aid of conoscopic observations. In addition to the expected uniaxial conoscopic light figures of polar cuts of SBN crystals (concentric circles) specific anomalies of birefringence are found to exist for some compositions (Fig. 1). The observed birefringence features are analyzed making use of the available theory of interference between the extraordinarily and the ordinarily polarized light beams affected by internal mechanical stresses. The role of the disorder in the distribution of Sr and Ba ions in the pentagonal positions in the SBN crystal lattice causing structural disordering resulting in deviations from the optical uniaxiality is discussed [1,2].

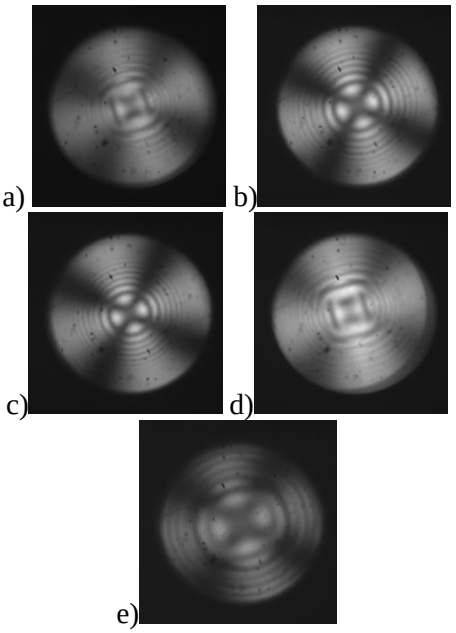

Fig.1 The conoscopic figures of SBN26 (a), SBN35 (b), SBN50 (c), SBN61 (d), SBN70 (e).

References

1. A Kolesnikov, I. Kaplunov, A.I. Ivanova, S.A. Tretiakov, O.V. Malyshkina, R. Grechishkin. *Ferroelectrics*, 2012, Vol. 441. P.84-91.

2. A.I. Kolesnikov, I.A. Kaplunov, A.I. Ivanova, S.A. Tretiakov, I.V. Talyzin, Yu.A. Malyshkin, R.M. Grechishkin. *Ferroelectrics*, 2012, Vol. 437. P. 45-51

DEUTERIUM DESORPTION TEMPERATURE FROM Mg-Ti COMPOSITES PREPARED BY METHOD OF ATOM-BY-ATOM MIXING OF COMPONENTS

O.M. Morozov, V.G. Kulish, V.I. Zhurba, I.M. Neklyudov, V.O. Progolaieva,
A.S. Kuprin, N.S. Lomino, V.D. Ovcharenko, I.V. Kolodiy, O.G. Galitskiy
National Science Center "Kharkov Institute of Physics and Technology", Kharkov, Ukraine
e-mail: morozov@kipt.kharkov.ua

An exclusive position of nanocrystalline materials as hydrogen storage materials is determined by their unique structural properties that can, probably, provide a high sorption capacitance and potentially high concentrations for hydrogen storage. One of the methods for obtaining materials in the nanocrystalline state is introduction of nanoformative elements. These are chemical elements with low solubility or non interacting with other elements in the composite being formed. The plasma evaporation-sputtering method was applied to make composite materials of the Mg-Ti system (the method of atom-by-atom mixing of components). The ion-implanted deuterium desorption temperature variations as a function of the component concentration were studied. It has been established that, by introducing Ti into Mg, the deuterium desorption temperature can be appreciably decreased (to 350-450 K) in comparison with the case of deuterium desorption from magnesium.

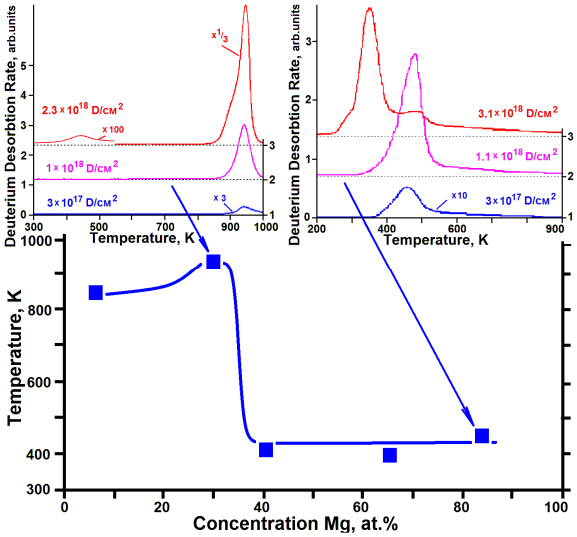

Fig.1. Deuterium desorption temperature versus the Mg-Ti composition for a deuterium dose of ~1×10^18 D/cm^2 (T_irr. ~100 K)

A step-like form of the curve of deuterium desorption temperature evidences on the presence of two different structure states of the Mg-Ti system depending on the ratio of components. The deuterium temperature decrease can be caused by filamentary inclusions formed, in the process of composite making and annealing, by the insoluble component (titanium) atoms providing the deuterium diffusion from the sample at a lower temperature (channels for deuterium diffusion through the surface barrier). A necessary high diffusion mobility of deuterium is provided by the amorphous state of samples. The deuterium desorption data obtained on the example of Mg-Ti and Mg-Zr [1], Mg-V [2] composites provide support for further research into hydrogen storage materials containing low-soluble chemical elements in the alloy components.

References

1. I.M. Neklyudov, O.M. Morozov, V.G. Kulish, V.I. Zhurba. N.S. Lomino, V.D. Ovcharenko, O.S. Kuprin, *IOP Conf. Ser.: Mater. Sci. Eng.* 23 (2011) 012028 doi:10.1088/1757-899X/23/1/012028.
2. I.M. Neklyudov, O.M. Morozov, V.G. Kulish, V.I. Zhurba. N.S. Lomino, V.D. Ovcharenko, O.S. Kuprin, *IOP Conf. Ser.: Mater. Sci. Eng.* 38 (2012) 012061 doi:10.1088/1757-899X/38/1/012061.

NEUTRON SCATTERING STUDY OF STRUCTURAL AND MAGNETIC SIZE EFFECTS IN NiO

Anatoly M. Balagurov[1], Ivan A. Bobrikov[1], Dmitrijs Jakovlevs[2], Alexei Kuzmin[3]
Mikhail Maiorov[4], Nina Mironova-Ulmane[3]

[1]Frank Laboratory of Neutron Physics, JINR, Dubna, Russia
[2]Riga Technical University, Latvia, Riga, Kalku Str. 1, LV-1048
[3]Institute of Solid State Physics, University of Latvia, Riga, Latvia
[4]Institute of Physics, University of Latvia, Salaspils, Latvia

E-mail of presenting author: nina@cfi.lu.lv

Effect of crystallite size on the atomic and magnetic structures of antiferromagnetic simple oxides such as MnO [1], CoO [2], NiO [3] remains an interesting topic of research. In particular, the existence of more than two magnetic sublattices as in a conventional massive NiO AFM structure has been found in NiO nanoparticles [3].

NiO nanopowders with crystallite sizes of 13-1500 nm were studied in [4] by several methods, including neutron diffraction. As a continuation of these studies, the diffraction patterns of the four NiO samples have been measured at HRFD diffractometer at the IBR-2 pulsed reactor in Dubna. The average grain sizes determined from the BET specific surface area measurements were 13 nm, 100 nm, 138 nm and 1500 nm. The morphology of all samples was studied by SEM, and the magnetic properties were characterized by Vibrating Sample Magnetometer (VSM).

We found that the atomic structure and the type of magnetic ordering are nearly independent of the average crystallite size. There is only a small (0.16%) increase in the cell volume when crystallite size decreases down to 13 nm. The average size of the coherently scattering regions and antiferromagnetic domains is large and coincides for the samples with the grain sizes of 138 and 1500 nm. For the sample with the grain size of 100 nm the size of crystal domains is close to that of the crystallites, whereas the magnetic coherence length is about 3 times smaller. Finally, the long-range magnetic order becomes largely destroyed in the sample of 13 nm.

References

1. I.V. Golosovsky et al., Phys. Rev. B **72** (2005) 144409.
2. A.N. Dobrynin et al., Phys. Rev. B **73** (2006) 245416.
3. R.H. Kodama, S.A. Makhlouf, A.E. Berkowitz, Phys. Rev. Lett. **79** (1997) 1393.
4. N. Mironova-Ulmane et al., Solid State Phenomena **168-169** (2011) 341.

EXFOLIATED GRAPHITE COMPOSITES: MICROWAVE APPLICATIONS

Nadzeya Valynets[1] (presenting author), Polina Kuzhir[1],
Alain Celzard[2], Jan Macutkevic[3], Stefano Bellucci[4]
[1]*Research Institute for Nuclear Problems, Belarusian State University,* [2]*IJL – UMR CNRS 7198,* [3]*Vilnius University,* [4]*INFN-Laboratori Nazionali di Frascati*
e-mail of presenting author: nadezhda.volynets@gmail.com

The latest trends, techniques and applications of microwave radiation in wireless network technologies, cellular phones, targeting radars, vehicle speed detection, and electron spin resonance apparatus, *etc* stimulate searching of new materials with desirable mechanical and thermal properties providing high electrical conductivity and electromagnetic interference shielding effectiveness (EM SE). For that purpose, a series of composite samples were prepared, based on epoxy resin (Epikote 828), a curing agent called A1 (a modified TEPA) and up to 2.0 wt.% content of exfoliated graphite (EG). EG was obtained by intercalation of natural graphite flakes, subsequently submitted to a thermal shock. Accordion-like particles were thus produced, leading to a material of low packing density, around 3 g/L [1]. The complex dielectric permittivity $\varepsilon^* = \varepsilon' - i\varepsilon''$ was measured by a LCR meter HP4284A in the frequency range 20 Hz–1 MHz at room temperatures. The spectra of S–parameters of epoxy/EG composites were measured in microwave range (26-37 GHz) with scalar network analyzer. The average value of power transmitted through the samples is 60%, 30%, and close to 0 for 0.25, 1 and 2 wt.% of EG embedded, respectively. Along with high EM performance in microwave range, composites based on EG are much easier to prepare than those filled with CNTs. Concluding, giving the benefit of being lightweight, using EG leads to exceptionally good EM attenuation ability, along with high dielectric permittivity in low frequency range (see Fig.1).

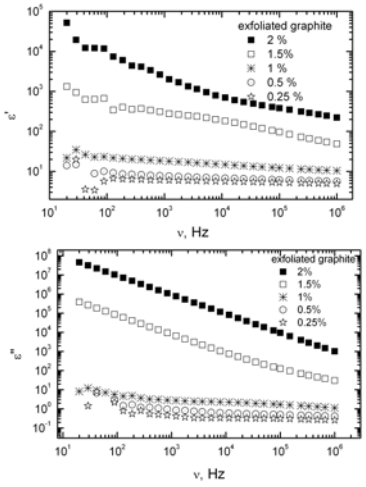

Fig.1. Dielectric permittivity of epoxy/EG in low frequency range.

This work was partially supported by EU FP7 projects FP7-266529 BY-NanoERA, FP7-247007 CACOMEL and PIRSES-GA-2012-318617 FAEMCAR.

[1] A. Celzard, J.F. Marêché, G. Furdin, *Progress in Materials Science* 50 (2005) 93-179.

Two point electrical measurements of 1D nanostructures

Mikk Vahtrus[1], Sergei Vlassov[1,2], Madis Paalo[1,2], Boris Polyakov[1,3], Leonid Dorogin[1,2], Mikk Antsov[1,2], Rünno Lõhmus[1,2], Imar Kink[1,2].

[1]Institute of Physics, University of Tartu, Estonia

[2]Estonian Nanotechnology Competence Centre, Riia 142, 51014 Tartu, Estonia

[3]Institute of Solid State Physics, University of Latvia, Latvia

e-mail: vahtrus@ut.ee

Investigation of electrical properties of 1D nanostructures like nanotubes, nanowires and nanofibers has gained considerable attention because of their potential applications in electronics, optical devices and sensors. Furthermore, nanostructures can exhibit different electrical properties compared to the bulk materials.

For electrical measurements of individual 1 D nanostructures, direct methods, where 2 or 4 electrodes are in direct contact with sample are commonly used. Electrodes can be made by fabricating contact pads on a substrate using nanolithography or applying conductive probes to the object by means of micromanipulators. One of the major problems of electrical measurements at the nanoscale is high contact resistance, especially in case of contacts between metal and semiconductor. 4 point probe method enables to exclude contact resistance. However, arrangement of four electrodes on small objects is highly problematic. Therefore 2 point method, where electrical contacts are made by two probes attached to manipulators and 1 D nanostructure is resting on a substrate, is preferable. As the resistance of an object is linearly proportional to the distance between the electrodes, plotting the resistance as a function of separation between electrodes will allow us to extract contact resistance from the intercept of the linear curve with Y (resistance) axes [1]. The main disadvantage of such approach is a possible influence of substrate, which is difficult to account for.

In present work we propose modified 2 point method where 1D object is resting half-suspended on a conductive substrate. Using single manipulator with conductive probe and moving it along the nanofiber or nanowire we are able to measure intrinsic resistance of those objects.

References

[1] M. Elawayeb, Y. Peng, K. J. Briston, B. J. Inkson, J. Appl. Phys. 111, 0343 06(2012)

DISSOLUTION-DEPENDENT ANTIBACTERIAL EFFECTS OF SILVER NANOWIRES

Meeri Visnapuu[1], Katre Juganson[2], Urmas Joost[1,3], Kai Künnis-Beres[2], Imbi Kurvet[2], Vambola Kisand[1,3], Angela Ivask[2]

[1]*Institute of Physics, University of Tartu, Estonia,* [2]*National Institute of Chemical Physics and Biophysics, Estonia,* [3]*Estonian Nanotechnology Competence Centre, Estonia*

e-mail: meeri.visnapuu@ut.ee

Silver nanoparticles (Ag NPs) are incorporated into various consumer products (http://www.nanotechproject.org/). Due to their microbicidal nature, the main applications of Ag NPs include antiseptic sprays and antimicrobial coatings. It has been argued that the antibacterial effects of Ag NPs are mainly derived from their dissolution and resulting Ag ions [1]. On the other hand, there are reports showing that in addition to solubility Ag NPs also exhibit particle-specific toxic effects due to their size, shape [2, 3] and surface defects [4]. In this research we studied whether the antibacterial effects of wire-shaped Ag NPs were dependent only on dissolution or whether the rod-like shape also contributed to the toxicity of these particles.

The wire-shaped Ag NPs (ø 60-80 nm, length > 2 μm; Seashell Technology, US) were characterized by visualizing their morphology and size using scanning electron microscopy, analyzing their UV-Vis spectra, measuring their z-potential and dissolution. Antibacterial effects of Ag nanowires were analyzed using bioluminescent *E.coli* cells. 1.4 mg of Ag nanowires/L decreased the bioluminescence of these bacteria by 50%. However, when this EC50 value was calculated based on dissolved Ag (0.4% was dissolved, i.e., the amount of dissolved Ag at EC50 was 0.005 mg/L) it was similar to that of $AgNO_3$. It was evident that all the observed antibacterial effects of the studied Ag nanowires were due to their dissolution. Also, dissolved Ag explained all the intracellular bioavailable Ag analyzed using recombinant Ag-induced bacterial cells.

Our research showed that the studied silver nanowires exhibited dissolution-dependent toxicity. One of the reasons for the absence of shape-dependent effect might be that the relatively big size of the wires prevented them from interacting with bacteria. Further investigation with smaller wires might lead to different results.

References

1. Z-m.Xiu, Q-b.Zhang, H.L.Puppala, V.L.Colvin, P.J.J.Alvarez, *Nano Lett.*, 2012, No.12, 4271-4275.

2. S.Pal, Y.K.Tak, J.M.Song, *Appl. Environ. Microbiol.*, 2007, No.6, 1712-1720.

3. L.C.Stoehr, E.Gonzalez, A.Stamfl, E.Casals, A.Duschl, V.Puntes, G.J.Oostingh, *Part. Fibre Toxicol.*, 2011, No.8, 36.

4. S.George, S.Lin, Z.Ji, P.S.Weiss, A.E.Nel, *ACS Nano*, 2012, No.6, 3745-3759.

EXAMINATION OF DIELECTRIC DISPERSION OF COMPLEX OXIDES ON THE BASIS OF BISMUTH-CONTAINING TITANATES

M.S. Shashkov[1], O.V. Malyshkina[1], E.V. Barabanova[1], M.S. Korolyova[2], I.V. Piyr[2]

[1]*Tver State University, Tver, Russia*

[2]*Komi Institute of Chemistry of Ural branch of Russian Academy of Sciences, Syktyvkar, Russia*

e-mail: Maksim.Shashkov@gmail.com

Much attention has recently been paid to the search of piezoceramic materials possessing dielectric properties similar to the properties of PZT ceramics but having no hazardous effect on the men's health and environment. In the present work we study the samples of non-toxic bismuth-containing compounds which are of interest with respect to utilizing their dielectric properties. Complex oxide compounds on the basis of bismuth titanates with chalcolamprite structure type and layered perovskite doped with Cr, Fe and Co inclusions were studied at room temperature by the method of dielectric spectroscopy in the frequency range of 30 to 10^6 Hz.

For a number of samples an influence of the conductivity on the low frequency dielectric spectra were found. The spectral analysis was performed with the aid of fractal-exponential approach. An empirical computational procedure was applied to find the relaxation time τ for the compositions $Bi_{1.6}Ti_2Cr_{0.16}O_{6.6}$, $Bi_{1.55}Ti_{1,97}Cu_{0.78}O_7$ and $Bi_4Ti_2Fe_1O_{11.5}$. To this end the relaxation time is defined as a value reciprocal to the frequency of a maximum on the graph of $\beta''(\omega)$ dependence (Fig. 1). It was ascertained that the integral dielectric parameters of a number of compounds follow the universal relaxation law of Jonscher [1]. Also, an analysis of the frequency dependence of the conductivity was performed and used to deduce suggestions on the mechanisms of conductivity for each of the samples under study in the given frequency interval.

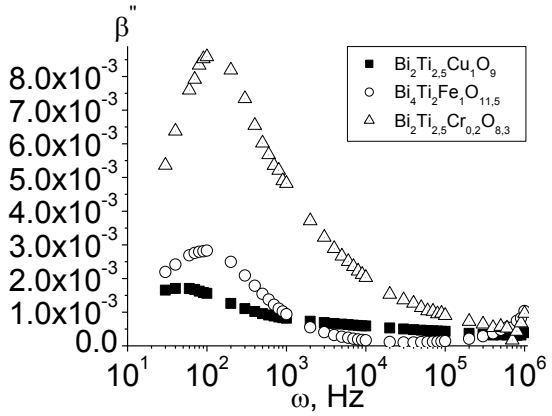

Fig. 1 Frequency dependence of the imaginary part of the dielectric module for $Bi_{1.6}Ti_2Cr_{0.16}O_{6.6}$, $Bi_{1.55}Ti_{1,97}Cu_{0.78}O_7$ and $Bi_4Ti_2Fe_1O_{11.5}$ compounds

References

1. A.K. Jonscher, Universal relaxation law, London, 1996. 415 p.

Elaboration of Alumina Nanofibers Reinforced Yttria Stabilized Zirconia nanocomposites by sol-gel method

Madis Umalas[1,2], Maarja Pohl[1], Ants Lõhmus[1], Rünno Lõhmus[1,2], Valter Reedo[1], Irina Hussainova[3] and Lauri Kollo[3],

[1]Institute of Physics, University of Tartu, Estonia,

[2]Estonian Nanotechnology Competence Centre,

[3]Department of Materials Engineering, Tallinn University of Technology, Estonia

e-mail: madis.umalas@gmail.com,

Ceramic matrix composites (CMCs) have been developed to overcome the intrinsic brittleness and mechanical unreliability of monolithic ceramics, which are otherwise attractive due to their high stiffness and strength [1]. One possibility of increasing materials` reliability and durability is to use ceramic nanofibers and whiskers as the reinforcement in ceramic matrices [2-4].

The aim of the present study was elaboration of aluminia (Al_2O_3) nanofibers reinforced 3 mol % yttria stabilized zirconia nanocomposites by the sol infiltration technique. Infiltrated sol was synthesized by sol-gel method from zirconium butoxide and yttrium nitrate hexahydrate. Al_2O_3 nanofibers with diameter 30 nm and length 24 mm were used as a reinforcing agent (Metallurg Engineering, Estonia).

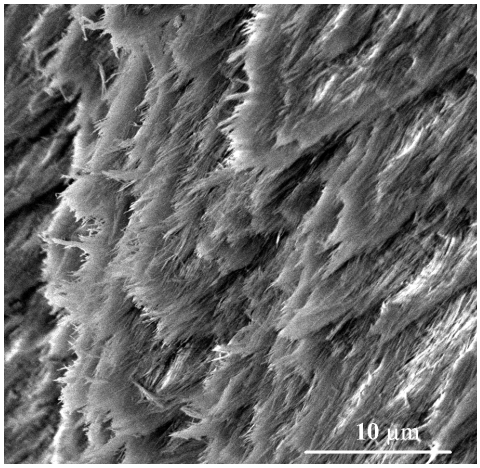

Fig.1SEM image of immersed Al_2O_3 nanofibers by ZrO_2 – 3 % Y_2O_3 sol.

The specimens of Al_2O_3 nanofibers with dimensions 24mm x 5 mm x 5mm were immersed into sol for 15 min and afterwards dried 30 min at 200 ^oC in air (Fig 1). The immersed specimens were sintered at 1500 ^oC in vacuum ~10^{-1} mBar. With the sol infiltration technique Al_2O_3 nanofibers were covered homogeneously with zirconia which resulted in the formation of dense and pore-free nanocomposite.

The composition and structure of the sintered specimens were characterized by X-ray diffraction, scanning electron microscope and energy dispersive X-ray spectroscopy. The hardness of the specimens was measured using the Vickers hardness test, hardness was 1275 HV0.5.

References

1. K.K. Chawla, Ceramic matrix composites, 2nd edn. Springer, New York, 2003.
2. B. N. Dudkin, A. Y. Bugaeva, G. G. Zainullin, V. N. Filippov, Inorg. Mater., 2010 46, 445.
3. J. Cho, A.R. Boccaccini, Mater Sci Forum., 2009, 606, 61-77
4. M.K. Naskar, M. Chatterjee, Ceram. Inter., 2004, 30, 257-265

PREPARATION AND CHARACTERIZATION OF ELECTRICALLY CONDUCTIVE METAL OXIDE CNT-COMPOSITES BY SOL-GEL METHOD

Madis Paalo[1], Tanel Tätte[1], Medhat Hussainov[1], Kelli Hanschmidt[1], Madis Lobjakas[1], Ants Lõhmus[1], Uno Mäeorg[2], Ilmar Kink[1]

[1]Institute of Physics, University of Tartu, [2]Institute of Chemistry, University of Tartu

e-mail of presenting author: madis.paalo@fi.tartu.ee

During the past decade, significant efforts have been made to transfer the extraordinary and unique properties of carbon nanotubes (CNT) to bulk materials in order to achieve novel functionality. Electrical conductivity and high aspect ratio of CNT materials for example enables their use as an alternative to transparent electrode materials [1]. Among the methods like powder processing, in situ growth of CNTs by chemical vapour decomposition, colloidal processing and electrophoretic deposition for obtaining CMCs, sol-gel method provides an attractive and alternative route to generate homogeneous and well-distributed dispersion of CNTs throughout a ceramic matrix. Unlike the aforementioned methods, sol-gel processing enables to achieve materials in various shapes (films, fibers, tubes, needles, bulk, as structured surfaces and ect.) at low cost and at low processing temperatures. In spite of metal oxides good optical, chemical and physical properties, research on metal oxide CNT-composites by sol-gel method is still very limited.

In the current paper we describe our studies of the preparation and characterization of ceramic composites obtained by using gelation of CNT doped titanium alkoxide nano sols. In our previous studies we have shown that it's possible to obtain selfstanding fibers and films from high viscosity transition metal oxides by using sol-gel method [2]. The effect of addition of CNTs to the rheological behaviour of alkoxide-based precursors was studied experimentally using specially constructed device to carry out measurements directly inside the synthesis vessel. Final materials were studied by SEM and FIB analysis and by 4-point eletrical measurements.

References

1. Cho J., Boccaccini A. R., Shaffer M. S. P., *J Mater Sci*, 2009, **44**, 1934.

2. Tätte T., Paalo M., Kisand V., Reedo V., Kartushinsky A., Saal K., Mäeorg U., Lõhmus A., Kink I., *Nanotechnology*, 2007, **18,** 531.

TITANIUM DIOXIDE THIN FILMS GROWN FROM TITANIUM CHLORIDE AND OZONE BY ATOMIC LAYER DEPOSITION

Lauri Aarik[1], Tõnis Arroval[1], Raul Rammula[1], Hugo Mändar[1], Väino Sammelselg[1,2], Jaan Aarik[1]

[1]*University of Tartu, Institute of Physics, Riia 142, 51014 Tartu, Estonia*

[2]*University of Tartu, Institute of Chemistry, Ravila 14A, 50411 Tartu, Estonia*

e-mail: lauri.aarik@ut.ee

Studies performed in last few decades have demonstrated that due to high chemical stability, photocatalytic activity, refractive index and dielectric constant of titanium dioxide (TiO_2) thin films prepared by atomic layer deposition (ALD) can be applied as a high-permittivity (high-*k*) dielectric film in microelectronics, high refractive index layers in optical coatings, protective material for anti-corrosive coatings in metal industry, etc. As in number of applications, films with low impurity content are needed. Thus, the goal of this study is to clarify the possibilities to deposited TiO_2 from $TiCl_4$ and ozone as hydrogen-free ALD precursors that could, in principle, ensure low hydrogen concentration in the films.

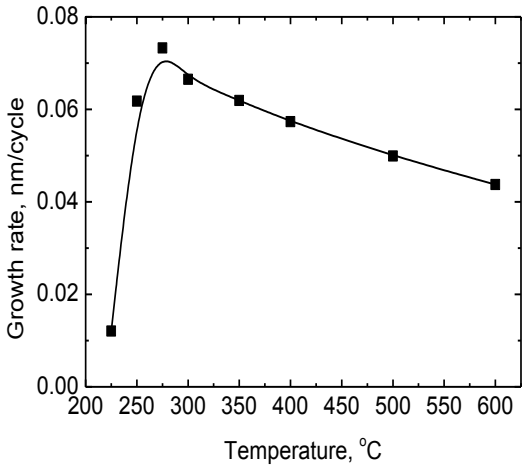

Fig.1 Growth rate as a function of temperature.

In order to investigate the film growth in real time and optimize the deposition process the quartz crystal monitor (QCM) was used. Growth of TiO_2 with acceptable rate was obtained at substrate temperatures 225–600°C (Fig.1). The composition studies made by X-ray fluorescence spectroscopy clearly demonstrated that O_3 was sufficiently reactive to ensure efficient replacement of chlorine by oxygen during the film growth. The films deposited from $TiCl_4$ and O_3 at 275°C contained only 0.12 ± 0.045 % of chlorine. This level was comparable to that obtained in the $TiCl_4$-H_2O process. The advantage of the $TiCl_4$-O_3 process is, however, the absence of possible sources of hydrogen contamination.

CHARACTERIZATION OF HYDROXIAPATITE BY TIME-RESOLVED LUMINESCENCE AND FTIR SPECTROSCOPY

Larisa Grigorjeva[1], Donats Millers[1], Krisjanis Smits[1], Dzidra Jankovica[2], Lasma Puķina[3]

[1]*Institute of solid State Physics, University of Latvia,*

[2]*Institute of Inorganic Chemistry, Riga Technical University, Latvia*
e-mail of presenting author: lgrig@latnet.lv

Hydroxyapatite $Ca_{10}(PO_4)_6(OH)_2$ (HAp), is inorganic component of bone and its synthetic version has been used for biomedical implant application. The present work deals with FTIR spectroscopy and time-resolved luminescence study of undoped and RE ions doped HAp nanocrystalline powders. RE ions substitute for Ca^{2+} in HAp structure and the charge compensations is required. On the other hand the RE ions luminescence was used as a local structure probe.

The samples were synthesized by co-precipitation method by using the ammonium dihydrogen phosphate $(NH_4)_2HPO_4$, calcium nitrate $Ca(NO_3)_2{\cdot}4H_2O$ and RE nitrates, for example $Eu(NO_3)_3{\cdot}6H_2O$. After the reaction the resulting material was washed several times and dried at 80^0C for 72h. The XRD measurements show hexagonal HAp structure; the grain size estimated from XRD measurements and is in range 20-25 nm.

The time–resolved photoluminescence (PL) has been measured at 300K. The YAG pulsed laser (266 nm, 2 ns pulse duration) was used for the PL excitation. PL measurements were carried out with a photon counting head (HAMAMATSU H8259) and photon counting board FastComTec Communication Technology module P 7887 and minimal time bins 250 ps. The radioluminescence and PL spectra were compared.

The Eu^{3+} ion luminescence is know as most studied luminescence dopand in HAp [2,3] due to luminescence bands sensitivity to local symmetry. The Eu^{2+} luminescence and intrinsic luminescence in undoped HAp were studied and analyzed.

References

1. R.Ternane. M.Th.Cohen-Adad, G.Panczer, C.Goutaudier, C.Dujardin, G.Boulon, N.Krib-Ariguib, M.Trabelski-Ayedi. Solid State Sciences, 2002, 4, 53-59.
2. O.A.Graeva, R.Kanakaja, A.Madani, B.C.Williams, K.C.Glass. Biomaterials, 2010, 31, 4259-42267.

Spark plasma sintering (SPS) of nanosized zirconia powders, obtained by azeotopic distillation

L.Kuznecova, A.Kuzmin

Institute of Inorganic Chemistry of Riga Technical University, Latvia

Tambov Scientific Institute of Chemical Researches,Russia

e-mail: leonora2002@yandex.ru

Scientific interest in the nano-dispersed zirconia is associated with the ability to change the properties obtained on its basis in a wide range of ceramics. Depending on the chosen technology can be as dense ceramics, designed for cutting tools and moderately porous suitable for bone implants. Properties of zirconia ceramics have greatly depend on the technology of its production, from the purity of the starting zirconium powder, alloy plant, particle size powders and sintering conditions.

Today, obtaining chemical zirconia compositions based on it most of the work is devoted to the issue of obtaining nanoproduct with desired properties, as it allows the chemical synthesis to produce nanopowder with a high degree of reproducibility and purity [1, 2].

We have analyzed properties of partially stabilized zirconia nanopowders, obtained by azeotropic distillation synthesis and ceramics, received by SPS sintering.

It was synthesized nanopowders with specific surface area in the range of 100-120 m^2/g (at temperature calcinations of 420 ^oC) and the crystallite size of the *t*-ZrO_2 in the range of 8-10 nm.

To be observe that received ceramics have high values of hardness (1465 HV at 5 kg of loading) and high density reaching to 98.4 % of theoretical density.

Thermal conductivity of the sintered ceramics were measured by the calorimeter IT λ 400 was 1,85 ± 0,09 W/(m·K).

References

1. J.C Ruiz-Morales, D. Marrero-López, J.T.S Irvine, P. Núñez. A new alternative representation of impedance data using the derivative of the tangent of the phase angle: Application to the YSZ system and composites. Mater. Res. Bull. 2004, 39 (9), pp. 1299-318. (Cites 10 times), IF-2011:1.284.

2. A.A. Voevodin, J.S. Zabinski. Nanocomposite and nanostructured tribological materials for space applications. Composites Sci. Technol. 2005, 65 (5 SPEC. ISS.), pp.741-748. (Cited 115 times), IF-2011:2.940. DOI: 10.1016/j.compscitech.2004.10.008

RARE EARTH DOPED ZIRCONIA NANOSTRUCTURED TRANSPARENT CERAMICS

Krisjanis Smits[1], Donats Millers[1], Larisa Grigorjeva[1], Dzidra Jankovica[2], Claude Monty[3]

[1]*Institute of solid State Physics, University of Latvia,*

[2]*Institute of Inorganic Chemistry, Riga Technical University,*

[3]*PROMES CNRS, France*

e-mail of presenting author: smits@cfi.lu.lv

Zirconia is one of the most promising oxides to be used as an up-conversion host material, because of the high chemical and physical stability as well as due to relatively low phonon energy of the matrix especially among oxides which is an important factor for the overall efficiency of the up-conversion processes in a material.

For practical luminescence applications the glasses or crystals and also nanostructured transparent ceramics are more preferable. There is also interest to obtain transparent nanostructured zirconia ceramic for laser optics as well for luminescent sensor applications. Some successful attempts to synthesize ZrO_2/TiO_2 transparent ceramics were reported earlier [1].

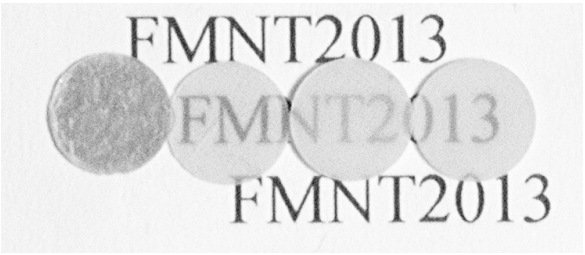

Fig.1 Pure and rare earth doped zirconia ceramics made by cold pressing from different raw nanocrystal powders

Optical semitransparent (translucent) polycrystalline ZrO_2 and ZrO_2 with Er, Yb and Nb ceramics were fabricated by cold and hot pressing (Fig.1). The nanocrystals were obtained by Solar Vapor condensation method realized in *Heliotron* reactor (PROMES CNRS France) [2]. As the raw materials for solar evaporation the Sol Gel nanocrystals were used.

The upconversion luminescence and the time resolved luminescence properties were compared of initial Sol Gel material with these of the Solar Vapor condensed nanocrystals.

References

1. U. Peuchert, Y. Okano, Y. Menke , S. Reichel, A. Ikesu*, J Eur. Ceram. Soc.,* 2009 No. 29 , 283–291

2. C.J.A.Monty, Arabian Journal for Science and Engineering. 2010, 35 (1C), 93-118].

NOVEL FINE-DISPERSE BIMETALLIC Pt-Pd/Al_2O_3 CATALYSTS FOR GLYCEROL OXIDATION WITH MOLECULAR OXYGEN

Konstantins Dubencovs[1], Svetlana Cornaja[1], Elina Sproge[1], Valdis Kampars[1], Daiga Markova[1], Lidija Kulikova[2], Vera Serga[2], Antons Cvetkovs[2]

[1]*Institute of Applied Chemistry, Riga Technical University, Latvia,* [2]*Institute of Inorganic Chemistry, Riga Technical University, Latvia*

e-mail: Konstantins.Dubencovs@rtu.lv

Increasing production of biodiesel which is one of the bio renewable energy sources causes surplus of glycerol. As its supply far away exceeds demand, many scientists look for other glycerol utilization fields. In this work selective glycerol oxidation which is one of the preferable glycerol conversion methods in the presence of novel fine-disperse bimetallic catalysts is studied.

Using new extractive-pyrolytic method we have synthesized several Pt-Pd bimetallic catalysts supported on plasma-processed alumina nanopowder (SSA 46 m^2/g). We have investigated catalysts synthesis and glycerol oxidation process parameter influence on catalyst activity and selectivity oxidizing glycerol in mild conditions. Change of Pt-Pd loading from 0.6 to 2.4% for each metal on the support didn't affect catalysts activity and selectivity significantly but influence of glycerol/Pt-Pd molar ratio and NaOH initial concentration was considerable. Best result (65% selectivity to glyceric acid with 96% glycerol conversion) was achieved using 1.2%Pt-1.2%Pd/Al_2O_3 catalyst when glycerol oxidation conditions were as follows: c_o(glycerol) = 0.3 M, c_o(NaOH) = 0.7 M, n(glycerol)/n(metal) = 300 mol/mol, t = 60 °C, P(O_2) = 1 atm, oxidation time 4 hours. Novel 1.2%Pt-1.2%Pd/Al_2O_3 catalyst was practically inactive in neutral water solutions (glycerol conversion was only 3%). In alkaline solutions novel bimetallic catalysts were more active and also selective to glyceric acid comparing them with analogous monometallic Pt/Al_2O_3 and Pd/Al_2O_3 catalysts [1, 2].

References

1. S.Chornaja, K.Dubencov, V.Kampars, O.Stepanova, S.Zhizhkun, V.Serga, L.Kulikova, *Reac. Kinet. Mech. Cat.* 2012, DOI) 10.1007/s11144-012-0516-3.

2. E.Palcevskis, L.Kulikova, V.Serga, A.Cvetkovs, S.Chornaja, E.Sproge, K.Dubencovs, *J. Serb. Chem. Soc.* 2012, 77, 1799–1806

Acknowledgments

This work was supported by the ERAF project Nr. 2010/0304/2DP/2.1.1.1.0/10/APIA/VIAA/087.

INVESTIGATION OF Ti DOPING EFFECT ON STABILIZATION OF R'-PLANE ORIENTED EPITAXIAL Cr_2O_3 THIN FILMS ON R-PLANE SAPPHIRE

Kaspar Roosalu, Taavi Pungas, Aivar Tarre, Jaan Aarik, Hugo Mändar

Institute of Physics, University of Tartu, Estonia

e-mail: roosalu@ut.ee

Titanium doped Cr_2O_3 (CTO) shows good gas sensing properties and has found use in commercial gas sensors. Manufacturing processes yielding great specific surface are preferred as gas sensing reactions occur on the surface CTO. Thus it is common that CTO with desired stoichiometry is produced for example by solid state reaction or flame evaporation followed by milling to suitable crystallite size and subsequent sintering. Although it is known that microcrystals of sintered CTO expose prevalently rhombohedral r-planes $(1\bar{1}\,02)$ [1], it is important to note that the other family of nonequivalent rhombohedral planes, the r'-plane $(\bar{1}\,102)$, has different surface configuration [2] and expectedly unique physical and chemical properties that have not yet been investigated for gas sensing applications.

In this report the structure and composition of atomic layer deposited epitaxial CTO thin films with various Ti content (<0.3 of total metal content) were studied by X-ray diffraction (XRD), X-ray fluorescence (XRF), X-ray reflectivity (XRR) methods. In our presentation we show that the ratio between r and r' orientations in epitaxial CTO films dependent on Ti content and the r' orientation became prevalent at a certain concentration of titanium in the films. We present the results of theoretical analysis of surface free energy and atomic configuration for r- and r'-planes of pure Cr2O3 and doped with Ti, calculated by molecular dynamics methods (GULP) and density-functional theory (CASTEP). The r'-plane was found to have one of the highest energies among low-index planes of α-Cr_2O_3. To our knowledge no prior work has been done on r'-plane atomic reconstruction and free energy calculations.

References

1. D.Scarano, A.Zecchina, S.Bordiga, G.Ricchiardi, G.Spoto, *J.Chem.Phys.*, 1993, No.177, 547-560.

2. H.Mändar, T.Uustare, J.Aarik, A.Tarre, A.Rosental, *Thin Solid Films.*, 2007, No.515, 4570- 4579.

DEVELOPMENT OF NANOFIBROUS 3D COLLAGEN/POLYANILINE COMPOSITES AS TISSUE ENGINEERING SCAFFOLDS

Kaido Siimon[1], Martin Järvekülg[2], Ivo Laidmäe[3]

[1]*Institute of Physics, University of Tartu, Estonia,* [2]*Estonian Nanotechnology Competence Centre, Estonia,* [3]*Department of Pharmacy, University of Tartu, Estonia*

Kaido.Siimon@ut.ee

Nanofibrous 3D collagen-based composite matrixes are being developed using electrospinning technique. The main objects of our studies are the effects of scaffold composition, polyaniline dopants and electrospinning parameters on scaffold properties and usability of the fabricated scaffolds as tissue engineering scaffolds.

3D scaffolds can be designed to closely mimic the environment of cells in a living organism, which is a considerable advantage compared to 2D surfaces. 3D collagen/polyaniline composite scaffolds can be made using electrospinning technique, resulting in a fibrous material, which is designed to have a nanofibrous collagen on the outside and a thin layer of polyaniline on the inside. The great porosity and relatively large specific surface area of the materials fabricated by electrospinning support cell adhesion and growth. Furthermore, electrospinning allows combining useful properties of both collagen and polyaniline.

Prior to electrospinning, polyaniline can be doped with various dopants, but is easely dedoped in water media. This in turn may lead to significant changes in solution pH even in buffer solutions, which makes the scaffolds unusable for cell culture. Therefore, techniques are being developed to make these scaffolds stable in water solutions.

The suitability of the scaffolds for cell culture is greatly determined by chemical composition, mechanical and electrical properties of the materials used. We are trying to elaborate scaffolds with properties similar to the growing environment of cells in a living organism.

INFLUENCE OF HE/ D_2 PLASMA FLUXES ON TUNGSTEN COATINGS MORPHOLOGY AND CRYSTALLINITY

K. Piip[1], P. Paris[1], A. Hakola[2], K. Bystrov[3], G. De Temmerman[3], M. Aints[1], I. Jõgi[1], J. Kozlova[1], M. Laan[1], J. Likonen[2], A. Lissovski[1], H. Mändar[1]

[1]Institute of Physics, University of Tartu, Estonia, [2]VTT, Finland, [3]DIFFER- Dutch Institute For Fundamental Energy Research, the Netherlands.

e-mail of presenting author: kaarel.piip@ut.ee

Tungsten coatings play a growing role in different appliances because of their thermal characteristics. Future fusion reactor walls in their most critical areas in divertor, where they suffer high plasma fluxes, will be made of tungsten. It makes important to study changes in tungsten surface morphology when exposed to high-flux He/D_2 plasmas.

Our previous study [1] showed that when samples with tungsten-containing coatings were exposed to hydrogen plasmas with moderate fluxes of low enough energy ions, the erosion of the coating was hardly detectable. In the present study, samples with pure tungsten coatings were tested using He-containing plasmas and higher surface temperatures. The main task of the study was to find the dependence of the surface morphology and its crystallinity on the plasma composition and the temperature of the sample coating.

Samples produced by DIARC-Technology Inc with 2 μm W-coatings on Mo were exposed to controlled plasma discharges in Pilot-PSI at DIFFER. Samples were exposed to pure He and D_2 and mixed He/D_2 plasmas. The maximum surface temperature of the samples was kept at 900^0C or 1200^0C and the ion energy in terms of the bias voltage was set to -40 V or -70 V.

SEM, EPMA and XRD as post mortem methods [1] were used to characterize the samples. SEM showed that the action of plasma beam caused at the sample surface formation of quasi-periodic structures of < 0.1 μm periodicity. According to XRD, plasma fluxes caused both a shift of XRD peaks and a decrease of the peak width.

References

1. P. Paris et al, Erosion of marker coatings exposed to Pilot PSI plasma, *J. Nuclear Materials*, Manuscript PSI2012, accepted

IMPEDANCE AND ADMITTANCE CHARACTERISTICS OF Bi_2S_3 NANOWIRE ARRAYS

Juris Katkevics[1], Gunta Kunakova[1], Arturs Viksna[1], Justin D. Holmes[2], Donats Erts[1]
[1]Institute of Chemical Physics, University of Latvia, Riga, Latvia
[2]Department of Chemistry, University College Cork, Ireland
e-mail: juris.katkevics@lu.lv

Nanowire arrays are advantageous building elements in fabrication of nanoelectronics and sensing devices. Their conductivity dependence on material and structure is the key parameter for potential practical applications. To control size distribution of nanowires diameter and obtain highly arranged arrays it is convenient to employ anodic aluminium oxide membranes (AAO) as templates for nanowire growth.

In this work we apply impedance and admittance measurements to characterize Bi_2S_3/AAO nanowire arrays. During electrochemical and electrical characterization of nanowires repeated action of current may influence their electrical properties; hence appropriate measurement conditions have to be established.

The influence of current frequency on the real, imaginary and complex electrochemical impedance and double layer capacitance for the Bi_2S_3 nanowire arrays was calculated. The changes in parameters of impedance and admittance with variable potential and constant current frequencies (1.5 Hz) were investigated.

Obtained experimental results show that Bi_2S_3 nanowire real resistance (Z_r) is constant within the measured potential region but imaginary resistance (Z_j) varies significantly. The real admittance (conduction) parameters of Bi_2S_3 nanowires are $2 \div 3$ $\mu\Omega^{-1}\cdot cm^{-2}$. Bi_2S_3/AAO nanowire array impedance parameters decreased and become stable after 5 hour conditioning in 0.1M CH_3COONa electrolyte at constant applied potential.

Calculated electrical properties of nanowire array and determined measurement conditions are important for characterization of large samples and in further studies of nanowires/ porous AAO membrane as complex electrode in nanowires array sensor applications.

CHARACTERIZATION OF GRAPHENE PREPARED BY CHEMICAL VAPOUR DEPOSITION ON NICKEL

Jekaterina Kozlova[a], Ahti Niilisk[a], Aarne Kasikov[a], Alar Gerst[a], Tauno Kahro[a], Arvo Tõnisoo[a], Harry Alles[a], Väino Sammelselg[a,b]

[a] *University of Tartu, Institute of Physics, Department of Materials Science, Riia 142, 51014 Tartu, Estonia*
[b] *Institute of Physical Chemistry, University of Tartu, Ravila 14a, 50011 Tartu, Estonia*
e-mail: jekaterina.kozlova@ut.ee

Graphene excellent electrical properties make it a promising material for nanoelectronics. The successful graphene implementation in electronics requires large-area high quality graphene synthesis. Chemical Vapor Deposition (CVD) on copper foils allows large-scale monolayer graphene production, but produced graphene sheets are polycrystalline with different graphene domains rotationally misoriented to each other, which leads to defects when the islands combine. On contrary, nickel does not introduce rotational disorder into graphene sheet and has smaller lattice mismatch with graphene, which can potentially lead to lower defect density and improved synthesized graphene quality in comparison to other catalysts. However, graphene growth on nickel is not self-limiting process which results in inhomogenious few-layer graphene growth.

In this work predominantely monolayer graphene was synthesized on nikel thin films. The nickel films were prepared by e-beam evaporation on silicon substrates covered with 300 nm layer of silicon dioxide. Graphene was synthesized onto these Ni films in a laboratory CVD reactor at low pressure from methane using argon as a carrier gas. Following the synthesis, graphene was covered with PMMA and nikel was etched away. The quality and thickness homogeneity of graphene samples were examined using μRaman spectroscopy, incl. spectroscopic mapping, and SEM techniques. Ti/Au contacts were fabricated onto prepared graphene structures by e-beam evaporation method. Electrical parameters of the graphene were determined and compared to values obtained on the copper catalyst.

Two limits of electron capture in a dynamic quantum dot

Janis Timoshenko[1,2], Vyacheslavs Kashcheyevs[1]

[1]Faculty of Physics and Mathematics, University of Latvia, Latvia

[2]Institute of Solid State Physics, University of Latvia, Latvia

e-mail: janis.timoshenko@gmail.com

Dynamic quantum dots are nano-sized areas of the 2D electronic system, electrostatically decoupled from the environment and controlled by time-dependent voltages, applied to gate electrodes [1]. They can be used, for example, as a basis for very precise current sources or as a physical implementation of a qubit – the elementary unit for quantum information processing.

The charge capture in a dynamic quantum dot is an essentially time-dependent and non-adiabatic process [1,2], which can be described by kinetic rate equations for the time-dependent probability distribution of the electron number in the quantum dot. In this study we identify two universal, device-independent limits of the charge capture process that correspond to opposing physical mechanisms: (i) *generalized grand-canonical* or *thermal limit* (temperature of the system is relatively high and the decoupling of the dot from environment is considered as sudden); and (ii) *generalized decay cascade* or *athermal limit* (temperature is low, and the decoupling of the quantum dot is gradual). We show that the dependencies of probability to capture given number of electrons on circuit parameters (e.g., gate voltage) are different in these two limits (Fig. 1), but in both cases they can be described by relatively simple expressions, where all complex system dynamics is encoded in one characteristic parameter per each charge state.

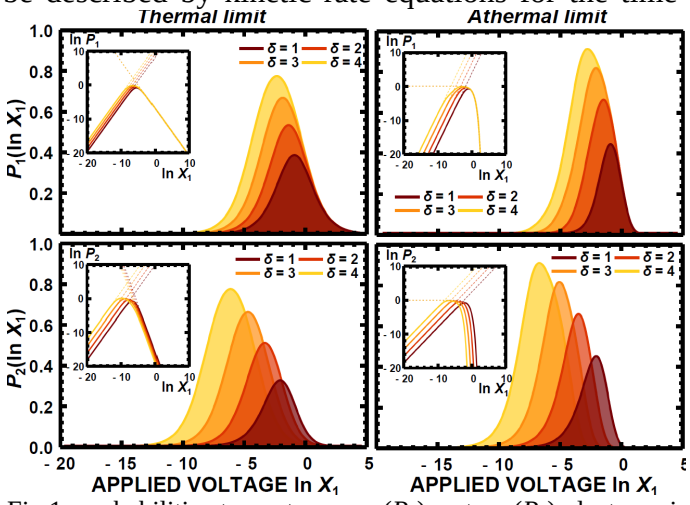

Fig.1. probabilities to capture one (P_1) or two (P_2) electrons in the quantum dot as functions of applied voltage in the thermal (*left panels*) and athermal (*right panels*) limits.

References

1. V. Kashcheyevs, B. Kaestner, Phys. Rev. Lett. **104**, 186805 (2010).
2. V. Kashcheyevs, J. Timoshenko, Phys. Rev. Lett. **109**, 216801 (2012)

STRUCTURE, MICROMECHANICAL AND MAGNETIC PROPERTIES OF POLYCARBONATE NANOCOMPOSITES

Janis Maniks[1] (presenting author), Roberts Zabels[1], Remo Merijs Meri[1], Janis Zicans[1]

[1]Institute of Solid State Physics, University of Latvia, [2]Institute of Polymer Materials, Riga Technical University

e-mail of presenting author: manik@latnet.lv

Modification of polymers with nanostructured fillers offers multiple advantages over traditional microcomposites. Nanocomposites usually possess considerably improved properties already at small nanofiller content. Depending on the intrinsic nature of the nanofiller, some specific properties such as magnetism, electrical conductivity and others can be assigned to polymers. There is much evidence about modification of primary aromatic thermoplastic polyesters, such as polycarbonate (PC), with inorganic anisometric fillers, particularly layered silicates [1], carbon nanotubes [2] and graphene [3]. Considerably less research has been devoted to modification of PC with magnetic nanofillers.

The current study evaluates the applicability of PC for development of magnetic polymer nanocomposites. Both, primary and secondary PC is used as a matrix for modified composites with commercial nanostructured cobalt ferrite ($CoFe_2O_4$). The nanocomposites are manufactured by the method of twin screw extrusion. The amount of nanostructured filler is changed from 0 to 5 wt. %. Ethylene-vinyl acetate elastomer in the amount of 10 wt. % is added as toughener. Structural characteristics of nanocomposites are determined by differential scanning calorimetry. Magnetic properties are characterized by means of vibrating sample magnetometer.

It is observed that upon introduction of the magnetic filler paramagnetic hysteresis loop is observed: at 5 wt. % of $CoFe_2O_4$ saturation magnetization of the nanocomposite is 2,17 emu/g, remanent magnetization is 0,8 emu/g and coercivity is 1200 G. Nanoindentation tests show that nanofiller-reinforced samples maintain reasonable plasticity characterized by work of plastic indentation, while their modulus and hardness are improved.

ACKNOWLEDGEMENTS: The research is carried out within the framework of the ERAF project Nr. 2010/0209/2DP/2.1.1.1.0/10APIA/VIAA/028

References

1. Guduri, B.R., Luyt, A.S. J. Nanosci. Nanotechnol., 2008, Apr;8(4):1880-1885.
2. Wang, M., Li, B., Wang, J. and Bai, P. Polym. Adv. Technol., 2011, 22, 1738–1746.
3. Yoonessi M, Gaier JR. ACS Nano, 2010, Dec 28;4(12), 7211-20.

MODIFICATION OF LiF STRUCTURE BY IRRADIATION WITH SWIFT HEAVY IONS UNDER OBLIQUE INCIDENCE

J. Maniks[1], R. Zabels[1], K. Schwartz[2], I. Manika[1], R. Grants[1], A. Dauletbekova[3], A. Rusakova[3], M. Zdorovets[4]

[1]*Institute of Solid State Physics, University of Latvia, Riga, Latvia,*

[2] *GSI Helmholtzzentrum für Schwerionenforschung, Darmstadt, Germany,*

[3]*L.N. Gumilyov Eurasian National University, Astana, Kazakhstan,*

[4]*Institute of Nuclear Physics, Astana, Kazakhstan*

e-mail: manik@latnet.lv

A significant progress in the research of track formation and surface nanostructuring has been achieved performing irradiations of various materials with swift heavy ion beams at grazing incidence [1]. In this work bulk-structure modifications in LiF irradiated with SHI under oblique angles have been investigated using AFM, chemical etching, nanoindentation and optical absorption spectroscopy. LiF crystals were irradiated under incidence angles of 30 and 70 degrees with 2.2 GeV Au (fluence 5×10^{11} ions·cm^{-2}) and 150 MeV Kr (fluence 10^{12}-10^{14} ions·cm^{-2}) ions. Investigations of the structure were performed on cross-sections produced by cleaving crystals perpendicular to the irradiated surface. Our recent studies on normally irradiated samples showed two typical structural zones: (1) a nanostructured region in the depth range where the electronic energy loss surpasses the threshold of 6-10 keV/nm and (2) a dislocation-rich region in the further part of the ion track [2]. The current results show that the characteristic zones of structural damage in samples irradiated under oblique angles are similar with those for normal irradiation. The dislocation loops in the dislocation-rich zone revealed by chemical etching in both cases have the <100> orientation. However, a variation of the thickness of irradiated layer with angle is observed. The nanoindentation measurements showed a higher hardness of samples irradiated under oblique angles. Such result can be attributed to differences in aggregation and ordering of defects in the mechanical stress field of ion tracks.

References

1. D.K.Avasthi, G.K.Mehta. Swift Heavy Ions for Materials Engineering and Nanostructuring. Springer Series in Materials Science, 2011, Capital Publishing Company, New Delhi, India.

2. A. Dauletbekova, J.Maniks, I.Manika, R.Zabels, A.T.Akilbekov, M.V.Zdorovets, Y.Bikhert, K.Schwartz, *Nucl. Instr. and Meth. B*, 2012, 286, 56-60

ELECTRODEPOSITION OF NANOPOROUS NICKEL LAYERS USING INDUCTIVE VOLTAGE PULSES

Martins Vanags, Janis Kleperis (presenting author), Gunars Bajars, Vladimirs Nemcevs
Institute of solid State Physics, University of Latvia,
e-mail of presenting author: kleperis@latnet.lv

Electrode/electrolyte interface with high active surface is important parameter for efficient electrolysis cell. The high surface-to-volume ratio as well as the very small particle size provides the higher activity of nanostructured catalysts [1]. We used inductive voltage pulses for electro-deposition of porous nickel thin film onto steel electrode. Short pulses (t_p<1μs) with variable amplitude (to ensure electro-deposition current density in region 124-224 A/dm^2) were applied to electrode and resulting coating were analyzed with electrochemical and microscopically methods. At lower current densities only smooth nickel coatings growth, while at higher current densities the bubbles appear and porous layer was formed. Electrochemical impedance spectra of smooth and porous layers are measured in deionized water (Fig.1) and in 1M KOH solution. The capacity C in equivalent scheme (Fig. 1 top right) is proportional to electrode surface, and from impedance spectra it is calculated that porous layer has 20 times larger active surface comparing to smooth layer (in KOH solution). From electrochemical measurements it is estimated that more efficient hydrogen evolution reaction occurs on electrode with porous nickel layer obtained at 223 A/dm^2. It is shown in this work that inductive short pulse method can be used to obtain nano-porous nickel coatings on electrodes for efficient electrolysis cell.

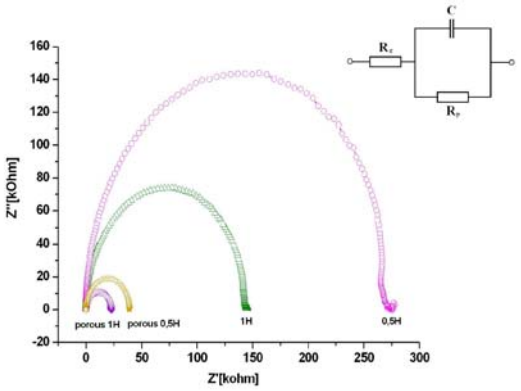

Fig.1 Nyquist impedance plots of smooth (larger semi-circles) and porous (smaller semi-circles) Ni coatings on steel electrode.

Acknowledgement: Authors acknowledge ERDF project Nr. 2010/0188/2DP/2.1.1.1.0/10/APIA/ VIAA/031 for financial support.

References:

1. L.P. Bicelli, B. Bozzini, C. Mele, L. D'Urzo, *Int. J. Electrochem. Sci.*, 2008, vol.3, 356 – 408.

CHEMICAL VAPOR DEPOSITED GRAPHENE ADSORBTION ABILITY

V.Grehov, J.Kalnacs, A.Murashov, A.Vilkens
Institute of Physical Energetics
e-mile of presenting author: jkalnacs@edi.lv

Nitrogen adsorption was studied for graphene, produced by chemical vapour deposition method (CVD) [1] . Typical isotherms of such samples are shown on Fig.1

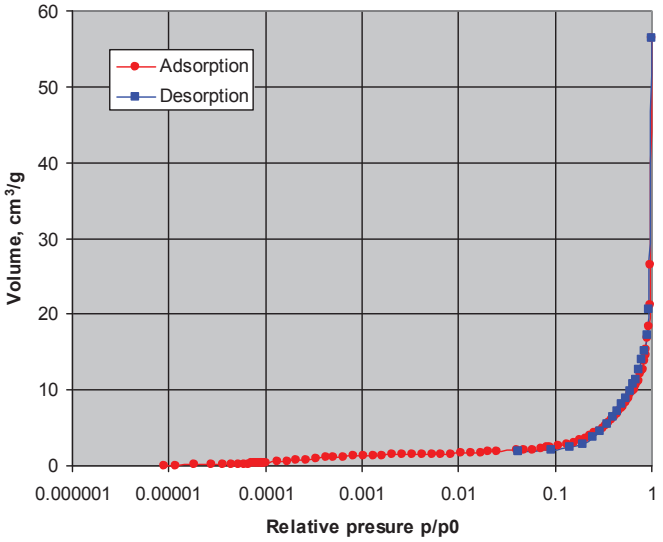

Fig.1 Tipical isotherms for CVD graphene.

The measurements were done using the manometric technique, in the range of relative nitrogen pressure from 10^{-6} to 1. The substance weight in each case was 5-15 mg. Before measuring adsorption, the sample was heated in vacuum at 300 °C for at least 24 h. Adsorption was measured after heating.

In determination of the specific surface area (S_{BET}) for the CVD graphene samples it was found that formally possible isotherms in BET approximation [2] are observed in two different pressure ranges.

Results:

Statistical analysis made it possible to distinguish two pressure regions for all the studied CVD samples - the region with greatest correlation and the region with greatest value S_{BET}.

The BET approximation at low pressure (Region 1) reflects a step-wise rise on the isotherm at a pressure of $p/p_0 \approx 0.0001$-0.001. It could be suggested that this step-wise adsorption of N_2 on CVD graphene is associated with the formation of a first adsorbed N_2 monolayer. In this case it is the Type IV isotherm due to the presence of mesopores. S_{BET} value 25 - 35 m^2/g was obtained in the BET approximation at low pressure. S_{BET} value 40-70 m^2/g was calculated in the higher pressure region with $p/p_0 \approx 0.2$-0.4.

The experimental results are discussed and their interpretation proposed.

References.

1. Zongping Chen, Wancai Ren, Bilu Liu, Libo Gao, Songfen Pei, Zhong-Shuai Wu, Jinping Zhao, Hui- Ming Cheng, Carbon 48 (2010) 3543-3550.
2. . Rouquerol, F., Rouquerol, J., & Sing, K. (1999). *Adsorption by Powder and Porows Solids*. Academic Press, p. 19.

CHARACTERISTICS OF STABILIZIED ZIRCONIA NANOPARTICLES PREPARED BY MOLTEN SALTS AND MICROWAVE SYNTHESIS

Janis Grabis, Dzidra Jankoviča, Jekaterina Sokolova, Ints Šteins
Institute of Inorganic Chemistry of Riga Technical University
e-mail of presenting author: grabis@nki.lv

Stabilizied zirconia nanoparticles due to their unique properties find application as solid electrolytes, gas sensors, catalysts, high-temperature corrosion resistant materials. Present trends in technology are directed to development of highly effective, economic and environmental friendly preparation methods of nanoparticles. From this point of view very perspective preparation methods of zirconia nanoparticles are fast microwave and solvent free molten salts synthesis. However, it is well known that properties of the prepared nanoparticles depend on the preparation method and used raw materials.

The aim of present work was comparison of properties and sinterability of stabilizied zirconia prepared by molten salts (MS) and microwave (MW) synthesis using $ZrOCl_2 \cdot 8H_2O$ or $ZrO(NO_3)_3 \cdot 2H_2O$ and $Y(NO_3)_3 \cdot 6H_2O$ as precursors. The MW synthesis was carried out in a Masterwave BTR, Anton Paar apparatus by heating salts solution in water or C_2H_5OH at temperature in the range of 150–190 ^oC during 20 min. The MS synthesis was carried out by heating mixture of the zirconia and yttria salts with NaCl and $NaNO_3$ at temperature in the range of 400–800 ^oC during one or two hours.

The prepared by the both methods YSZ crystalline nanoparticles containing 3 mol% Y_2O_3 consist from t-ZrO_2 and possible also c-ZrO_2 phase. The specific surface area of the nanoparticles prepared by MS and MW was in the range of 124–146 m^2/g and 90–117 m^2/g respectively in dependence on the synthesis parameters.

The crystallite size of YSZ nanoparticles prepared by MS synthesis was in the range of 4–14 nm and increases with temperature and duration time of the process as well as with decrease of molar ratio of oxides and sodium salts. The crystallite size of YSZ nanoparticles prepared by MW synthesis was in the range of 6–9 nm and was determined by the process temperature and used solvents.

The prepared samples were densified by using spark plasma sintering (SPE-825-CE, SPS Syntex Inc.). Densification of YSZ nanoparticles starts at 850 ^oC and samples with fine-grained microstructure with relative density of 98 and 96% respectively were obtained at 1300 ^oC. Therefore the both methods allow produce YSZ nanoparticles with controlled crystallite size and high sinterability.

ELECTRICAL PERCOLIATION IN ONION LIKE CARBON COMPOSITES

Jan Macutkevic[1], Juras Banys[1], Suzane Hens[2], Vesna Borjanovic[2], Olga Shenderova[2], Vladimir Kuznetsov[3], Sergei Moseenkov[3]

[1]Vilnius university, Vilnius, Lithuania, [2] International Technology Center, Raleigh, USA, [3] Boreskov Institute of Catalysis SB RAS, Novosibirsk, Russia

e-mail of presenting author: jan.macutkevic@gmail.com

Electrically percolative polymer-based composites have been attracting much attention because of their potential applications such as electroactive materials, sensitive materials, and electromagnetic coatings. Owing to the advanced electrical, thermal, and mechanical properties, various carbon nanoparticles like carbon nanotubes or carbon black have been widely studied and often used as nanofillers in the past few years. The main advantage of carbon nanotubes versus other carbon nanofillers is their extremely low percolation threshold [1]. The onion-like carbons (OLCs), consisting of stable defected multishell fullerenes, exhibit high conductivity similar to carbon nanotubes. It was also find that percolation threshold in OLC composites can be 10 vol % [2]. In this presentation we have investigated how further reduce percolation threshold in onion like carbon composites. The search of electrical percolation was performed in composites with various polymer matrix like Polymethylmetacrylate (PMMA), Polyurethane (PU), Polydimethylsiloxane (PDMS) and epoxy resin. It was demonstrated that after annealing of OLC/PMMA and PU composites above glass transition temperature however below melting point percolation threshold decreases. It was find also that percolation threshold is dependent from OLC aggregate size. Close to the percolation threshold the value of complex dielectric permittivity is high in all investigated frequency range from hertz to terahertz. Therefore, investigated OLC composites are promising candidates for various electronic applications.

This research is funded by the European Social Fund under the Global Grant measure.

[1] W. Bauhofer, J. Z. Kovacs, Composites Science and Technology 69, 1486 (2009).

[2] J. Macutkevic, D. Seliuta, G. Valusis, J. Banys, V. Kuznetsov, S. Moseenkov, O. Shenderova, App. Phys. Lett. 95, 112901 (2009).

INFLUENCE OF PREPARATION TECHNOLOGY ON THE DIELECTRIC PROPERTIES OF CARBON NANOTUBES POLYMER COMPOSITES

Jan Macutkevic[1], Alesya Paddubskaya[2], Polina Kuzhir[2], Ieva Kranaviciute[1], Juras Banys[1], Sergey Maksimenko[2],
Vladimir Kuznetsov[3], Ilya Mazov[3], Dmitri Krasnikov[3]

[1]Vilnius university, Vilnius, Lithuania, [2]Institute of Nuclear Problem of Belarus State university, Minsk, Belarus, [3] Boreskov Institute of Catalysis SB RAS, Novosibirsk, Russia

e-mail of presenting author: jan.macutkevic@gmail.com

The dielectric properties of Polymethylmetacrylate (PMMA) composites filled with CVD made multi-walled carbon nanotubes (MWCNT) of different mean outer diameters (d ~ 9 nm and 12-14 nm) were investigated in temperatures from 300 K to 450 K and in wide frequency range (20 Hz-1 MHz). Composites were prepared by *in-situ* polymerization and coagulation. At room temperature and below percolation threshold the dielectric permittivity was found to be higher for composites with thicker carbon nanotubes. For composites prepared by coaguliation percolation threshold is higher as 2 wt%. In contrast, for composites prepared by *in-situ* polymerization it is lower, for composites with thin nanotubes it is about 1 wt% and 2 wt% for thick nanotubes composites. Such difference of percolation threshold value is caused by better distribution of thin carbon nanotubes. Temperature dependence of complex dielectric permittivity of investigated composites below percolation threshold is mainly caused by β relaxation in pure PMMA polymer matrix. The potential barrier for PMMA molecules rotation is higher in composites with thicker MWCNT and demonstrates non-monotonous concentration dependence. Above and close to percolation threshold on heating to 450 K the complex dielectric permittivity increase due negative temperature effect. The temperature dependence of DC conductivity of composites with 2 wt% MWCNT (on cooling below 300 K) was fitted with fluctuation induced tunneling model

$$\sigma_{DC} = \sigma_0 \exp(-(T_1/(T+T_0))), \quad (1)$$

where T_1 represents the energy required for an electron to cross the insulator gap between conductive particles aggregate and T_0 is the temperature above which thermal activated conduction over the barriers begins to occurs. Obtained parameters are σ_0=0.01 S/m, T_1=174 K, T_0=63 K for composite with thin nanotubes and σ_0=8.71 μS/m, T_1=139 K, T_0=62 K for composite with thick nanotubes.

Acknowledgment

This research is funded by the European Social Fund under the Global Grant measure.

MAGNETIC MOMENT OF SINGLE VORTICES IN YBCO NANO-SUPERCONDUCTING PARTICLES: EILENBERGER APPROACH

Ivan Zakharchuk[1,2], Polina Belova[1,3], Mikhail Safonchik[1,4], Konstantin Traito[1], Erkki Lähderanta[1]

[1]Lappeenranta University of Technology, Finland, [2]Saint-Petersburg State Electrotechnical University, Russia, [3]Petrozavodsk State university, Russia, [4]A. F. Ioffe Physico-Technical Institute, Russia

email: ivan.zakharchuk@lut.fi

Temperature dependence of single vortex magnetic moment in nanosize superconducting particles is investigated in the framework of quasiclassical Eilenberger approach. Such nanoparticles can be used for preparation of high-quality superconducting thin films with high critical current density [1]. In contrast to bulk materials where the vortex magnetic moment is totally determined by flux quantum, in nano-sized specimens (with characteristic size, D, much less than effective penetration depth, λ_{eff}) the quantization rule is violated and magnetic moment is proportional to $D^2/\lambda_{eff}^2(T)$. Due to strong repulsion between vortices in nanoparticles only a single vortex can be trapped in them. Because of small size of particles the screening current of the vortex is located near the vortex core where the current is quite high and comparable to depairing currents. Therefore, the superconducting electron density, n_s, depends on the current value and the distance from the vortex core. This effect is especially important for superconductors having gap nodes, such as YBCO.

The current dependence of n_s in nanoparticles is analogous to the Volovik effect in flux-line lattice in bulk samples. The magnitude of the effect can be obtained by comparing the temperature dependence of magnetic moment in the vortex and in the Meissner states. In the last case the value of screening current is small and superconducting response to the external field is determined by London penetration depth. Because of importance of nonlinear and nonlocal effects, the quantum mechanical Eilenberger approach is applied for description of the vortex in nanoparticles. The flattening of $1/\lambda_{eff}^2(T)$ dependence has been found. A comparison of the theoretical results with experimental magnetization data in Meissner and mixed states of YBCO nanopowders has been done. The presence of nonlinear and nonlocal effects in vortex current distribution is clearly visible. The obtained results are important for the description of pining in nanostructured high-T_c thin films.

References

1. M. Peurla, H. Huhtinen, M. A. Shakhov, K. Traito, Yu. P. Stepanov, M. Safonchik *et al.*, *Phys. Rev. B*, 2007, No.75, 184524.

Corrosion protection of metals using multilayer thin films based on TiO_2 and Al_2O_3 grown by ALD

Ivan Netšipailo[1], Lauri Aarik[1], Väino Sammelselg[1,2]

[1]*Institute of Physics, University of Tartu, Riia 142, 51014 Tartu, Estonia*

[2]*Institute of Chemistry, University of Tartu, Ravila14a, 50411 Tartu, Estonia*

email: vanes@ut.ee

Corrosion destruction of chemically active metals from their surface side is a big problem in industry and society also nowadays. Thus, the methods that consist of using chemically resistive sealing coatings on top of samples surfaces, playing gas barrier role, are well appreciated. Widely used paint-coatings that are as a rule relatively thick, up to tens micrometers, and despite of this have low mechanical resistivity, thin and ultra-thin inorganic films can be used instead if they fulfill all necessary sealing properties: high chemical inertness, low gas diffusion, good adhesion to the substrate surfaces, necessary elasticity, are homogeneous and defect free. It is known that atomic layer deposition (ALD) method ensures ideal surface coverage and should also yield defectless thin films with high density. Therefore the method should have marked application perspectives in preparation of thin anti-corrosion coatings.

In this work multilayer ALD thin films based on 6 sublayers: $3\times(Al_2O_3+TiO_2)$ were examined. Difference of etching rates the films deposted at different substrate temperatures onto Si or steel substrates was determined for different concentrated acid environments.

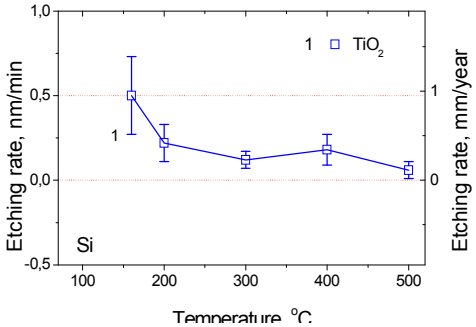

Figure 1.

It is shown that titania subfilms with anatase structure have significant resitance even in hot 80% sulphur acid and the ones with rutile structure are good in 37% hydrochloric acid (see Fig. 1).

HYDROGEN CHLORIDE AS A POSSIBLE REACTANT FOR SYNTHESIS OF TITANIUM CARBIDE DERIVED CARBON POWDERS FOR HIGH-TECHNOLOGY DEVICES

Indrek Tallo, Thomas Thomberg, Alar Jänes, Enn Lust

Institute of Chemistry, University of Tartu, Estonia

e-mail: Indrek.tallo@ut.ee

Molecular chlorine has been dominantly used for the synthesis of carbide derived carbons. Based on preliminary data, hydrogen chloride might prove to be a safer and cheaper replacement. The main aim of this work was to establish the influence of hydrogen chloride as the reactant on the carbon synthesis conditions and consider the suitability of the prepared carbon for supercapacitor electrode material.

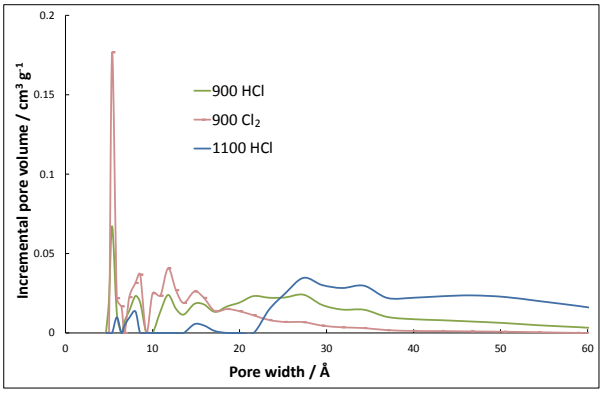

Fig.1 Pore size distributions of different synthesized materials obtained from low temperature N_2 sorption measurements.

Carbon powders were synthesized from titanium carbide within the temperature range from 700 to 1100°C using either molecular chlorine or hydrogen chloride as reactant. High-resolution transmission electron microscopy, X-ray diffraction, Raman spectroscopy, low temperature N_2 sorption, cyclic voltammetry, constant power and electrochemical impedance methods were used to study the synthesized materials.

Based on experimental results, titanium carbide derived carbon powders synthesized by using molecular chlorine showed somewhat better performance if used as the electrode material for non-aqueous electrolytes based supercapacitors. The somewhat different more mesoporous morphology of the obtained carbon, when using hydrogen chloride as reactant, might be interesting for applications other than supercapacitors.

This work was supported in part by the Estonian Ministry of Education and Research (project SF0180002s08), by the Estonian Centre of Excellence in Science: High Technology Materials for Sustainable Development, Estonian Energy Technology project 3.2.0501.10-0015, Estonian Materials Technology project 3.2.1101.12-0019, by the graduate school "Functional Materials and Technologies", receiving funding from the European Social Fund under project 1.2.0401.09-0079 in Estonia and by the Estonian Science Foundation under project no. 8172.

References

I.Tallo, T.Thomberg, H.Kurig, A.Jänes, K.Kontturi,E.Lust, *J. Solid State Electr.*, 2013, No.17, 19-28.

DIELECTRIC SPECTROSCOPY OF GRAPHITE LOADED EPOXY RESIN COMPOSITES

I. Kranauskaite[1], J. Macutkevic[1], J. Banys[1], A. Celzard[2], S. Bellucci[3]

[1]*Vilnius university,* [2]*IJL – UMR CNRS 7198 AND LERMAB – ENSTIB,* [3]*INFN-Laboratori Nazionali di Frascati*

e-mail: ieva.kranauskaite@ff.stud.vu.lt

Polymer composites with various carbon inclusions, like single- or multi- walled carbon nanotubes, carbon black, graphite or graphene are interesting for fundamental research and very attractive for various applications due to possibility to manipulate composite properties at nanoscale. The value of dielectric permittivity and electrical conductivity of these composites could be very high close to percolation threshold. However, despite of lot of publications is a lack of deep understanding relation between carbon filler microscopic properties and composite dielectric properties [1].

In this contribution were investigated epoxy resin composites filled with various size graphite flake inclusions, namely natural graphite (diameter of the graphite flakes are d = 500 – 750 μm), coarse graphite (d = 150 – 800 μm), medium graphite (d = 44 – 75 μm), fine graphite (d = 15 – 44 μm) and exfoliated graphite. The concentration of graphite inclusions was from 0.25 to 2.0 wt. %. Dielectric investigations were performed in frequency range from 20 Hz to 1 MHz, while the temperature interval was from 10 K to 450 K, by measuring loss tangent and capacity with LCR meter (HP – 4284A). The dielectric properties of all investigated composites, except composites with exfoliated graphite, are very similar to the dielectric properties of pure resin. At temperatures close to room temperature the dielectric dispersion in these composites is mainly caused by alfa relaxation in pure epoxy resin. At higher temperatures, similarly to pure epoxy resin electrical conductivity appears.

This research is funded by the European Social Fund under the Global Grant measure.

[1] W. Bauhofer, J. Z. Kovacs, *Composite Science and Technology* 69, 1486 (2009).

MANUFACTURING, STRUCTURE AND PROPERTIES OF RECYCLED POLYETHYLENE TEREPTHALATE/LIQUID CRYSTAL/MONTMORILLONITE CLAY NANOCOMPOSITES

Guntis Japins[1] (presenting author), Rita Berzina[1], Janis Zicans[1], Remo Merijs Meri[1], Tatjana Ivanova[1], Valdis Kalkis[2], Ingars Reinholds[2]

[1]Institute of Polymer Materials, Riga Technical University, [2]Department of Chemistry, University of Latvia

e-mail of presenting author: guntisjapins@gmail.com

Every year global amount of solid waste increase, extremly fast is increase in the amounts of polymer waste. More than half of polymer waste are coming from packing industry. Recycling is rational and environmentally friendly way to solve this problem. Significant part of polymer waste is covered by well known and widely used thermoplastic polymer – polyethylene terephthalate (PET). PET can be relatively easy recycled. Most often the source of recycled PET (RPET) is post-consumer beverage bottles. First PET bottle recycling attempts were launched in 1977, in 2011 about 1.6 million tons of PET bottles were recycled [1]. Thus novadays RPET can be regarded as considerable alternative source for development of novel materials.

In this study RPET or PET have been melt mixed with nanostructred montmorillonite clay (MMT) and liquid crystal polymer (LCP) by using twin screw extruder. It is well known that addtion of MMT to PET allows considerably increase its mechanical and barrier properties [2]. It is also known that addition of LCP improves mechanical, rheological and barrier properties of PET and other thermoplastic polyetsters [3]. The simultaneous effect of both of these modifiers on the structure and properties of PET, however, has not been considerably investigated. In this research the effect of LCP and MMT on the structure and properties (mechanical, reological, calorimetric and thermal properties) of RPET and PET are investigated. The amount of LCP has been changed from 2 to 10 wt%, while that of MMT from 1 to 5 wt.%. Synergetic effect has been observed. For example, adding 5 wt% of LPC and 5% of MMT, the highest rise of the modulus of elasticity has been observed.

References

1. http://www.foodproductiondaily.com/Packaging/EU-PET-bottle-recycling-rate-rises-report
2. S.Pavlidou, C.D.Papaspyrides. A review on polymer–layered silicate nanocomposites. *Prog. Polym. Sci.*, **2008**, 33(12), 1119-1198.
3. M.Mucha. Polymer as an important component of blends and composites with liquid crystals. *Prog. Polym. Sci.*, **2003**, 28(5), 837-873.

TRANSPORT PROPERTIES OF INDIUM ANTIMONIDE WITH MAGNETIC NANOPRECIPITATES

Erkki Lähderanta[1], Alexei Kochura[1,2], Boris Aronzon[1,3], Konstantin Lisunov[1,4], Alexander Lashkul[1] and Mikhail Shakhov[1,5]

[1]Lappeenranta University of Technology, Finland, [2]Kursk State University, Russia, [3]Kurchatov Institute, Moscow, Russia,[4]Institute of Applied Physics, Kishinev, Moldova,[5]Ioffe Institute, StPetersburg, Russia

e-mail of presenting author: erkki.lahderanta@lut.fi

Interest to the group III-V diluted magnetic semiconductors (DMS) is connected to their high potential for use in spintronics applications [1]. Indium antimonide (InSb) is known among the group III-V semiconductors as the material with the narrowest band gap and the highest carrier mobility. Doping of InSb with Mn leads to interesting magnetic properties of $In_{1-x}Mn_xSb$ connected to presence of different types of magnetic systems. These include (i) the substitutional Mn ions, (ii) the atomic-size Mn complexes and (iii) the MnSb nanoprecipitates [2].

Here we present investigations of the resistivity, magnetoresistance and the Hall effect in $In_{1-x}Mn_xSb$ with x = 0.02, 0.03 and 0.06. Samples were prepared by direct alloying of indium antimonide, manganese and antimony, followed by a fast cooling of the melt with a rate of 10 – 12 K/s. The resistivity in zero magnetic field exhibits below T ~ 20 K an upturn, which has been interpreted as the manifestation of the Kondo effect characterized by the Kondo temperature T_K ~ 3 – 8 K. The Hall resistivity demonstrates presence of the normal and the anomalous Hall components, where the latter is connected to the ferromagnetically ordered spin system of MnSb nanoprecipitates. The magnetoresistance, $\Delta\rho/\rho_0$, below T ~ 10 K is negative (n-MR) reaching the value up to 15 % at 1.6 K. The magnetic field and temperature dependences of n-MR are interpreted with the Khosla-Fischer model of spin-dependent scattering by localized magnetic moments.

References

1. I. Žutić, J. Fabian, S. Das Sarma, *Rev. Mod. Phys.*, 2004, Vol. 76, 323 – 410.

2. A.V. Kochura, B.A. Aronzon, K.G. Lisunov, A.V. Lashkul, A.A. Sidorenko, R.De Renzi, S.F. Marenkin, M. Alam, A.P. Kuzmenko, E. Lähderanta, *J. Appl. Phys.*, 2013, 2013, Vol. 113, 083905.

DIELECTRIC AND ULTRASONIC INVESTIGATIONS OF COMPOSITES OF POLY(ε-CAPROLACTONE) AND $Mo_6S_3I_6$ NANOWIRES

D. Jablonskas[1], A. Kuprevičiūtė[1], Š. Svirskas[1], V. Samulionis[1], J. Banys[1] and T. McNally[2]

[1]*Vilnius University, Faculty of physics, Saulėtekio av. 9, III b., LT-10222 Vilnius, Lithuania*

[2]*School of Mechanical and Aerospace Engineering, Queen's University Belfast, BT9 5AH, UK*

e-mail of presenting author: dziugas.jablonskas@ff.stud.vu.lt

$Mo_6S_3I_6$ (MoSI) nanowires have excellent conductivity and are good alternative to carbon nanotubes as functional one dimensional (1D) nanofiller for polymeric materials used in electrostatic discharge, EMI shielding, flexible electronic substrate and electrode applications [1].

A Poly(ε-caprolactone) (PCL) is one of the most commonly used polymers in biomedical applications, mainly because it is biodegradable and non-toxic. Chemical formula of PCL is $[[CH_2]_5COO]_n$, where n ≈ 300. It is A2-type polymer, it consists of monomers, which contain dipoles of carboxyl group, which are separated by non-polar methyl group. Dielectric spectroscopy of PCL has shown three relaxation processes, which are noted α, β and γ. α relaxation resides in lower frequencies and it is the dielectric manifestation of the cooperative motions that occur at the dynamic glass transition temperature. β and γ relaxations, which resides in higher frequencies, are related with more localized dipole motions of polymer [2].

Some structural and mechanical characteristics of PCL-x%MoSI composite were investigated earlier and presented in [1]. However, there are very little data about dielectric properties of PCL-x%MoSI composite. Thus, the aim of this report is to present the results of dielectric spectroscopy of PCL-x%MoSI composites.

Also, the temperature dependencies of longitudinal ultrasonic velocity and attenuation in PCL-x%MoSI composites will be presented. The influence of nanowires in composite on ultrasonic properties will be discussed.

References

1. S. J. Chin, P. Hornsby, D. Vengust, D. Mihailovič, J. Mitra, P. Dawson, T. McNally, Pol. Adv. Tech., vol. 23(2), pp. 149-160 (2010).
2. V. Sencadas,M. Grimau, E. Laredo, M. C. Pérez Y., A. Bello J. Chem. Phys. Vol. 114 (14) pp. 6417-6425 (2001).

NANOTUBES FOLDED FROM CUBIC AND ORTHORHOMBIC $SrZrO_3$: FIRST-PRINCIPLES STUDY

Andrei Bandura, Robert Evarestov, Dmitry Kuruch

Department of Chemistry, Quantum Chemistry Division, St. Petersburg State University, Russia

e-mail: di_ma_rex@front.ru

In this work we consider the different types of stoichiometric nanotubes (NTs) folded from the cubic and orthorhombic $SrZrO_3$ (SZO). The first (I) types of NTs have been obtained by rolling up of (001) slabs of the cubic phase ($Pm\bar{3}m$), the second (II) and the third (III) types were folded from (001) and (110) slabs of the orthorhombic (*Pbnm*) phase, accordingly. The calculations have been performed in the LCAO approximation using the hybrid exchange-correlation functional PBE0. The stability of the single-wall nanotubes of chiralities (n, 0) and (n, n) for the cubic, and (n_1 0) and (0 n_2) for the orthorhombic SZO have been investigated in dependence on their diameter, the number of layers (2 or 4) in the slab, and the outer surface termination (SrO or ZrO_2).

Type I NTs folded from 2-layer slabs, generally, keep the initial structure while maintaining the original symmetry during the optimization procedure. However, if the symmetry decreases due to removing of the screw rotations, the nanotube structure exhibits considerable reconstruction with splitting of ZrO_2 shells into two atomic (O and Zr) subshells, thus resembling the surface of SZO orthorhombic phases. Strain energy of those NTs is significantly less than that for the tubes with a full set of symmetry operations. Also, it has been observed spontaneous splitting of the SrO-terminated (n, n) 4-layer nanotubes into two separated NTs. The resulted double-wall nanotubes are energetically more favorable than the two isolated single-wall nanotubes consisting of SrO–ZrO_2–SrO and ZrO_2 shells, correspondingly.

The NTs folded from the orthorhombic phase (of types II and III), generally, preserve the atomic distortions inherent to the SZO orthorhombic phases. However, the concrete NT surface structure depends on the chirality, the number of layers and termination type. The reconstruction of ZrO_2-terminated outmost surfaces because of break of the Zr–O bonds has been found in all types of NTs simulated from 4-layer slabs.

Acknowledgements

Author thanks St. Petersburg State University for the financial support (Grant 12.37.142.2011).

Numerical investigation of arrays of concentration microstructures in dispesions of magnetic nanoparticles

Dmitry Zablotsky[1] (presenting author), Ansis Mezulis[1]

[1]*Institute of Physics, University of Latvia, Latvia*

e-mail of presenting author: dmitrijs.zablockis@gmail.com

Magnetic colloidal dispersions exhibit pronounced Soret effect in the presence of temperature gradients and so the creation of thermal nonhomogeneities by absorption of incident optical intensity is a convenient method for the formation of concentration microstructures in layers of ferrocolloid. In external magnetic fields these formations acquire complex internal structure established by the simultaneous and self-consistent thermophoretic, magnetic, diffusive and advective interactions.

We observe by numerical simulations the emergence and evolution of periodic 2D arrays of these microstructures of magnetic nanoparticles (Fig. 1) induced through photoabsorption and thermodiffusion in a thin layer of magnetic colloid in the applied magnetic field. The observable parameters are formulated on the grounds of obtained detailed microscopic information and are compared with the results of experimental measurements in forced Rayleigh scattering arrangement.

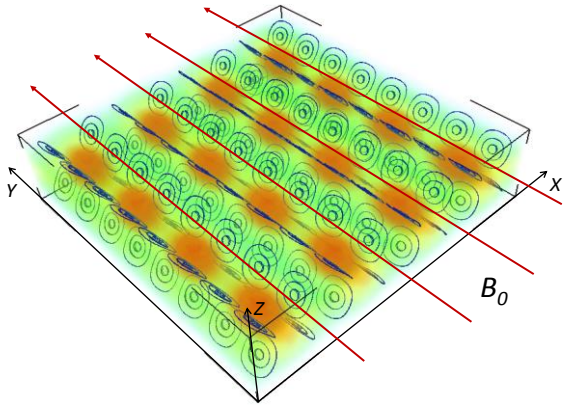

Fig.1 Photoabsorptive 2D grid in magnetic field (distribution of ferroparticle concentration and microconvective streamlines)

The stability of the extended convective-diffusive microstructures is examined as well. We conclude that these structures are relatively stable if the magnetic field is applied along the temperature gradient. The perpendicular configuration, if the external field is oriented normally to the sidewall of the layer, is rather unstable due to the defining influence of the transversal boundary. The destabilization of the microstructure and the emergence of the unstable perturbations are observed above the threshold of the instability.

Acknowledgements

The work has been supported by the European Regional Development Foundation, Project 2011/0001/2DP/2.1.1.1.0/10/APIA/VIAA/007

THE INFLUENCE OF EXTERNAL WEAK MAGNETIC FIELD ON ANHARMONIC NANOCONTACTS OF JOSEPHSON TYPE

Daulet Sergeyev[1,2], Kuanyshbek Shunkeyev[1], Nurgul Zhanturina[3]

[1]Aktobe State Pedagogical Institute, [2]Military Institute of Air Defense Forces, [3]Al-Farabi Kazakh National University, Kazakhstan

e-mail: serdau@rambler.ru

The researchers' interest to anharmonic behaviour of supercurrent in Josephson's contacts (JC) is determined with wide application of such objects in the contemporary micro- and nanoelectronics [1, 2]. The present work considers the influence of external weak magnetic field on JC with anharmonic current of $I_s(\varphi) = I_{c1}\sin\varphi - I_{c2}\sin 2\varphi$ type, where I_c – critical current, φ – difference in phase of wave functions [3, 4]. In the framework of modified Ferrel-Prange equation describing the influence of magnetic flied on JC $\frac{d^2\varphi}{dx^2} = \frac{1}{\lambda_J^2}(\sin\varphi - k\sin 2\varphi)$ the influence of weak magnetic field on JC is studied. (Here k – anharmonism parameter, λ_J – Josephson depth of magnetic field's penetration). The distribution of difference in phase, supercurrent, and magnetic field along JC are found for weak external magnetic field (Fig. 1). It is established the external weak magnetic field influences on anharmonic in more passive way in comparison with traditional JC ($k = 0$).

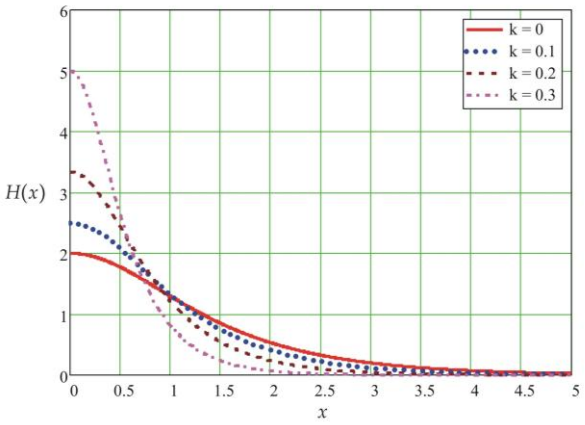

Fig.1 The distribution of magnetic field at different values of anharmonism parameter.

References

1. S.Bakurskiy, N.Klenov, T.Karminskaya, et al. *Supercond. Sci. Technol.*, 2013, Vol.26, 015005.

2. D.Sergeyev, K.Shunkeyev, *Rus. Phys. J.*, 2009, No.8/2, 556-559.

3. D.Sergeyev, K.Shunkeyev, *J. of Intern. Sci. Publ.: Materials, Methods & Technology*, 2010, No.4, 398-408.

4. D.Sergeyev, K.Shunkeyev, *Chemical and Radiation Phys*., 2011, Vol.4, 100-109.

Preparation of Short Range Ordered Nanodot Arrays and Analysis of Particle Optical Properties

I.Apsīte[1], R.Popļausks[1], U.Maļinovskis[1], A. Vīksna[1, 2], J.Prikulis[1], G.Bergs[1], D.Erts[1]

[1]*Institute of Chemical Physics, University of Latvia, Riga, Latvia*
[2]*Faculty of Chemistry of University of Latvia, Riga, Latvia*

Nanoporous anodized aluminium membrane masks are used for production of short range ordered metal nanoparticle arrays with diameter 10-30 nm. The masks are prepared by two step anodization and immersed in paraffin wax as transport substrate. DC voltage of 10-20 V and 40 V were used for pore formation in sulphuric and oxalic acids respectively. Resulting membrane thickness using sulphuric acid is 60-100 nm [1]. Free standing mask are obtained after removal of wax and PMMA by oxygen gas at elevated temperature. Metal nanoparticles are made by sputtering through the AAO mask. Nanoparticles have uniform size and spatial distribution. Nano-pore structure, density and diameter can be controlled by variation of process parameters, e.g. voltage or electrolyte.

Ag, Au, Cr/Au nanoparticle arrays were prepared. To analyse particle optical properties we use optical scattering imaging. Optical properties are measured to nanoparticles on glass surface.

Size of nano-pores and thickness of membrane using sulphuric acid is smaller than previously reported [2, 3].

Keywords: AAO, nanoparticles.

References:

1. I. Pastore, R. Poplausks, I. Apsite, I. Pastare, F. Lombardi, D. Erts Fabrication of ultra thin anodic aluminium oxide membranes by low anodization voltages. IOP Conference Series: Material Science and Engineering, 23 (2011) 012025 doi:10.1088/1757-899X/23/1/012025
2. Ding G.Q., Zheng M.J., Xu W.L.Shen W., Nanotechnology, 2005, Vol.16, 1285-1289
3. Woo L., Hee H., Lotnyki A., Schubert M., Hesse D., Baik S., Gosele U., Nature Nanotechnology, 2008, Vol. 3 402-407

FORCE-FIELD CHOICE FOR THE SIMULATION OF TiO_2- AND ZrO_2-BASED NANOTUBES

Andrei Bandura, Vitaliy Teil, Robert Evarestov

Department of Chemistry, Quantum Chemistry Division, St. Petersburg State University, Russia

e-mail: andrei@ab1955.spb.edu

A combination of quantum mechanical methods and classical force-fields forms an approach which gives the possibility to extend the results of *ab initio* calculations obtained for relatively small systems to the nanosystems of reliable dimensions. In this work we check the applicability of the existing parameterizations of the Born-Mayer potential to the simulation of the titania and zirconia nanotubes. The different modifications of the bulk TiO_2 and ZrO_2 crystals have been used as the primary test systems to select the suitable force fields. Finally, three parameterizations [1–3] have been chosen for TiO_2 systems and two parameterizations [2,3] for ZrO_2 systems.

The nanotubes under consideration have been folded from the different layers of cubic and tetragonal phases of titania and zirconia. The 3-plane (111) layers of fluorite ($Pm\bar{3}m$) structure have been employed for construction of the nanotubes with the hexagonal morphology. The 6-plane (001) layers of tetragonal ($P4_2/nmc$) modification have been used to obtain the nanotubes with lepidocrocite morphology, and 6-plane (101) layers of anatase ($I4_1/amd$) structure have been used for the nanotubes with the corresponding morphology.

Force-field based calculations of nanotubes of the different chirality and with the diameter about 20 Å have demonstrated that only parameterizations [1,3] are able to reproduce the nanotubes strain energy correctly. All the selected fields produce the reliable nanotube structure; however none of them can give the reasonable formation energy of the nanotubes and nanolayers.

Acknowledgements

The authors are grateful for the support to RBRF (grant 11-03-00466a).

References

1. M. Matsui, M. Akaogi, *Mol. Simul.*, 1991, 6, 239.

2. S.M. Woodley, P.D. Battle, J.D. Gale, C.R.A. Catlow, *Phys. Chem. Chem. Phys.*, 1999, 1, 2535.

3. S.I. Lukyanov, A.V. Bandura, R.A. Evarestov, *Surf. Sci.*, 2013, http://dx.doi.org/10.1016/j.susc.2013.01.002.

Near-infrared sensitive organic solar cell

Anastasija Ivanova[1], Igors Kaulachs[1], Gunta Shlihta[1], Peteris Shipkovs[1], Modris Roze[2]
1 – Institute of Physical energetics,21 Aizkraukles Str., Riga LV-1006, Latvia;
2 – Riga Technical University, Azenes 14, Riga, Latvia

The efficiency of organic solar cells has steadily increased in the past few years. Still the main shortcoming of these cells is their limited spectral range up to a wavelength of 800 nm. In order to broaden the spectral coverage of the cells we are looking for tandem partner with photosensitivity in infrared spectral region. It is known that lead phthalocyanine (PbPc) in triclinic phase has large and strong intermolecular charge transfer (CT) band around 900 nm which enables considerable efficiency in planar solar cells with C_{60} as electron acceptor and transporter up to 990 nm. Yet open circuit voltage (V_{OC}) of these cells doesn't exceed 0.5 V. In present work we are trying to replace C_{60} with C_{60} derivatives with higher LUMO level than for C_{60} to increase V_{OC} value of the cell.

All layers of the cell were prepared by thermal evaporation in vacuum ~ 10^{-6} mbar in the same system without breaking the vacuum. ITO glass was covered by 10 nm thick hole conducting and exciton blocking molybdenum oxide layer, which was followed by 50-100 nm thick PbPc layer by slow evaporation to obtain triclinic phase, then followed 40-60 nm thick fullerene derivative. This layer was covered by 10 nm thick 1,10-bathophenantroline (BPhen) layer. As electrode was used thermally evaporated Al or Yb covered by Al. Active cell area was 7 mm^2.

All photoelectric measurements will be made in the same home made vacuum cryostat where cell was manufactured at p ~ 10^{-6} mbar without breaking the vacuum and moving the cell.

The spectral dependences of short circuit photocurrent external quantum efficiency (EQE), fill factor (FF) and open circuit voltage (V_{OC}) will be investigated in spectral range 370-1100 nm by measuring current-voltage dependences in every spectral point, using synhro-detection technique and PC controlled data storage equipment. Obtained results will be discussed.

SPECTROSCOPY OF THE $5d^1$-$4f^1$ TRANSITIONS OF Ce^{3+} IN NANOCRYSTALLINE XENOTIME- AND RHABDOPHANE-TYPE YTTRIUM PHOSPHATES

Alexandr Popov[1,2], Yurii Orlovskii[1,2], Alexander Vanetsev[1], Chong-Geng Ma[1,4], Olga Gaitko[3], Elena Orlovskaya[2], Sven Lange[1], Ilmo Sildos[1]

[1] *Institute of Physics, University of Tartu, Estonia,* [2] *General Physics Institute RAS, Moscow, Russia,* [3] *Chemistry Department of Lomonosov Moscow State University, Russia,* [4] *College of Mathematics and Physics, Chongqing University of Posts and Telecommunications, P.R. China*

e-mail of presenting author: alexandr.popov@ut.ee

Our work is supported by European Social Fund (MTT50, MJD167, MJD054)

We measured and calculated for the first-time the crystal-field splitting (CFS; Fig. 1, a, b) of the $5d^1$ state of Ce^{3+} in the hexagonal xenotime-type $YPO_4 \cdot 0.8H_2O$:Ce^{3+} nanocrystallites (NCs) (the hexagonal D_2 optical center of Ce^{3+}), which fit each other. The CFS of D_2 center is about 1.5 times larger than that of the tetragonal rhabdophane-type YPO_4:Ce^{3+} NCs (Fig. 1, c) (the tetragonal D_{2d} optical center of Ce^{3+}). The later have the same CFS as in the YPO_4:Ce^{3+} bulk crystal [1].

The spontaneous emission decay time of the lowest $5d^1$ level of hexagonal D_2 center found from the slope of the final stage of the D_2 center fluorescence kinetics (Fig. 2, a) is $\tau(D_2)$ = 33.6 ns. The $\tau(D_2)$ as twice as long than the spontaneous emission decay time of $\tau(D_{2d}$ center) = 18.4 ns (Fig. 2, b). The deactivation of this $5d^1$ level by the multiphonon relaxation process is negligible, because the $4f^1(^2F_{7/2}) - 5d^1(^2\Gamma_1)$ energy gap is too much (~30000 cm^{-1} for both Ce^{3+} centers) in comparison with $h\nu(OH^-)$ = 3600 cm^{-1} and even more so with $h\nu(PO_4^{2-})$ = 1000 cm^{-1}.

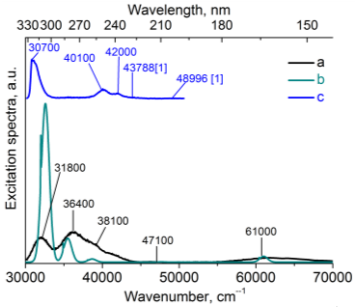

Fig. 1. The excitation spectra of the $5d^1$ state of Ce^{3+} in the $YPO_4 \cdot 0.8H_2O$ NCs (a, b), the YPO4 NCs (c). The curve (b) is calculated spectra. We use the exchange charge model [2] for calculation of the CFS of $5d^1$ level. The notes on the graph indicate the CF levels positions.

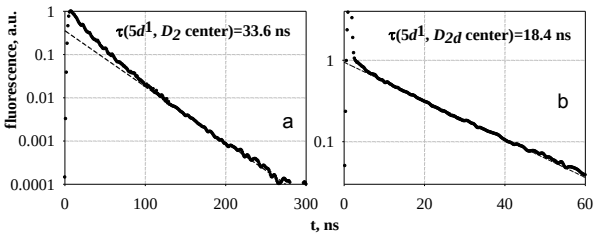

***Fig. 2.** The fluorescence kinetics from the lowest $5d^1$ level of Ce^{3+} in the YPO_4*$0.8H_2O$:0.2% Ce^{3+} NCs (a) at laser excitation (λ_{exc}=266 nm, f=5 kHz, t_p=9 ns, λ_{det}=380 nm, T=300K) and the YPO_4:2% Ce^{3+} bulk crystal (b) at synchrotron excitation (λ_{exc}=323 nm, f=10.87 MHz, t_p=1 ns, λ_{det}=353 nm, T=10K); the dash lines are fitting curves.*

References

1. L. van Pieterson, M.F. Reid, R.T. Wegh, S. Soverna, A. Meijerink, Phys. Rev. B 65 (2002) 045113.
2. B. Z. Malkin, A. A. Kaplyanskii, R. M. Macfarlane. *North-Holland Publishing Company (Elsevier)*, **1987**, p. 13.

MICROWAVE-HYDROTHERMAL SYNTHESIS OF NANOCRYSTALLINE XENOTIME- AND RHABDOPHANE-TYPE YTTRIUM PHOSPHATES DOPED WITH CE^{3+} IONS

Alexander Vanetsev [1], Olga Gaitko [2], Yurii Orlovskii [1,3], Alexandr Popov [1,3], Elena Orlovskaya [3], Ilmo Sildos [1]

[1] *Institute of Physics, University of Tartu, Estonia,* [2] *Chemistry Department of Lomonosov Moscow State University, Russia,* [3] *General Physics Institute RAS, Russia,*

e-mail of presenting author: alexander.vanetsev@ut.ee

In present work we propose a novel method for microwave-hydrothermal (MW-HT) synthesis of tetragonal yttrium orthophosphate (YPO_4) with xenotime-type structure and hexagonal hydrate of yttrium orthophosphate ($YPO_4 \cdot 0.8H_2O$) with rhabdophane-type structure doped with Ce^{3+} ions.

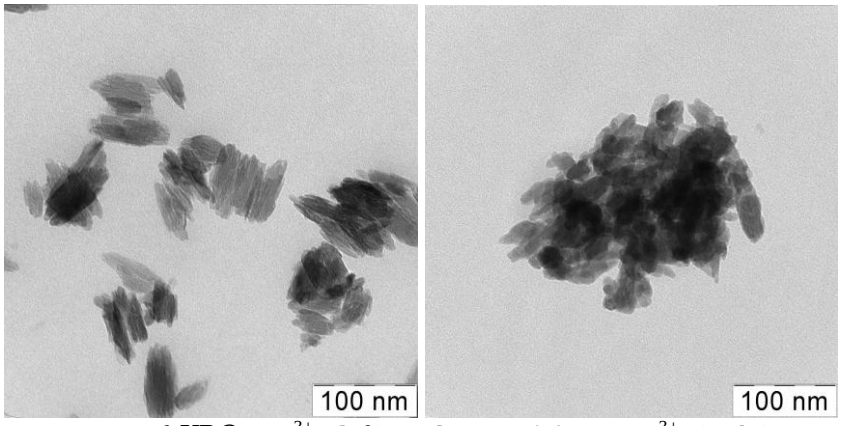

Fig.1 TEM images of $YPO_4:Ce^{3+}$ (left) and $YPO_4 \cdot 0.8H_2O:Ce^{3+}$ (right) nanoparticles synthesized at 200°C for 2 hours.

Synthesis includes rapid precipitation of phosphates and subsequent MW-HT crystallization of obtained gels. We've established the dependence of phase composition and morphology of particles on reagents ratio and duration of MW-HT treatment. We've shown the possibility to obtain well-crystalline and easily dispersible nanoparticles of named phosphates with mean sizes in the range of 30-50 nm and narrow size distribution using proposed synthetic technique. This work was supported by European Social Fund (grants # MTT50 and MJD167).

SURFACE ANALYSIS OF SUPERCAPACITOR ELECTRODES AFTER LONG-LASTING CONSTANT CURRENT TESTS

Jaanus Eskusson, Alar Jänes, Enn Lust

Institute of Chemistry, University of Tartu, Estonia

e-mail of presenting author: alar.janes@ut.ee

FIB-SEM, XPS, TOF-SIMS and electrochemical methods have been used for the characterisation of physical properties and chemical composition of microporous carbide derived carbon electrodes, prepared from TiC at 950 ºC (noted as TiC-CDC) after 40000 charge/discharge cycles. Some changes in surface chemical composition of TiC-CDC electrodes and Al current collectors has been established including partial dissolution of Al from positively charged electrode and deposition of Al onto the negatively charged TiC-CDC electrode surface. The values of gravimetric energy calculated before and after constant current charge/discharge cycling at cell voltage 3.4 V are quite similar (35 and 34 W h kg^{-1}, respectively). At starting moment the gravimetric power was nearly 1.4 times higher (195 kW kg^{-1}, 146 kW dm^{-3}) than that calculated after 40000 charge/discharge cycles (144 kW kg^{-1}, 104 kW dm^{-3}). The characteristic relaxation time constant (0.94 and 1.23 s, respectively) increases somewhat in accordance with the decrease of power density during long-lasting cycling at higher cell voltage range from 0.2 to 3.4 V. TOF-SIMS data are in a good agreement with XPS (Fig. 1) and FIB-SEM results.

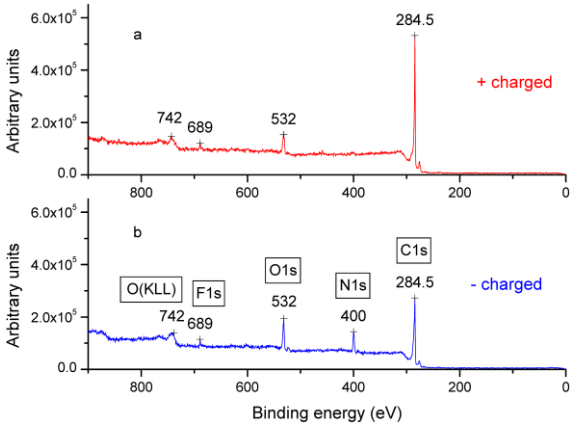

Fig.1 XPS spectra for positively (a) and negatively (b) charged electrodes after 40000 charge and discharge cycles.

References

1. A. Jänes, J. Eskusson, R. Kanarbik, A. Saar, E. Lust, *J. Electrochem. Soc.* 2012, 159 A1141-A1147.

ATOMIC LAYER DEPOSITION OF HAFNIUM AND ZIRCONIUM OXIDES ON CARBON NANOPARTICLES

Aile Tamm[1], Anna-Liisa Peikolainen[2], Jekaterina Kozlova[1], Lauri Aarik[1], Jun Lu[3], Kaspar Roosalu[1], Hugo Mändar[1], Jaan Aarik[1] , Kaupo Kukli[1,4]

[1] University of Tartu, Institute of Physics, Department of Materials Science, Riia 142, EE-51014 Tartu, Estonia, [2] IMS Lab, Institute of Technology, University of Tartu, Nooruse 1, EE-50411 Tartu, Estonia, [3] Department of Physics, Chemistry and Biology, IFM, Linköping University, 581 83 Linköping, Sweden, [4]University of Helsinki, Department of Chemistry, P.O.Box 55, FI-00014, Univ. Helsinki, Finland

e-mail of presenting author: aile.tamm@ut.ee

Nonvolatile semiconductor memory based on storing electric charge on non-contacted floating gates is the dominant memory concept for portable devices [1], including ways to design floating-dot memories containing conductive nanodots in (multilayer) gate dielectrics. Therefore appears to be important to study the deposition of materials possibly forming a further basis for this kind of device prototypes.

In this report we describe preparation of structures containing carbon nanoparticles covered by coatings grown by atomic layer deposition (ALD). The structures shown in Fig. 1 contain e.g. HfO_2 or ZrO_2 as a control oxide and Al_2O_3 as a tunnel oxide layer. The carbon nanoparticles were deposited by dip-coating substrate into organic solution. Carbon nanoparticles were synthesized from 5-methylresorcinol and formaldehyde via base catalysed polycondensation reaction and distributed over silicon wafers. Before deposition of nanoparticles the substrates were covered with 1-2 nm thick Al_2O_3 layer grown from $Al(CH_3)_3$ and O_3. The HfO_2 films were grown from $HfCl_4$ and H_2O and ZrO_2 from $C_5H_5Zr[N(CH3)_2]_3$ and H_2O.

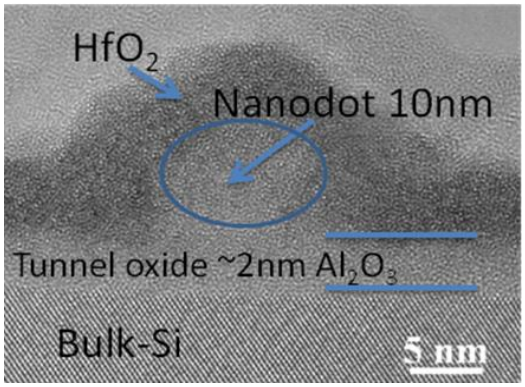

Fig.1. Cross-sectional HRTEM image of a carbon nanoparticle on Al_2O_3 covered with HfO_2.

References

1. K.H. Kuesters, M. F. Beug, U. Schroeder, N. Nagel, U. Bewersdorff, G. Dallmann, S. Jakschik, R. Knoefler, S. Kudelka, C. Ludwig, D. Manger, W. Mueller, A. Tilke, *Adv. Eng. Mater*. 2009 No.11, p. 241

EXPLOTITATION AND STRUCTURAL PROPERTIES OF MODIFIED POLYACETAL NANOCOMPOSITES

Agnese Grigalovica[1] (presenting author), Remo Merijs Meri[1], Janis Zicans[1], Tatjana Ivanova[1], Janis Grabis[2]

[1]Institute of Polymer Materials, Riga Technical University, [2]Institute of Inorganic Chemistry, Riga Technical University

e-mail of presenting author: a.grigalovica@gmail.com

Polyacetal polymers are among most widely used engineering polymers. They are used in different branches of national economy, such as, building, automotive, house holding, medicine and others due to it good mechanical and chemical properties. In the same time application of polyacetals in engineering is somewhat limited because of insufficient ductility in subzero temperatures, relatively low thermal resistance, especially at prolonged exposure times etc. Purposeful modification of polyacetals is promising for increasing certain exploitation characteristics of the polymers. Polyacetals, modified with elastomers such as ethylene copolymers [1], styrene rubber [2] or thermoplastic polymer TPU [3] have advanced impact strength, processability and yielding behavior. Polyacetals, modified with anisometric nanostructured fillers possess [4-7] have improved thermal resistance, mechanical properties as well as some specific properties such as, magnetic or electric, dependent on the nanostructured modifier itself [4-6].

The current research looks on the effectiveness of modification of POM with both anisometric nanoparticles of ZnO and ethylene-octene copolymer (EOC). The amount of EOC in the nanocomposites has been changed from 0 to 50 weight %, while that of ZnO from 0 to 5 weight %. Nanocomposites with varying POM:EOC:ZnO ratios have been obtained by using melt compounding.

It is shown that addition of 10 weight % of EOC allows increase impact strength and flexibility of POM. Simultaneously modification of the investigated compositions with 2 wt. % of anisometric ZnO improves stiffness and thermal stability of the materials.

References

1. Pan, G.O., Chen, Y.J., Li, H.L. Plast. Rubber Compos. Process.Appl., 2007, 36, 291-296.
2. Gao, X., Qu, C., Fu, C., Peng, Y., Zhang, Q. Macromol. Mater. Eng., 2004, 289, 41-48.
3. R.N.Uthaman, A.Pandurangan, S.S.M.A.Majeed.. J. Polym. Res., 2007, 14, 441-447.
4. L.H.Sun, Zhen-Guo Yang, X.H.Li, Polym. Eng. Sci, 48, 2008, 1824-1832
5. X.Zhao,L.Ye. J.Appl.Polym.Sci.,111,2009,759-767
6. N.Yu, L.He, Y.Ren, Q.Xu, Polymer, 52,2011, 472-480
7. S. Siengchin, G. C. Psarras, J. Karger-Kocsis, Journal ofApplied Polymer Science,Vol. 117,2010,1804–1812

CATHODOLUMINESCENCE STUDY OF Al-DOPED ZnO NANOFILMS

A.I. Popov[a], V. Savchyn[b], J. Purans[a], A. Dabrowska[c], A. Huczko[c], Birendra Pathak[d] and D. P. Subedi[d]

[a]*Institute of Solid State Physics, University of Latvia, Kengaraga 8, 1063 Riga, Latvia*
[b]*Department of Electronics, Ivan Franko National University of Lviv, 107 Tarnavskogo str, 79017 Lviv, Ukraine*
[c]*Department of Chemistry, Warsaw University, 1 Pasteur str., 02-093 Warsaw, Poland*
[d]*Department of Natural Sciences, School of Science, Kathmandu University, Dhulikhel, Nepal*

e-mail: popov@ill.fr, popov@latnet.lv

Nowadays, Al-doped ZnO is one of the most widely used materials for transparent conductive oxide coatings. Here we report on temperature dependent cathodoluminescence characterization of Al-doped (mole concentration of Al within 0-10%) and un-doped ZnO nanofilms on quartz substrate which were obtained by ultrasonic spray pyrolysis.

It was demonstrated that the relative intensity of the 10 keV-electron-beam induced luminescence bands at 1.9; 2.3 eV and complex band at 3.3 eV depends on both temperature and Al content. The influence of quartz substrate on cathodoluminescence emission spectra is evaluated. Finally, on the base of ab-initio calculations, the model of the radiative recombination in Al-doped ZnO is proposed

Femtosecond excitonic dynamic and relaxation in solid ZnO: dependence of the luminescence decay time on nano particles size and excitation mode

P. Martin[1], A. Belsky[2], M. Dumergue[1], B. Masenelli[3], P. Mélinon[2]

[1]*CELIA, Université de Bordeaux-CNRS-CEA, Talence F-33405, France*

[2]*Institut Lumière Matière, CNRS-Université Lyon 1, F-696222 Villeurbanne, France*

[3]*Institut des Nanotechnologies de Lyon et INSA, F-69621 Villeurbanne, France*

e-mail: martin@celia.u-bordeaux1.fr

We present some new results on time resolved luminescence of ZnO monocrystal (MC) and nanoparticles (NP) excited by femtosecond IR, UV and VUV pulses between 15K and 300K. The samples have been excited in multiphoton regime by the 800 nm, single photon regime by the 266 nm, 40 fs light pulses provided by Ti:Sa laser source with cadence of 1 kHz and VUV fs pulses generated by High Harmonic Generation (HHG). The excitation intensity on the sample was controlled.

ZnO nanoparticles with different sizes were elaborated by Low Energy Cluster Beam Deposition with high crystalline quality (quasi no defects). The optical properties of the NPs have been studied by photoluminescence (PL) and no defect related visible or excitonic luminescence have been evidenced [1]. The time resolution was about 40 ps using MCP photomultiplier in start-stop mode. The frequency mixing technique with time resolution of 300-400 fs, was used for the study of rise time and faster decays.

The dynamics of the free (FX) and bound (DX) excitons are discussed depending on the excitation mode formation, excitation density, temperature and size of the solid system. The role of the electronic relaxation is also taken into account for higher photons energy.

The study of the bound exciton lifetime NP size dependence is of importance firstly to understand the mechanisms which drive this dependence and then to define an optimized nanostructure for reaching the faster luminescence.

References

[1] D. Tainoff, B. Masenelli, P. Mélinon, A. Belsky, G. Ledoux, D. Amans, C. Dujardin, N. Fedorov and P. Martin, *Phys. Rev. B*, **2010**, 81, 115304.

Multifunctional materials

ON THE POSSIBILITIES FOR IMPROVING THE EFFICIENCY OF RADIATION IN HETEROSTRUCTURES BASED ON THE IV-VI SEMICONDUCTORS

A.M. Pashaev[1], O.I. Davarashvili[2], M.I. Enukashvili[2], Z.G. Akhvlediani[2,3], L.P. Bychkova[2] and M.A. Dzagania[2]

[1]*National Aviation Academy of Azerbaijan, Baku , Azerbaijan*
[2]*Iv. Javakhishvili Tbilisi State University , Georgia,*
[3]*E.Andronikashvili Institute of Physics, Tbilisi, Georgia*
E-mail : omardavar@yahoo.com , zairaak@yahoo.com

The experiments with isoperiodic heterostructures in the system of IV-VI semiconductors PbSeTe-PbSnSeTe showed that, under different methods of epitaxy (from the gaseous and liquid phases), during their fabrication mutual diffusion of the components between the layers takes place. The isoperiodity is disturbed, and near the heteroboundary, most often in the active area PbSnSeTe of the structure, are formed the areas of certain thickness where the mismatch could approach the level when the strain reaches the limit of elasticity. This could result in the formation of a net of dislocations on the areas of this kind, its formation could be aggravated in actual experiments depending on the conditions of fabrication of heterostructures. As a result, in the active area the lifetime of current carriers reduces and the efficiency of spontaneous radiation is impaired – the quantum yield of radiation decreases by an order. According to the estimates, the measured threshold current in lasers increases 5-6 times, whereas their operating temperature decreases.

In the IV-VI semiconductors with high concentration of nonstoichiometric defects, the diffusion coefficients of the components, especially of chalcogenides, are relatively high. At ~500^{0}C the diffusion coefficient of tin makes up 10^{-14} cm^2/s and of tellurium - 10^{-12} cm^2/s. Such a difference between the diffusion coefficients determines a noticeable diffusion mismatch.

With consideration for the specific features of the band structure of IV-VI semiconductors, we studied the structures the active areas of which contained sub-inverse or sup-inverse compositions. The obtained values of mismatch $\frac{\Delta a}{a}$ near heteroboundary were compared with the interpolation results. The values were closed for the sub-inverse compositions of the active area. For preventing the formation of a net of dislocations in the active area, the composition of the emitter was "pulled up" to the composition of the active area by making closer the content of tellurium in both areas, decreasing the content of tin upon reaching the isoperiodity at the heteroboundary and doping the emitters with calcium or strontium.

For the sup-inverse compositions of the active area, the critical mismatch is so high that only "pulling up" of the compositions is not enough, and doping is essential, which results in the increase in the modulus of elasticity of the layers. As a result the ultimate strains at the same deformations increase and their relaxation is put off. The investigation of doped IV-VI semiconductors by the method of internal friction revealed that the impurities of this kind are chrome and manganese [1]. They decrease the lattice constant, while the modulus of elasticity increases twice as much. Such doping could be successfully used for the sub-inverse compositions of active areas as well. Manganese is most efficiently used in the structures with temperature "self-controlling" heterostructures: in the latter the emitter is formed on the base of the sub-inverse composition, whereas the active layer – on the base of the sup-inverse one. The compositions are to be chosen so that at T=77K the width of their forbidden gaps coincided, but, because of different signs of coefficients $\frac{dE_g}{dT}$, the heterobarrier could exceed 0.2eV at room temperature.

References:

1.A.M.Pashaev, O.I.Davarashvili, V.A.Aliyev. In:*Proceedings of the International Conference on Microelectronic Sencors, Baku, 2005, pp.57-58.*

INVESTIGATION OF MECHANICAL AND ELECTRICAL PROPERTIES OF Li DOPED SODIUM NIOBATE CERAMIC SYSTEM

Włodzimierz Śmiga[1], Barbara Garbarz-Glos[1], Wojciech Piekarczyk[2],
Monika Karpierz[1] and Maris Livinsh[3]

[1]*Institute of Physics, Pedagogical University of Cracow, Poland*
[2]*Faculty of Materials Science and Ceramics,*
AGH-University of Science and Technology, Cracow, Poland
[3] *Institute of Solid State Physics, University of Latvia*
e-mail of presenting author: w.smiga@gmail.com

The perovskite niobates constitute a very interesting group of functional materials, because of their extreme physical parameters sensitive to external factors. Some solid solutions based on a sodium niobate have i.a. a very good piezoelectric properties, moreover, they contain no lead and so they fulfil a very important demand of high technology industry concerning a reduction of the environmental pollution. One of the most interesting and extensively studied system is a lithium niobate -sodium niobate solid solution ($LiNbO_3$-$NaNbO_3$).

Pure and 4wt.% Li-added sodium niobate ceramics were prepared by a two-stage hot-pressing technology in the Institute of Solid State Physics at the University of Latvia. The preliminary structural studies were carried out by X-ray diffraction technique showed the formation of single perovskite phase in the investigated compositions. The effect of Li doping on a microstructure and mechanical properties of the $LiNbO_3$-$NaNbO_3$ solid solution was investigated at room temperature. The microstructure and EDS measurements were performed by means of scanning electron microscope with field emission Hitachi S4700 and microanalyses system Noran-Vantage. To determine the elastic constants (the Young′s modulus E, the shear modulus G, bulk modulus K and the Poisson′s ratio v) of $Li_{0.04}Na_{0.96}NbO_3$ a method of measurement of the longitudinal (V_L) and transverse (V_T) ultrasonic wave velocities for this type of material was developed. The electric properties of $NaNbO_3$ and $Li_{0.04}Na_{0.96}NbO_3$ ceramics were investigated in the frequency range from 100 Hz to 200 kHz and from room temperature up to 750 K, both in the process of heating and cooling. Both electric permittivity and conductivity exhibit an anomaly as a function of the temperature and frequency. The a.c. electric conductivity as a function of angular frequency $\sigma(\omega)$ follows the relation $\sigma(\omega) = A\omega^s$. The local minima of electrical conductivity σ were observed, which are probably associated with a polaronic transport mechanism.

DIELECTRIC AND PYROELECTRIC PROPERTIS OF CALCIUM-BARIUM NIOBATE SINGLE CRYSTALS

Olga Malyshkina[1], Vladimir Lisitsin[1], Jan Dec[2], Tadeusz Łukasiewicz[3]

[1]Tver State University, Tver, Russia

[2]University of Silesia, Institute of Materials Science, Katowice.

[3]Institute of Electronic Materials Technology, Warsaw

e-mail: Olga.Malyshkina@mail.ru

Single crystals of $Ca_xBa_{1-x}Nb_2O_6$ (CBN) with nominal concentrations of calcium in the solution 28% (CBN28), 30% (CBN30) and 32% (CBN32) were studied. According to [1] these materials are characterized by high (~35 C/cm^2) coercive fields (E_c) and remanent polarization (P_r) depending on the value of the applied electric field. In the present work temperature dependence of E_c and P_r were studied by the Sawyer-Tower method together with the pyroelectric properties examined by the TWS method [2].

It was found that the increase of the temperature results in a decrease of the E_c accompanied by an increase of the switchable remanent polarization (Fig.1, *a,b*). The hysteresis loop transformation into an elliptic shape was observed at temperatures of 35-50 degrees above the maximum of dielectric permittivity (Fig.1, *c*), corresponding to the sharp increase of the electric conductivity. In contrast to dielectric hysteresis loop the polarization of the samples depends on the Ca(*x*) concentration. Uniform polarization distribution was observed only in CBN32. For CBN30 the polarization magnitude at the +Ps side is lower than at the –Ps side, while in CBN28 the surface layer at this side is completely depolarized.

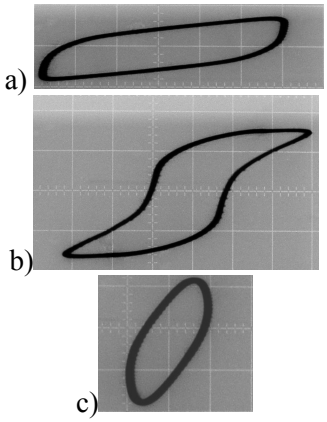

Fig.1 Dielectric loops of CBN32 crystal at 335 K (a), 407 K (b) and 539 K (c). Scale OX: 3 kV/cm; OY: 2 (a), 4 (b) and 8 (c) μC/cm2.

References

1. Y.J. Qi, C.J. Lu, J. Zhu, X.B. Chen, H.L. Song, H.J. Zhang, X.G. Xu, *Appl. Phys. Lett.,* 2005, Vol. 87, P.082904.
2. O.V. Malyshkina, A.A. Movchikova, R.M. Grechishkin, O.N. Kalugina, *Ferroelectrics*, 2010. Vol. 400. P.63-75.

LUMINESCENCE OF $LaBr_3$:Ce,Hf SCINTILLATION CRYSTALS UNDER UV-VUV-XUV and X-RAY EXCITATION

Vladimir Ivanov[1], Vladimir Pustovarov[1], Artem Razumov[1], Oleg Ignat`ev[1], Dmitry Vyprintsev[2]

[1]*Ural Federal University, Yekaterinburg, Russia,* [2]*LTD Company "Stark", Obninsk, Russia*

e-mail: ivy@dpt.ustu.ru

The LaBr:Ce scintillator has been recently introduced as a very valuable alternative to the most conventional scintillators. This crystal manufactured by the Saint-Gobain corporation, in fact, is characterized by a high light output (~60.000 photons/MeV), fast decay time (25 ns), brilliant energy resolution as well as high stability of parameters in wide temperature range. All of these features make this scintillator very attractive for both spectrometric applications and for medical imaging [1-2]. The present study was carried out by the means of the luminescence UV-VUV-XUV spectroscopy. The time-resolved photoluminescence (PL) spectra ((in region of 1.5-6.0 eV), the PL excitation spectra (in region of 3.7-320 eV) as well as the PL decay kinetics has been measured at T=7.5 and 300K using SR on the SUPERLUMI station and BW3 beam-line (HASYLAB, DESY). The nonproportional PL response was investigated. The absorption spectrum, thermo-stimulated and X-ray excited luminescence were studied in temperature region of 90-500K in Ural Federal University. The spectrometric parameters of scintillation $LaBr_3$:Ce,Hf detectors (diameter 18-38 mm, h=3-10 mm) in combination with PMT or photodiode were studied at T=(-25) – (+55)ºC with using of γ-ray isotopes.

The examined single crystal with high optical quality (3-5 % of cerium and 0.05-0.5 % hafnium in primary charger) have been grown using Bridgman process in the Russian Company "Stark" [3]. The synthesized single crystals were certificated by a XRD and inductive-bound plasma methods, both the chemical and RFA analysis were used also. Introduction of hafnium ($HfBr_4$) in the melt reduces a hygroscopicity of grown single crystals significantly. The spectrometric parameters of $LaBr_3$:Ce,Hf detectors are stable and do not degrade. Some selected results of our studies in this topic are presented in Refs [4-6] in detail.

References

1. E.V.D. van Loef, P.Dorenbos, C.W.E. van Ejik, K.Kramer, H.U.Gudel, *Appl. Phys. Lett.,* 2001, Vol.79, 1573-1575.

2. http://www.detectors.saint-gobain.com/Brillance380.aspx

3. D.I.Vyprintsev, Patent of Russian Federation No. 2426694, priority from 15.02.2010.

4. V.A.Pustovarov, V.Yu.Ivanov, D.I.Vyprintsev, N.G.Shvalev, *Technical Phys. Letters,* 2012, Vol.38, 784–788.

5. V.A.Pustovarov, A.N.Razumov, et. al. *Bulletin of the Russian Academy of Sciences. Physics*, 2013, Vol.77, 217–220.

6. V.A.Pustovarov, V.Yu.Ivanov, D.I.Vyprintsev, N.G.Shvalev, *DESY, HASYLAB Annual Report-2011*. 20111577.

INVESTIGATION OF LUMINESCENCE MECHANISM OF PERSISTENT STRONTSIUM ALUMINATE PHOSPHOR

Virginija Liepina[1], Krisjanis Smits[1], Dzidra Jankovica[2], Larisa Grigorjeva[1], Donats Millers[1]

[1]*Institute of solid State Physics, University of Latvia,*

[2] *Institute of Inorganic Chemistry, Riga Technical University*

e-mail of presenting author: virginija.liepina@gmail.com

Eu and Dy doped strontium aluminates are widely known for their intensive long lasting phosphorescence. Phosphors of the aluminate family doped with rare earth materials exhibit extremely long and intensive afterglow – up to 30 hours. The luminescent properties of strontium aluminate phosphors have been studied for some time in order to obtain the longer lasting and more intensive phosphorescence, but the mechanism responsible for the long lasting afterglow is not yet clear, though many authors have proposed different possible models. Knowing the model, it would be possible to purposefully change the synthesis parameters to obtain a more efficient phosphor. The goal of this research is to clarify the knowledge of the mechanism responsible for the long lasting phosphorescence.

In this report the analysis of the luminescence kinetics of $SrAl_2O_4$: Eu, Dy has been described, as well as the investigation of thermally stimulated luminescence (TSL) accumulated under different excitation (X-ray lamp, deuterium lamp, 266 nm Nd:YAG laser). By TSL measurements and comparison of their spectral distribution dependence on temperature the depth and the nature of the charge trapping centers has been determined. The luminescence and afterglow of the sample after selective dopant excitation has been investigated. The luminescence kinetics dependence on the population of the filled trapping centers has been shown. The possible recharging process of the rare earth dopants has been investigated by electron paramagnetic resonance. The possible mechanism of energy transfer has been discussed.

V.Dimza, L.Kundzina, M.Kundzins, K.Kundzins, M.Livins, M.Antonova, A.Plaude

„The effect of Cu admixture on relaxor properties of the PLT8/65/35 electrooptical ceramics”

The complex dielectric permeability $\varepsilon^* = \varepsilon' - \varepsilon''$ measured within the thermal range of 20–400 °C and the 10^2–10^6 Hz frequency range in the PLT 8/65/35 ceramics containing 0.005, 0.1, 0.5, 1.0, and 3.0 % Cu by weight is reported presenting analysis of the frequency dependence of ε' and ε'' at different temperatures (Vogel-Fulcer relation, Arrhenius law and the Cole-Cole diagrams) hysteresis loops P(E) along with the results X-ray diffraction, Raman, EPR, and Electron Microscopy (Fracture Mode Behaviour) studies.

It is observed that, with increasing the concentration of Cu:

1) the temperature $T_{m\varepsilon}$ of the $\varepsilon'(T)$ maximum shifts to a higher temperature;
2) two additional low-frequency relaxation mechanisms interfering with each other appear and overlap with that of the “classical” nano-size domain relaxors.

The microscopic mechanisms of the observed effects are discussed.

OPTICAL PROPERTIES OF NATURAL TOPAZ

Vera Skvortsova, Nina Mironova- Ulmane, Laima Trinkler, Georg Chikvaidze

Institute of solid State Physics, University of Latvia

e-mail: vera@cfi.lu.lv

The study the optical properties of topaz can be used to determine the quality of jewelry topaz, for the successful use of these crystals in thermoluminescence dosimetry as well as for evaluation of physical and chemical conditions of formation of mineral. Topaz is an aluminium fluorsilicate with a general composition of $Al_2(SiO_4)(F,OH)_2$. It crystallizes in a rhombohedral structure, belonging to the space group Pbnm**.** Usually in nature topaz occurs in the form of colourless crystals. Colouration of topaz crystals is possible through the incorporation of transition metal impurities or by irradiation. The paper presents study of infrared and Raman spectroscopy, UV-Visible absorption and photoluminescence spectra of natural topaz crystals from Ukraine before and after fast neutron irradiation.

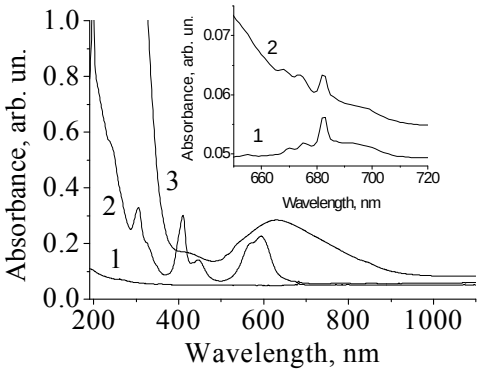

Fig.1 Topaz absorption spectra before (1) and after neutron irradiation (2), natural blue topaz from Volodar sk Volynskii, Ukraine(3).

In absorption spectra of colourless topaz before fast neutron irradiation were observed several lines in the region of the Cr^{3+} ion electron transition $^4A_{2g} \rightarrow {}^2E_g$ (Fig. 1, inset). After irradiation in the absorption spectra (Fig.1) there appears an intense absorption band at 230 nm and occur the characteristic bands at 250, 305, 334, 410, 446, ~ 590 nm. With increase of neutron fluence the absorption band 590 nm broadens and its maximum shifts to 620 nm. We assume that the band ~ 620 nm is complex and includes not only radiation defects but also the bands associated with the presence of impurities of Cr^{3+}, Fe^{2+} and Mn^{2+} ions. The photoluminescence spectra of colourless topaz crystals contain bands centred around 350 and 420 nm at λ_{ex} = 251 nm and broad bands with maxima 570 and 800 nm at λ_{ex} = 447 nm. The Raman spectra of colourless topaz have a narrow band with a maximum at 350 cm^{-1}. After neutron irradiation the intensity of this narrow band increases. The series of sharp bands in the range 250-500 and 800- 1000 cm^{-1} are observed in the Raman spectrum of natural blue topaz. The origin of the luminescence bands in topaz crystals and bands in Raman spectra is discussed.

LUMINESCENT PROPERTIES AND ENERGY TRANSFER IN $Y_XLu_{1-X}PO_4:RE^{3+}$ (RE = Eu, Ce) SOLID SOLUTIONS

V.S. Levushkina[1], D.A. Spassky[2,3], V.V. Mikhailin[1,2], M.S. Tretyakova[4], B.I. Zadneprovski[4], I.A. Kamenskikh[1]

[1]Physics Faculty, M.V. Lomonosov Moscow State University, Moscow, Russia, [2]Skobeltsyn Institute of Nuclear Physics, M.V. Lomonosov Moscow State University, Russia, [3]Institute of Physics, University of Tartu, Estonia, [4]Central Research and Development Institute of Chemistry and Mechanics, Moscow, Russia

e-mail: bestpum@mail.ru

Phosphates doped with rare-earth ions are considered as perspective materials for scintillating detectors, X-ray imaging and as phosphors in plasma display panels [1]. Increase of the light yield is one of the most actual problems for scintillating detectors. Enhancement of the light yield can be expected for scintillators based on the solid solutions of phosphates. In the solid solutions clusters may appear. In this case the distance between the components of generic electron-hole pair is constrained and hence the probability to be captured on the emission center is increased. Actually it was shown that superior light yield is observed just for perovskite solid solutions $Lu_xY_{1-x}AlO_3$:Ce in comparison with YAP:Ce or LuAP:Ce [2]. Also enhancement of luminescence intensity under X-ray excitation has been already detected for $Lu_xSc_{1-x}BO_3:Ce^{3+}$ [3] and $Lu_xY_{1-x}BO_3:Eu^{3+}$ [4]. Here the luminescence properties of the set of phosphates solid solutions $Y_xLu_{1-x}PO_4$ (x = 0, 0.1, 0.3, 0.5, 0.7, 0.9, 1) doped with 0,5 mol % Eu^{3+} or with 0,5 mol % Ce^{3+} were investigated. Special attention was attended to the energy transfer processes from the host states to the activator luminescence centers. Spectroscopic studies of the samples were carried out using synchrotron radiation in the energy region 3.7-22 eV at the SUPERLUMI station, DESY and using the laboratory set-up in UV spectral region. Synchrotron radiation is an ideal light source for the luminescence spectroscopy in VUV region due to its continuous spectrum, high intensity and temporal structure. Measurements were carried out at temperatures 10 and 300 K. Investigated samples were synthesized by sol-gel method.

References

1. M. Balcerzyk, Z. Gontarz et al., *J.Lum*, 2000, v.87-89, 963.

2. A. N. Belsky, C. Dujardin, C. Pedrini, et al., Proc. of the 5th International Conference on Inorganic Scintillators and Their Applications, August 16-20, 1999, Moscow, p.363.

3. Y. Wu, D. Ding, S. Pan, F. Yang and G. Ren, *J. Alloys Comp*., 2011, v. 509, 366.

4. D.A. Spassky, V.S. Levushkina, V.V. Mikhailin, et al., Abstracts of the Satellite workshop of the Int. Conf. "Functional Materials" ICFM'2011, October 3-8, 2011, Simferopol, DIP, Ukraine, p. 415.

OPTICAL-FIELD INDUCED SURFACE-RELIEF FORMATION PHENOMENON IN THIN FILMS OF VITREOUS CHALCOGENIDE SEMICONDUCORS

Ugis Gertners, Janis Teteris
Institute of solid State Physics, University of Latvia,
e-mail: gertners@gmail.com

The demand of lower cost surface-relief based optical instruments such as grating-based resonators or filters for waveguides, diffractometers, spectrometers, etc. is one of the main driving forces for the investigation of direct light-induced relief formation. The most common techniques for fabricating and investigating these surface-relief gratings involve an interferometric or holographic recording setup.

We have investigated that the light-induced mass transfer process strongly depends on the material itself and polarization of the light. The behavior of mass transfer and thus the resulting recording could be related to interaction between the polar photo-induced defects and the polarized electric field of recording beam. It has been shown that the mass transfer can be directed both ways – towards or away from the electric field intensity gradient. The evolution of surface relief in dependence from the recording time and polarization has been investigated in detail. The mechanism of the direct recording of surface relief on amorphous chalcogenide films based on the photo-induced plasticity has been discussed.

A direct recording technique is a comparatively new solution for lithography and, as shown in this report, provides new experimental techniques for better understanding of the interaction between the light and matter. The obtained gratings are very stable at room temperature, so this method can replace some of the chemical etching techniques and find a practical application in the applied physics.

CELL GROWTH ON PATTERNED SURFACES PREPARED BY A NOVEL SOL-GEL PHASE SEPARATION METHOD

Triin Kangur[1,2], Paula Reemann[3], Liis Nurmis[1,2], Viljar Jaks[4], Martin Järvekülg[1,2]

[1]Institute of Physics, University of Tartu, Estonia, [2]Estonian Nanotechnology Competence Centre, [3]Department of Physiology, University of Tartu, Estonia, [4]Institute of Molecular and Cell Biology, University of Tartu, Estonia

kangur@ut.ee

Cell behavior can be influenced by modifying properties of the environment surrounding the cells. Nano- and micro-topographical features[1,2], mechanical properties[3] and chemical functionality[4] of substrates have been shown to affect cell behavior. Sol–gel is a range of simple and flexible methods for preparing materials with a variety of properties and shapes[5].

We have applied a novel sol-gel phase separation based method to prepare silica micro- and nanopatterned surfaces with round surface structure features (Fig.1) from simple TEOS-alcohol sol composition. Variation in the size of structure elements was achieved by solvent variation and adjustment of sol concentration. To determine the effect of the patterned surfaces on fibroblast growth, morphology and cytoskeletal organization, we evaluated several markers of cell proliferation and differentiation.

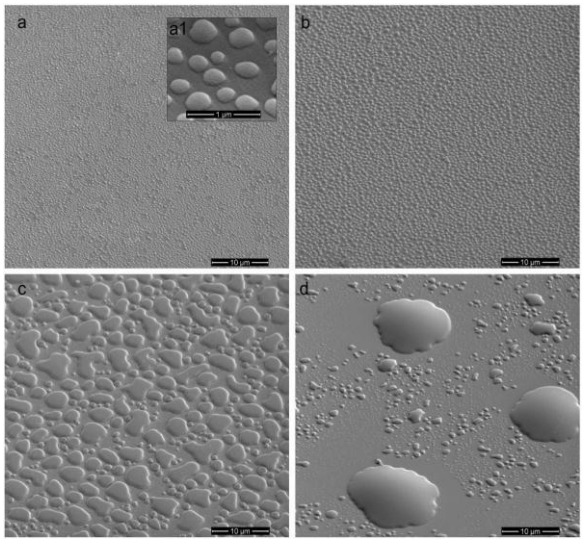

Fig.1. SEM images of silica domes. Scale bar corresponds to 10 µm. The insert a1 shows magnification of "a" surface, where scale bar corresponds to 1 µm.

Growth characteristics and morphology of primary human dermal fibroblasts were found to be modulated by the microstructure of the substrate. The increase in the size of the structural elements, lead to the increased inhibition of the cell growth, changes in the morphology and the enhancement of cell senescence. These effects are likely mediated by the decreased contact between the cell membrane and the growth substrate.

References

1. S. Verma et al., *Nanomedicine* , 2011,6:157–81.
2. C.K.. Choi et al., *Trends Cell Biol*, 2010, 20:705–14.
3. A.J. Engler, et al., *Cell*, 2006, 126:677–89.
4. M. Tirrell, et al., *Surf Sci*, 2002, 500:61–83.
5. K. Saal, et a., *Int J Mater Prod Technol*, 2011, 40:2–14.

ELECTRON AND HOLE CENTERS IN X-RAY- OR UV-IRRADIATED OXYORTHOSILICATE CRYSTALS

Valentin Laguta[1], Martin Nikl[1], Svetlana Zazubovich[2] (presenting author)

[1]*Institute of Physics AS CR, Cukrovarnicka 10, 162 53 Prague, Czech Republic*

[2]*Institute of Physics, University of Tartu, Riia 142, 51014 Tartu, Estonia*

e-mail of presenting author: **svet@fi.tartu.ee**

Ce^{3+}-doped oxyorthosilicates of the type of Lu_2SiO_5 and Y_2SiO_5 have excellent scintillating performances and are presently key materials for applications in positron emission tomography. Lu_2SiO_5:Ce presents the best figure-of-merit due to its high density, fast scintillation decay, much smaller concentration of shallow electron traps as compared with aluminum perovskites and garnets, high light output, and satisfactory energy resolution [1]. However, the presence of an afterglow negatively influences the characteristics of Lu_2SiO_5 and Y_2SiO_5. To clarify the origin of the defects responsible for the afterglow, a detailed study of the TSL and EPR characteristics of undoped and Ce^{3+}-doped Y_2SiO_5 and Lu_2SiO_5 crystals has been carried out. In the irradiated Ce^{3+}-doped crystals, the holes are mainly trapped at Ce^{3+} ions. The recombination of thermally released electrons with the hole Ce^{4+} centers is accompanied with the Ce^{3+} emission. The recombination of thermally released holes with electron centers should be accompanied with the intrinsic emission or the emission of the impurity rare-earth ions (e.g., Eu^{3+} or Sm^{3+}) which can trap electrons.

Unlike previous TSL studies of these materials (see, e.g., [2, 3]), we have measured the TSL glow curves separately for the Ce^{3+} emission (≈3.0 eV) and for the Sm^{3+} or Eu^{3+} emission (2.0-2.1 eV) after X- or UV-irradiation at 80 K and 295 K of Ce^{3+}-, Eu^{3+}-, or Sm^{3+}-containing Lu_2SiO_5 and Y_2SiO_5 crystals. This allows us to separate the TSL peaks arising from the thermal destruction of electron and hole centers. For example, in the Y_2SiO_5-based crystals, the TSL peaks arising from the thermal release of holes from various O^--type hole centers are located at 155 K, 243 K, and 323 K (at the heating rate of 0.2 K/s). The peaks arising from the thermal release of electrons are located at 95 K, 120 K, 213 K, 388 K, and 443 K. Only the latter peaks appear at the TSL glow curve of the UV-irradiated crystals. The origin and structure of the electron and hole centers are clarified by EPR. The parameters of the corresponding traps (trap depths and frequency factors) are defined.

References

1. M.Nikl, V.V.Laguta, A.Vedda, *Phys. Stat. Sol. B*, 2008, 245, 1701-1722.

2. A.Vedda, et al., *Phys. Rev. B*, 2008, 78, 195123-1-8.

3. E.Mihokova, et al., *IEEE Trans. Nucl. Sci.*, 2012, 59, 2085-2088.

THE EFFECT OF AGING ON THE SUPERCONDUCTING TRANSITION TEMPERATURE AND RESISTIVITY OF Y-Ba-Cu-O CERAMICS AFTER HIGH TEMPERATURE TREATMENT

Sergey Nikoghosyan[1,2], Vachagan Harutyunyan[2], Valeri Baghdasaryan[2], Edgar Mughnetsyan[1], Erjanik Zargaryan[1] and Albert. Sarkisyan[1]

[1] *International Scientific-Educational Center of NAS RA, Armenia,* [2] *A.I. Alikhanyan National Research Laboratory (Yerevan Physics Institute) Foundation, Armenia*

e-mail of presenting author: nick@mail.yerphi.am

The effect of aging on the superconducting transition temperature (T_c) and resistivity (r) of Y-Ba-Cu-O ceramic samples is studied after heating at 400°C (30 minutes), quenching in air and subsequent aging at 290 K for about 11 days. By periodic measurements of current-voltage characteristics within the temperature range of (78-290) K, r dependences on the transport current I and temperature T are found for different storage periods t_a (aging time). It is shown that at earlier stages of aging (lower t_a), r measured at 78 K increases first slowly with the transport current I and then significantly sharply. It is also found that for a fixed I, r behaves - with a rise in t_a - similarly at both 78 K and 290 K. However, if at 78 K after the aging period r increases by almost 4000 times, at 290 K the increase factor only makes 50.

The observed results for the investigated high temperature superconducting (HTSC) samples are explained by the presence of weak and strong superconducting links, which break down under the effect of the transport current I at low and high I, correspondingly. It is revealed that for the samples treated at longer t_a, the destruction of weak links is observed at lower I. It is suggested that in the course of aging, the oxygen sublattice of the HTSC unit cell undergoes a certain redistribution of its atoms, as a result of which O4 atoms occupy the previously vacant O5 sites. It is found that in the course of the whole aging process, T_c reveals its maximum approximately in a week, whereas at room temperature r increases continuously, probably due to the rise of the volume fraction of dielectric phase in the aging sample.

OPTICAL AND ELECTROLUMINESCENCE PROPERTIES OF TERC-BUTIL GROUP CONTAINING PIRANILIDEN DERIVATIVES.

Santa Popova, Aivars Vembris
Institute of solid State Physics, University of Latvia, LV 1063 Riga, Latvia
e-mail: esse.sommeil@gmail.com

Electroluminescent layer in commercial organic light emitting diodes mainly is processed by expensive thermal evaporation in vacuum. The cost of such devices can be significantly reduced if this layer is made from solution. Various polymers for the electroluminescence thin films were synthesized and investigated. Nevertheless repeatability of the polymer synthesis is low. This issue can be solved by low weight organic compound that forms amorphous layer from solutions. In this work we present three original organic compounds with various electron acceptor groups and piranilyden fragment as a backbone. Trityloxyethyl and terc – butyl group leads to amorphous thin film forming from solution and increases yield of the synthesis, respectively.

Photoluminescence quantum yield of investigated compounds in dichloromethane solution is in range from 0.27 to 0.80. Thin films on glass substrate were prepared for absorption and photoluminescence measurements by spin coating method from dichloromethane solution. Photoluminescence of presented compounds covers spectral region from 550 to 750 nm. Stronger electron acceptor group gives red-shift of luminescence spectra. Multilayer devices with the structure ITO/PEDOT:PSS(50 nm)/organic layer(~100 nm)/BaF(1 nm)/Al(100 nm) were made to determine electroluminescent properties of the compounds. Photoluminescence and electroluminescence spectrum are identical which indicate to the same origin of the emission. The electroluminescence efficiency of such samples appeared to be quite low. Tris (8-hydroxyquinoline) aluminum (Alq_3) layer was added between electroluminescence layer and BaF to optimize the structure. We assume that it could block the excitons in luminescence layer and increase electron transport. Inserted layer did not affect electroluminescence spectra and slightly increased the electroluminescence efficiency as we presumed.

Acknowledgement:

This work has been supported by Latvian State Research Program No.2 in Materials Sciences and Information Technologies and ERAF project Nr. 2010/0204/2DP/2.1.1.2.0/10/APIA/VIAA/010.

IMPROVEMENT OF CdS FILM OPTICAL PROPERTIES BY LASER RADIATION FOR APPLICATION IN SOLAR CELLS

Artur Medvid[1], Rimas Janeliukstis[1], Edvins Dauksta[1], Pavels Onufrijevs[1], José Luis Plaza[2], Sandra Rubio[2], Ernesto Diéguez[2], Igor Dmitruk[3] and Natalia Berezovska[3]

[1]*Institute of Technical Physics, Riga Technical University, Latvia*

[2]*Universidad Autónoma de Madrid, 28049 Madrid, Spain*

[3]*Kyiv National Taras Shevchenko University, Kyiv, Pr. Glushko 1-2, Ukraine*

e-mail: medvids@latnet.lv

CdS plays an important role as a window layer forming n-CdS/p-CdTe heterojunction in photovoltaic cells based on CdTe. Closed space sublimation (CSS) technique is one of the main methods to form CdS layer. However, the polycrystalline layers formed by this method contain a lot of defects [1], which decrease lifetime of charge carriers. So, the aim of the work is to improve properties of CdS layer formed on ITO layer by CSS method using Nd:YAG laser radiation. The surface of CdS layer on ITO/glass structure was irradiated by pulsed Nd:YAG laser with different intensities. The measurements of topography by SEM after irradiation of the surface by laser showed micro-ripples formation. Two bands in photoluminescence (PL) spectra at 8 K were found – the red band at about 1.719 eV and the yellow band at 2.030 eV. Both bands correspond to donor – acceptor pair (DAP) recombination [2]. Laser irradiation caused a redistribution of intensities of these bands, which is explained by generation and recombination of intrinsic defects in DAP. A new intense PL band, containing two subbands, attributed to exciton bound to a neutral acceptor at ≈ 2.535 eV [2-3] and exciton, bound to a neutral donor at ≈ 2.540 eV [2-3] (at 1.6 K), appeared after irradiation by maximum laser intensity. Thermal quenching of PL band intensities was studied by determining defect activation energies. Activation energy of exciton band was found to be 38.9 ± 0.5 meV. After irradiation the intensity of Raman LO line increased about 3 times and phonon replica with energy of about 37 meV appeared. These facts indicate that our CdS film has crystallized and therefore, its quality has improved after irradiation by maximum laser intensity.

References

1. Paul Besomi and Bruce Wessels, *Journal of Applied Physics*, **51**, 4305 (1980).

2. Anke E. Abken, D.P. Halliday, Ken Durose. *Journal of Applied Physics*, **105**, 064515 (2009).

3. J. Humenberger, G. Linnert, K. Lischka. *Thin Solid Films*, **121**, 75 (1984).

Acknowledgement

The authors gratefully acknowledge the support provided by the FP7-ERANET-MATERA project: NANOSTRUCTURED CdTe SOLAR CELLS.

STRUCTURE AND DIELECTRIC PROPERTIES OF $Na_{1/2}Bi_{1/2}TiO_3$-$BaTiO_3$ SOLID SOLUTIONS IN THE PHASE TRANSITION REGION

Reinis Ignatans, Marija Dunce, Maija Antonova, Aina Plaude, Eriks Birks
Institute of Solid State Physics, University of Latvia, Latvia
e-mail of presenting author: reinis.ignatans@gmail.com

$Na_{1/2}Bi_{1/2}TiO_3$-$BaTiO_3$ solid solutions exhibit good piezoelectric properties and attract interest as a lead-free ferroelectric material. In this work structure and dielectric properties of solid solutions $(1-x)Na_{1/2}Bi_{1/2}TiO_3–xBaTiO_3$ above the morphotropic phase boundary in the concentration range $0.10\leq x\leq 0.97$ are studied as function on temperature and concentration. Character of splitting of [200] diffraction maximum indicate coexistence of tetragonal and cubic phases in the region of the phase transition. The width of the coexistence region depends on the content of $BaTiO_3$, reaching minimum at average concentrations x. Treatment of the experimental data by the Rietveld method allows us to extract temperature dependence of percentage of these phases in the concentration range, starting from x=0.4. The fail of the method at lower $BaTiO_3$ concentrations apparently reflects influence of local deformations on the width of the diffraction maxima, making separation of the phases difficult. The phase diagram of solid solutions is completed. Only one structural phase transition between paraelectric cubic and ferroelectric tetragonal phases is established in all studied concentration range, but there can be distinguished concentration ranges with different character of dielectric properties. The dielectric properties in low Ba concentration range are comparable with pure $Na_{1/2}Bi_{1/2}TiO_3$. In a wide concentration range, where relaxor behaviour prevails, the temperature of the phase transition weakly depends on Ba content.

MODIFICATION OF CARBON NANOTUBES AND CELLULOSE COTTON FIBERS USING HYBRID IONIC LIQUID – SOL-GEL APPROACH.

Raul Välbe[1*], Marta Tarkanovskaja[1,2], Uno Mäeorg[2], Valter Reedo[1], Andres Hoop[3], Ants Lõhmus[1]

[1] *Institute of Physics, University of Tartu, Riia 142, 51014 Tartu, Estonia.*
[2] *Institute of Chemistry, University of Tartu, Ravila 14A, 50411 Tartu, Estonia.*
[3] *Haine Paelavabrik OÜ, Tehase 21, 50106 Tartu, Estonia.*
e-mail: raul.valbe@ut.ee

Modification of materials with ionic liquids (IL) have been in the focus of a rapidly growing number of studies in the last decade [1;2]. Moreover IL synergy with other materials may influence their properties significantly. Nevertheless, their advantageous liquid state turns out to be an impediment for applications in devices, which need solid state shaping.

In current study we present a method where new type of ILs act as modificators for CNT-s and cellulose fibers. This simple route carried out by interconnected and entangled ionic liquid, sol gel and solid carbon nanotube networks opens up opportunities for ceramic transparent electrodes as well as opportunities for functionalisation of different shape and zized sol-gel materials. Ionogel modified cellulose fibers can be utilized in the formation wich have UV-shielding properties as well for antibacterial use.

Characterization studies of the product were carried out by energy-dispersive X-ray spectroscopy (EDX), scanning electron microscopy (SEM) and optical microscopies; also infrared spectra (IR) were recorded. Thermal analyses were performed by differential scanning calorimetry (DSC).

References

[1] M. Freemantle, An Introduction to Ionic Liquids, Royal Society of Chemistry, Cambridge, 2009.
[2] L. Vidal, ML. Riekkola, A. Canals, Ionic liquid-modified materials for solid-phase extraction and separation: a review, Anal Chim Acta. (2012) 19-41.

BAND TAIL ABSORPTION SATURATION IN $CdWO_4$ WITH 80-fs LASER PULSES

R. Laasner[1], N. Fedorov[2], V. Nagirnyi[1], S. Guizard[2], M. Kirm[1], V. Makhov[3], S. Markov[1,3], A. Vasil'ev[4], S. Vielhauer[1], I.A. Tupitsyna[5]

[1]Institute of Physics, University of Tartu, Estonia, [2]Laboratoire des Solides Irradiés, CEA-CNRS Ecole Polytechnique, France, [3]P.N. Lebedev Physical Institute, Moscow, Russia, [4]Skobeltsyn Institute of Nuclear Physics, Moscow, Russia, [5]Institute for Scintillation Materials, National Academy of Sciences of Ukraine

e-mail: raullaasner@gmail.com

In scintillators based on excitonic emission, the phenomenon of nonproportional response can be explained in terms of the nonlinear interactions of relaxed excitons [1-4], where the nonradiative losses of luminescence are explained in terms of the Förster energy transfer mechanism of dipole-dipole interactions.

At sufficiently high excitation densities the effects of saturated absorption become important, effectively decreasing the absorption coefficient and giving rise to induced transparency [4]. In the present work we report on the decay kinetics of $CdWO_4$ under excitation by 80-fs laser pulses. Using a gated imaging CCD camera the luminescence decay is recorded across a 520x520 μm^2 spot on the crystal surface with a spatial resolution of 0.5 μm. Having both spatial and temporal resolutions allows a wider analysis of exciton quenching compared to the previous studies [1-4]. At the excitation energy of 4.66 eV, less than the optical gap of $CdWO_4$, electron-phonon interaction becomes necessary for exciton formation. The fact that the pulse duration is shorter than the characteristic time of vibronic relaxation sets an upper limit to the exciton density and leads to absorption saturation. The Förster dipole-dipole interaction model is extended to include the effect of saturated absorption. The model is successfully tested on experimental data. The limit to the exciton density in $CdWO_4$ is calculated to be 1.9×10^{19} cm^{-3} at 4.66 eV excitation with 80-fs laser pulses.

References

1. S. Vielhauer, V. Babin, M. De Grazia, *et al.*, Phys. Sol. State, 50(9) 1789 (2008).

2. M. Kirm, V. Nagirnyi, E.Feldbach, *et al.*, Phys. Rev. B **79**, 233103 (2009).

3. V. Nagirnyi, S. Dolgov, R. Grigonis, *et al.*, IEEE Trans. Nucl. Sci. **5(3)**, 1182 (2010)

4. R. T. Williams, J.Q. Grim, Qi Li, *et al.*, Phys. Stat. Sol. (b) **248**, 426 (2011)

ATMOSPHERIC PRESSURE PLASMA JET IN MICROTUBES

Rasmus Talviste[1] , Indrek Jõgi[1], Marko Part[1], Tanel Tätte[1], Jüri Raud[1], Matti Laan[1]

[1]*Institute of Physics, University of Tartu, Estonia*

e-mail: rasmus.talviste@ut.ee

Atmospheric pressure non-thermal plasma jets (APPJ-s) have received considerable attention because of their applicability in medicine [1], for surface treatment of temperature-sensitive materials, in analysis of chemical elements [2] and possibly as hall thrusters in space technology [3]. The miniaturization widens the usability of the plasmajets but also demands the use of new dielectric materials and preparation methods. Novel ZrO_2 microtubes with superior temperature stability and dielectric properties and internal diameter as low as 20 μm have been prepared in the Institute of Physics of University of Tartu.

Usually the plasmajets are investigated at diameters above 1 mm. The aim of our study was to find out the lowest limits of the diameter of microtubes where a stable plasmajet could still be ignited. The effect of scaling down of the tube diameter was studied using a series of quartz tubes with small but well-defined diameters (500, 300, 200 and 100 μm) and wall thickness (10 μm).

The electrical and spectral characteristics such as the breakdown voltage (V_{BD}) and the intensity relationships of various spectral emission lines of characteristic plasma species (He, N_2, OH, O) have been measured (Fig. 1). The spectral characteristics further allowed the determination of plasma parameters such as rotational and vibrational temperature of nitrogen and excitation temperature of He which characterize the chemical activity of plasma.

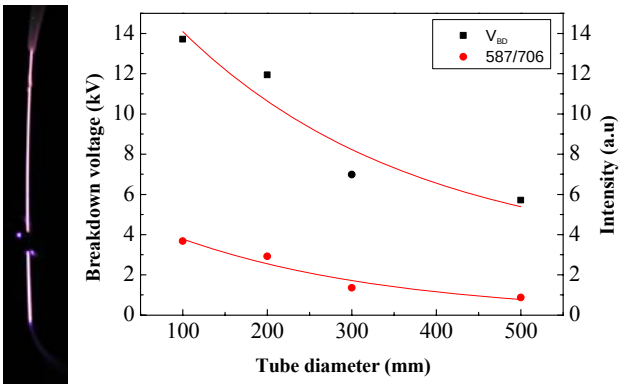

Fig.1. Picture of the pla smajet inside of the ZrO 2 microtube (left). V_{BD} *and the 587/706 line intensity relationship as a function of tube diameter in the case of quartz microtubes (right). Solid lines are a guide for the eye.*

References

1. X. Lu, Z. Jiang, Q. Xiong, Z. Tang and Y. Pan, *Appl. Phys. Lett.*, 2009, No.4, 151504-3.
2. C. Meyer, S. Müller, E.L. Gurevich and J. Franzke, *Analyst*, 2011, 136, 2427-2440.
3. C. Charles and R.W. Boswell, *Plasma Sources Sci. Technol.*, 2012, 21, 022002-4.

LASER CONOSCOPY OF LARGE-SIZED OPTICAL CRYSTALS

A.I. Kolesnikov[1], R.M. Grechishkin[1], S.A. Tretiakov[1], V.Ya. Molchanov[2], A.I. Ivanova[1], E.I. Kaplunova[1], E.Yu. Vorontsova[1]

[1]*Tver State University, Tver, Russia*

[2]*Acousto-Optic Research Centre, MISIS, Moscow*

e-mail: rostislav.grechishkin@tversu.ru

Conoscopic interferometry provides a simple method of non-destructive control of the quality of a number of ferro-piezoelectric and optical crystals. Standard optical microscopes, including some commercial instruments, are easily adapted for implementation of conoscopic studies, though limited to small handy samples with a thickness of the order of 0.5 mm. In the present work we show that the usage of wide convergent or divergent conical laser beams in a simple benchtop configuration makes it possible to examine large-sized optical crystals by the method of conoscopy, including samples elongated along the optical axis direction. As distinct from traditional optical microscopy the conoscopic figures obtained with the aid of the laser installment may contain tens and hundreds of isochromate fringes (Fig. 1,*a*), thus increasing the informative capabilities of the method. Large-sized crystals of $LiNbO_3$ (∅65×95 mm), $LiTaO_3$ (∅70×40 mm), TeO_2 prisms (50×50×30 mm) were examined experimentally at different angles between the optical axis and normal to the crystal surface. Shown in Fig. 1, *b* is a typical optical striation in a large (∅65×95 mm) Czochralsky grown $LiNbO_3$ crystal revealed by its influence on the regular shape of the isochromes. The experimental studies of different optical anomalies are confirmed by calculations based on the theoretical analysis given in [1].

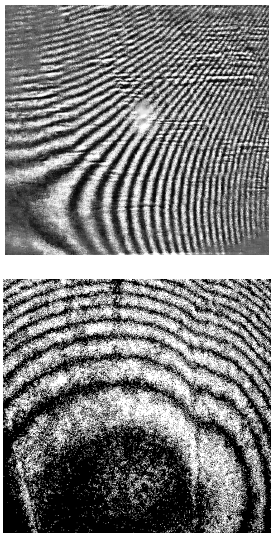

(*a*) (*b*)

Fig.1 Family of high-order isochromes (a) and distortion of the isochrome shape due to striation in a bulk $LiNbO_3$ crystal (b).

References

1. A.I. Kolesnikov, I.A. Kaplunov, A.I. Ivanova, S.A. Tretiakov, I.V. Talyzin, Yu.A. Malyshkin, R.M. Grechishkin, E.Yu. Vorontsova, Isochrome Shapes in the Conoscopic Patterns of Uniaxial Crystals, Ferroelectrics, 2012, v. 441, 75-83.

DIELECTRIC AND IMPEDANCE SPECTROSCOPY OF Fe DOPED $0.94(Na_{0.5}Bi_{0.5}TiO_3)$-$0.06BaTiO_3$ CERAMICS

Kęstutis Bučinskas[1], Rūta Mackevičiūtė[1], Maksim Ivanov[1], Robertas Grigalaitis[1], Jūras Banys[1], Eva Sapper[2], Jürgen Rödel[2]

[1] *Faculty of Physics, Vilnius University, Lithuania,*

[2] *Institute of Materials Science, Technische Universität Darmstadt, Germany*

e-mail of presenting author: kestutis.bucinskas@ff.stud.vu.lt

Ever since the discovery of piezoelectric effect, piezoelectric materials have been rapidly developed and widely used. The most widely used piezoelectric materials are $Pb(Zr,Ti)O_3$(PZT)-based ceramics because of their superior piezoelectric properties. However due to legislative enforcements, representatively the European RoHS/WEEE regulations [1], lead-free piezoelectric materials have been extensively studied last decade. Among the studied materials, $(1-x)(Na_{0.5}Bi_{0.5}TiO_3)$-$xBaTiO_3$ ceramic family has been of particular interest because of the similar piezoelectric properties to PZT ceramics [2].

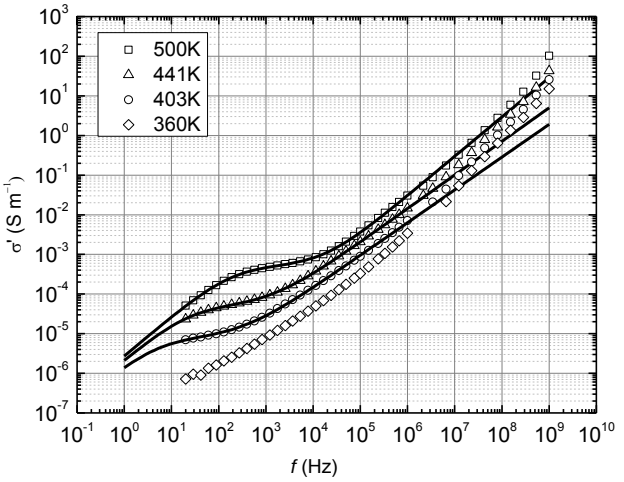

Fig.1 Frequency dependency of real part of complex conductivity of Fe doped $0.94(Na_{0.5}Bi_{0.5}TiO_3)$-$0.06BaTiO_3$ ceramics

In the present work the dielectric and impedance properties of Fe doped $0.94(Na_{0.5}Bi_{0.5}TiO_3)$-$0.06BaTiO_3$ ceramics in 20Hz-1GHz frequency range and 300-500K temperature range are investigated. The measurements of dielectric permittivity were performed during freezing cycle with 1K/min temperature variation rate. Conductivity was calculated using dielectric permittivity data. Fig. 1 shows frequency dependency of the real part of complex conductivity. Experimental data was fitted with generalized universal Jonscher's law [3]. The best fits were obtained for 403K-500K temperature range. One conductivity process was distinguished with Arrhenius behavior of σ_{DC} and possible cause of conductivity process is discussed.

References

1. *Official Journal of the European Union* 46 (L37) pp. 19-23 (2003).
2. Thomas R. Shrout, Shujun J. Zhang, *J. Electroceram*. 19, pp. 111-124 (2007).
3. I. I. Popov, R. R. Nigmatullin, A. A. Khamzin, and I. V. Lounev, *J. Appl. Phys*. 112, 094107 (2012).

HIGH-FREQUENCY DIELECTRIC PROPERTIES OF $Pb(Fe_{1/2}Nb_{1/2})O_3$ CERAMICS AND SINGLE CRYSTAL

R. Mackevičiūtė[1], J. Banys[1], A. Kania[2], V. Goian[3], D. Nuzhnyy[3], S. Kamba[3]

[1] *Vilnius University, Faculty of Physics, Vilnius, Lithuania*

[2] *A. Chelkowski Institute of Physics, University of Silesia, Katowice, Poland*

[3] *Institute of Physics, Academy of Sciences of the Czech Republic, Czech Republic*

Multiferroic materials, like bismuth ferrite (BFO), lead iron niobate (PFN) and others draw a lot of scientific attention in recent years, as the possibility to control magnetization with electric field, or polarization with magnetic field. It opens the route to a wide variety of new applications. However, despite the fact that PFN ceramic was studied more than 50 years [1], a dispersion of dielectric permittivity is still not investigated in a wide frequency range.

Dielectric measurements were performed between 300 and 500 K in the frequency range from 20 Hz to 0.8 THz. PFN ceramics are known to undergo a single diffuse phase transition between 370 K and 380 K [1]. This is characterized by a broad peak in ε'(T), whose position does not move with frequency. Our experimental data exhibit relaxor ferroelectric behavior, because the peak of ε'(T) moves to higher T with increasing frequency. Detail frequency analysis of dielectric dispersion revealed two anomalous dielectric relaxations; one in sub-THz region and the second in microwave and radio-frequency region. In contradiction to ceramics, we observed two dielectric anomalies in PFN single crystal [2], one at ~370K, and additional one, coming from structural phase transition, at ~355K. The rise of the dielectric permittivity near the temperature of phase transitions is much sharper in single crystal than in ceramics, and the temperatures of maxima of the dielectric permittivity do not depend on frequency, i.e. no relaxor or diffuse phase transition behavior was observed.

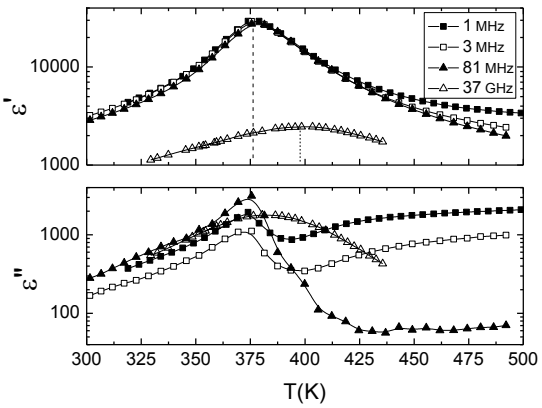

Fig. 1 Temperature dependence of the real and imaginary parts of dielectric permittivity of PFN ceramics.

References

1. V. A. Bokov, I. E. Mylnikova, and G. A. Smolenskii. *Sov Phys–JETP*, 1962, 15, 447–449.

2. A.Kania, E.Talik, and M.Kruczek. *Ferroelectrics*, 2009, 391, 114-121.

SEMI-MICROSCOPIC VIBRONIC THEORY OF QUANTUM PARAELECTRICITY AND FERROELECTRICITY

Peet Konsin[1], Boris Sorkin[1]

[1]*Institute of Physics, University of Tartu, Riia 142, Tartu, Estonia*

e-mail: konsin@fi.tartu.ee; e-mail: sorkin@fi.tartu.ee

In [1-5] the vibronic theory of displacive ferroelectric phase transitions with an order-disorder component for the $BaTiO_3$-type ferroelectric-perovskites is developed. In the present report we have developed the semi-microscopic electron-phonon theory of the quantum paraelectrics and ferroelectrics of the $SrTiO_3$-type. At this, it is shown that the local short-range electron-phonon coupling causes the occurrence of nanoregions and local ferroelectricity in $SrTi(^{16}O_{1-x}{}^{18}O_x)_3$. For quantum paraelectrics-ferroelectrics of the ABO_3-type we have shown that the ground and excited (F_{1u}) electronic states of the BO_6 cluster are mixed, hybridized by the potential ferroelectric F_{1u} vibration which becomes soft due to interband vibronic couplings. The electron-lattice interaction of the electronic states of the BO_6 cluster with the F_{2u} optical phonons at the corner of the Brillouin zone ($R=(\frac{\pi}{a},\frac{\pi}{a},\frac{\pi}{a})$) leads to the antiferrodistortive phase transition from the cubic phase (O_h) to the tetragonal (D_{4h}) one.

The dependences of the dielectric constants on temperature in $SrTiO_3$ and $KTaO_3$ along c-and a-axes. The staggered rotation-like distortion of the BO_6 octahedra in strontium titanate and other quantities are found. The external factors (the electrostatic field, the changing of the isotopic substitution in $SrTiO_3$ ($^{16}O \rightarrow {}^{18}O$), the application of pressure either uniaxial or hydrostatic etc, can lead to the occurrence of the quantum ferroelectricity in the $SrTiO_3$-type oxides. We obtained the Gibbs and Helmholtz free energies for this type of compounds. The theory is compared with the experimental data and some theoretical predictions are made.

Acknowledgments

The research was supported by the Estonian Research Council (project IUT2-27) and by the European Union through the European Regional Development Fund (projects TK114 and SF0180013s07AP).

References

1. P.I.Konsin and N.N.Kristoffel (1987). In: Interband model of ferroelectrics.Ed.Bursian E.V., Hertzen Pedagogical Institute, Leningrad, p.32.
2. P.Konsin and N. Kristoffel, Ferroelectrics 226, 95 (1999).
3. P.Konsin, Phys. Stat. Sol. (b) 86, 57 (1978).
4. I. B. Bersuker, The Jahn-Teller Effect, Cambridge: Cambridge University Press (2006).
5. P. Konsin and B. Sorkin, Ferroelectrics, 359, 63 (2007).

THE INFLUENCE OF ELASTIC STRESS ON THE SURFACE OF ADIABATIC POTENTIAL OF KI CRYSTAL AT FIXED TEMPERATURES

Nurgul Zhanturina[1], Kuanyshbek Shunkeyev[2], Viktor Tkachenko[2]

[1]*Al-Farabi Kazakh National University, Kazakhstan*

[2]*Aktobe State Pedagogical Institute, Kazakhstan*

e-mail: nzhanturina@mail.ru

We explained theoretically χ - shaped temperature line of luminescence intensity of the free and self-trapping excitons (STE) KI crystal by the temperature dependence of the self-trapping excitons potential barrier (Fig. 1). According to Fig. 1 the potential barrier of exciton's self-trapping is maximum at 4.2K in KI crystal, and there are monohalogen excitons. All excitons transits in a self-trapped state at the temperature about 60K, as evidenced by the lack of a barrier on the adiabatic potential surface in KI crystal. The deformation of 2% at fixed temperature leads to a smoothing of the surface of the adiabatic potential. This explains the increased luminescence of self-trapped excitons in the application of uniaxial compression. Expression for the probability of radiative annihilation of excitons in the crystal KI $\eta_a = \left[1+\tau_q\left(1/\tau' + \nu\exp(-E/kT)\right)\right]^{-1}$, obtained on the basis of the Mott formula qualitatively explains the increase in the efficiency of non-radiative decay of the STE to the primary radiation defects (*F*, *H*-pairs), where τ_q - the timelife of the self-trapped excitons, τ' - the timelife of the luminescence, ν - the frequency of the V_k -center, E - the height of the STE.

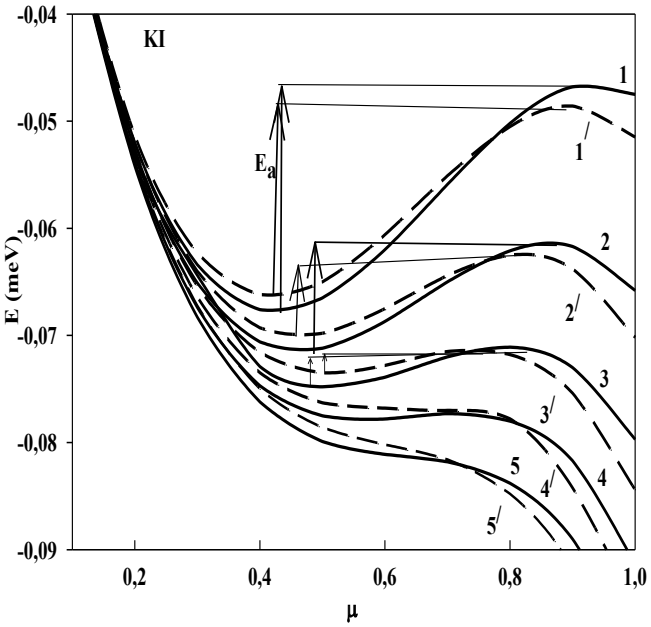

Fig 1. Adiabatic potential surface in KI crystal (1, 2, 3, 4, 5 respectively – at 4.2K, 20K, 40K, 60K, 80K, dashed – at elastic deformation).

References

1. L.N. Myasnikova, N.N. Zhanturina, K.Sh. Shunkeyev, B.A. Aliev, M. Grinberg, V.S. Tkachenko, *3-rd International Congress on Radiation Physics and Cchemistry of Condensed Matter High Current Electronics and Modification of Materials with Particle Beams and Plasma Flows.* Tomsk, 2012, 28.

THE STUDY OF CORRELATION BETWEEN MICROSTRUCTURE OF FERRITES ADN THEIR COMPLEX PERMEABILITY SPECTRA

Janis Jankovskis[1], Nikolajs Ponomarenko[1], Nina Mironova-Ulmane[2], Dmitrijs Jakovlevs[1]
[1]*Riga Technical University,* [2]*Institute of solid State Physics, University of Latvia*
e-mail: nikolaj.ponomarenko@gmail.com

Complex permeability spectra ($\dot{\mu}(f) = \mu'(f) - j\mu''(f)$, where $\mu'(f)$ is real (dispersion) part and $\mu''(f)$ is imaginary (absorption) part), obviously are housing large amount of information on inner processes of high frequency basic magnetic materials – polycrystalline ferrites (PF). The interpretation of the data coming from spectra has been in progress for several decades but as a rule they are only qualitative (except one specific point of the spectrum – the static permeability). These interpretations as well as direct experiments reveal the close correlation between the details of spectrum and microstructure of the sample. Our quantitative modeling of spectra based on account of grain size distribution effects includes several principal premises: grains are magnetically independent; grain size D probability distribution function is lognormal: $f(D) = \left(\sqrt{2\pi}\sigma D\right)^{-1} exp[-(lnD - lnD_{med})^2/2\sigma_{lnD}^2]$; magnetization processes within grains resemble the ones established for large variety of real PF samples with different microstructure. Statistical averaging of corresponding equations bring to analytic presentation of absorption component of spectrum: $\mu'' = \mu''_{max} exp[-(logf - logf_u)^2/2\sigma^2]$, where f_u and $\mu''_{max} = \mu''(f_u)$ are parameters of maximum absorption, and σ is the microstructure characteristic - dispersion. The equation quantitatively relates characteristics of magnetic spectrum of the sample with its microstructure (at least in principle). It is the concern of this investigation to add to it the real experimental data for the samples from the two main groups of ferrites - NiZn and MnZn.

The experiments were performed on PF toroidal samples of different inner/outer diameter (ID/OD), cross section area (A), number of winding turns, and microstructure. Magnetic spectra were measured for PF with similar and dissimilar microstructure. The truthfulness of spectra were systematically verified by the use of Kramers-Kronig relations. The results prove the importance of statistical characteristics of the microstructure.

The results gained allow to conclude that for NiZn ferrites correlation of experimental spectra and the modelling is evident. Still, the correlation of spectra and model for MnZn samples becomes inexact for rather high ID/OD and A of samples, obviously, due to dimensional effects in PF.

TRITIUM RETENTION STUDIES IN W COATED JET DIVERTOR CFC TILES

Mihails Halitovs[1], Gunta Kizane[1#], Liga Avotina[1], Jari Likonen[2], Nicolas Bekris[3], Catalin Stan-Sion[4] and JET-EFDA contributors*

JET-EFDA, Culham Science Centre, Abingdon, OX14 3DB, UK
[1]Institute of Chemical Physics, University of Latvia, Latvia;
[2]VTT Technical Research Centre of Finland, Finland;
[3]Karlsruhe Institute of Technology, Germany;
[4]H. Hulubei National Institute of Physics and Nuclear Engineering, Romania
e-mail: gunta.kizane@lu.lv

The Joint European Torus (JET) is currently operated with an ITER-like Wall (ILW) in which the plasma-facing material in the main vacuum chamber is beryllium while tungsten is used in the divertor in a similar manner foreseen for ITER. Tungsten has been selected for ITER not only because of its outstanding physical properties (high melting point and high conductivity) but also because of its low affinity for hydrogen, limiting thus the tritium inventory in Plasma Facing Components (PFCs). As tungsten has higher density than carbon, it is much less affected by physical and chemical sputtering and therefore the total amount of co-deposited or accumulated tritium on these PFCs is noticeably reduced [1]. In particular, in JET tungsten coatings on Carbon Fibre Composite (CFC) tiles are presently used in the divertor area where only CFC tiles have been used in the past. In this work the effects of W coating are evaluated in terms of tritium retention.

Samples of two divertor tiles (3 and 7) used in JET during the experimental campaign in 2007-2009 with an MkII-HD divertor configuration were compared. Tile 2IWG3A is a pure CFC tile with no additional coating while tile 2OWG7B had ~ 25 μm tungsten coating with molybdenum interlayer [2].

Examined samples of tile 2IWG3A show the average tritium activity of $5 \cdot 10^5$ Bq·g^{-1} for the plasma-exposed surface of the tile while the bulk activity is approximately $3 \cdot 10^3$ Bq·g^{-1}. Samples of W-coated tile 2OWG7B show tritium activity for the top layer being approximately 10 times smaller than the corresponding samples of uncoated tile.

As observed in previous studies for full CFC tiles [3, 4], the tritium activity measured for the upper layer of a divertor tile, can be up 1000 - 100000 times higher than the bulk activity.

The present work provided an experimental confirmation that tungsten will lead to decreased tritium inventory in divertor tiles. Due to the smaller permeability of tritium through tungsten, as well as to its lower affinity to form hydrides, tungsten is valuable for use in the divertor region of any fusion machine such as ITER and DEMO.

Acknowledgments: This work was supported by EURATOM and carried out within the framework of the European Fusion Development Agreement. The views and opinions expressed herein do not necessarily reflect those of the European Commission.The meeting of planning activities was supported by ERAF Project 2010/0202/2DP/2.1.1.2.0/10/APIA/VIAA/013 Support for the international cooperation projects and other international cooperation activities in research and technology at the University of Latvia.

* See the Appendix of F. Romanelli et al., Proceedings of 24th IAEA Fusion Energy Conference 2012, San Diego, USA

References:

[1] V. Philipps. Tungsten as material for plasma facing-components in fusion devices J. Nucl. Mater. **415** (2011) S2–S9

[2] C. Ruset *et al.* Development of W coatings for fusion applications. Fus. Eng. Des. **86** (2011) 1677–1680

[3] N.Bekris *et al.* Tritium Depth profiles in 2D and 4D CFC tiles from JET and TFRT. J. Nucl. Mater. **313-316** (2003), 501-506.

[4] E. Pajuste *et al.* Structural changes and distribution of accumulated tritium in the carbon based tiles. J. Nucl. Mater. **415** (2011) S765–S768

INFLUENCE OF TEMPERATURE ON PHOTOISOMERISATION PROCESS OF POLYMER FILMS DOPED BY AZOBENZENE DERIVATIVES

M.Narels, E.Laizane, A.Vembris

Institute of solid State Physics, University of Latvia

e-mail: martins.nar@gmail.com

Azobenzene derivatives are recognized for their capability to isomerize under illumination. However it is known that isomerization can be induced not only by light but also by heat in the *cis→trans* direction due to the metastable cis state. The thermal reaction in most of the azobenzene derivatives at room temperature is hard to distinguish from the photoreaction nonetheless it could have significant impact on the isomerization process at longer time scale. Analysis of the kinetics of isomerization process at various temperatures is useful to obtain information about temperature influence on molecular switching.

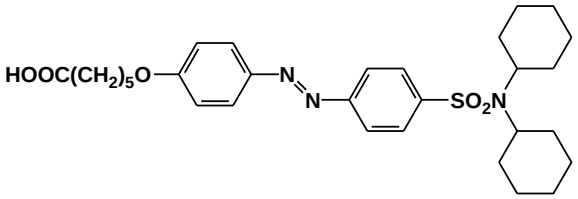

Fig.1. Azobenzene derivative

In the work 6-[4-(4-Dicyclohexylsulfamoylphenylazo)phenoxy]hexanoic acid was chosen (see Fig.1). Molecules were doped in polymer matrix at various concentrations from 3 to 15wt%. Host-guest systems were prepared from chloroform solutions by spin-coating method. Samples were irradiated by alternate light in ultraviolet spectral region at ~360nm and visible spectral region at ~450nm, which correspond to *trans→cis* and *cis→trans* isomerization, respectively. At the same time light intensity at 360nm which pass through the sample was recorded. Double exponential process was observed in low temperature region from 100 to 250K and one exponential process at temperature higher than 250K. Time constants of *cis→trans* isomerization decrease by temperature but *trans→cis* increase. Temperature influence on parameters of photoisomerization kinetics will be discussed.

Acknowledgment:

This work has been supported by Latvian State Research Programm No.2 in Materials Sciences and Information Technologies and ERAF project Nr. 2010/0204/2DP/2.1.1.2.0/10/APIA/VIAA/010.

ZrO_2 MICROTUBES AS SUBSTRATES IN ALD PROCESSES

Marko Part, Aile Tamm, Jekaterina Kozlova, Hugo Mändar, Tanel Tätte, Kaupo Kukli

Institute of Physics, University of Tartu, Riia 142, 51014, Tartu, Estonia

e-mail of presenting author: markopa@ut.ee

Materials with microtubular geometry have attracted considerable attention during the past few decades due to their possible applications in microfluidic devices used for energy storage and production, like SOFC, where microtubular geometry could possess better thermo-mechanical properties and sealing simplicity compared to other geometries [1]. Another possible application of microtubes is to use these as miniature plasma chambers. For the use in these applications, the tubes should be functionalized by different coatings, like MgO films which can promote catalytic splitting of water and enable hydrogen storage. MgO is also considered as a seed layer for growing various kinds of materials including thin films from another kinds of precursors that normally dismatch with the original substrate [2]. Simple NaCl-like structure makes it an attractive material to investigate oxide surface chemistry in ALD [3].

To favor emission of electrons form the inner surface of the tubes, required for plasma chamber applications, atomic layer deposition (ALD) of MgO has been carried out on tubes. The films were deposited from 2,2,6,6-tetramethyl-heptanedionato-3,5-magnesium(II) at 220 °C on the surface of YSZ microtubes. Controlled growth of films enable to achieve ultrathin and dense films both on the inner and outer surface. $Mg(thd)_2$ was evaporated at 104 °C from an open boat inside the reactor. Nitrogen was used as both carrier and purging gas and O_3 was used as oxygen precursor. The cycle times used for the growth of MgO were 5-2-2-5 s for the sequence $Mg(thd)_2$ pulse-purge-O_3 pulse-purge. The tubes were obtained by novel route via hydrolysis of zirconium butoxide ($Zr(OBu)_4$) with large excess of water and heat treated at 800 °C under atmospheric pressure.

The tubes covered with MgO films met all the requirements for plasma chamber applications. Due to homogeneity of the nanocrystalline structure formed, the tubes could also be applied as optical waveguides or miniature light sources in photonics.

References

1. R. Campana, A. Larrea, J.I. Pena, V.M. Orera, *Journal of the European Ceramic Society* 29 (2009) 85-90.

2. S.H. Rhee, Y. Yang, H.S. Choi, J.M. Myoung and K. Kim, *Thin Solid Films* 396 (2001) 23-28

3. M.C. Gallagher, M.S. Fyfield, L.A. Bumm, J.P. Cowin and S.A. Joyce, *Thin Solid Films* 445 (2003) 90-95

GREEN LUMINESCENCE DECAY KINETICS ANALYSIS IN $NaLaF_4:Er^{3+}$

Maris Springis, Jurgis Grube, Anatolijs Sarakovskis
Institute of Solid State Physics, University of Latvia
e-mail of presenting author: springis@cfi.lu.lv

In this work luminescence spectra and kinetics of $NaLaF_4:Er^{3+}$material at different Er^{3+} concentration are studied under excitation in UV, VIS and IR spectral region at different temperatures.

A luminescence spectrum for $NaLaF_4:Er^{3+}$ (0.2mol%) at 489nm excitation reveals characteristic Er^{3+} ion luminescence bands in the green (540 nm), red (640 nm) and infrared (980 nm) spectral regions. The green luminescence band responsible for the transition $^4S_{3/2} \rightarrow {}^4I_{15/2}$ is dominating the spectrum. As the concentration of the activator is increased the positions and the shapes of the luminescence bands do not vary remarkably while the intensity of all luminescence bands changes significantly. The proportional increase of the red band intensity with increasing Er^{3+} concentration under direct excitation should be caused by the increase of the number of the activator ions. The superlinear increase of infrared luminescence intensity with the increase of Er^{3+} concentration as well as the quenching of the green luminescence for the concentrations higher than 2 mol% can be attributed to the cross-relaxation process between the activator ions.

The green luminescence decay kinetics under pulsed direct excitation reveals rather complicated, nonexponential behavior and can be divided in several sequential stages. Both activator concentration and temperature dependence of the green luminescence decay kinetics are discussed in the frame of various energy relaxation models, involving direct relaxation at short times and small activator concentration, migration accelerated relaxation at higher activator concentration and migration-limited relaxation at longer times.

The financial support of ERDF project Nr. 2010/0204/2DP/2.1.1.2.0/10/APIA/VIAA/010 and VPP IMIS is greatly acknowledged.

PHASE TRANSITIONS AND PHYSICAL PROPERTIES IN Ca MODIFIED $Na_{1/2}Bi_{1/2}TiO_3$-$SrTiO_3$-$PbTiO_3$ SOLID SOLUTIONS

Marija Dunce, Eriks Birks, Maija Antonova,
Anatoly Mishnov, Maris Kundzinsh, Andris Sternbergs
Institute of solid State Physics, University of Latvia, Latvia
e-mail of presenting author: marija.dunce@cfi.lu.lv

Composition $0.4Na_{1/2}Bi_{1/2}TiO_3$-$0.4SrTiO_3$-$0.2PbTiO_3$, which belongs to a family of $0.4Na_{1/2}Bi_{1/2}TiO_3$-$(0.6-x)SrTiO_3$-$xPbTiO_3$ solid solutions, is located in the region of the phase diagram (T,x), where stability of the relaxor state, evaluated as width of the temperature region between the maximum of dielectric permittivity T_m and the temperature of the spontaneous phase transition between the relaxor and the ferroelectric states T_t, diminishes. In the present work, Sr in $0.4Na_{1/2}Bi_{1/2}TiO_3$-$0.4SrTiO_3$-$0.2PbTiO_3$ is gradually replaced by Ca and the influence of this substitution on the relaxor state and the phase transition is studied.

The concentration dependence of the tetragonal cell's volume gradually decreases if the concentration of Ca increases, confirming replacement of Sr by Ca in the lattice, while the tetragonality in a certain concentration range remains independent of Ca content. Stability of the relaxor state and the temperature of the phase transition is also weakly-dependent on Ca content in the range of low concentrations, and steeply increases, starting from certain Ca concentration. Stability of the phase transition and polarization from Ca at low concentrations of Ca, on one hand, and steep decreasing of dielectric properties, on the other hand, is explained assuming that at low concentrations Ca resides inside polar nanoregions preventing their reorientation in the weak external electric field.

CHARACTERIZATION OF FUNCTIONAL GROUPS OF AIRBORNE PARTICULATE MATTER

Margarita Baitimirova[1], Juris Katkevics[2], Eduards Bakis[3], Arturs Viksna[4]

[1-4]*University of Latvia, Latvia*

e-mail: puma3b@inbox.lv

In this research solid particles of smoke were collected on the filters from burning of various combustibles in a burning chamber and from atmosphere of city of Riga by dichotomous impactor. The functional groups of black carbon were determined by Fourier-transform infrared spectroscopy (FTIR). A thin tablet was formed from particulate matter and KBr powder. FTIR spectra were measured using PerkinElmer Spectrum Two spectrometer with computer program PerkinElmer Spectrum v.10.03.07. The spectral signal was measured from 4000 to 400 cm^{-1} wave lengths.

In the FTIR spectra of particulate matter from city atmosphere and from burning of various combustibles were observed aromatic C-C and C-H groups (Fig. 1). These signals were observed not only in the spectra of solid particles of kerosene smoke and of city atmosphere, but these signals were in the spectra of solid particles of stearin and paraffin candles burning, too. As we know, components of stearin wax are saturated and unsaturated fatty acids, and components of paraffin wax are saturated aliphatic hydrocarbons. From this, it may conclude that aromatic hydrocarbons are forming in the burning process and particulate matter is formed from them. This fact conforms to literature data [1]. Also particulate matter contained O-H, aliphatic C-H, C≡C, C=O and C-O groups.

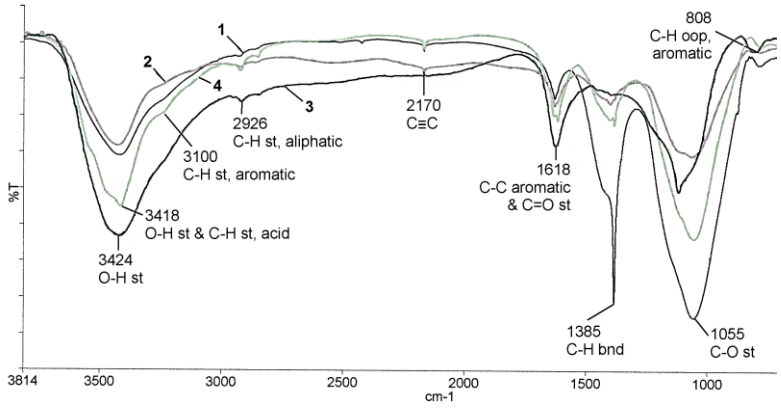

Fig.1. FTIR spectra of particulate matter from stearin (1) and paraffin (2) candles burning, kerosene combustion (3) and from atmosphere of city (4)

Acknowledgements

This work has been supported by the European Social Fund within the project «Support for Master Studies at University of Latvia».

References

1. J.S. Lighty, J.H. Veranth, A.F. Sarofim. *Air & Waste Manage. Assoc.*, 2000, No.50, 1565-1618.

INFLUENCE OF GRATING PERIOD ON SURFACE RELIEF HOLOGRAM RECORDING EFFICIENCY IN AMORPHOUS AS_2S_3 AND $AS_{40}S_{15}SE_{45}$ FILMS

M. Reinfelde, J.Teteris
Institute of solid State Physics, University of Latvia, LV 1063 Riga, Latvia
e-mail: mara.reinfelde@cfi.lu.lv

Recently a number of studies on direct surface structure formation by holographic recording were carried out in thin layers of chalcogenide semiconductors [1, 2]. This phenomenon is due to photoinduced mass transport during comparatively long light illumination. Dependence on recording conditions - light polarization, film thickness and grating period - was studied. Efficiency of recording is defined by distribution of electric field vector of resulting interference pattern inside the recording media. In this work we will present the results obtained on As_2S_3 and $As_{40}S_{15}Se_{45}$ films for wide range grating periods overlaying ~1 ÷ ~80 μm.

References

1. M.Reinfelde, R.Grants, J.Teteris, *Photoinduced mass transport in amorphous As-S-Se films*, Phys.St.Sol.C, 9, No.12 (2012) 2586-9.
2. J.Teteris, U.Gertners and M.Reinfelde*, Photoinduced mass transfer in As2S3 films*, Phys.St.Sol.C, 8 (2011) 2780-4.

INFLUENCE OF RADIATION ON EPR AND OPTICAL SPECTROSCOPY OF HUMAN BLOOD

Maksims Polakovs[1], Nina Mironova-Ulmane[1], Ilmo Sildos[2], Ainars Aboltins[3]

[1]*Institute of Solid State Physics, University of Latvia, Riga, Latvia*

[2]*Institute of Physics, University of Tartu, Riia 142, Tartu 51014, Estonia*

[3]*Pauls Stradins Clinical University Hospital, Riga, Latvia*

e-mail of presenting author: maksims.polakovs@gmail.com

In the present work we report results of study EPR and optical absorption spectra of blood of patients examined by radio-isotopes diagnosis (Tc99m). Venous blood was donated by consenting patients before and after radio-isotopes diagnosis and collected under air in glass tubes containing of anticoagulant. The EPR spectra were recorded using an EMX-6/1 spectrometer (BRUKER) working at X-band frequency with 100 kHz modulation. The EPR spectra of blood have been studied at 80K temperature. It is shown that EPR spectra of blood of patients after examination by radio-isotopes diagnosis has signal of the ion Fe^{3+} (methemaglobin) in low-spin state with g = 2.003 and in the high spin state with g=6.0. We can also detect EPR signals from the metal-protein transferrin (g=4.3) that contains the non-haem rhombic iron. The EPR signal of human blood mixed with Tc^{99m} has signal Fe^{3+} (methemaglobin) in low-spin state with g = 2.003 only.

The optical absorption spectra of blood were measured in the energy range which includes all d-d electronic transition in ions of Fe^{2+} and Fe^{3+}. We observed the additional absorption band in absorption spectra of blood of patients after radio diagnosis. These additional bands belong to the Fe^{3+} ions are, because the Fe^{2+} ions of hemoglobin is oxidized to the Fe^{3+} ions by radiation to form methemaglobin (MetHb). These data shows that the blood of patients after radio-diagnosis has methemaglobin higher normal. The Fe^{2+} in heme of hemoglobin is oxidized to the Fe^{3+} by radiation.

Acknowledgement

This work was partially supported by Latvian National Research Program in Materials Science.
This work was supported by ERDF project Nr.2DP/2.1.1.2.0/10/APIA/VIAA/010.

HALL-EFFECT STUDIES IN DOPED ZnO THIN FILMS

M. Zubkins, R. Kalendarev, K. Vilnis, A. Ecis, A. Azens, J. Purans

Institute of Solid State Physics, University of Latvia, Riga, Latvia

zubkins@cfi.lu.lv

Transparent conducting oxide (TCO) thin films are heavily doped semiconductors (E_g > 3.0 eV) with a wide range of applications, such as transparent electrodes for flat panel displays and photovoltaic cells, window defrosters, light emitting diodes, etc. For technological applications, the TCO should have the electrical resistivity of $\rho \sim 1.0 \cdot 10^{-4}$ Ωcm, with the optical transmission in the visible range of around 90 %. Doped zinc oxide films are a good alternative to the commonly used and expensive tin doped indium oxide (ITO) films, because the source material is inexpensive and non-toxic.

Doped ZnO films have been deposited by reactive DC magnetron sputtering from metallic targets made of Zn mixed with doping element, such as Al or Ir. For reference, pure ZnO thin films have been deposited as well. Sputtering power, deposition time and argon gas flow were kept constant at 100 W, 40 min and 50 sccm, respectively. Substrate temperature, work pressure and oxygen flow were varied to investigate the dependence of films electrical properties on these parameters. The process was controlled by plasma optical emission spectroscopy, based on Zinc emission line at 480.05 nm.

Hall effect of doped ZnO films was measured by equipment HMS5000, using *Van der Pauw* technique. The parameters measured were electrical resistivity and magnetoresistance, Hall coefficient, charge carrier concentration and mobility in the temperature in range 80 – 350K.

Acknowledgement

The work has been performed within ERDF project:
2010/0272/2DP/2.1.1.1.0/10/APIA/VIAA/088.

DIELECTRIC PROPERTIES OF $Ba_2NdFeNb_{3,7}Ta_{0,3}O_{15}$ SOLID SOLUTION

D. Gabrielaitis[1], M. Kinka[1], M. Albino[2], M. Josse[2], V. Samulionis[1], R. Grigalaitis[1], M. Maglione[2] J. Banys[1]

[1] *Vilnius University, Faculty of Physics, Lithuania*

[2] *CNRS, Université de Bordeaux, ICMCB-CNRS, France*

e-mail of presenting author: martynas.kinka@delfi.lt

Tetragonal Tungsten Bronze (TTB) structural family attracted much attention in recent years. It is one of the largest oxygen octahedral ferroelectric families next to the ferroelectric perovskites [1]. Three types of open channels that develop within its octahedral framework give raise to its unique properties. More open crystalline network makes TTB a more flexible material. A wide range of substitutions available in TTB framework enables scientists to synthesize many different compounds. This feature makes it a better candidate (as compared to perovskites) in search of relaxors, ferroelectrics and even multiferroics.

$Ba_2NdFeNb_{3,7}Ta_{0,3}O_{15}$ ceramic under investigation here belongs to TTB structural family. Dielectric measurements of complex permittivity in a frequency range from 20 Hz to 37 GHz upon heating and cooling were performed. Obtained results show ferroelectric phase transition at 315 K while heating. On cooling a huge shift of permittivity maxima is observed. Permittivity dispersion at lower temperatures indicates appearance of a second phase. Wide hysteresis loop ranging over 50 K is also seen. Such wide hysteresis loop is unusual however similar results were reported for $Ba_2NdFeNb_4O_{15}$ compound [2]. The main interest is to find explanation for observed behaviour upon heating and cooling which could be done by examining frequency dependence of complex permittivity. It clearly shows two separate, temperature dependent processes. Approximation with Cole-Cole equation and obtained parameters will be used to explain undergoing processes.

References

1. R. Guo, H. T. Evans, A. S. Bhalla, *Crystal Structure Analysis of Ferroelectric Tetragonal Tungsten Bronze* $Pb_{0.596}Ba_{0.404}Nb_{2.037}O_6$, *Applications of Ferroelectrics,*. 1996, 241 - 244 vol 1.

2. J. Banys, S. Bagdzevicius, M. Kinka, V. Samulionis, R. Grigalaitis, E. Castel, M. Josse, M. Maglione. *Dielectric Studies Of* $Ba_2Pr_xNd_{1-x}FeNb_4O_{15}$ *Ceramics*, Applications of Ferroelectrics (ISAF/PFM), 2011 International Symposium on Piezoresponse Force Microscopy and Nano scale Phenomena in Polar Materials.

HEMP FIBER NON-WOVENS PROPERTIES ANALYSIS

Liga Freivalde[1] (presenting author), Silvija Kukle, Stephen Russell[3]

[1, 2] Institute of Textile Technology and Design, Riga Technical University, [3] School of Design, Centre for Technical Textiles, University of Leeds, United Kingdom

e-mail of presenting author: Liga.Freivalde@rtu.lv

This paper describes non-woven samples which were developed for insulation (thermal, acoustic), intended to be used in building industry. The development of high-performance materials made from natural resources is increasing worldwide. Latvia is searching for a new ways to develop materials with a high added value by using locally obtained raw materials. In Latvian climate high hemp straw yields are obtainable, fibres proportion reaches 22-25 % [1], and acquired fibres have good physical and mechanical properties. [2;3] Non-woven samples were made by using local hemp and the EU introduced variety farmed in climatic and soil conditions found in Latvia. A comprehensive review of nonwoven samples made of the hemp fibers by three different manufacturing technologies, such as hydro-entanglement, thermal bonding and needle-punching, will be presented. Specimen's physical properties are tested and compared between methods as well as between varieties. The review also encloses samples comparison with conventional insulation materials. The fiber processing techniques as well as the factors (growing conditions, fiber type and content etc.) affecting these processes will be discussed. In this work we focus on nonwoven materials acustic properties as well as properties who directly affect them, i.e., thickness, density, mass per unit area).

Acknowledgements

This research has been supported by the European Social Fund within the project "Support for the Implementation of Doctoral Studies at Riga Technical University".

References

1. V.Stramkale, L.Freivalde, S.Kukle, *Analysis of the renewable fiber properties and uses in scale of Latvia*, Proceedings of the 41st International Symposium on Novelties in Textiles, Ljubljana, Slovenia, 2009, 320-325.
2. I. Baltina, Z.Zamuska, *Scientific Journal of RTU Material Science*. Effects of Late Hemp Straw Harvesting on Fiber Quality 2010, vol.5, 194-198.
3. S.Kukle, V.Stramkale, D.Kalniņa, R.Soliženko, *Comparision of Hemp Fibre Properties.* 6th International Textile Clothing and Design Conference "Magic World of Textiles" (ITC&DC): Book of Proceedings, Dubrovnik, Croatia, 2010, 76-80.

ANALYSIS OF FULLERENE C_{60} POSSIBLE FORMED IN THE DIVERTOR AREA OF A TOKAMAK LIKE DEVICES

Liga Avotina[1], Gunta Kizane[1*], Janis Kalnacs[2], Larisa Baumane[1], Linda Ansone[3]

[1]*Institute of Chemical Physics, University of Latvia, Latvia,* [2]*Institute of Physical Energetics, Latvia,* [3]*Departament of Geography and Earth Science, University of Latvia. Latvia*

e-mail: liga.avotina@lu.lv

Carbon fiber composite (CFC) materials are used in tokamak's type fusion reactors due to low Z and good thermal conductivity. In vacuum vessel plasma-wall interaction phenomena induces flake, dust production and tritium trapping in them [1]. There have been observed similarities between tokamak flakes, dust and C_{60} films [2]. The fact that fullerene like compounds might be in dust of tokamak divertor, does not preclude the formation of fullerenes or long-chain hydrocarbons during plasma operations.

The aim of this research is to investigate structure and properties of decomposition of fullerene (C_{60}) containing samples in order to understand formation and structure of flakes and dust in a fusion machine.

Thermal analysis of samples was realized in air an argon atmosphere, using different heating rates. Structure of fullerene containing samples was analyzed with FT-IR and electron spin resonance spectroscopy and with powder X-ray diffractometry (p-XRD).

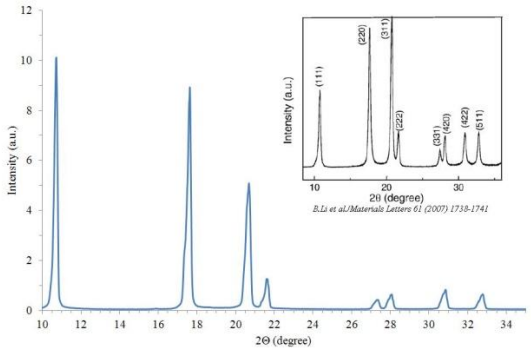

Fig.1. p-XRD pattern of C_{60} bulk crystal (right upper corner) and syntetic fullerene C_{60} containing sample

Characteristic reflexes of C_{60} are observed (Fig.1). In p-XRD pattern, most intensive reflexes are at 10.7 (111), 17.6 (220) and 20.7 (311) 2Θ angle. In FT-IR spectra all the four allowed vibration bands of C_{60} fullerene [3] at about 525, 576, 1182 and 1428 cm^{-1} are observed. Characteristic parameters of C_{60} containing sample could be used for detection presence of C_{60} in plasma exposed carbon based deposits.

*Acknowledgement: The research was supported by ERAF Project 2010/0202/2DP/2.1.1.2.0/10/APIA/VIAA/013 Support for the international cooperation projects and other international cooperation activities in research and technology at the University of Latvia

References:

[1] F. Le Guern et al. *Fusion Engineering and Design* 86 (2011) 2753-2757

[2] N.Yu.Svechnikov et al. *Fusion Engineering and Design* 75-79 (2005) 339-344

[3] G.V. Andrievsky et al. *Chemical Physics Letters* 364 (2002) 8-17

AFTERGLOW AND THERMOLUMINESCENCE OF ZrO_2 NANOPOWDERS

Laurits Puust, Valter Kiisk, Kathriin Utt, Ilmo Sildos

Institute of Physics, University of Tartu

e-mail of presenting author: laurits.puust@ut.ee

Phosphors with persistent photoluminescence (PL) are potentially important components of sustainable energetics. Moreover, nanoparticles with persistent afterglow can be used as fluorescent biolabels for *in-vivo* medical research. Wide-gap oxides ZrO_2 and HfO_2 with low phonon frequencies are perspective matrices for optical doping. Nanomaterials of these oxides have revealed a PL with afterglow in the time frame of hundreds of seconds.[1]

Hereby we prepared ZrO_2 nanopowders by sol-gel technique based on fast hydrolysis and polymerisation of zirconium(IV)butoxide. PL and its afterglow were recorded after 266 nm excitation. A combined heating/cooling stage was used to record thermoluminescence (TL) glow curves over the range of –100…300°C. TL intensity was detected in dependence on driving temperature at maximum of emission band (480 nm) which can be ascribed to oxygen vacancies (V_O) in the monoclinic ZrO_2.[2] Most intense PL afterglow at room temperature was obtained from material annealed at 1250°C and the afterglow was found to be correlated with 6°C and 110°C TL peaks (Fig. 1).

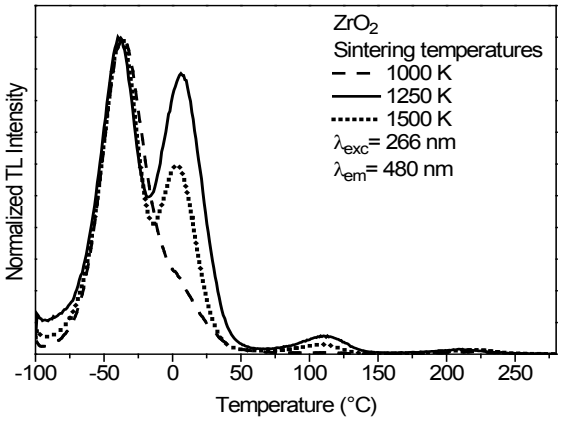

Figure 1. TL glow curves of ZrO_2 nanopowders annealed at different temperatures (heating rate 20 K/min) after 266 nm irradiation of 3 minutes.

References

1. José M. Carvalho, Lucas C. V. Rodrigues, Jorma Hölsä, Mika Lastusaari, uiz A. O. Nunes, Maria C. F. C. Felinto, Oscar L. Malta, and Hermi F. Brito, *Optical Materials Express*, 2012, Vol. 2, No. 3, 331-340.
2. Cuikun Lin, Cuimiao Zhang, and Jun Lin, *J. Phys. Chem. C*, 2012, Vol. 111, No. 8, 3300-3307.

EXCITON-PHONON INTERACTION IN ALKALI HALIDE CRYSTALS AT LOW TEMPERATURE UNIAXIAL ELASTIC STRESS

Kuanyshbek Shunkeyev[1], Lyudmila Myasnikova[1], Nurgul Zhanturina[2]

[1]Aktobe State Pedagogical Institute, [2]Al-Farabi Kazakh National University, Kazakhstan

e-mail: shunkeev@rambler.ru

The obtained experimental results of the work allow to determine the following mechanisms of luminescence and exciton-phonon interaction in KI, RbI, NaBr and KBr crystals at low temperature uniaxial elastic stress.

The decrease of emission halfwidth (ΔH) for self-trapped excitons at fixed temperature (100K) for elastic stressed crystals was experimentally determined: KI (for π: ΔH=0.03 eV; for σ: ΔH=0.02 eV), RbI (for σ: ΔH=0.03 eV), NaBr (for π, σ: ΔH=0.03 eV), KBr (for σ: ΔH=0.006 eV).

The frequency increase of active fluctuations of self-trapped excitons [1] in elastic stressed crystals was experimentally determined: KI (for π: $\Delta\omega=0.44\cdot10^{12}$ s^{-1}; for σ: $\Delta\omega=0.41\cdot10^{13}$ s^{-1}), RbI (for σ: $\Delta\omega=0.25\cdot10^{13}$ s^{-1}), NaBr (for π, σ: $\Delta\omega=0.56\cdot10^{13}$ s^{-1}), KBr (for σ: $\Delta\omega=0.04\cdot10^{13}$ s^{-1}).

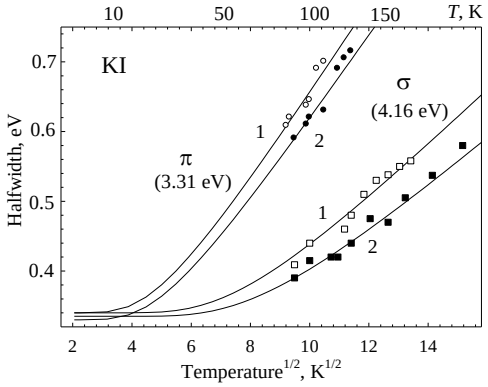

Fig.1 The temperature dependence of emission of the halfwidth the KI crystal before (1) and after low temperature uniaxial elastic stress (2).

The decrease of Huang-Rhys parameter in elastic stressed crystals was experimentally determined: KI (for π: ΔS=31; для σ: ΔS=26), RbI (for σ: ΔS=40), NaBr (for π, σ: ΔS=29), KBr (for σ: ΔS=4).

On the basis of the increase of activation energy of temperature luminescence quenching, emission band contraction of self-trapped excitons, frequency increase of active fluctuations of self-trapped excitons, decrease of Huang-Rhys parameter the attenuation of exciton-phonon interaction in elastic stressed KI, RbI and NaBr crystals is established [2].

References

1. H.Nishimura, T.Tsujimoto, M.Nakayama, T.Horiguchi, M.Kobayashi, *J.Phys.Soc.Japan*, 1994, V.63, №7, 2818-2824.
2. L.Myasnikova, K.Shunkeev, *Rus. Phys. J.*, 2009, №8/2, 129-132.

SPECIFICITY OF STABILIZATION OF *H*-CENTERS IN CRYSTAL KBr AT LOW TEMPERATURE DEFORMATION

Kuanyshbek Shunkeyev, Alexandra Barmina, Sagynbek Shunkeyev

Aktobe State Pedagogical Institute, Kazakhstan

e-mail: shunkeev@rambler.ru

The influence of low temperature elastic stress on the stabilization of movable interstitial halogen atom of KBr crystal is experimentally studied [1]. The main radiation defects of KBr crystal (previously elastic stressed at 80K) are F - and Br_3^- -centers (curve 1, Figure 1).

With the elastic stress increase at the same X-ray radiation exposures an effect of Br_3^- -center concentration decrease is observed; it is accompanied with the Br_2^- -center concentration increase (curves 2, 3, 4, Figure 1).

The insert shows differential absorption spectra at elastic stress (curve 4-1) and after its removal (curve 5-1) where an absorption band with maximum at 3.25 eV disappears. The arrows show maximums positions of absorption bands V_K -, V_{KA}(Na)-, H_A(Na)- and H -centers. According to spectral structure and thermal destruction as a result of the self-trapping of interstitial halogen atom in the field of elastic stress the found absorption band (3.25 eV) is ascribed to V_K -center.

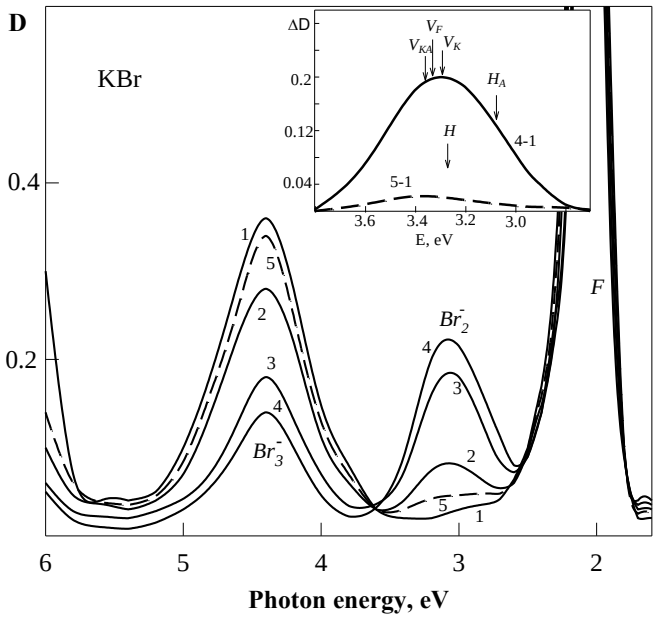

before stress (1), after stress at 80K (2 – ε = 0.4%, 3 - ε = 0.8%, 4 - ε = 1.2%), after stress removal (5). The insert shows differential absorption spectra curves 4-1and 5-1.

Fig.1 KBr *crystal absorption spectra X-rayed at 80K in isodose mode for 3 hours.*

References

1. K.Shunkeyev, A.Barmina, S.Shunkeyev, *Rus. Phys. J.*, 2006, No. 10, 148-149.

REAL-TIME OPTICAL CHARACTERIZATION OF ATOMIC LAYER DEPOSITION OF DIELECTRICS ON GRAPHENE

Kristel Möldre, Aivar Tarre, Peep Adamson, Tauno Kahro, Ahti Niilisk, Jaan Aarik
Institute of Physics, University of Tartu, Riia 142, 51014, Estonia
e-mail of presenting author: kristel.moldre@ut.ee

High intrinsic mobility of charge carriers in graphen makes this material extremely attractive for application in field effect transistors. For this application, thin gate dielectrics with high permittivity should be deposited on graphene. As accurate control of film thickness is needed in preparation of gate stacks, atomic layer deposition (ALD) seems to be the most appropriate technique for this purpose. Unfortunately, due to chemical inertness of the graphene surface, ALD of dielectrics on this material is still a challenge. In development of new process technologies, possibility to employ real-time characterization would be a great advantage. Incremental dielectric reflectance (IDR) is a method that allows real-time monitoring of ALD of dielectrics on the atomic layer level on different kind surfaces [1]. Therefore we used IDR to characterize ALD of TiO_2 on graphene that was grown by chemical vapor deposition on copper foils and then transferred to SiO_2 substrates. For monitoring TiO_2 growth, a laser beam was directed onto a substrate under the Brewster angle and the reflection was measured during the film deposition. In this way we were able to monitor deposition of TiO_2 on graphene with sufficient sensitivity from the very first ALD cycles (Fig. 1). The studies confirmed that pretreatment of graphene had a crucial influence on behavior of the optical signal in the initial stage of deposition. Calculations performed to interpret the results showed that uniformity of film nucleation was the most possible reason for this effect and, thus, could have been characterized on the basis of IDR data.

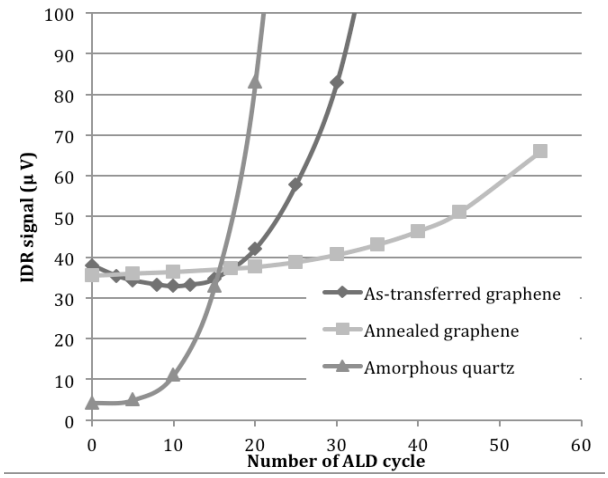

Fig.1 Dependence of IDR signal on number of ALD cycles applied.

[1] A. Rosental, P. Adamson, A.Gerst, A. Niilisk „Monitoring of atomic layer deposition by incremental dielectric reflection“, Appl. Surf. Sci. 107 (1996) 178

PHOTOINDUCED MASS TRANSPORT IN AZO-BENZENE CONTAINING COMPOUNDS

K. Klismeta, J.Teteris
Institute of solid State Physics, University of Latvia, LV-1063 Riga, Latvia
e-mail: k.klismeta@gmail.com

The photoinduced changes of optical properties in azobenzene containing compound solution layers and thin films were studied under influence of polarized and non-polarized 532 nm laser light.

Under influence of non-polarized light azo compounds experience *trans-cis* isomerisation process, that can be observed in the absorbance spectrum of the sample. If the light is linearly polarized, molecules align perpendicularly to the electric field vector and as a result photoinduced dichroism and birefringence is obtained. If a lateral polarization modulation of a light beam is present, a mass transport of the azo-benzene containing compound occurs. By studying the absorbance of used wavelength, concentration distribution in the solution and the direction of mass transport can be determined.

The mechanism of mass transport based on photoinduced dielectrophoretic phenomenon has been discussed. The studies of this work show that direct holographic recording of surface relief gratings can be used in optoelectronics, telecommunications and data storage [1, 2].

References

1. N. K. Viswanathan, D. Y. Kim, S. Bian, J. Williams, W. Liu, L. Li, L. Samuelson, J. Kumara, S. K. Tripathy *Surface relief structures on azo polymer films,* Journal of Materials chemistry, 1999, No. 9, 1941-1955 p.
2. R.H, El Halabieh, O. Mermut, C.J. Barett *Using light to control physical properties of polymers and surfaces with azobenzene chromophores* Pure and Applied Chemistry, 2004, Vol. 76, 1445-1465 p.

MODELLING OF CRUST THICKNESS FOR SILICON PURIFYING PROCESS WITH ELECTRON BEAM

Kirils Surovovs[1], Kristaps Bergfelds[2], Andris Muiznieks[2], Armands Krauze[2], Matiss Plate[2], Georgijs Chikvaidze[1]

[1]*Institute of solid State Physics, University of Latvia,*

[2]*Faculty of Physics and Mathematics, University of Latvia*

e-mail: ks10172@lu.lv

One possibility of purification of metallurgical grade silicon for photovoltaic needs is the melting of polycrystalline silicon in a copper crucible by an electron beam (see Fig.1). High overheating temperatures (about 1000 K) ensure effective evaporation of some impurities [1]. Crucible wall is water-cooled which creates a solid silicon layer, i.e., crust, on the crucible wall.

The melt flow is calculated in 3D numerically and obtained heat flux densities (see Fig.2) at crust boundary are used to analyse crust thickness. Influence of different crucible materials and different ways of cooling is investigated (see Fig.3).

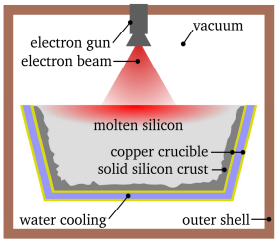

Fig.1 Scheme of considered system

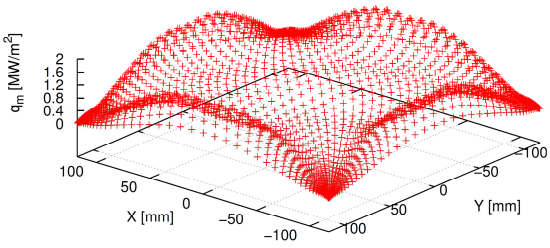

Fig.2 Heat flux density distribution along the bottom surface of the melt.

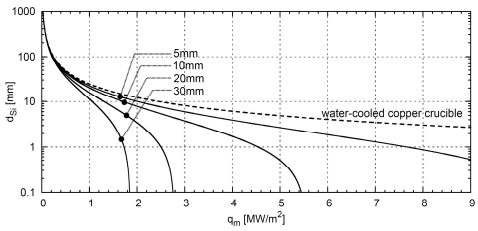

Fig.3 Solid silicon crust thickness in case of water-cooled graphite crucible.

Acknowledgements

The present work has been supported by the European Regional Development Fund project No. 2010/0245/2DP/2.1.1.1.0/10/APIA/VIAA/114

References

1. Kazuhiro Hanazawa, Noriyoshi Yuge, Yoshiei Kato, Materials Transactions, 45(3):844–849, 2004.

2. A. Krauze, A. Muiznieks, K. Bergfelds, K. Janisels, G. Chikvaidze, Magnetohydrodynamics, 47(4):369–383, 2011.

TRIPHENYLPENTANE SUBSTITUENTS CONTAINING MOLECULAR GLASSES WITH NONLINEAR OPTICAL ACTIVITY

Kaspars Traskovskis[1], Andrejs Tokmakovs[2], Valdis Kokars[1], Martins Rutkis[2]

[1]*Institute of Applied Chemistry, Riga Technical University, Latvia*

[2]*Institute of Solid State Physics, University of Latvia, Latvia*

e-mail: kaspars.traskovskis@rtu.lv

Molecular organic glasses, the compound class where amorphous glassy state is formed by relatively small molecules without the presence of plasticizers has many potential applications as optical materials. Incorporation of donor-(π electron bridge)-acceptor type chromophores in such compounds and achieving non-centrosymmetrical molecular order by external electric field polling allows to obtain materials with nonlinear optical (NLO) activity. Our group has successfully developed NLO materials where amorphous phase stability of molecular compounds is ensured by incorporation of triphenyl substituents [1].

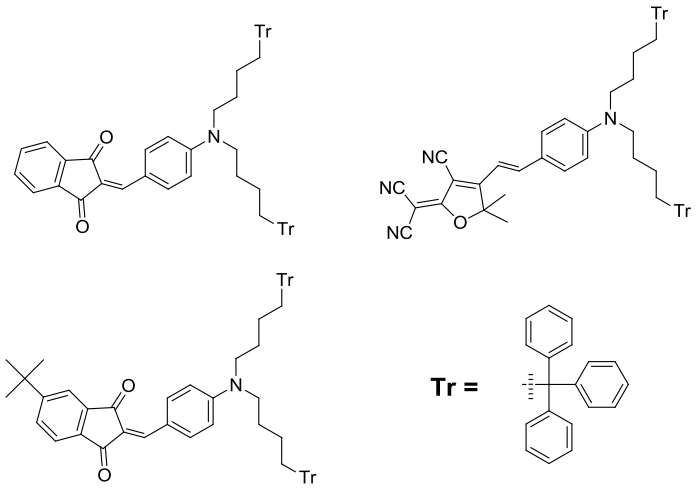

Fig.1 Chemical structures of synthesized NLO active molecular compounds

Here we present the improved design of mentioned materials where we increased the chemical stability of compounds by replacing labile triphenyl-oxygen bound with C-C bound. Chromophores containing indanedione or tricyanofuranyl acceptors have been synthesized (Fig. 1). Compound synthesis, chemical characterization and experimentally obtained linear and nonlinear optical properties of materials will be presented.

References

1. K. Traskovskis , I. Mihailovs , A. Tokmakovs , A. Jurgis , V. Kokars, M. Rutkis, *J. Mater. Chem*., 2012, No.22, 11268-11276.

CHARGE CARRIER MOBILITY IN THIN FILMS OF GLASS FORMING LOW MOLECULAR ORGANIC COMPOUNDS

Kaspars Pudzs, Aivars Vembris
Institute of solid State Physics, University of Latvia,
e-mail: kaspars.pudzs@cfi.lu.lv

One of the easiest thin film processing methods is solution casting. Therefore, compounds that form amorphous structure from solution are perspective in optoelectronic devices. Especially low molecular weight organic compounds should be mentioned due to their repeatable synthesis. Electrical properties of organic compounds are important in such devices. This leads to the necessity to study charge carrier mobility which is one of the key parameter that characterizes electrical properties. Unfortunately, often dispersive charge carrier transport in thin amorphous film has been observed, which makes it difficult to determine charge carrier mobility.

In this work charge carrier mobility in “sandwich” type samples consisting of thin film of glass forming low molecular compound for example indandione or pyranyliden derivatives as an active layer between ITO as bottom and semi-transparent Al as top electrode were studied. The organic thin films were made by spin-coating or blade casting method from chloroform solution with the thickness of 0.4 to 4 μm. Current voltage characteristics were analysed before charge carrier mobility measurements to define the ohmic region in the sample and to avoid space charge limited current effekts on mobility measurement. Charge carrier mobility at various electrical fields was determined by carrier extraction by linearly increasing voltage (CELIV), photo-CELIV and Time of Flight (ToF) methods. Thin (~30 nm) FePc or Se charge generation layer between electrode and organic film was used for the compounds which absorbtion or charge generation was very low. Mobility measurements were made in air condition. Application limits and possible solutions of charge carrier mobility determination methods for investigated compounds will be discussed.

Acknowledgment:

This work has been supported by Latvian State Research Programm No.2 in Materials Sciences and Information Technologies and ERAF project Nr. 2010/0204/2DP/2.1.1.2.0/10/APIA/VIAA/010.

REFLECTANCE AND MULTISPECTRAL EVALUATION OF COLOR VISION ASESSMENT PLATES

Kaiva Luse[1], Maris Ozolinsh[1,2], Sergejs Fomins[2]

[1]*Optometry and vision science dept., University of Latvia,*

[2] *Institute of solid State Physics, University of Latvia.*

e-mail: kaiva.luse@gmail.com

Previous work has resulted in the creation of a set of 24 pseudoisochromatic plates for the assessment of red-green color vision deficiencies. The design of the experiment for acquiring corresponding pairs of achromatic and chromatic color matches is described earlier [1]. For printing of the tests a calibrated *Canon PIXMA mp550* inkjet photo printer on glossy photo paper was used.

The scope of the study is to (1) evaluate the distance of the acquired chromatic values of the test stimuli to corresponding confusion lines for each type of deficiency and to compare to those values of tests used in clinical practice, (2) evaluate the spread of the chromatic values induced by printing method, (3) model the vision perception in terms of cone signals and thus predicting the outcome perception in case of deficiency.

Reflectance measurements with the halogen bulb irradiance spectrum was measured with Ocean Optics USB400-VIS-NIR spectrometer through the calibrated Ocean Optics optical fiber (Color temperature ~ 4000K) and multispectral imagery (by tunable liquid crystal filters system *CRI Nuance Vis 07*) data analysis show that:

1) printing quality in terms of color dispersion for printing methods used is much smaller than in case of commercially available color vision deficiency tests.

2) the distance from the confusion lines in case of all stimuli was less than 0.02 units (x,y) in CIE xy color diagram.

Results for cone signals and analysis in case of tests used in clinical practice are in process.

Acknowledgments:

This work has been supported by the European Social Fund within the project «Support for Doctoral Studies at University of Latvia».

References

1. Luse, K., Fomins, S., Ozolinsh, M. *IOP Conf.Series: Materials Scienceand Engineering*, 38, 2012, p. 2 – 4

EFFECT OF TITANIUM(IV)ISOPROPOXIDE AND ACETYLACETONE MOLAR RATIO IN THE SOLUTION ON SPRAY DEPOSITED TiO_2 FILMS

Ilona Oja Acik[1], Malle Krunks[1], Arvo Mere[1], Kairi Otto[1], Valdek Mikli[2]

[1]Department of Materials Science, Tallinn University of Technology, Estonia, [2]Centre for Materials Research, Tallinn University of Technology, Estonia

e-mail: kairi.otto@gmail.com

TiO_2 thin films have numerous applications, they have been used for example in solar cells [1], photocatalyst [2] and gas sensor [3] devices. TiO_2 thin films were prepared by the sol-gel method using chemical spray pyrolysis technique. The spray solution contained of titatium(IV)isopropoxide (TTIP) and acetylacetone (acacH) in ethanol at Ti^{4+} concentration of 0.2M. The TTIP:acacH molar ratio in the spray solution was varied from 1:1, 1:2, 1:3 to 1:4. The films were deposited onto Si (100) and borosilicate glass substrates at substrate temperatures of 260°C and 450°C using pulsed spray solution feed. As-deposited films were subjected to annealing at 500°C and 700°C for 30 minutes. The structural development of the TiO_2 films was studied as a function of TTIP:acacH molar ratio in the solution. The films were characterized by Raman, UV-VIS, FT-IR and AFM measurements. According to Raman measurements, as-deposited films at 260°C and 450°C were amorphous, independent on the TTIP:acacH molar ratio in the solution. Anatase to rutile phase transformation temperature depends on the film deposition temperature and the TTIP:acacH molar ratio in the spray solution. The films deposited from the solution with TTIP:acacH=1:4 indicated smooth surface whereas a porous structure was observed when the solution of TTIP:acacH=1:1 was sprayed. The TiO_2 film thickness increased with the TTIP:acacH molar ratio in the spray solution.

References

1. I.Oja Acik, A.Katerski, A.Mere, J.Aarik, A.Aidla, T.Dedova, M.Krunks, *Thin Solid Films*, 2009, No.517, 2443-2447.

2. O.Carp, C.L.Huisman, A.Reller, *Progr. Solid State Chem*., 2004, No.32, 33-177.

3. V.Kiisk, M.Šavel, V.Reedo, A.Lukner, I.Sildos, *Phys. Proc*., 2009, No.2, 527-538.

INFLUENCE OF COMPRESSIVE STRESS ON DIELECTRIC AND FERROELECTRIC PROPERTIES OF THE $(Na_{0.5}Bi_{0.5})_{0.7}Sr_{0.3}TiO_3$ CERAMIC

J.Suchanicz[1,*], G.Klimkowski[1], M.Karpierz[1], U.Lewczuk[1], I.Faszczowy[1], A.Pękala[1], K.Konieczny[1], M.Antonova[2], A.Sternberg[2]

[1]*Institute of Physics, Pedagogical University, 30-084 Krakow, Poland*
[2]*Institute of Solid State Physics, University of Latvia, LV-1063 Riga, Latvia*

Good quality lead-free ceramic of $(Na_{0.5}Bi_{0.5})_{0.7}Sr_{0.3}TiO_3$ have been produced by a solid phase sintering process at 1200°C. X-ray diffraction and Raman spectroscopy studies show that obtained samples possess perovskite structure. The micrograph of the fractured surface showed a dense structure ceramics, in a good agreement with 96% relative density determined by the Archimedes method. The dependence of dielectric and ferroelectric properties on the uniaxial pressure (0-1500 bar) of this ceramic was investigated revealing significant influences of the external stress on these properties. This includes a shift of the phase transition, a diffuseness of the permittivity characteristics, increase of the thermal hysteresis and a decrease of polarization. We have shown that $(Na_{0.5}Bi_{0.5})_{0.7}Sr_{0.3}TiO_3$ ceramic is capable of sustaining large compressive stress without any mechanical degradation. The electrostrictive coefficient Q_{11} and differential permittivity were evaluated from obtained data. We discuss our results based on hardening of the soft-mode and domain switching processes under the action of pressure. The $(Na_{0.5}Bi_{0.5})_{0.7}Sr_{0.3}TiO_3$ ceramic is expected to be a new promising candidate for lead-free electronic material.

THE EFFECT OF ANNEALING ON SPECTRA AND DECAY TIME OF X-RAY LUMINESCENCE OF ZINC OXIDE POWDERS

K. Chernenko[1], O. Klimova[1], E. Gorokhova[2], P. Rodnyi[1]

[1]*Saint-Petersburg State Polytechnical University,* [2] *Research and technological institute of optical materials all-russia scientific center "S.I. Vavilov State Optical Institute"*

e-mail: nuclearphys@yandex.ru

Zinc oxide (ZnO) is a direct wide band gap (3.37 eV) semiconductor material with a large exciton binding energy (60 meV). It gained significant attention motivated by potential applications as an oxide electronic material, and in optoelectronic and lighting applications. Luminescence of ZnO, generally, has two bands: near band edge luminescence (NBEL), ascribed to excitons, and green luminescence (GL). The origin of the GL is still a matter of debates, despite a great number of studies. In most cases it is attributed to zinc or oxygen vacancies. Some authors assume that GL can be connected to both defects. By applying different annealing atmospheres one can indicate if an increase/decrease in the concentration of a specific intrinsic defect is correlated with the GL properties. In this work, we present the effect of vacuum and air annealing on intensity and decay time luminescence changes, and a shift of the emission, of the studied ZnO powders.

Chemical purity powder #1 (99.5%, Russia) and high purity powder #2 (99.999%, USA) were used. Annealing was performed at 800÷1050°C in vacuum and air for 2 h. After vacuum annealing GL maximum of powder #1 is around 513 nm and intensities of GL are about 10 (for 800°C) and 20 (for 1050°C) times greater than the initial one. Decay time curves of powders are well approximated by two exponential decay functions. For powder annealed at 800°C decay constants are τ_1=126 ns, τ_2≈1.6 μs and amplitudes ratio is I_1/I_2=1.88. For powder annealed at 1050°C decay constants are τ_1=128 ns, τ_2≈1.2 μs and amplitudes ratio is I_1/I_2=2.18. GL maximum of air annealed powders is around 525 nm and intensity is 5 times greater than the initial one. Decay time curves of air annealed powders are identical and can be roughly approximated by two exponential decay functions with decay constants τ_1=48 ns, τ_2≈4.5 μs and amplitudes ratio I_1/I_2=4.48. Annealing of powder #2 in vacuum has completely different result: intensity of NBEL grows up towards to GL ones, but complete intensity of luminescence didn't change significantly. Maximum of GL is at 510 nm. Air annealing provides result completely the same to powder #1. We assume that such results come from uncontrolled trivalent impurity.

Physical processes behind the obtained results will be discussed in report.

PHOTOREFRACTIVE LIGHT SCATTERING IN $LiNbO_3$:B, $LiNbO_3$:Y, $LiNbO_3$:Y:Mg, AND $LiNbO_3$:Ta:Mg CRYSTALS

N.V. Sidorov[1], A.V. Syuy[2], A.A. Janichev[1], A.A. Gabayn[1], M.N. Palatnikov[1], A.A. Kruk[1], and K. Bormanis[3]

[1]*Institute of Chemistry, Kola Science Centre RAS, Russia*

[2] *Far Eastern State Transport University, Khabarovsc, Russia*

[3]*Institute of Solid State Physics, University of Latvia, Latvia*

E-mail: bormanis@cfi.lu.lv

Lithium niobate ($LiNbO_3$) single crystals of low photo-refractivity, prospective materials for transformation and generation of laser radiation, can be grown from congruent melt (R = Li/Nb = 0.946) containing admixture of inactive photovoltaic cations (Mg^{2+}, Zn^{2+}, Gd^{3+}, B^{3+}, and some other) maintaining charge under illumination. Optically resistant $LiNbO_3$ crystals of negligible photo-refraction modified by coupled admixtures are of practical interest. Such crystals would be efficient used as inverters of the wave front, for transformation of radiation and generating harmonics in lasers.

Reported in the paper are results of studies of the photo-refractive (photo-induced) light scattering (FRLS) in single crystals of lithium niobate modified by Mg^{2+}, B^{3+}, Y^{3+}, and Ta^{5+} cations. Only circular light scattering is present in congruent crystals the FRLS being absent. Admixtures are found to suppress photo-refraction. Coupled (Mg^{2+} and Y^{3+}) and (Mg^{2+} and Ta^{5+}) admixtures suppress photo-refraction by partial autofocusing of the radiation during illumination. The speckle pattern of FRLS and dynamics of its evolvement depending on the intensity of the exciting radiation are affected by the kind of the inactive admixtures. In the case of B^{2+}, Ta^{5+}, and Y^{3+} the scattering indicatrix practically retains its shape. Any changes in the speckle pattern being completely absent is characteristic to the $LiNbO_3$:B (0.12 % mass) crystal confirming earlier data on reducing photo-refraction in lithium niobate crystals by admixture of B^{3+} cations. Another evidence supporting the same conclusion is the absence of Raman bands prohibited by selection rules in the spectra of the $LiNbO_3$:B (0.12 % mass) single crystals.

FERROELECTRIC LEAD NICKEL-NIOBIUM TITANATE CERAMICS: PHASE TRANSITION STUDIES

K. Bormanis [1], S.N. Kallaev[2], Z.V. Omarov[2], R.G. Mitarov[3],
S.A. Sadykov[2], A.R. Bilalov[2], and A. Kalvane[1]

[1] *Institute of Solid State Physics, University of Latvia, Riga, Latvia*

[2] *Institute of Physics, Dagestan Science Centre, RAS, Makhachkala, Russia*

[3] *Dagestan State Technical University, Makhachkala, Russia*

E-mail: bormanis@cfi.lu.lv

The multi-component mixed perovskites of extraordinary crystal structure and unique properties, an enormous dielectric permittivity, strong piezoelectricity and electrostriction in particular, for decades have been of increasing interest. The $PbNi_{1/3}Nb_{2/3}O_3$ – $PbTiO_3$ (PNN-PT) solid solution system is one of mixed ferroelectric relaxors.

The presented study is focused on heat capacity and dielectric properties of the $0.7PbNi_{1/3}Nb_{2/3}O_3$ – $0.3PbTiO_3$ solid solution ferroelectric ceramics within the 120 – 800 K range of temperature. The PNN-PT samples were obtained by conventional ceramics technology.

Results of measurements of dielectric permittivity ε(T) show the broaden region of phase transition. Dispersion of the dielectric permittivity peak value ε_m specific to ferroelectric relaxors is observed in case of the $0.7PbNi_{1/3}Nb_{2/3}O_3$–$0.3PbTiO_3$ compound.

Broad anomalies on the curve of heat capacity are revealed in the 250 – 450 K and 450 – 650 K intervals and a λ-anomaly at T≈ 225 K. An anomaly on the $C_p(T)$ curve specific to phase transition is found at T = 520 K.

The obtained results and available reported data allow to assume that randomly distributed polarised nano-size formations of rhombohedric structure emerge within the nonpolar cubic phase of $0.7PbNi_{1/3}Nb_{2/3}O_3$ – $0.3PbTiO_3$ at cooling upon reaching the Burns temperature T_d≈650 K while macroscopic polarisation in samples is absent as far down as to the room temperature. The anomalous behaviour of heat capacity $C_p(T)$ characteristic to relaxors within the range of 250 – 650 K is related to changes and interactions in the system of reorienting nano-size polar units.

The anomalous component of heat capacity in the range of phase transition was found as the difference between the measured value and calculated phonon heat capacity. The features of the dependence of heat capacity and its anomalous part on temperature in $0.7PbNi_{1/3}Nb_{2/3}O_3$ – $0.3PbTiO_3$ indicate to absence of a thermodynamic phase transition within the range of dielectric permittivity maximum.

EFFECTS OF ILLUMINATION ON THE DIELECTRIC RESPONSE OF BARIUM-STRONTIUM NIOBATE CERAMICS

K. Bormanis[1], A.I. Burkhanov[2], Luu Thi Nhan[3], S.V. Mednikov[3], and M. Antonova[1]

[1] Institute of Solid State Physics, University of Latvia, Riga, LV-1063, Latvia

[2] Volgograd State Architectural and Engineering University, Volgograd, Russia

[3] Volgograd State Technical University, Volgograd, Russia

E-mail: bormanis@cfi.lu.lv

A study of the low- and infra-low frequency relaxation in the SBN-75 ceramics under white irradiation is reported. Effective dielectric permittivity $\varepsilon'_{\text{eff}}(E)$ and dielectric loss $\varepsilon''_{\text{eff}}(E)$, $tg\delta_{\text{eff}}$ are determined from measurements performed on a modified Sawyer-Tower circuit of polarisation loops at frequencies of 0.1, 1.0, and 10 Hz and different field intensities E. Anomalies on the $\varepsilon'_{\text{eff}}(E)$ and $\varepsilon''_{\text{eff}}(E)$ curves of SBN-75 (Fig. 1) are observed before and after illumination.

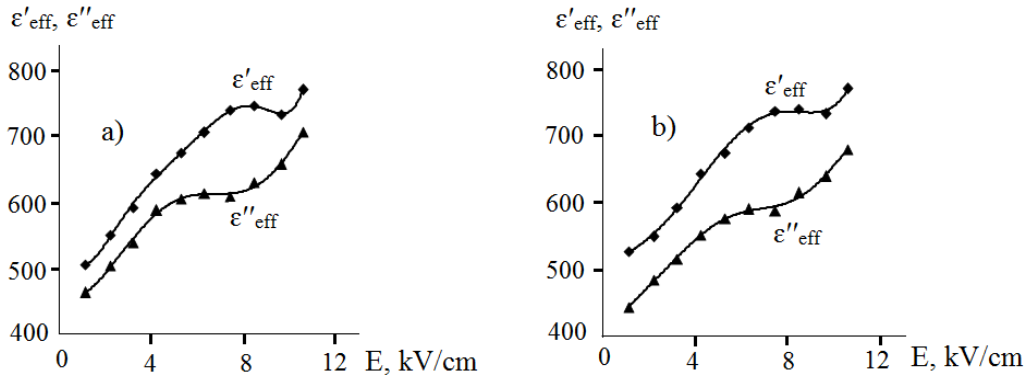

Fig. 1. Dependence on field intensity of $\varepsilon'_{\text{eff}}(E)$ and $\varepsilon''_{\text{eff}}(E)$ at frequency 0.1 Hz and T = 62 ˚C: a – non-irradiated SBN-75 sample, b – irradiated SBN-75 sample.

Effective parameters $tg\delta_{\text{eff}}(E), \varepsilon'_{\text{eff}}$, and $\varepsilon''_{\text{eff}}$ obtained from polarisation loops before and after irradiation at frequencies below 10 Hz, the interval representative of relaxation of polarisation in the relaxor phase of the SBN-75 ceramics, show that irradiation mainly causes some decrease of the values of $tg\delta_{eff}$ and $\varepsilon''_{\text{eff}}$.

Most likely the anomalies are due to relaxation of the space charge. Irradiation is shown to reduce the contribution of space charge at temperatures (i.e., near T_m) corresponding to the range of the relaxor phase. The decrease of dielectric loss at irradiation of the SBN-75 ceramics points to rise of unbalanced carriers compensating the space charge in the material.

UP-CONVERSION LUMINESCENCE OF $NaLaF_4$ DOPED WITH Tm^{3+} AND Yb^{3+}

Jurgis Grube, Guna Doke, Anatolijs Sarakovskis, Maris Springis

Institute of Solid State Physics, University of Latvia

e-mail: Jurgis.Grube@cfi.lu.lv

Our previous studies have showed that $NaLaF_4$ doped with rare-earth elements is a perspective material for up-conversion luminescence [1]. It is possible to obtain up-conversion luminescence in a wide spectral region (red, blue, UV) using this material doped with Tm^{3+} and Yb^{3+}.

Therefore polycrystalline $NaLaF_4$ doped with Tm^{3+} and Yb^{3+} ions was synthesized. An intensive blue up-conversion luminescence under 980nm excitation was observed in these samples. When the samples were treated in different ways, for example grinding or deposited on a substrate using laser ablation technique, we could achieve also relative intensive ultraviolet up-conversion luminescence (Fig. 1).

Based on the experimental results peculiarities of different processes which take place in $NaLaF_4$:Tm^{3+},Yb^{3+} ions will be discussed.

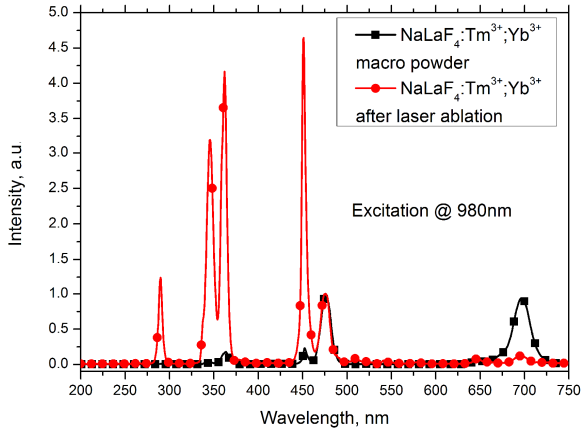

Fig.1 Up-conversion luminescence spectra for $NaLaF_4$ doped with Tm^{3+} (2mol%) and Yb^{3+} (20mol%) as macro powder and after laser ablation, excitation at 980nm. Spectra are normalized to 480nm up-conversion luminescence band

Acknowledgements:

The financial support of State Research Program IMIS (project 1), ERDF project 2010/0204/2DP/2.1.1.2.0/10/APIA/VIAA/010 and ESF project 2009/0138/1DP/1.1.2.1.2/09/IPIA/VIAA/004 is highly appreciated.

References

1. A. Sarakovskis, J. Grube, A. Mishnev, M. Springis, Optical Materials **31**, 1517-1524 (2009)

PHOTOELECTRICAL PROPERTIES OF DMABI DERIVATIVES AS MATERIALS FOR SOLAR CELLS

Janis Latvels[1], Raitis Grzibovskis[1], Dagnija Blumberga[2], Ilze Maderniece[2]

[1]Institute of Solid State Physics, University of Latvia, [2]Institute of Energy Systems and Environment, Riga Technical University

e-mail: janis.latvels@gmail.com

Increasing demand of energy gives rise to search for new and perspective energy sources. The innovative solution is solar energy obtained using organic materials. The advantages of organic materials are lower costs, easy processing and a wide range of materials which cover broad spectral range.

In this work N,N'-dimetilaminobenziliden-1,3-indandione (DMABI) and seven its derivatives were investigated. The molecule N,N'-dimetilaminobenziliden-1,3-indandione (DMABI) forms the base of these materials. 1,3-indandione works as an electron acceptor while dimetilaminobenzene as an electron donor. Exciton is formed by photoinduced electron transfer between electron donor and acceptor parts.

DMABI and its derivatives represent the class of photosensitive molecular crystals. The photocurrent efficiency for DMABI is 10^{-2} el/phot. Derivatives with various functional groups were selected in order to improve energetic parameters and photoelectrical properties.

The knowledge of energetic parameters of materials are fundamental to design solar cells. An ionization potential and energy gap directly affect such important electronic processes as charge carrier generation and transport. In order to characterize energy structure several parameters were determined- an optical energy gap E_{GOpt}, a threshold energy of quantum efficiency of photoconductivity E_{th}, a difference between oxidation and reduction potential (U_{redox}).

The very first results of efficiency of organic solar cells containing DMABI molecules will be discussed.

This work has been supported by the European Social Fund within the project «Support for Doctoral Studies at University of Latvia».

ROLE OF DIFFUSION IN FORMATION AND PROPERTIES OF SOL-GEL MICRO-STRUCTURES

Jakob Jõgi[1], Martin Järvekülg[1], Aigi Salundi[1], Marko Part[1], Kelli Hanschmidt[1], Tanel Tätte[1], Alexey Romanov[1], Jaan Kalda[2], Ants Lõhmus[1]

[1]Institute of Physics, University of Tartu, [2]Institute of Cybernetics, Tallinn University of Technology

e-mail: jakob27@fi.tartu.ee

Low-dimensional IVB group metal oxide materials produced using the sol-gel method are of great interest due to the possible applications in biotechnology, photocatalysis, electronics, high-temperature isolation and solar cells industry. The elaboration of different strategies for the synthesis of micro- and nanoscale oxide materials is essential for improving the properties and finding new applications for these materials.

We have previously reported tubular micro-structures obtained by spontaneous rolling of gel film segments formed by cracking and fragmentation of the film on highly viscous substrate [1,2]; and micro-tubes obtained by direct pulling from viscous precursor followed by solidification of the jets [3].

The purpose of current work is to elaborate the mathematical aspects of diffusion-limited formation and properties of sol-gel micro-structures. Formulas for diffusion in a plane and for cylindrical geometries are presented and compared with each other and with experimental results.

References

1. J. Jõgi, M. Järvekülg, J. Kalda, A. Salundi, V. Reedo, A Lõhmus, Europhys. Lett., 2011, 95(6), 64005-p1 - 64005-p6.

2. M. Järvekülg, R. Välbe, J. Jõgi, A. Salundi, T. Kangur, V. Reedo, J. Kalda, U. Mäeorg, A. Lõhmus, A. E. Romanov, Phys. Status Solidi A, 2012, 209(12), 2481 - 2486.

3. M. Part, K. Riikjärv, K. Hanschmidt, A. Tamm, H. Mändar, G. Nurk, K. Kukli, T. Tätte, Trends in Nanotechnology International Conference (TNT2012), 2012.

PO-136

LATTICE DYNAMICS OF $CdWO_4$

J.Gabrusenoks

Institute of Solid State Physics, University of Latvia

e-mail: gabrusen@latnet.lv

The first-principle calculations are emploed to study lattice dynamics of cadmium tungstate. The equilibrium structure of wolframite-type crystal and lattice vibrations were calculated within the density functional theory using CRYSTAL09 program. Calculated phonon frequencies 8Ag+10Bg+7Au+8Bu in Γ point are compared with experimental Raman and IR spectra. Also symmetrie of the Raman and IR vibrations are discused.

THERMALLY AND OPTICALLY STIMULATED LUMINESCENCE IN LI2B4O7 DOPED WITH METAL IONS

I. Romet[1], G. Corradi[2], M. Danilkin[3], M. Kerikmäe[3], A. Kotlov[4], V. Nagirnyi[1], V. Seeman[1]

[1] Institute of Physics, University of Tartu, Estonia, [2]Institute for Solid State Physics and Optics, Wigner Research Centre for Physics, Hungary, [3]Institute of Chemistry, University of Tartu, Estonia, [4]DESY, Hamburg, Germany

e-mail of presenting author: Ivo.Romet@ut.ee

Lithium tetraborate ($Li_2B_4O_7$ or LTB) has been recognized as a promising tissue-equivalent material for thermoluminescent dosimetry suitable in particular for neutron detection. Doped with multiple impurities Cu, Ag, P it demonstrates an outstanding sensitivity exceeding that of the well-known LiF:Mg,Ti [1]. We substituted phosphorus impurity for more convenient Mn^{2+} or Be^{2+}, and studied the role of particular impurities in recombination luminescence relevant for dosimetry. The results of a study of LTB:Cu,Mn, LTB:Cu,Be, LTB:Ag,Mn, and LTB:Ag,Be ceramics using a wide range of spectroscopic methods are presented. Excitation and emission spectra of the samples excited by synchrotron radiation were measured at the SUPERLUMI station of HASYLAB at DESY, Germany. X-ray excited luminescence, cathodoluminescence (CL), and thermostimulated luminescence (TSL) curves and TSL spectra were studied in the range of 5-600 K. The low-temperature X-ray excited luminescence and CL spectra of the samples studied are represented by complex broad bands. None of the impurity emission bands except that of Mn^{2+} can be explicitly distinguished in these spectra. Low-temperature TSL peaks near 80 K are mainly presented by the emission bands of impurity-perturbed excitons. High-temperature TSL peaks in the region of 330-540 K have impurity-related origin. The hole trapping in the boron-oxide framework is shown to play a crucial role in increasing the TSL efficiency. Mn^{2+} and Be^{2+} may substitute either for Li^+ or B^{3+} ions, thus forming both electron and hole traps at the substitution sites [2]. Cu^+, Ag^+, and Mn^{2+} ions can play the role of efficient recombination centres. Charge carrier recombinations near Mn^{2+} or at Cu^+ and Ag^+ ions result in the emission at 2.03, 3.35 and 4.6 eV, respectively. Such a well-separated structure of optical spectra provides a powerful tool for distinguishing electron and hole processes in an irradiated material.

References

1. M. Prokic. Radiat. Prot. Dosim., 2002, 100, 265–268.
2. M. Danilkin et al., Radiat. Meas., 2010, 45, 562-565.

THE EFFECT OF RADIATION MODIFICATION ON PROPERTIES OF POLY(ETHYLENE-1-OCTENE) MAGNETIC NANOCOMPOSITES

Ingars Reinholds[1], Valdis Kalkis[1], Janis Zicans[2], Remo Merijs-Meri[2], Agnese Grigalovica[2]

[1]Faculty of Chemistry, University of Latvia, [2]Institute of Polymer Materials, Riga Technical University

e-mail of presenting author: ingars.reinholds@lu.lv

Magnetic elastomer composites of selected poly(ethylene-1-octene) copolymers (POEs) filled with different content (up to 10 wt.%) of zinc-nickel ferrite nanoparticles have been made. The composites have been irradiated with ionising radiation (accelerated electrons) up to irradiation doses equal to 100, 300 and 500 kGy.

POE copolymers belong to a relatively new class of ethylene elastomers with high flexibility, rubber like mechanical properties and a processability of thermoplastics. Radiation or chemically cross-linked POEs are suitable for formation of heat shrinkable materials [1]. These properties are highly dependent on the content of flexible 1-octene chains in copolymer.

Stress-strain and structural properties of radiation modified composites with POEs with different content (17 and 38 wt.%) of 1-octene filled with ferrite nanoparticles have been researched.

Thermomechanical properties – thermorelaxation stresses formed in thermal heating and the thermo residual stresses resulting in the process full setting and cooling of materials – have been investigated for orientated up to 100-300 % specimens. It was found that gel content increases up to 85% with increased radiation dose up to 500 kGy due to the formation of cross-linked structures. That coincides with increased thermomechanical characteristics, which increased with decrease of the content of 1-octene content in POEs. Formation of cross-linked structures in the electron beam irradiated samples was confirmed also by the investigation of specimens with FTIR and DSC methods. Improvement of the strength properties (increase of stiffness, tensile and residual stresses) was observed with increase of the filler content in composites.

References

1. J. K. Mishra,Y. W. Chang, B. C. Lee, S. H. Ryu, *Rad. Phys. Chem.*, 2008, No.77, 675-679.

BROADBAND DIELECTRIC INVESTIGATION OF $(Sr_{1-1.5x}Bi_x)TiO_3$ (x=0.15, 0.1, 0.05)

Ieva Kranauskaitė[1], Maksim Ivanov[1], Šarūnas Bagdzevičius[1], Karlis Bormanis[2], Jūras Banys[1]

[1]*Faculty of Physic, Vilnius University, Sauletekis str. 9/3, 10222 Vilnius, Lithuania*

[2]*Institute of Solid State Physic, University of Latvia, Kengaraga str. 8, 1063 Riga, Latvia*

e-mail of presenting author: i.kranauskaite@yahoo.com

Lead containing piezoelectric ceramics and single crystals as $Pb(Zr_xTi_{1-x})O_3$ (PZT) or (1-x)$[Pb(Mg_{1/3}Nb_{2/3})O_3]$-x$[PbTiO_3]$ (PMN-PT) are widely used as actuator, transducer, and sensor materials. However, the toxicity of lead has led to a demand for alternative materials that are more human and environment friendly. $(Sr_{1-1.5x}Bi_x)TiO_3$ - strontium bismuth titanate (SBT for short) is one of such compounds.

It is well known that in pure incipient ferroelectrics, like $KTaO_3$ or $SrTiO_3$ polar phonons are responsible for the dielectric permittivity and no pronounced dielectric dispersion is observed below the soft-mode response [1]. The ferroelectricity in such materials can be induced by application of strong enough electric field, uniaxial stress or substitution of A-site ions by isovalent or heterovalent ions. The broadband dielectric studies on SBT ceramic (up to $x \leq 0.17$) [2, 3] showed that Bi doping induces formation of local antiferrodistortive and polar regions. This causes a complex relaxational dynamic below the phonon frequency range. The aim of this work was to extend the investigations of dielectric dispersion and calculate the relaxation distribution function.

The dielectric properties of SBT ceramic have been investigated from 20 mHz to 30 GHz in wide temperature range. Obtained results showed the pronounced dielectric dispersion which looks similar to the one typically observed in disordered materials. In contrast to the proposals in [2], which claimed that the dispersion in SBT ceramic looks relaxor-like, we have to point its close similarity to the dispersion typically found in dipolar glasses. The calculated distribution of relaxation times $f(\tau)$ confirms our findings because no splitting into two parts of $f(\tau)$ can be seen.

[1] K.A. Muller and H. Burkard, Phys. Rev. B. 19, 3593 (1979).

[2] V. Porokhonskyy et.al. Phys. Rev. B. 69, 144104 (2004).

[3] Ang Chen, Yu. Zhi, J. Hemberger, P. Lunkenheimer, and A. Loidl, Phys. Rev. B 59, 6665 (1999).

ELECTRONIC EXCITATIONS AND SELF-TRAPPING OF ELECTRONS IN $CASO_4$

I. Kudryavtseva[1], M. Klopov[2], A. Lushchik[1], Ch. Lushchik[1] and A. Pishtshev[1]

[1]*Institute of Physics, University of Tartu,* [2]*Tallinn University of Technology, Estonia*

e-mail of presenting author:irina.kudrjavtseva@ut.ee

In many wide-gap materials, self-trapped (ST) *p*-type holes were revealed long ago. In Sc_2O_3 with empty 3*d* electron shell of unexcited Sc^{3+}, the possibility of ST 3*d*-electrons was suggested and then experimentally proved under low-temperature excitation [1]. A search for ST electrons in materials containing Ca^{2+} cations with similar electron structure was started long ago as well. Recent comparative first-principles studies have examined the role calcium *3d* empty electronic states play in structural energetics and bonding of Ca-containing crystalline systems [2]. In the case of $CaSO_4$, more detail DFT calculations performed within PBE0-based hybrid functional scheme have given the value of the fundamental energy gap of about 9.6 eV, and demonstrated in terms of electronic orbitals the principal feature of the band structure – the presence of the significant contribution of Ca *3d*-states into the lower part of the conduction band (which in turn can be filled in via allowed dipole O *2p* $\rightarrow$ Ca *3d* transitions). A complex peak of thermostimulated luminescence (TSL) at 45–65 K, which can be efficiently induced by the irradiation with photons of $h\nu > 10$ eV, was detected in extra pure or doped $CaSO_4$ (anhydrite) and tentatively dicribed as unfreezing of ST electrons [3]. It is worth noting that thermally stimulated hopping diffusion of ST electrons occurs with extremely low frequency factor (~10), i.e. 12 orders of magnitude lower than it is typical of diffusion of self-trapped *p*-holes along [110] anion rows in alkali halides. The calculated electronic structure is compared with the experimental spectra of reflection, excitation of several emissions and phosphorescence, as well as with the creation spectra of TSL peaks.

References

1. Ch. Lushchik, I. Kuusmann, V. Plekhanov, *J. Lumin.*, 1979, 18/19, 11-18.

2. A. Pishtshev, M. Klopov, *Abstr. Intern. Conf. FM&NT*, Riga, 2012, p.117.

3. A. Lushchik, Ch. Lushchik, I. Kudryavtseva, et al., *Radiat. Meas.*, 2013, in press.

FEATURES OF LITHIUM NIOBATE SINGLE CRYSTALS MODIFIED BY RARE EARTH ADMIXTURES

M.N. Palatnikov[1], N.V. Sidorov[1], V.A. Sandler[2], K. Bormanis[3], and I. Smeltere[3]

[1]*Institute of Chemistry, Kola Science Centre RAS, Apatity, Murmansk Region, Russia*

[2]*Ivanovo State University, Ivanovo, Russia*

[3]*Institute of Solid State Physics, University of Latvia, Latvia*

E-mail: bormanis@cfi.lu.lv

A number of anomalies of conductivity and of optical, dielectric and pyroelectric properties of lithium niobate crystals within a range of temperatures (300—400 K) has been observed by different authors. The lack of quantitative repeatability of the results depending on the history of the sample is typical to most studies of anomalous thermal behaviour of various physical parameters of ostensibly pure lithium niobate crystals and particularly of crystals containing admixtures.

Examining of the micro- and nano-structures of domains and specific structural ordering features of lithium niobate crystals containing admixture of rare earth elements ($LiNbO_3$:REE) and grown under stationary and non-stationary conditions has revealed formation of regular micron-scale domain structures (RDS) of changeable or fixed steps and periodic nano-size fractal structures of steps between 10 and 100 nm. A super-structural sub-lattice of clustered defects forming in the cation sub-lattice of REE-modified lithium niobate crystals is observed to have steps of the size of a few lattice translation periods.

Static and dynamic piezoelectric properties, dielectric dispersion and conductivity of lithium niobate crystals modified by REE (Gd, Er, Tm, and Gd:Mg), containing micro- and nano-structures, and grown under stationary and non-stationary conditions are studied within the 290 – 840 K and 0.5 – 10^6 Hz range of temperature and frequency, respectively. Abrupt increase of the d_{33} piezoelectric modulus up to the value of single domain ostensibly pure lithium niobate crystal is observed up to 340 K at heating poly-domain $LiNbO_3$:REE crystals. The actual observed values of physical parameters and kinetics of the processes to a considerable extent are determined by the particular micro- and nano-structure of the sample.

IMPROVEMENT OF SOL-GEL DEPOSITED ZnO:Al THIN FILMS BY LASER RADIATION

Artur Medvid, Harijs Cerins, Edvins Dauksta, Gundars Mezinskis, Agneta Vezenkova, Baiba Auzina

Riga Technical University, LV-1048, Riga Azenes Str.14-24, Latvia

e-mail: Harijs.Cerins@rtu.lv

Zinc oxide (ZnO) is very important semiconductor with wide band gap (E_g=3.37 eV) and large exciton binding energy of 60 meV at room temperature. It is very promising candidate for such devices like gas sensors[1], light emitting diodes[2], solar cells[3], lasers[4]. Doping of ZnO with group III elements is commonly employed to enhance n-type conductivity of ZnO transparent electrodes. The ZnO doping by Al generates a free electron in the conduction band. Al atoms in thermodynamic equilibrium condition substitutes Zn atoms in ZnO crystal, but concentration of Al depends on growth method: sol-gel method, hydrothermal method, atomic layer deposition.

In this work, we investigated structural, optical and electrical properties of pure ZnO and Al-doped ZnO samples prepared by sol-gel method. Sol-gel process is a wet-chemical method widely used in material science and ceramic engineering. This method is used for materials fabrication starting from a colloidal solution (sol) that acts as the precursor for an integrated network (gel). In our work, precursor is zinc acetate ($Zn(CH_3COO)_2$). For surface topography studying we used atomic field microscope (AFM). We also measured ZnO and ZnO:Al photoluminescence (PL) spectra before and after irradiation by Nd:YAG laser fourth harmonic (λ=266nm, I~15MW/cm^2, τ=15ns). 4-point probes method to measure samples surface resistivity was used.

After the laser radiation two orders decrease of resistivity was observed, which is very important for transparent electrodes. PL measurements showed changes of optical properties in irradiated ZnO:Al sample. Moreover, from AFM measurements we obtained that grain size increase twice. Explanation of obtained results will be proposed.

References

1. Dayan N J, Sainkar S R, Karekar R N and Aiyer R C 1998 *Thin Solid Films* **325** 254
2. Saito N, Haneda H, Sekiguchi T, Ohashi N, Sakaguchi L and Koumoto K 2002 *Adv. Mater.* **14** 418
3. Chopra K L and Das S R 1983 *Thin Film Solar Cells* (New York: Plenum) 321
4. Huang M H, Mao S, Feick H, Yan H, Wu Y, Kind H, Weber E, Russo R and Yang P 2001 *Science* **292** 1897

SYNTHESIS AND PHOTOLUMINESCENCE IN Eu^{3+} DOPED $NaLaF_4$ MATERIAL

G. Doke, M. Voss, J. Grube, A. Sarakovskis, M. Springis
Institute of Solid State Physics, University of Latvia
e-mail: guna.doke@gmail.com

It is known that most of the fluoride and complex fluoride materials have relatively high chemical stability, moreover, these materials have small phonon energy which suppresses the rate of nonradiative transitions. These properties make fluorides very attractive as host materials for optically active trivalent rare-earth ions. Numerous studies on optical properties of fluoride and complex fluoride materials have been conducted for several decades, however not much information can be found about processes in europium doped $NaLaF_4$ material. This research is a part of extensive studies of different rare-earth doped and codoped $NaLaF_4$ materials, their synthesis, optical properties and possible applications [1, 2].

In this work $NaLaF_4$:Eu^{3+} samples with different Eu^{3+} concentrations were synthesized by solid-state reaction. The synthesis was performed using different annealing temperatures and atmospheres (air or fluorine). For these samples photoluminescence spectra, excitation spectra, luminescence decay kinetics and X-ray diffraction patterns were measured.

From the analysis of the obtained experimental data conclusions about composition and optical properties of the material was made. Optical transitions and cross-relaxation processes in the activator system as well as formation of oxygen related defects and their impact on material optical properties are discussed.

The financial support of ERDF project Nr. 2010/0204/2DP/2.1.1.2.0/10/APIA/VIAA/010 and VPP IMIS is greatly acknowledged.

References

1. A. Sarakovskis, J. Grube, A. Mishnev, M. Springis, *Optical Materials*, 2009, 31, 10, 1517 – 1524.

2. J. Grube, G. Doke, M. Voss, A. Sarakovskis, M. Springis, *IOPConf. Series: Materials Science and Engineering*, 2011, 23

RAMAN SCATTERING ANALYSES OF DEFECTS IN SiC

George Chikvaidze[1], Nina Mironova-Ulmane[1], Aina Plaude[1], Oleg T. Sergeev[2]

[1]*Institute of solid State Physics, University of Latvia*

[2]*V.E.Lashkaryov Institute of semiconductor physics, National Academy of science of Ukraine*

e-mail of presenting author: georgc@cfi.lu.lv

The limitations of the SiC technology are due to defects for SiC, such as point defects, line defects or two dimensional plane defects and stacking faults, which is very bad for the devices. Structural characterization was performed by micro-Raman spectroscopy, which represents a powerful technique for the characterization of SiC, because it is non destructive and requires no special preparation of samples. The parameters of the Raman signal such as intensity, width, peak frequency and polarization of Raman bands provide fruitful informations on the crystal quality. In present work, X-ray diffraction, FTIR absorption have been performed on single crystals SiC, plate 6H- SiC and 3C- SiC also. Investigated samples of SiC were grown by direct synthesis from silicon and carbon vapour in deep vacuum in quasi-close system produced of a high purity graphite. Samples were deposities onto substrates of SiC. All samples of 6H-SiC have hexagonal wurtzite structure with C^4_{6v} space group that was confirmed by x-ray diffraction measurements. A preliminary investigation has been performed by optical microscopy and SEM to determine the defect morphology.

The first- and second-order Raman spectra of 6H - SiC are given and analyzed in detail. We have performed Raman scattering investigations for semi-insulating 6H-SiC and doped 6H-SiC crystalline plates at room and at liquid nitrogen temperatures. A semi-insulating single crystals of 6H–SiC was also examined as a reference. Significant changes were observed in the shape, intensity and position of the A_1(LO). The changes in peak position, spectral shape, and width of the A_1(LO) phonon could be attributed to plasmon–phonon coupling.

Acknowledgement.

This work was supported by ERAF Project Nr.2010/0245/2DP/2.1.1.1.0/10/APIA/VIAA/114.

STRONG SECONDARY EMISSION OF OPAL-BASED PHOTONIC CRYSTAL: LIGHT LOCALIZATION AND DEFECT LUMINESCENCE

Galyna Dovbeshko[1], Olena Fesenko[1], Vitalii Boiko[1], Leonid Dolgov[2], Valter Kiisk[2], Ilmo Sildos[2], Vladimir Gorelik[3]

[1]Institute of Physics, Natl. Acad. of Sci. of Ukraine. Ukraine, [2]Institute of Physics, University of Tartu, Estonia, [3]P.N. Lebedev Physical Institute of the Russian Academy of Sciences, Russia

e-mail of presenting author: gd@iop.kiev.ua

The primary photonic crystal demonstrates light scattering and photoluminescence (PL) in wide region starting from 350 to 700 nm with two intensive maxima at about 400 and 500 nm, and several weak bands in the interval of 600 – 700 nm. PL of synthetic opal is connected with the presence of defects and impurities. The band with a maximum at a wavelength near 520 nm is related to the surface states of Si – H, whereas the band with maxima near 650 and 690 nm to the bulk and surface states Si – O. The nature of the blue band at about 400 nm is associated with the presence of various impurities such as zinc, calcium, sodium, iron, zirconium oxides, etc [1]. The fraction of these impurities is less than 10^{-5}. The PL intensity for the primary synthetic opal changed from point to point under the scanning over its surface [2] and depends on the presence of forbidden zone.

For synthetic opal the most efficient excitation wavelengths λ_{exc} lies in 310-370 nm range for the blue luminescent band of silica and in 240-270 nm range for the greenish-red bands. Therefore we selected λ_{exc}=250 nm and λ_{exc}=350 nm pulsed excitations and applied them for measurement of fluorescent kinetics from photonic crystals. For each emission wavelength we obtained multi component decay curves in nanosecond and microsecond time scales, which can be associated with different types of defect centers in the samples, while it was established that reference amorphous quartz sample has long decay time components of several tens or even one hundred microseconds, which are rather bigger, than in microsecond range decay times obtained from the photonic crystal samples of synthetic opal. Photonic structure seems causes localization of optical modes and light [3]. We acknowledge support from Nanotwinning FP7 (project ID 294952), Russian-Ukrainian project 60-02-12. References

1. A.N. Gruzintsev, G.A. Emel'chenko, V.M. Masalov, and E.E. Yakimov, *Neorgan. Mater.,* 2009, **45**, 302-305.
2. G.I. Dovbeshko, O.M. Fesenko, V.V. Boyko, V.F. Gorchev, S.O. Karakhin, N.Ya. Gridina, V.S. Gorelik, V.N. Moiseenko, *Ukr. J. Phys.,* 2012, **57(7)**, 732.
3. T. Sperling, W. Buhrer, C.M. Aegerter, G. Marter, *Nature photonics,* 2013, **7,** 48-52.

FIRST-PRINCIPLES CALCULATIONS OF DEFECTS IN MgF_2

F.U.Abuova[1], A.T. Akilbekov[1], E.A. Kotomin[2], S.Piskunov[2]

[1]*L. N. Gumilyov Eurasian National University, 3Munaitpasova, Astana, Kazakhstan*

Fatika_82@mail.ru

[2]*Institute of Solid State Physics, 8 Kengaraga str., University of Latvia, Riga*

Kotomin@latnet.lv

MgF_2 with rutile structure is important wide-gap optical material with numerous applications. It is also radiation-resistant material, the energy required to form a stable primary radiation defect known as the *F* center (fluorine vacancy with trapped electron) between 5K and room temperature is much higher than in other alkali halides. We present and discuss here the results of calculations for basic colour centers (F-, H-, Frenkel defects) in the crystal bulk. This study is based on the large scale *ab initio* DFT calculations using hybrid B3PW exchange-correlation functional as implemented into CRYSTAL code.

In order to understand the behaviour of the material with respect to irradiation and its optical properties, we analyzed the electronic structure, atomic geometry, charge density distribution as well as defect- and surface formation energies using several types of supercells. We compared properties of close and well separated F-H (Frenkel) defect pairs and migration of defects. We simulated also formation and demonstrated energetic preference of inert F_2 interstitial molecules as sinks of mobile interstitials atoms. We discuss how this is related to the material radiation stability.

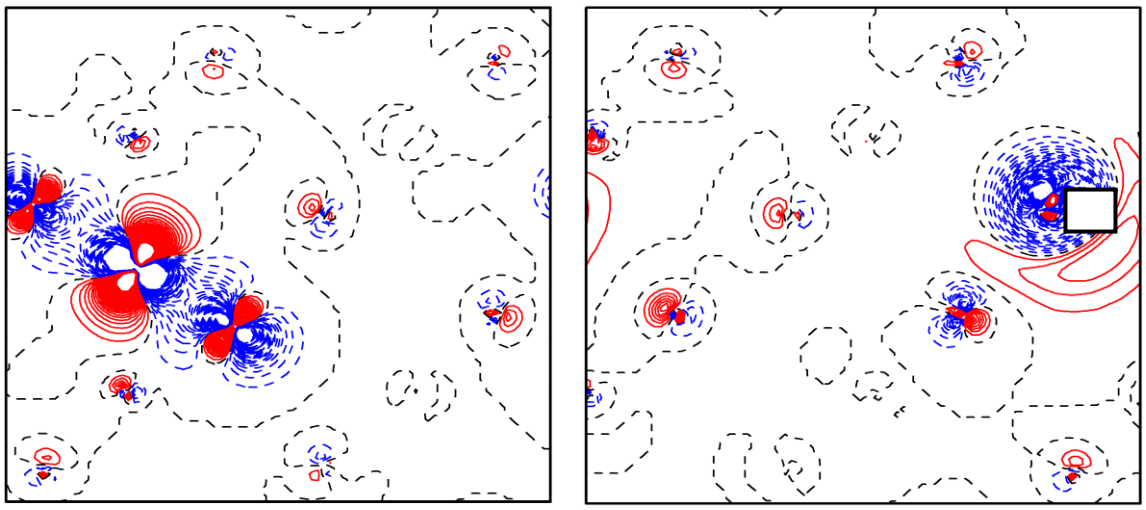

a) b)

The electronic density redistribution around the H center (a) и F center b).

PHOTO-INDUCED FORMATION OF SURFACE RELIEF IN AMORPHOUS AS_2S_3 FILMS

Elina Potanina, Janis Teteris

Institute of solid State Physics, University of Latvia, LV 1063 Riga, Latvia
elina.potanina@gmail.com

In this report we study the formation of surface relief in arsenic trisulfide films under laser light radiation, with modulated polarization direction.

Arsenic trisulfide is known as inorganic polymer, which is often used in holography due to large photoinduced changes of its chemical and optical properties. However, formation of surface relief is obtained with method, different from holographic recording. Only one laser beam with modulated polarization direction was used.

Samples with different thickness were made using vacuum evaporation. The photoinduced changes on the surface were initiated by DPSS laser light (532 nm). Profiles of surface reliefs were observed and reliefs depth dependence on film thickness and exposure was studied.

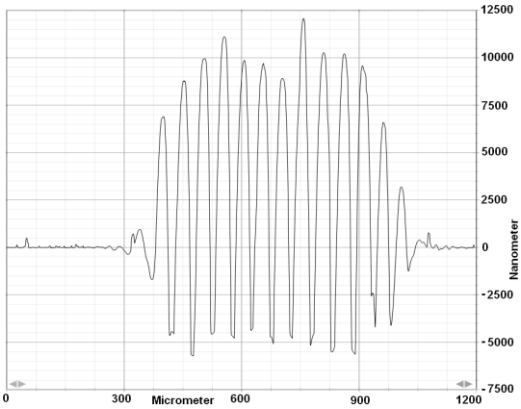

Fig.1 Profile of 17 μm high surface relief in 5,5 μm thick film

References

1. U.Gertners, J.Teteris, *The impact of light polarization on the direct relief forming processes in As_2S_3 thin films*, IOP Conf. Series:Materials Science and Engineering, 38 (2012) 012026.
2. H.Hisakuni, K.Tanaka, *Giant photoexpansion in As_2S_3 glass*, Applied Physics Letters Vol. 65 No. 23, 1994, 2925 – 2927 p.

IMPROVEMENT OF CdZnTe DETECTOR PROPERTIES BY LASER

E. Dauksta[1], A. Medvid[1], A. Mychko[1], E. Dieguez[2], H. Bensalah[2]

[1]Riga Technical University, Riga, Latvia

[2]Universidad Autónoma de Madrid, Madrid, Spain

e-mail: edvins.dauksta@rtu.lv

One of the most promising materials for X-ray and gamma ray detectors are cadmium telluride (CdTe), and cadmium zinc telluride (CdZnTe) compound semiconductor crystals [1, 2]. The main reason for this is the possibility to use those materials at room temperature. However, Te inclusions, crystal twins, dislocations, grain boundaries and other defects degrade crystal performance as radiation detector.

Several researchers have studied a possibility to improve crystal quality by CO_2 laser irradiation [3, 4]. However, this method has some disadvantages - processing time of about 100 h and damage of the crystal surface.

We have studied the influence of laser radiation on CdZnTe crystal electrical properties and radiation detector parameters.

CdZnTe crystal was grown by vertical gradient freezing method and had high concentration of non-controllable impurities and Te inclusion. CdZnTe samples where treated by Nd:YAG (λ=1064 nm) laser to decrease defect influence on electrical properties. Current voltage characteristic measurements (IV) were performed to detect changes in electrical conductivity. IV characteristic showed that the sample resistivity increased after irradiation by $2 \cdot 10^4$ laser pulses. This effect is more pronounced with higher Te inclusion concentration. Moreover, energy-dispersive X-ray spectroscopy did not show any changes of chemical composition, but measurements of ^{241}Am radiation spectrum showed increase of peak to valley ratio.

Laser treated CdZnTe detectors showed reduction of leakage current, improved spectral energy resolution and peak to valley ratio.

References

1. T. E. Schlesinger, J. E. Toney, H. Yoon, YE. Lee, B. A. Brunett, L. Franks, R. B. James, Mat. sci. eng. R, **32**, 103 (2001)

2. F. Lebrun. Nucl. instrum. meth., A. **563**, 200 (2006)

3. M. Meier, M. J. Harrison, S. Spalsbury, D. S. McGregor, J. cryst. growth. **311**, 4247 (2009)

4. S. V. Plyatsko, L. V. Rashkovetskyi, Semiconductors+, **40**, 287 (2006)

EFFECT OF POROSITY ON THE ELECTRICAL PROPERTIES OF PZT CERAMICS

E.V. Barabanova[1], O.V. Malyshkina[1], A.I. Ivanova[1], E.M. Posadova[1], K.M. Zaborovskiy[1], A.V Daineko [2]

[1]*Tver State University, Tver, Russia,* [2]*Research Institute "ELPA", Zelenograd, Russia*

e-mail: pechenkin_kat@mail.ru

Ferro-piezoelectric ceramics on the basis of lead zirconate titanate perovskite solid solutions $PbZr_{1-x}Ti_xO_3$ (PZT) continue to be the most important ferroelectric and piezoelectric materials in commercial devices [1]. The properties of PZT-based materials as well as of other solid solutions depend strongly on the preparation conditions, in particular on the porosity formed during sintering [2, 3].

In the present work a study was made of the dielectric properties of PZT ceramics with varying porosity in the frequency range of 25 Hz – 1 MHz. The grain size and porosity were examined with the aid of scanning electron microscopy (JEOL JSM 6510LV).

It was found that the porosity has a direct influence on the dielectric permittivity and specific conductivity as illustrated in Fig. 1. The magnitude of the above parameters decrease with the increase of porosity, while the types of their frequency dependence remain the same.

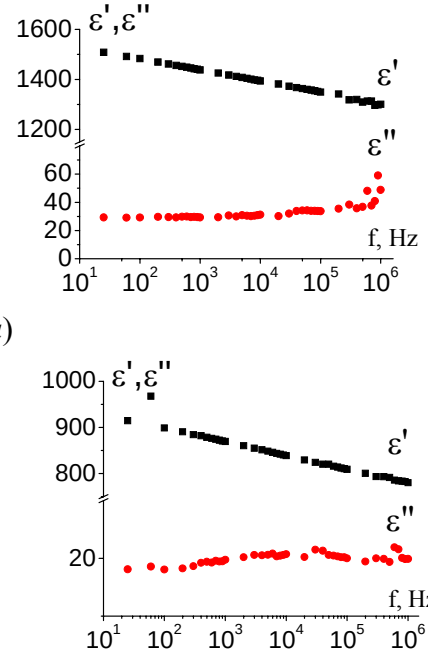

Fig.1 Frequency dependence of the real and imaginary parts of the dielectric permittivity of PZT-19 pore-free ceramics (a) and that with porosity of 25% (b)

References

1. W. Heywang, K. Lubitz, W. Wersing. Piezoelectricity Evolution and Future of Technology. Springer – Verlag Berlin Heidelberg, 2008.

2. R. Guo, C.A. Wang, A.K. Yang, J.T. Fu. *J. Appl. Physics*, 2010, V. 108, 124112.

3. B. Praveenkumar, H.H. Kumar, D.K.Kharat. *Bull. Mater. Sci.*, 2005, V. 28, 453-455.

DIELECTRIC PROPERTIES OF $BaTiO_3$ BASED MATERIALS WITH ADDITION OF TRANSITION METAL IONS WITH VARIABLE VALENCE

Dorota Sitko[1], Barbara Garbarz-Glos[1], Wojciech Bąk[1],
Andrzej Budziak[2], C.Kajtoch[1] and Anna Kalvane[3]
[1]*Institute of Physics, Pedagogical University of Cracow, Poland*
[2] *The H.Niewodniczanski Institute of Nuclear Physics PAN, Cracow, Poland,*
[3]*Institute of Solid State Physics, University of Latvia*
e-mail of presenting author: sitko.dorota@gmail.com

A comparative analysis of the dielectric properties of $BaTiO_3$, $BaTiO_3$+0.1 wt.% MnO_2 and $BaTiO_3$+0.1 wt.% Fe_2O_3 ceramics was performed. The temperature dependence of dielectric properties and an electrical conduction for both the samples were measured at the temperature ranging from 130 K to 500 K and at the frequency from 10 - 10^7 Hz. The influence of substitution has a pronounced effect on the electrical properties of the ceramics. In the case of Fe-ions doped $BaTiO_3$, was observed one board peak slightly dependent on frequency at T_C and one board hump with a maximum at about 250 K which exhibits relaxor behavior. The ε(T) characteristics for $BaTiO_3$+0.1wt.%MnO_2 are qualitatively similar to those known for $BaTiO_3$. The observed transition temperatures for the sample doped with Mn-ions and pure BT are almost equal but the amplitudes of all peaks are much smaller. The multivalence nature of incorporated ions is supposed to cause such a behavior of the investigated polycrystalline materials.

PO-151

FOURIER TRANSFORM-EPR SPECTROSCOPY OF TRANSITION METAL IONS IN ZnO

D. V. Azamat[1], A. G. Badalyan[2], J. Lancok[1], V. A. Trepakov[1,2], L. Jastrabik[1] and A. Dejneka[1]

[1] *Institute of Physics AS CR, 182 21, Prague 8, Czech Republic*

[2] *Ioffe Physical-Technical Institute, RAS, 194021, St. Petersburg, Russia*

e-mail: azamat@fzu.cz

Diluted magnetic semiconductors based on ZnO with transition metal ions (TM=Ni, Co, Mn, Fe) are widely used nowadays as model objects for testing concepts for spintronics applications. The $3d^5$ transition metal ions such as Fe^{3+} and Mn^{2+} with electron spin S=5/2 potentially provide a spin multiplet for use in the implementation of quantum algorithms.

Magnetic properties of Co^{2+} ions in ZnO have been probed by use of Fourier Transform-Electron Paramagnetic Resonance (FT-EPR). The EPR data reveal the formation of Co dimer centers in heavily doped hydrothermally grown ZnO single crystals. Well separated magnetic dimers of Co^{2+} ions embedded in ZnO matrix are anti-ferromagnetically coupled nearest-neighbour S^{eff}=1/2 spins leading to an S=1 ground state of the pairs.

Rabi oscillations have been studied on the ground state of Co^{2+} ions in ZnO. These quantum oscillations of electron-nuclear states of Co^{2+} (nuclear spin I=7/2) indicates the long-lived quantum coherence at helium temperature. The measurements were performed at different cobalt concentrations using a Pulsed EPR Bruker E-580 X- and Q-band spectrometer.

Acknowledgments

This work was supported by the project SAFMAT CZ.2.16/3.1.00/22132

STRUCTURAL, MICROSTRUCTURAL AND DIELECTRIC SPECTROSCOPY STUDY OF FUNCTIONAL FERROELECTRIC CERAMIC MATERIALS BASED ON BARIUM TITANATE

Barbara Garbarz-Glos[1], Wojciech Bąk[1], Andrzej Budziak[2] and Maija Antonova[3]

[1]*Institute of Physics, Pedagogical University of Cracow, Poland,*

[2] *The H.Niewodniczanski Institute of Nuclear Physics PAN, Cracow, Poland,*

[3]*Institute of Solid State Physics, University of Latvia*

e-mail of presenting author: barbaraglos@gmail.com

In this work the differences between the physical properties of barium titanate $BaTiO_3$ and newly obtained $BaHf_xTi_{1-x}O_3$ were identified. These ceramics were prepared by solid-phase reaction of simple oxides and carbonates using the conventional method. This method made possible to obtain ceramic materials with optimal and well-defined properties and thus to extend the scope of the functional electroceramics BT-type in modern electronics. Phase composition and crystal structure of the samples was studied by X-ray diffraction. The experiments was performed using X-ray diffractometer with X'Pert PRO (Pananalytical) with CuKα radiation and a graphite monochromator, at various temperatures in the temperature range between 130 and 500 K, both in the process of heating and cooling. A profile-fitting program FULLPROF based on the Rietveld method was used to analyse and fit the spectra. Investigations of the chemical compositions and microstructure of the specimens were performed on polished sections and fractures by using the Hitachi S4700 electron scanning microscope with field emission and the Noran Vantage EDS system. The obtained results allowed to determining the stoichiometry of the materials and evaluate their microstructure: grain and pore sizes, shapes and orientation. The application of dielectric spectroscopy, known also as impedance spectroscopy method or admittance spectroscopy as well, made it possible to characterize of the material in the terms of electrical properties: dielectric permittivity (ε*), electric modulus (M*; M* = 1/ε*) as well as electric impedance (Z*) and admittance (Y*; Y* = 1/Z*). Investigations of dielectric properties were performed by means of a Alpha-AN modular measurement system together with cryogenic temperature control system - Quatro Cryosystem and WinDETA Novocontrol software. The comprehensive studies were conducted to determine the relationship between the conditions of the production process: the sintering, the formation and growth of grains of electroceramics and dielectric and mechanical properties. On the basis of experimental data, was concluded that the lead free material based on barium titanate solid solutions possesses better parameters than pure BT and is one of the promising candidate for the manufacture of transducers.

BROADBAND DIELECTRIC INVESTIGATION OF BARIUM TITANATE AND NICKEL-ZINC FERRITE COMPOSITE CERAMICS

Aurimas Sakanas[1], Robertas Grigalaitis[1], Jūras Banys[1], Liliana Mitoseriu[2], Vincenzo Buscaglia[3], Paolo Nanni[4]

[1]*Faculty of Physics, Vilnius University, Lithuania,* [2]*Physics Department, University "Alexandru Ioan Cuza", Romania,* [3]*Institute of Energetics & Interphases IENI-CNR, Italy,* [4]*Department Chemical & Process Engineering, University Genoa, Italy*

e-mail of presenting author: aurimas.sakanas@ff.vu.lt

Ferroelectric barium titanate and nickel-zinc ferrite composite ceramics belong to a multifunctional materials group called multiferroics. Multiferroics are materials combining at least two ferroic properties in the same structure and have drawn major scientific and technological attention in recent years. One of the most promising candidates is barium titanate and nickel zinc ferrite composite. Although dielectric properties of this material were already investigated, the results up to only megahertz frequencies were presented [1, 2].

Here we demonstrate the results of the broadband dielectric spectroscopy of xBaTiO$_3$-(1-x)Ni$_{0.5}$Zn$_{0.5}$Fe$_2$O$_4$ composite ceramics with x=0.5, 0.6 and 0.7 molar ratios in the 20 Hz to 50 GHz frequency range. The real part of dielectric spectra of the composite ceramics (Fig. 1) manifests conductivity contribution up to a few megahertz frequencies followed by a relaxation process. At high enough frequencies, where the conductivity contribution is greatly reduced, diminished permittivity with the increasing concentration of nickel-zinc ferrite can be observed.

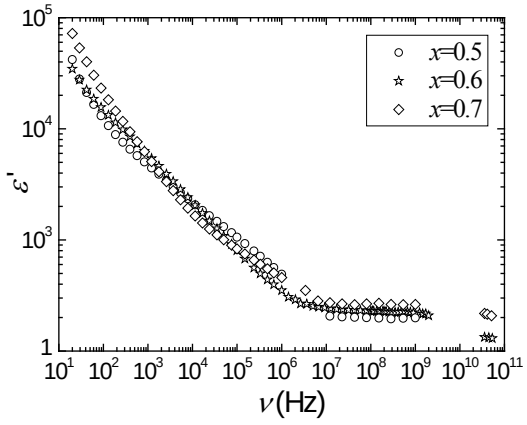

Fig.1 Frequency dependence of the real part of dielectric permittivity at 500 K for $xBaTiO_3$-(1-x)$Ni_{0.5}Zn_{0.5}Fe_2O_4$ composites with different x.

References

1. L. Mitoseriu, V. Buscaglia, *Phase Transitions,* 2006, Vol.79, No.12, 1095-1121.

2. L. P. Curecheriu, M. T. Buscaglia, V. Buscaglia et al., *J. Appl. Phys.,* 2010, Vol.107, No.104106, 1-11.

INFLUENCE OF Li_2TiO_3 ON CHEMICAL REACTIVITY OF Li_4SiO_4 PEBBLES

Arturs Zarins[1], Gunta Kizane[1], Arnis Supe[1], Regina Knitter[2], Mathias Kolb[2], Oliver Leys[2]

[1]*University of Latvia, Institute of Chemical Physics, 4 blvd. Kronvalda, LV-1010, Riga, Latvia*

[2]*Karlsruhe Institute of Technology, Institute for Applied Materials, 76021 Karlsruhe, Germany*

e-mail of presenting author: arturs.zarins@lu.lv

Lithium orthosilicate pebbles with 2.5wt% additions of SiO_2 ($Ø_{peb.}$=0.25-0.63 mm, 90mol% Li_4SiO_4 and 10m ol% Li_2SiO_3) are one of European Union approved tritium breeding ceramics for fusion reactors [1]. A lithium carbonate containing sub-surface layer forms on pebbles (eq.) at thermal treatment – due to exponential quenching (Fig.1.), and at storage, from air atmosphere. Radiation unstable Li_2CO_3 influences main properties of tritium breeder: tritium diffusion and desorption [2], mechanical and radiation stability of pebbles [3].

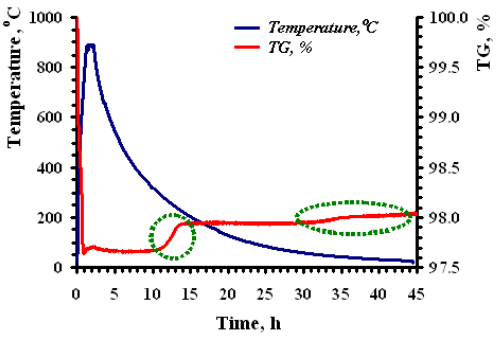

Fig.1. Chemisorption of CO_2 and H_2O vapor on surface of Li_4SiO_4 pebbles with 10mol% of Li_2SiO_3 ($Ø_{pebbl.}$≈500 µm) at thermal treatment (T_{max}=900°C, t_{max}=1 h, air atmosphere)

$$Li_4SiO_{4(cryst.)} + CO_{2(g.)} \xrightarrow{H_2O_{(g.)}} Li_2CO_{3(amorph.)} + Li_2SiO_{3(amorph.)}$$ ***(Air atmosphere)*** (eq.)

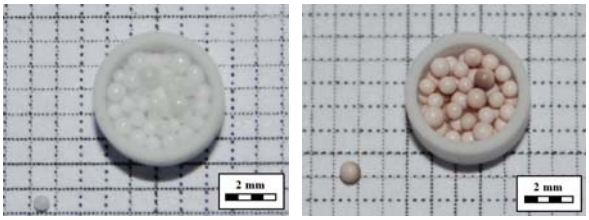

Fig.2. Li_4SiO_4 pebbles ($Ø_{pebbl.}$=560-900 µm) with 10mol% of Li_2SiO_3 (left) and 10mol% of Li_2TiO_3 (right) after thermal treatment (T_{max}=950°C, t_{max}=504 h, air atmosphere)

Therefore, to improve chemical and physical properties of Li_4SiO_4 pebbles it has been proposed to change composition of ceramic [4]. In place of Li_2SiO_3, as secondary phase could be us ed a less reactive and radiation stable Li_2TiO_3 phase [5]. Aim of this investigation was for the first time to compare chemical reactivity of Li_4SiO_4 pebbles with additions of Li_2TiO_3 and Li_2SiO_3 (Fig. 2.). It has been observed that Li_2TiO_3 additions reduce reactivity of Li_4SiO_4 pebbles with H_2O vapour and CO_2 at thermal treatment with exponential quenching.

References

1. M. Zmitko et al. Journal of Nuclear Materials 417 (2011) 678-683.
2. M.H.H. Kolb et al. Journal of Nuclear Materials 427 (2012) 126-132.
3. A. Zarins et al. Journal of Nuclear Materials 429 (2012) 34-39.
4. A. Zarins et al. Book of abstracts, 29th Conference of Institute of solid state physics, 20-22 February, 2013, *submitted*.
5. R. Knitter et al. Journal of Nuclear materials, 2012, *in press*.

APPLICATION OF SEDIMENTATION EXPERIMENTS WITH SUSPENDED NANOPARTICLES

Ansis Mezulis, Elmars Blums, Mikhail Maiorov
Institute of Physics, University of Latvia
e-mail of presenting author: ansis@sal.lv

As a matter in fact, sedimentation experiments examine the integral sedimentation velocity of suspended particles. If the particles are nano-sized (10…50 nm in diameter), due to a small Peclet number the sedimentation effect is very weak; the experiment tooks at least 10 days to measure particle excess in the boundary layer, gained by the sedimentation.

Nevertheless, in some points the sedimentation experiments become reasonable. It is the simpliest way to study the influence of particle interaction. G.K. Batchelor in the eighties has devepoled the sedimentation model, taking into account the particle interaction. The experimental results of sedimentation can be compared to both the Batchelor and the Stokes non-interaction model to conclude about degree of interaction, moreover, to calculate the polydispersity of suspended particles. The particles with ferromagnetic properties are of particular interest. Indeed, if the test-tube is submitted to a gradiental magnetic field, the magnetic force acts besides the gravitational one, and the sedimentation velocity of a particle can be calculated as:

$$U = \frac{2gR_m^3(\rho - \rho_0 + \mu_0 M_S \nabla H / g)}{9\eta_0 R_H},$$

where R_m and R_H are the magnetic and hydrodynamic radius of a particle, ρ and ρ_0 the density of hard particle and of the solvent.

We perform sedimentation experiments with suspended polydisperse ferromagnetic nanoparticles, charactrized by log-normal size distribution, proved by independent measurements with the vibrating sample magnetometer (VSM) and the size analyzer (DLS). The particle concentration changes in the boundary layers are measured by the inductance coils, placed at the top and at the bottom of the test-tube. Additionaly, after the experiment is finished, we take the samples from both ends of the test-tube in amount of 1 mm layer to perform VSM and DLS analysis to conclude about particle size separation.

The work is supported by European Regional Development Foundation, Project 2011/0001/2DP/2.1.1.1.0/10/APIA/VIAA/007

References

1. G. K. Batchelor, C.-S. Wen, J. Fluid Mech., 124, 495-528 (1982)
2. E. Blums, Yu. A. Mikhailov, R. Ozols, Heat and Mass Transfer in MHD Flows, World Scientific, Singapore (1987)

INVESTIGATION OF IODINE IMPLANTED C12A7 CERAMICS

Annika Pille[1], Eliko Tõldsepp[1], Eduard Feldbach[1], Viktor Denks[1], Marco Kirm[1], Anders Hallén[2]

[1] *Institute of Physics, University of Tartu, Estonia,* [2] *KTH Royal Institute of Technology, Sweden*

e-mail: annika.pille@ut.ee

$12CaO \cdot 7Al_2O_3$ (C12A7) is a nanoporous compound which has been extensively studied due to its unique crystal structure and electronic properties. Its flexible lattice is composed of positively charged framework of Ca-Al-O cages (free space Ø ~0.4 nm) and O^{2-} ions occupying 1/6 of the cages in the stoichiometric case. By different chemical treatments, the encaged O^{2-} anions can be replaced by other anions (F^-, Cl^-, H^-, OH^-, Au^- [1,2] etc) and even by electrons [3] resulting in unusual changes in materials properties. The latter replacement converts insulating C12A7 into a persistent electronic conductor making this compound suitable for transparent electrodes. Optical properties of various derivatives of C12A7 have been studied by our research group [4,5], however, there are no reports on the largest halogen – the iodine ion, which can be encaged into C12A7. The aim of this work was to prepare iodine doped C12A7 using ion implantation technique as it was successfully used earlier for implementing Au^- ions into C12A7 lattice [2].

Powder of C12A7 was synthesized by self-propagating combustion method using stoichiometric ratio of metal nitrates and a mixture of urea and β-alanine as fuels. The synthesized powder was used as a starting material for melt-solidification process in a carbon crucible followed by heat-treatment in air to obtain high density C12A7 ceramics containing various encaged oxygen species (mainly O^{2-} , O_2^-, OH^-). Iodine implantation at 300 keV, using fluence of 10^{15} and 10^{16} cm^{-2}, and a target temperature of 600 ºC was carried out at the Ion Technology Centre (Uppsala, Sweden). Iodine concentrations in the C12A7 ceramic samples were estimated by Rutherford backscattering spectrometry and XPS. Raman spectroscopy of the implanted samples showed no evidence of the crystal lattice destruction, despite the high fluence. Therefore iodine anion formation and incorporation into the cages of C12A7 lattice is expected, analogously to Au^- [2].

References

1. K. Hayashi, P.V. Sushko, D.M. Ramo, et al., *J. Phys. Chem. B 111*, 2007, 1946.
2. M. Miyakawa, H. Kamioka, M. Hirano, et al., *Phys. Rev. B 73*, 2006, 205108.
3. K. Hayashi, S. Matsuishi, T. Kamiya, et al., *Nature 419*, 2002, 462.
4. E. Feldbach, V.P. Denks, M. Kirm, et al., *J Mater Sci: Mater Electron 20*, 2009, S260.
5. E.Tõldsepp, T. Avarmaa, V.P. Denks, et al., *Optical Materials 32*, 2010, 784.

MULTIFUNCTIONAL MATERIALS FROM HEMP FIBERS TREATED WITH STEAM EXPLOSION TECHNOLOGY

Anna Putnina[1,2], Silvija Kukle1, Janis Gravitis[2]

[1]*Riga Technical University, Institute of Textile Materials Technologies and Design, Azenes St. 14, LV – 1048, Riga, Latvia*

[2] *LSIWC Laboratory of Biomass Eco-Efficient Conversation, Dzerbenes St. 27, Riga LV-1006, Latvia*

anna.putnina@rtu.lv

Multifunctional materials include properties of smart material systems (e.g. smart textiles) as well as biologically synthesized materials (case of biomimetic). Natural wood, flax and hemp fibres are examples of such multifunctional materials – polymer composite systems. In current research attempt has been made to analyse hemp fibres treated with steam explosion (SE) technology. During the SE process, fibres are chemically modified and mechanically defibrillated. At the end of the steaming process, the instantaneous release of pressure stops the reaction and separates the fibres. Disintegration of hemp fibres separated from non-retted, dew-retted and dried stems of hemp plants grown in the Agricultural Science Centre of Latgale (Kraslava) at 2010 vegetation season of Latvian local genotype 'Purini'[1] by alkali treatment and steam explosion (SE) were investigated.

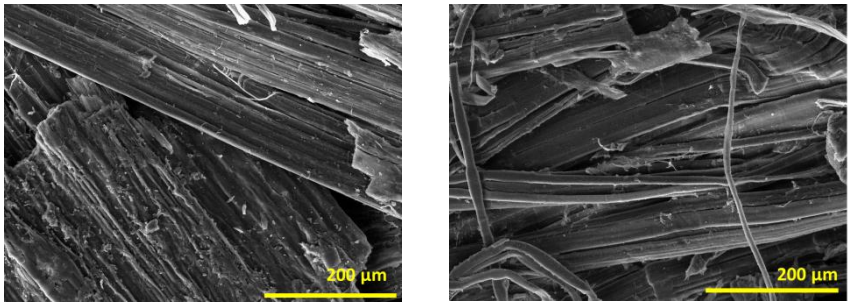

Fig. 1. SEM micrograph of bundles of the hemp fibres before and after SE

An average intensive SE in combination with the hydro-thermal and alkali after-treatment allows decreasing the diameter of hemp fibres and reduce the concentration of non-celluloses components, among them hemicelluloses, lignin, pectin, waxes and water [1;2].

References

1. Putnina A., Kukle S., Gravitis J. Effect of Steam Explosion Treatment on Hemp Fibres Microstructure. 12th World Textile Conference AUTEX 2012 *"Innovative Textile for High Future Demands": Book of Proceedings*, Croatia, Zadara, 13.-15. June, 2012, 871 -874

2. Kukle S., Gravitis J., Putnina A. Processing Parameters Influence on Disintegration Intensity of Technical Hemp Fibres. *Journal of Biobased Materials and Bioenergy*. Vol.6, No.4, 2012, 440-448.

EXPERIMENTAL SETUP FOR ANALYSIS OF SORPTION AND DESORPTION OF TRITIUM IN LIQUID LITHIUM UNDER DIFFERENT EXTERNAL CONDITIONS

A. Lescinskis[1,2], G. Kizane[1], A. Vitins[1], E. Platacis[2], O. Lielausis[2], A.Romanchuks[2], K. Kravalis[2]

[1] Institute of Chemical Physics, University of Latvia, [2] Institute of Physics, Agency of University of Latvia

E-mail: andris.lescinskis@lu.lv

Liquid lithium is a perspective material and it's intended to be used it in the D – T fusion devices (like JET, ITER) as a cooling agent, which protects a surface of divertor (inside the lower part of the plasma chamber) from complete thermal destruction ($800\,^0C$). Lithium is flowing over the surface of divertor and cools it down. During this process lithium gets polluted with plasma chamber gases (He, ^{2}H and ^{3}H) and with chemically eroded particles of divertor surface as well. In order to not disrupt complex process of nuclear plasma, concentration of tritium in lithium shall not exceed certain acceptable standards (less than 1 appm) [1]. Still to these days this is a problem of decontamination lithium from tritium. The particular research aims is to study tritium sorption and thermal desorption processes in molten lithium under different external conditions (temperature, magnetic field, atmosphere and others). Investigate lithium - tritium chemically bonded forms which also includes a number of polymorphic forms (Li_nT) [2]. Develop and optimize conditions for effective separation of tritium from lithium.

An original complex device has been designed and created especially for this research. Some of tritium sorption and thermal desorption in liquid lithium experiments has been successfully done already. First experiment series were carried out under reduced pressure (vacuum) to rule out other operating gases (Ar, He) that may also interact with liquid lithium. Experiments showed good tritium desorption which highly depends on the temperature. Collected and mathematically treated data from tritium monitor. Further investigations under different conditions are in progress.

Acknowledgments

This work was supported by the European Regional Development Fund, project No. 2010/0262/2DP/2.1.1.0/10/APIA/VIAA/176 "Advanced lithium-ion technology for plasma treatment equipment (divertor) for the protection of the active surface".

References

1. D. K. Sze, R.F. Mattas, J. Anderson, R. Haange, H, Yoshia, O. Kventon, *Tritium Recovery from Lithium Based On Cond Trap.* Third International Symposium on Fusion Nuclear Technology, University of California, Los Angeles, June 27 - July 1, 1994, 19p
2. C.H. Wu, R.O. Jones, *Stability and structure of Li_nH molecules (n=3-6): Experimental and density functional study.* Journal of Chemical Physics, 2004, **11,** 5128 – 5132

INVESTIGATION OF CARBONIZED LAYER ON SURFACE OF NaAlSi GLASS FIBERS

Evalds Pentjuss, Andrejs Lusis, Gunars Bajars, Jevgenijs Gabrusenoks
Institute of solid State Physics, University of Latvia
e-mail of presenting author: lusis@latnet.lv

Glass fiber fabrics are used in dry and wet atmosphere and in water at elevated and changeable temperatures. The changes in environment can initiate processes in fabric that lead to a new its equilibrium state and changed physical properties. Some of them may be irreversible. It is accepted [1] that interaction of alkali silicate glasses with water or mineral acids proceeds by ionic exchange by diffusion of Na^+ ions to glass surface and H^+ or H_3O^+ from water into the bulk of glass to fill the vacancies of Na^+ ions. It looks that Na^+ ions and H_2O and CO_2 from atmosphere during the months form the shell of $Na_3H(CO_3)_2 \cdot 2H_2O$ or its mixture with $Na_2CO_3 \cdot H_2O$ on the surface of glass fibers. Such shell can be dissolved in water and acids [2]. The heating leads to weight loss associated with decomposition by reaction of $2(Na_3H(CO_3)_2 \cdot 2H_2O) \rightarrow 3Na_2CO_3 + CO_2\uparrow + 5H_2O\uparrow$ at temperature over 55-57 ^{0}C, and dehydration of $Na_2CO_3 \cdot H_2O$ over 100 ^{0}C. There are studied the weight uptake after different thermal treatment of unleached and leached fabrics for K-glass fabric (initial composition of (18-22) Na_2O (3-5) Al_2O_3 (73-79) SiO_2) and powder of carbonates leached in water. The experimental weight-time curves were analyzed using regression technique. There are observed fast uptake of weight during the first tenths of minutes after heating for both types of samples and much slower (hundreds of hours) uptake up to equilibrium weight for unleached samples. Analysis indicated that fast weight uptake consist of two simultaneously going processes on surface of shell. One of them should be associated with water absorption, and second, with water diffusion from surface inside the shell. The late uptake should be associated with hydration of bulk of shell. The irreversible weight loss should be associated with loss of Na atoms in evolving process of vapor of H_2O and CO_2 during heating of samples. In a case of leached samples the surface process are much faster. An increased temperature (170 ^{0}C) leads to increase of weight losses and decrease of absorption rate that should be caused by increase of roughness of glass surface.

References

1. B.W.Veal, D.J.Lam, D.P.Karim. *Nucl. Tech.* **51** (1980) 136.

2. E.Pentjuss, A.Lusis, G.Bajars, J.Gabrusenoks, L.Jekabsone. *IOP Conf. Ser.: Mater.Sci. Eng.* **38** (2012) 012021.

PHOTOSENSITIVE PROPERTIES OF COMPOSITE FILMS BASED ON COPPER CHLORIDE IN POLYMER MATRIX

Andrejs Gerbreders [1,2], Andrejs Bulanovs[2], Eriks Sledevskis [2], Vjaceslavs Gerbreders[2], Janis Teteris[1]

[1]*Institute of solid State Physics, University of Latvia,* [2]G. *Liberts' Innovative Microscopy Centre, Daugavpils University*

e-mail of presenting author: andrejmah@gmail.com

The composite films based on PMMA, free radical photoinitiator and $CuCl_2$ were prepared. Transmission spectra of the films before and after illumination by different laser lines (405, 456 nm) were measured. The reversible character of the composite photosensitivity was fixed. Possibility of metal nanoparticles formation as a result of reduction reaction has been discussed.

The holographic gratings were recorded by different exposure (200 – 500 J/cm^2) in the films with different concentration (8-20 wt. %) of copper salt. The film sensitivity dependence on polymer molecular weight was studied. Surface relief of the gratings was measured by AFM.

PECULARITIES OF DEFECT CREATION IN LiF-WO_3, LiF- TiO_2 AND LiF- Fe_2O_3 CRYSTALS UNDER PULSED ELECTRON IRRADIATION

R. Kassymkanova, A. Abdrakhmetova, A. Dauletbekova, A. Akilbekov, Z. Kidiraliyeva

L.N. Gumilyov Eurasian National University, Astana, Kazakhstan,
e-mail alma_dauletbek@msil.ru

Radiation defects creation in LiF –WO_3, LiF- TiO_2, LiF- Fe_2O_3 crystals under pulsed electron radiation is researched with high time (20 ns) and spectral (2 nm) resolution measurement techniques.

LiF crystals were grown by Stocbarger method in fluoridizing atmosphere in Vavilov State Optical Institute(Saint Petersburg). Other crystals were grown in air by Czochralski method in the Institute for Scintillation Materials of NAS of Ukraine Kharkov).

The analysis of initial defects the investigated crystals was performed by the absorption spectroscopy in the infrared region byFT-IR spectrometer Nicolet 5700, and in the visible region of the spectrum by the spectrometer SP-256. The electron pulse parameters were as follows: 10 ns duration, energy density per pulse up to 0.1 $J \cdot cm^{-2}$, 1.10^{-2}-1.10^{-3} Hz pulse repetition rate. The crystals were irradiated over the interval of 15-300 K, the absorbed dozes varied in range of 10^1-10^5 Gy. The spectral kinetic characteristics of pulsed cathodoluminescence and pulsed photoluminescence (excitation quantum energy equal to 4.66 eV) and the absorption spectra after crystal irradiation have been studied.

LiF –WO_3, LiF- TiO_2, LiF- Fe_2O_3 crystals contain also oxygen in two types of modification: O^{2-} and OH^-. The concentration of free OH^- ions was determined by Smakula formula with oscillation strength 0.942. The concentration of OH^- ions was found to be about 6×10^{17} cm^{-3} for all crystals.

Formation and accumulation processes of color centers in regular lattice of LiF –WO_3, LiF- TiO_2, LiF- Fe_2O_3 crystals are determined by following parameters:

a) concentration of defect regions containing polyvalent cations (W, Fe, Ti)
b) size of nanodefect regione (defect nanostructure)
c) stabilization places of hole centers

TSL EQUIPMENT DEVELOPMENT AND APPLICATION FOR CRYSTALLINE SILICON DIOXIDE STUDY

A.Zolotarjovs, A.N. Trukhin, K.Smits, D.Millers

Institute of Solid State Physics, University of Latvia

Thermostimulated luminescence (TSL) and fractioned glow technique (FGT) equipment were built and measurements on SiO3:Ge crystal carried out.

TSL measurement equipment consists of spectrometer and temperature control module. Equipment is set up in such way, that allows easy modulation of linear heating with different heating rate as well as step-like heating of sample. The cryostats used could be liquid nitrogen cryostat and closed cycle helium cryostat. To acquire spectra Andor Shamrock SR-303I-B spectrometer supplied with Andor IDus CCD camera was used. Equipment setup can be easily modified to resolve specific tasks (e.g. attaching photomultiplier tube).

For software development National Instruments Labview 9 environment was used. For each cryostat different application suite was made, witch allows quick modification of a particular measurement algorithm without affecting the other ones. Various data processing applications were made – output matrix adaptation to fit Origin 8 data analysis environment, the spectrometer lattice correction, as well as some other operations.

Crystalline α-quartz doped with germanium was studied using described above equipment. The sample was chosen because previously it is known that Ge in quartz is effective trap for electrons, there fore it could be used for detection of hypothetic self-trapped hole in α-quartz. However previous investigations of ODMR and TSL [1, 2] shows that in α-quartz the hole still mobile and trapping occurs only on defect states. The TSL peaks below 70K in quartz doped with Ge belong to hole trapped on Ge.

References:

1. W. Hayes, J.T.Jenkin, *Phys. C: Solid State Physics 18* (1985) L849-L853
2. A. N. Trukhin. *Sov. Solid State Physics 28* (1986) 1460-1464

SURFACE RELIEF GRATING RECORDING IN AZO POLYMER FILMS

Jelena Aleksejeva, Janis Teteris

Institute of solid State Physics, University of Latvia,

e-mail: aleksejeva.jelena@gmail.com

In this work holographic recording of surface relief grating in organic Poly(Disperse Red 1 – methacrylate) thin films was studied. In this compound azo dye is chemically bonded to monomers making mass transport very efficient in the presence of optical field gradient [1,2].

Sample preparation was performed using different solvents and coating methods. In the obtained samples holographic recording was performed by solid-state diode pump laser with 532 nm wavelength. Polarization grating and surface relief grating formation was studied by diode laser with 660 nm wavelength. Diffraction efficiency's dependence on read-out laser beam polarization state was investigated. The depth of surface relief grating was measured by AFM and studied in dependence on recording beam intensity, exposure and thickness of the sample.

References

1. L. Rocha, V. Dumarcher, E. Malcor, C. Fiorini, C. Denis, P. Raimond, B. Geffroy, J.-M. Nunzi, *Synthetic Metals*, 2002, **127**, p. 75-79.
2. Shane J. Strutz, L. Michael Hayden, *Journal of Polymer Science: Part B: Polymer Physics*, 1998, Vol **36**, p. 2793-2803.

A comparative DFT study of structural energetics and chemical bonding features in crystalline lithium borates

A. Pishtshev[1], M. Klopov[2]

[1]*Institute of Physics, University of Tartu, Tartu, Estonia*

[2]*Tallinn University of Technology, Tallinn, Estonia*

e-mail: aleksandr.pishtshev@ut.ee

In the present work, by using PAW-PBE GGA functional schemes, we have carried out DFT calculations on the electronic structures of single crystals of the ternary lithium borates $LiBO_2$, LiB_3O_5, and $Li_2B_4O_7$. The electron localization function and effective charges were evaluated to determine the bonding arrangement. The obtained results were used to outline the overall bonding picture in the given materials, and to examine relative strengths and weaknesses of ionic bonds and covalent linkage. Special attention was focused on a comparative analysis of local charge geometries, cation-anion electron transfer, and the interplay between the lattice and electronic degrees of freedom associated with the certain structural and compositional features. In the context of cation substitutions in the Li-B-O systems, the effects of partial H and Cu substitutions for Li in *alpha* and *gamma* phases of $LiBO_2$ were studied.

Acknowledgments

This work was supported by the European Union through the European Regional Development Fund (Centre of Excellence ``Mesosystems: Theory and Applications", TK114). It was also supported by the Estonian Science Foundation grant No 8991.

ENERGY STRUCTURE AND PHOTOELECTRICAL PROPERTIES OF GLASS FORMING PYRANYLIDEN DERIVATIVES IN THIN FILMS

Aivars Vembris[1], Raitis Grzibovskis[1], Kaspars Pudzs[1], Baiba Turovska[2]

[1]*Institute of Solid State Physics, University of Latvia,*

[2]*Latvian Institute of Organic Synthesis*

e-mail of presenting author: aivars.vembris@cfi.lu.lv

Organic solar cells would have such advantages as low cost and simple production compared to inorganic solar cells. Photosensitive part consists of at least two compounds to provide heterojunction - charge separation on interface. Two types of active layer can be made: heterojunction at two layer interface or bulk heterojunction. Thick layer (high absorption) and large interface area (more probable charge separation) is advantages of the bulk heterojunction samples. Nevertheless mismatch of energy levels can reduce charge separation therefore determination of energy structure of the molecules is critical to obtain good heterojunction at the interface.

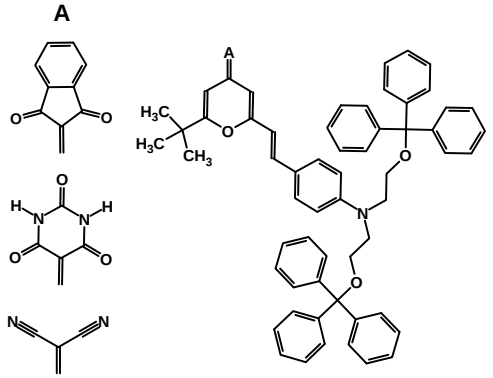

Fig.1 Investigated pyraniliden derivatives.

In the work optical, photoelectrical and photovoltaic properties of thin films glass forming pyranyliden derivatives (see. Fig.1) was investigated. In all cases organic thin films were deposited by spin-coating method. Energetical structure of compounds where studied in solutions by cyclic voltamperogrammes and in sandwich type samples (ITO/ organic compound/ Al). Optical gap and photoconductivity threshold energy of investigated compounds were determined.

Solar cell with the structure ITO/PEDOT:PSS/Organic compound:PCBM/BaF/Al where prepared. Volt-ampere characteristics were measured while illuminating samples by Solar simulator with AM1.5G with at 100mW/cm2 intensity. Influence of molecular structure on energy levels and solar cell efficiency will be discussed.

Acknowledgment:

This work has been supported by the ERAF Project Nr. 2010/0252/2DP/2.1.1.1.0/10/APIA/VIAA/009.

FIRST PRINCIPLES CALCULATIONS OF ZnO CRISTALS DOPED WITH HYDROGEN

A. Usseinov[1], E.A. Kotomin[2], Yu. Zhukovskii[2], Ju. Purans[2], A. Sorokin[2], A. Akilbekov[1]

[1]*L.N. Gumilyov Eurasian National University, Kazakhstan*

[2]*Institute of Solid State Physics, University of Latvia, Latvia*

e-mail: useinov_85@mail.ru

Understanding of the atomic and electronic structure of defective/doped ZnO is of great importance for improving performance of electrodes in optoelectronic devices based on transparent conducting oxides, e.g. LED displays etc. of particular interest is understanding of a role of hydrogen impurities penetrating into ZnO thin films from plasma.

We report results of the *ab initio* modeling of atomic hydrogen in interstitial positions (H_i) of the ZnO structure based on hybrid DFT method (PBE0 exchange-correlation functional) as incorporated into the CRYSTAL-2009 computer code [1] using the supercell model and linear combination of atomic orbitals (LCAO) basis set. This approach allows us to obtain very accurate calculations of the optical gap and defect level positions therein. We compare properties of the hydrogen in the bulk with that on ZnO ($1\bar{1}00$) surface. The defect-induced electronic charge redistribution, lattice distortion, defect formation energy are calculated for the bulk and on the surface, as well as density of electronic states (DOS) and the band structure.

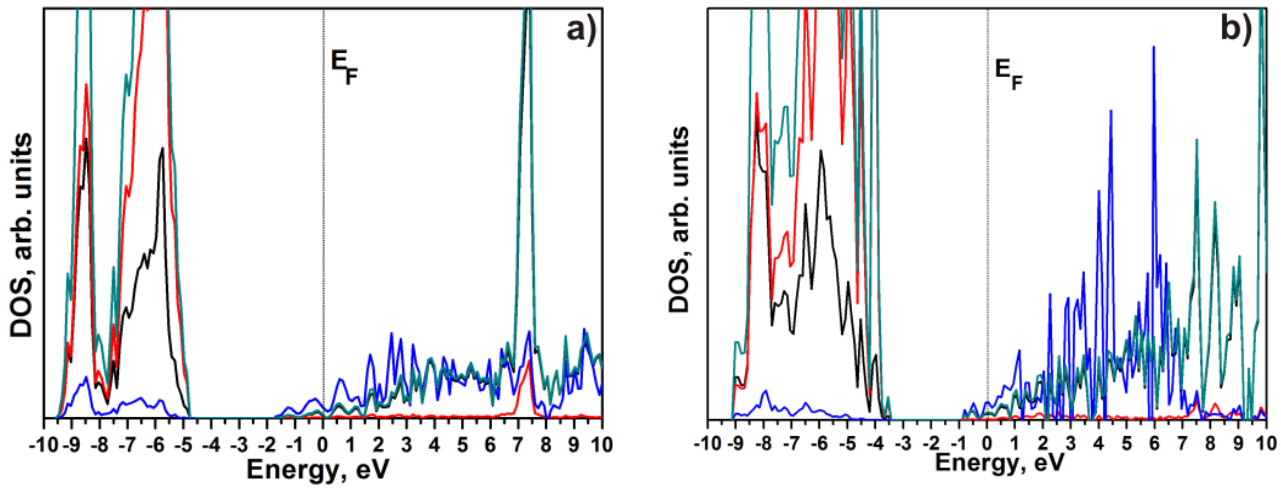

Figure 1. DOS projected onto all orbitals Zn (black), O (red), H (blue), and the total density of states (cyan); a) hydrogen in (2x2x2) supercell ZnO; b) hydrogen adsorbed on the ($1\bar{1}00$) surface of ZnO . For the hydrogen atom PDOS increased by 50 times. E_F - Fermi level.

It is confirmed that H_i in the bulk is a shallow donor with a considerable contribution into the conduction band bottom. At the surfaces hydrogen shows a strong binding to oxygen ions. Despite the charge redistribution the OH bond length in the bulk and on the surface are similar, surface hydrogen contribution into the electronic states of the conduction band is much larger than that in the bulk.

Reference

[1] Dovesi R, Saunders V R, Roetti R, Orlando R, Zicovich-Wilson C M, Pascale F, Civalleri B, Doll K, Harrison N M, Bush I J, D'Arco P and Llunell M 2009 *CRYSTAL09 User's Manual* University of Torino, Torino.

FIRST-PRINCIPLES CALCULATIONS OF ELECTRONIC STRUCTURE AND PHONON PROPERTIES OF Al- AND H-DOPED ZnO

A.V. Sorokine, D. Gryaznov, E.A. Kotomin, J. Purans
Institute of Solid State Physics, University of Latvia, Latvia
e-mail: as08504@lu.lv

Zinc oxide (ZnO) is commonly considered as a promising material for manufacturing of transparent conducting films used in solar cells and LCD screens. Properties of ZnO vary with the concentration and the type of defects and dopants. The main impurities considered important for practical applications are substitutions of Zn with other metal atoms (Al, Ga, etc.) and/or hydrogen atoms substituting for oxygen ions or placed in interstitial positions [1]. In the present first principles calculations we have analysed properties of oxygen vacancy in pure ZnO, as well as those of Al_{Zn}- (substitution for Zn) and H_O- (substitution for O) doped ZnO within LCAO method and hybrid exchange-correlation functional as implemented in CRYSTAL09 code [2]. Our calculations were based on the supercell approach with the concentrations of defects 6.25 % and 2.78 %. Gaussian basis set was optimised for each impurity. Lattice structure of defective ZnO was fully relaxed to calculate phonon frequencies at fixed volume using frozen-phonon method. Impurity-induced phonon modes were carefully identified, and corresponding changes related to their concentrations were analysed. These phonon frequencies were then used to calculate Gibbs free incorporation energies for impurities. In addition, Gibbs free formation energy of oxygen vacancy was also estimated. We demonstrate that phonon contribution to Gibbs free formation energy of oxygen vacancy in ZnO is relatively small, unlike in many other oxides [3]. Notice that our calculations included contribution of van der Waals interactions (using parameters of Grimme and the so-called DFT-D method [4]) to the defect energetics.

This study was supported by ERAF 2010/0272/2DP/2.1.1.1.0/10/APIA/VIAA/088 project

References

1. L. Schmidt-Mende, J. L. MacManus-Driscoll, *Mater. Today* **10**, 40 (2007).
2. R. Dovesi, V.R. Saunders, C. Roetti, et al., *CRYSTAL-2009 User Manual*, Turin:University of Torino (2009).
3. D. Gryaznov et al., *J. Phys. Chem. C* (submitted).
4. S. Grimme, J. Comput. Chem. **27**, 1787 (2006).

NANOCRYSTALLINE TiN FILMS AFTER DEUTERIUM IONS IRRADIATION

A.S. Kuprin, O.M. Morozov, V.D. Ovcharenko, E.N. Reshetnyak, G.N. Tolmachova
National Science Center "Kharkov Institute of Physics and Technology", Kharkov, Ukraine
e-mail: kuprin@kipt.kharkov.ua; morozov@kipt.kharkov.ua

In the present work we studied the influence of irradiation dose of deuterium on the structure and hardness of TiN coatings. The coatings were deposited from filtered vacuum arc plasma [1]. Films with thickness of 5 μm, were deposited on stainless steel samples at a bias potential of -100 V and a nitrogen pressure of 0.4 Pa. Irradiation was carried by ions D_2^+ energy of 24 keV, at dose of 5×10^{16} D/cm^2 to $1{,}5\times10^{18}$ D/см^2 at room temperature. Nanohardness measured at Nanoindenter G200.

High nanohardness (Fig. 1) is typical for vacuum-arc nitride condensates with high compressive internal stresses. Its small decline by 10-15% at doses up to 5×10^{17} D/cm^2 due to the reduction of internal stresses. At doses greater than 1×10^{18} D/cm^2 nanohardness of coatings drastically decreased.

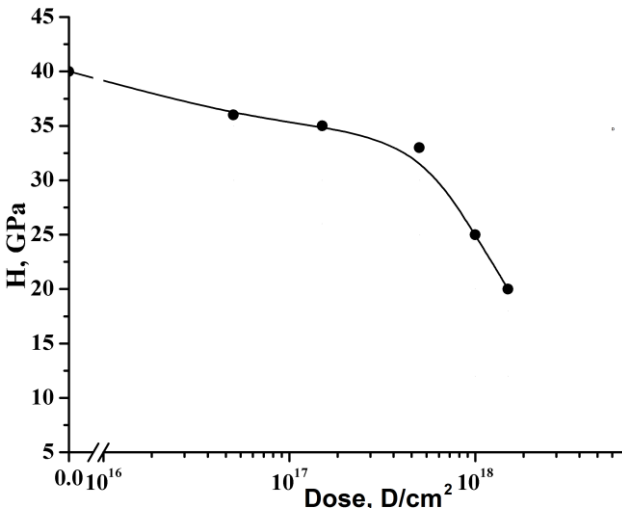

Fig.1. Influence of deuterium irradiation dose on the hardness of TiN coatings.

According to X-ray analysis TiN coatings have a cubic structure of the type NaCl, the crystallite size of ~22 nm. Deuterium implantation by dose of 1.5×10^{18} D/cm^2 led to a shift in the diffraction lines to smaller angles, indicating an increase in the lattice (from 0.43 nm to 0.431 nm), and due to the formation of a solid solution of deuterium in the lattice of TiN. Deuterium desorption temperature range with increasing implantation dose expanded in the direction of decreasing temperature.

References

1. I.I. Aksenov, V.M. Khoroshikh, Filtering shields in vacuum-arc plasma sources. *Proc. TATF"98, Regensburg (Germany)*, 1998, 283-288.

ENGINEERING ASPECTS OF MULTILAYER PIEZOCERAMIC ACTUATORS

V.A. Golovnin[1], I.A. Kaplunov[2], A.I. Ivanova[2], R.M. Grechishkin[2]

[1]*Research Institute ELPA, JSC, Zelenograd, Russia*

[2]*Tver State University, Tver, Russia*

e-mail: rmgrech@yandex.ru

Piezoelectric multilayer monolithic stacks (MLMS) (Fig. 1(*a*)) are increasingly used in a great variety of high-precision actuators and microelectromechanical systems (MEMS) [1]. The application-specific adjustment of the working parameters of the MLMS is achieved by the choice of the piezoelectric material (mainly high-strain PZT ceramics), MLMS geometry, electrode material, etc. The microstructure of the MLMS is defined generally by the sintering process, though the result depends on the composition of PZT and electrode [2].

The volumetric ratio of the PZT/electrode interfaces increases inevitably with the miniaturization trend of the chip devices, so it is imperative to investigate the co-fired interfaces in greater detail. In the present work we study the cofiring process with the aid of scanning electron microscope (JEOL) and X-ray microanalysis (Oxford). Fabrication of the samples included paste preparation, multiple printing and drying, isostatic compression, co-firing, cutting, electrical connection, poling and testing. 70%Ag-30%Pd powders with a liqiudus temperature of ~1150°C served to form the inner electrodes. Typical strain vs voltage hysteresis curve of the prepared samples of 30 mm height is presented in Fig. 1(*b*).

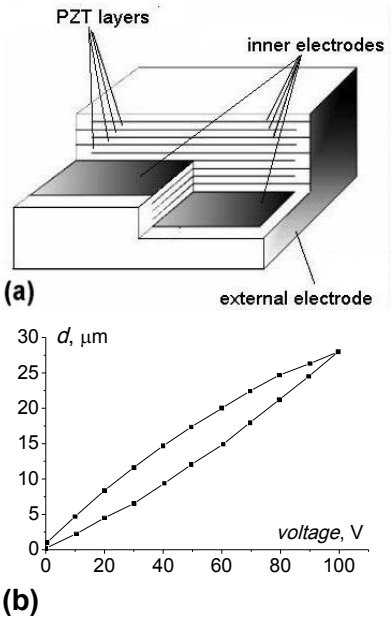

Fig.1 Scheme of the stack actuator (a) and strain vs voltage hysteresis curve (b).

The microanalysis has shown that the atomic composition of the electrode after co-firing coincides with that of the initial Ag-Pd powder except for Pb traces observed in the electrode at distances ≤ 500 nm from the PZT/Ag-Pd interface. 90%Ag-10%Pd paste may be used to decrease the MSML price.

References

1. W. Heywang, K. Lubitz, W. Wersing, *Piezoelectricity – Evolution and Future of a Technology*. Berlin/Heidelberg: Springer, 2008.

2. T. Kühnlein, A. Stiegelschmitt, A. Roosen, M. Rauscher, *Development of a model for the sintering of PZT multilayer ceramics and their dielectric properties, J. Eur. Ceram. Soc.,* 2013, V. 33, 991-1000.

LUMINESCENCE OF STISHOVITE

A. N.Trukhin [1], K.Smits[1], T. I. Dyuzheva [2], L. M.Lityagina [2]

[1]*Institute of solid State Physics, University of Latvia,* [2] *L.F.Verechshagin Institute of High pressure Physics of RAS, Troitsk, Russia*

e-mail of presenting author: truhins@cfi.lu.lv

Stishovite is a dense, octahedral structured crystalline silicon dioxide. Previously found [1] two luminescence bands, a blue one at ~400 nm (~3.1 eV) and an UV one ~260 nm (~4.7 eV). a new luminescence of stishovite we had found now under excitation of F_2 (157 nm), ArF (193 nm), KrF (248 nm) excimer lasers as well as under green diode laser (532 nm). It is a band in near infrared range of spectra (750 – 900 nm). This luminescence possesses several sharp lines showing on quasimolecular nature of corresponding defect. There is zero phonon line at 787 nm (1.57 eV) growing with cooling and anti-stokes line at 771 nm (1.68 eV) disappearing with cooling. The spectrum of luminescence resembles that of defect luminescence in diamond. NIR luminescence is attributed to carbon impurity presence in stishovite, creating some molecular center together with oxygen and silicon. The decay kinetics of NIR luminescence is of long duration (~ 400-800 μs) independent on temperature (studied in the range 8 – 380 K). A long tail of blue luminescence overlaps with NIR luminescence. This tail possesses shorter decay than NIR luminescence and coincides with the blue band main time constant ~17 μs.

Now, we have found that UV luminescence of stishovite (at 260 nm) can be also excited using F_2 excimer laser (157 nm). The intensity and the decay of UV band are independent on temperature in the range 8 – 290 K. Low yield and fast time constant are explained with efficient deactivation of corresponding electronic level of the defect. We ascribe the fast UV luminescence to singlet-singlet transitions whereas slow blue band to triplet-singlet transitions of the same defect.

The UV band of stishovite could be x-ray excited with high energetic yield (~ 10 %) and the intensity of UV luminescence grows significantly during x-ray irradiation time. This could show at least on some transformation of a complex defect from luminescence silent state to active state. X-ray irradiation separates parts of complex defect, liberating luminescence active part, and therefore increases the UV band intensity. Another part of complex defect presumed the carbon related molecular defect and/or OH groups.

References

1. A.N. Trukhin ,T.I.Dyuzheva ,L.M.Lityagina, N.A. Bendeliani, J.Phys.: Condens. Matter 20 (2008) 175206 (5pp).

DIELECTRIC AND ELECTRIC PROPERTIES OF $CuFeP_2S_6$ CRYSTAL

A. Dziaugys[1], J. Banys[1], Yu. Vysochanskii[2]

[1]*Departament of Radiophysics, Faculty of Physics, Vilnius University, Lithuania*

[2]*Institute of Solid State Physics and Chemistry of Uzhgorod University, Ukraine*

andrius.dziaugys@ff.vu.lt

Various ferroic phases were recently shows to occur in the layered compounds AMP_2S_6 (A= Cu, Ag; M= Cr, In;) at low temperatures [1-3]. These compounds consist of lamellae defined by a sulphur framework in which the metal cations and P - P pairs fill the octahedral voids; within a layer, the metal cations and P-P form triangular patterns [2]. In the low temperature phase metal cations sublattice exhibit some kind of ordering. Depending of the type of the ordering, phase transition can be ferrielectric as in $CuInP_2S_6$ [2], antiferroelectric and antiferromagnetic as in $CuCrP_2S_6$ [1]. In disorder (high temperature) phase metal cations exhibit high mobility and can migrate through the lattice. This is main cause of high ionic conductivity in these and similar compounds [4].

In this contribution the broad band dielectric spectra of newly synthesized $CuFeP_2S_6$ crystal are presented. No ferroelectric phase transition was detected by broadband dielectric investigations in the temperature range from 25 K to 300 K. The dielectric dispersion is mainly caused by electrical conductivity. The volume conductivity has been distinguished from contact effect. The DC conductivity has been extracted from experimental results. From this DC conductivity the activation energy has been calculated and compared with $CuCrP_2S_6$ and $CuInP_2S_6$. The frequency dependent anomaly in the temperature range is related with Maxwell-Vagner relaxation.

Acknowledgment

We wish to acknowledge the support of the Research Council of Lithuania funding this work according to the project “Postdoctoral Fellowship Implementation in Lithuania”.

Reference

[1] V. Maisonneuve, C.Payen, V.B Cajipe. Chem. Mater. **5**, 758 (1993).

[2] V. Maisonneuve, V. B. Cajipe, A. Simon, R. Von der Muhll and J. Ravez, Phys. Rev.B **56,** 10860 (1997).

[3] J. Banys, J. Macutkevic, V. Samulionis, A. Brilingas and Yu. Vysochanskii, Phase Transitions **77,** 345 (2004).

[4] J. Macutkevic, J. Banys and Yu. Vysochanskii, phys. stat. sol. a **206,** 167 (2009).

Pulse-EPR studies of transition metal impurities in $SrTiO_3$

D. V. Azamat[1], A. G. Badalyan[2], J. Lancok[1], V. A. Trepakov[1,2], L. Jastrabik[1] and A. Dejneka[1]

[1] *Institute of Physics AS CR, 182 21, Prague 8, Czech Republic*

[2] *Ioffe Physical-Technical Institute, RAS, 194021, St. Petersburg, Russia*

e-mail: azamat@fzu.cz

We use magnetic resonance spectroscopy for the accurate determination of the different oxidation states and local environment of manganese and chromium impurities in $SrTiO_3$. Pulse-electron paramagnetic resonance (pulse-EPR), which is used in our study, offers a direct way to investigate the nature of defects in $SrTiO_3$ and gives a clear indication for spin-lattice relaxation mechanisms.

A multi-frequency (9.3, 34.5, 49 and 70 GHz) EPR study has been performed on $SrTiO_3$ single crystals doped with manganese. The EPR spectra originating from the $S = 2$ ground state of the Mn^{3+} ions are shown to belong to three distinct types of Jahn-Teller centers. The results indicate the strong covalent reduction of the density of unpaired spins (Fermi term) at the manganese nucleus for the various types of centers. Our results show the formation of exchange coupled Mn^{4+} dimers, which are substituted for the second-nearest-neighbor Ti^{4+} sites in $SrTiO_3$ crystals.

The electron spin echo technique has been used to measure the spin lattice relaxation of the most prevalent Cr^{3+} impurities in $SrTiO_3$. The relaxation of longitudinal magnetization is dominated by the sum of two exponentials with two time constants (i.e., a slow and a fast constant) at liquid-helium temperatures. The results of fitting the temperature variation of T_1 suggest that the dominant exponential contribution is related to the spin-phonon relaxation time arising from the local phonon mode.

Acknowledgments

This work was supported by the project SAFMAT CZ.2.16/3.1.00/22132

Synchrotron radiation

VUV SYNCHROTRON RADIATION SPECTROSCOPY OF PLZT CERAMICS

A.I. Popov[1], L. Shirmane[1], V. Pankratov[1], V. Dimza[1], M. Antonova[1],
M. Livinsh[1], A.Kotlov[2] and J. Zimmermann[3]

[1]*Institute of Solid State Physics, University of Latvia, 8 Kengaraga, Riga, LV-1063, Latvia*

[2]*HASYLAB, DESY, Notkestrasse 85, D-22761 Hamburg, Germany*

[3]*Electronic Materials Division, Institute of Materials Science, Darmstadt University of Technology, D-64287 Darmstadt, Germany*

e-mail: popov@ill.fr

Lanthanum-modified lead zirconium titanate ferroelectric ceramics $Pb_{1-y}La_y(Zr_xTi_{1-x})O_3$ (PLZT) are very interesting because of their high optical transparency in optical applications. PLZT ceramics are desirable candidates for most device applications, such as light shutters, modulators, color filters, memories and image storage devices.

In this report, for the first time the luminescence properties of PLZT 8/65/35 compounds well known for relaxor behavior as well as Eu, Co, Cr, Ce, Mn, Ni and Fe doped PLZT were studied under vacuum ultraviolet (VUV) and ultraviolet (UV) synchrotron radiation (3.6 – 25.0 eV) emitted from DORIS III storage ring at SUPERLUMI station at HASYLAB, DESY, Hamburg, in the wide temperature range of 10–293 K.

As it is known for some PLZT, their experimentally determined band gap energy is 3.3 - 3.7 eV and thus use of synchrotron radiation provides ideal conditions for the multiplication of electronic excitations, when each absorbed photon produces two or more electronic excitations. To study this effect, we have measured the appropriate excitation spectra of the intrinsic emission (~600 nm) in the case of undoped, Ce or Eu-doped PLZT, or that of Fe-related emission (~440 nm) in the case of Fe-doped sample.

In all cases, a prominent threshold for excitation multiplication at about 14.0 eV (as high as (3-4) Eg) was discovered. The results obtained are compared with the appropriate reflection spectra, all measured at 10 K. The temperature dependence of the intrinsic emission band was studied in details in temperature range 10-150 K and the appropriate quenching parameters are determined.

A comparison with the results of electronic structure calculations is also presented.

X-RAY EXCITED EMISSION OF YAG AND YAG:Nd^{3+} SINGLE CRYSTALS

Vachagan Harutunyan[1], Vladimir Makhov[2], Eduard Aleksanyan[1,3]

[1]*A.Alikhanian National Scientific Labor. Brs.2,375036 Yerevan, Armenia*

[2] *Lebedev Physical Institute, Leninsky Prospect 53,119991 Moscow, Russia*

3 Institute of Physics, University of Tartu, Riia 142, Tartu, Estonia

e-mail: aeduard@fi.tartu.ee

Yttrium aluminum garnet ($Y_3Al_5O_{12}$ or YAG) is a well-known host material for rare earth (RE) doped active media of solid-state lasers [1]. Besides, Nd^{3+} doped compounds can be considered as promising candidates for application as scintillators [2] or upconverters [3]. Our previous studies [4,5] have shown that YAG crystals doped with RE^{3+} show excellent optical properties because of their low phonon energy (~700 cm^{-1}). The investigation of the optical properties of YAG single crystals under high-energy excitation is of great importance for understanding the physical processes occurring during relaxation of electronic excitation in both pure and Nd^{3+} doped crystals.

In this work we study the nature of emission centers in both pure YAG and YAG:Nd^{3+} (0.5%-1%) under X-ray synchrotron radiation (SR) excitation. Specificity of this method is the participation of many elementary excitations (excitons, electrons-hole pairs) in RE^{3+} excitation. Investigated crystals were grown by the Czochralsky method.

In pure YAG the broad emission band centered at 4.2 eV is observed at 300 K. When temperature drops to 80 K the maximum of the band shifts to 4.6 eV. In fact this low-temperature emission band has a nonelementary shape and can be decomposed into the sum of two bands centered at ~4.7 and ~4.1 eV. These emissions correspond to radiative decay of self-trapped excitons localized at regular and near-defect sites.

The presence of characteristic lines of Nd^{3+} f-f emission in the emission spectrum of YAG:Nd^{3+} indicates that Nd^{3+} luminescence is also efficiently excited under X-ray SR excitation.

References

1. Y. Ma, H. Li, J. Lin, X. Yu, *Optics & Laser Technology*, 2011, Vol. 43, 1491-1494.

2. V.N. Makhov, N.Yu. Kirikova, M. Kirm et.al., *NIM A*, 2002, 486, 437-442.

3. D. Lo, V.N. Makhov, N.M. Khaidukov, J.C. Krupa, J.Y. Gesland, *J. Lumin.*, 2004, 106, 15-20.

4. L. Ning, P.A. Tanner, V.V. Harutunyan, E. Aleksanyan, V.N. Makhov, M. Kirm, *J. Lumin.*, 2007, 127, 397-403.

5. E. Aleksanyan, V. Harutunyan, R. Kostanyan, E. Feldbach, M. Kirm, P. Liblik, V.N. Makhov, S. Vielhauer, *Optical Materials*, 2009, 31, 1038-1041.

TEMPERATURE DEPENDENCE OF ENERGY TRANSFER TO THE LUMINESCENCE CENTERS IN $ZnWO_4$ AND $ZnWO_4$:Mo

N.R. Krutyak[1], V.V. Mikhailin[1,2], A.N. Vasil'ev[2], D.A. Spassky[2,3], I.A. Tupitsyna[4], A.M. Dubovik[4], E.N. Galashev[5], V.N. Shlegel[5], A.N. Belsky[6]

[1]Physics Faculty, M.V. Lomonosov Moscow State University, Russia, [2]Skobeltsyn Institute of Nuclear Physics, M.V. Lomonosov Moscow State University, Russia, [3]Institute of Physics, University of Tartu, Estonia, [4]Institute for Scintillation Materials, NAS of Ukraine, Ukraine, [5]Nikolaev Institute of Inorganic Chemistry SB RAS, Russia, [6]Universite Claude Bernard Lyon 1, France

e-mail: krutyakn@yahoo.com

Zinc tungstate is a perspective scintillation material for the cryogenic scintillating bolometers [1]. High energy resolution, low background level and discrimination between different types of particles makes it suitable for the registration of rare processes such as double beta decay, neutrinoless double beta decay and weakly interacting massive particles [2].

In this work the energy transfer processes to emission centers is studied in $ZnWO_4$ and $ZnWO_4$:Mo single crystals in the temperature range 10-300 K. Nominally undoped $ZnWO_4$ was grown by the low temperature gradient Czochralski technique. $ZnWO_4$:Mo single crystal was grown by the conventional Czochralski method.

The temperature dependence of energy transfer to the intrinsic emission centers in $ZnWO_4$ is connected with the modification of Onsager sphere radius, the numerical simulation describing the process is presented. The competitive role of radiative relaxation channel related to the attendant impurity of molybdenum is studied in $ZnWO_4$:Mo. It is shown that below 60 K the energy transfer of interband excitations to the MoO_6 emission centers is terminated due to the localization of holes at WO_6 complexes.

References

1. H.Kraus, F.A.Danevich, S.Henry, V.V.Kobychev, V.B.Mikhailik, V.M.Mokina, S.S.Nagorny, O.G.Polischuk, V.I.Tretyak, *Nucl. Instr. Meth. A*, 2009, v. 600, 594–598.

2. S.Pirro, J.W.Beeman, S.Capelli, M.Pavan, E.Previtali, P.Gorla, *Phys. Atom. Nucl.,* 2006, v. 69, 2109-2116

LOCAL STRUCTURES AND VALENCES OF DOPANTS IN PERSISTENT LUMINESCENCE MATERIALS

Mika Lastusaari[1,2], Hermi F. Brito[3], Stefan Carlson[4], Jorma Hölsä[1-3], Taneli Laamanen[1,2], Lucas C.V. Rodrigues[1,3], Edmund Welter[5]

[1]University of Turku, Department of Chemistry, Turku, Finland, [2]Turku Center for Materials and Surfaces (MatSurf), [3]Universidade de São Paulo, Instituto de Química, São Paulo-SP, Brazil, [4]MAX-Lab, Lund University, Lund, Sweden, [5]DESY, a Research Centre of the Helmholtz Association, Hamburg, Germany

e-mail of presenting author: miklas@utu.fi

Persistent luminescence is emission observed long after the removal of the excitation source. The best performing materials (*e.g.* $Sr_2MgSi_2O_7:Eu^{2+},Dy^{3+}$) can emit for 24+ h. Though Eu^{2+} is the luminescent center, the roles of the co-doping rare earth (R^{3+}) ions and other lattice defects are still uncertain [1]. The existence and effect of different $R^{2+/3+/IV}$ ions in $MAl_2O_4:Eu^{2+},R^{3+}$ and $M_2MgSi_2O_7:Eu^{2+},R^{3+}$ (M: Ca, Sr, Ba) persistent luminescence materials was studied with XANES and EXAFS. The co-existence of Eu^{2+} and Eu^{3+} in all co-doped materials was observed, but only Eu^{2+} in $CaAl_2O_4:Eu^{2+}$. Eu and R occupied the regular M sites. The co-doping created local structural distortions around Eu^{2+} due to defect aggregation.

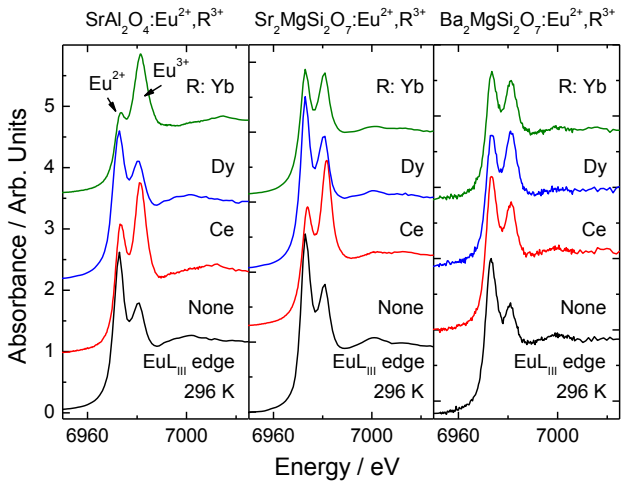

Fig. EuL_{III} edge XANES spectra for Eu^{2+},R^{3+} doped $SrAl_2O_4$ and $M_2MgSi_2O_7$ (M: Sr, Ba) at 296 K.

References

1. H.F. Brito, J. Hölsä, T. Laamanen, M. Lastusaari, M. Malkamäki, L.C.V. Rodrigues, *Opt. Mater. Expr.*, 2012, **2**, 371-381.

LUMINESCENCE STUDIES OF ULTRA-POROUS ALUMINA NANOPOWDERS

Marek Oja[1], Eduard Feldbach[1], Marco Kirm[1], Luc Museur[2], Mohamed Amamra[3], Andrei Kanaev[3]

[1]*Institute of Physics, University of Tartu, Estonia*

[2]*Laboratoire de Physique des Lasers, CNRS, Université Paris 13, France*

[3]*Laboratoire des Sciences des Procédés et des Matériaux CNRS, Université Paris 13, France*

e-mail: marek.oja@ut.ee

Aluminium oxide (Al_2O_3) is widely used technological material in the form of ceramics and single crystals. In addition to well-known and studied α-Al_2O_3 (see [1] and references therein), there are metastable polymorphs (δ, θ, γ etc.) known as transition alumina. The most important transition alumina is γ-Al_2O_3, which is used as a support for metal catalyst due to its high surface to volume ratio. In α-Al_2O_3 all Al ions have only octahedral coordination (AlO_6 units), whereas in transition alumina tetrahedrally coordinated (AlO_4) units can be found. The number of occupied tetra- or octahedral sites varies for different polymorphs, which leads to remarkable differences in their properties. Earlier our group has been studying intrinsic electronic properties of transition alumina for θ-and δ-Al_2O_3 [2] and mixed phase Al_2O_3 powders [3]. It is important to note that preparation of transitions alumina results in samples, which contain several phases thereby complicating data analysis. The main goal of this work is to study electronic properties of transition alumina prepared by another method and compare results to powders obtained using combustion synthesis.

The samples were produced by oxidation of laminated metallic aluminium through a mercury/silver amalgam film, which leads to a formation of nanoporous monoliths with characteristic fibrils diameter of 5 nm of high porosity of ~90% and specific area ~300 m^2/g [4]. Structural analysis of thermally treated hydrated raw alumina confirmed phase purity of α-, γ-, and θ-Al_2O_3 samples. Low temperature time-resolved luminescence spectroscopy under VUV-XUV synchrotron radiation excitation and cathodoluminescence were the main experimental methods. The revealed emission band in VUV at 7.5 and 7.2 eV for α- and θ-Al_2O_3 respectively, were assigned to the radiative decay of self-trapped excitons (STE) like in α-Al_2O_3. In UV-visible region broad emission bands with more distinct maxima at 3 eV and 4.3 eV were revealed. Their decay kinetics and presence of excitation bands below intrinsic absorption (< 9 eV) tentatively assigned to defects as F-centre emission and F^+-centre overlapping with intrinsic STE emission, respectively. The relaxation of electronic excitations and energy transfer processes in transition alumina will be discussed.

References

1. M. Kirm, G. Zimmerer, E. Feldbach, et al, *Phys. Rev. B, 1999*, 60, 502.
2. M. Kirm, E. Feldbach, et al, *Rad. Meas.*, 2010, 45, 618-620.
3. M. Oja, E. Feldbach, A. Kotlov, et al, *Rad. Meas.*, (accepted).
4. J-L. Vignes, C. Frappart, T. Di Costanzo, et al, *J Mater Sci*, 2008, 43, 1234-1240.

PERSISTENT LUMINESCENCE OF CADMIUM SILICATES

Lucas C.V. Rodrigues[1,2], Mika Lastusaari[1,3], Hermi F. Brito[2], Maria C.F.C. Felinto[4], José M. Carvalho[2], Jorma Hölsä[1-3], Oscar L. Malta[5]

[1]University of Turku, Department of Chemistry, Turku, Finland, [2]Universidade de São Paulo, Instituto de Química, São Paulo-SP, Brazil, [3]Turku Center for Materials and Surfaces (MatSurf), [4]Instituto de Pesquisas Energéticas e Nucleares (IPEN), São Paulo-SP, Brazil, [5]Universidade Federal de Pernambuco, Departamento de Química, Recife-PE, Brazil

e-mail of presenting author: lucascvr@iq.usp.br

The most studied persistent luminescence phosphors contain Eu^{2+} as the emitting center [1,2]. In some systems, persistent luminescence is observed to originate from trivalent rare earths (R^{3+}), instead. $CdSiO_3:R^{3+}$ presents persistent luminescence arising from the R^{3+} ions (Tb^{3+}, Pr^{3+}), from defects (La^{3+}, Gd^{3+}, Lu^{3+}) or from both (Dy^{3+}, Sm^{3+}) [3]. Cd_2SiO_4, however, does not show persistent luminescence when doped with *e.g.* Tb^{3+}. To understand this anomaly, the position of $R^{2+/3+}$ levels in the band gap was determined based on the synchrotron radiation (SR) VUV-UV-Vis spectroscopy yielding the band gap and charge transfer energies. For Tb^{3+}, the emitting excited levels are inside CB, and, thus, no persistent luminescence is observed. The position of Pr^{3+} levels suggests that $Cd_2SiO_4:Pr^{3+}$ material should show persistent luminescence, what is observed after ceasing the 300 nm irradiation. Finally, based also on structural data and other SR techniques as XANES/EXAFS, the mechanisms of the R^{3+} doped $CdSiO_3$ and Cd_2SiO_4 persistent luminescence were developed. A better understanding of the mechanisms may be achieved by simultaneous theoretical DFT studies.

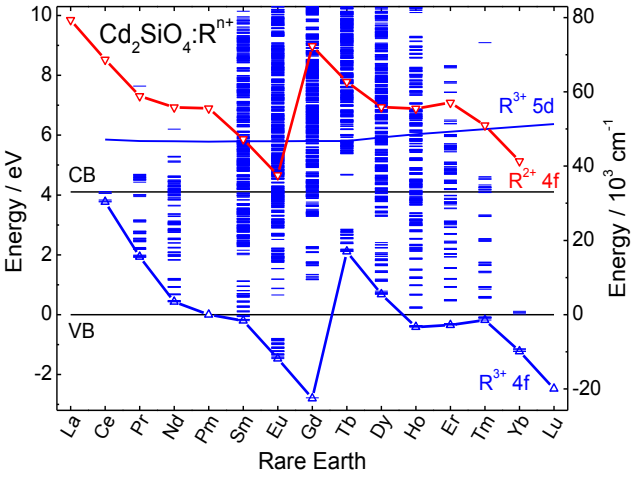

Fig. Location of the $4f^n$ ground and excited levels of $R^{2+/3+}$ in Cd_2SiO_4.

References

1. T. Matsuzawa, Y. Aoki, N. Takeuchi, Y. Murayama, *J. Electrochem. Soc.*, 1996, **143,** 2670-2673.

2. T. Aitasalo, J. Hölsä, H. Jungner, M. Lastusaari, J. Niittykoski, *J. Phys. Chem. B*, 2006, **110**, 4589-4598.

3. H.F. Brito, J. Hölsä, M. Lastusaari, M.C.F.C. Felinto, J.M. Carvalho, L.C.V. Rodrigues, 8th International Conference on f-Elements (ICfE8), August 26-31, 2012, Udine, Italy.

X-RAY SPECTROSCOPY OF $Li_6YB_3O_9$ AND $Li_6GdB_3O_9$ SINGLE CRYSTALS

Ivar Kuusik[1], Tanel Käämbre[1], Arvo Kikas[1], V. Pustovarov[2], Vladimir Ivanov[2]

[1]*Institute of Physics, University of Tartu, Estonia*

[2]*Urat State Technical University-UPI, Yekaterinburg, Russian Federation*

E-mail: ivar@fi.tartu.ee

Borates containing crystals have useful properties and are being widely used for non-linear optical, isolation, luminescence and phosphorescence purposes. Investigators have demonstrated a high efficiency of borate crystals as scintillation materials as well as in neutron detection [1, 2].

Recently special attention is given to complex alkali rare-earth borates, which have anion groups consisting of boron and oxygen. $Li_6YB_3O_9$ doped with rare earth ions is considered to be a promising laser medium [3].

Nonlinear optical (NLO) materials are used (among other non-linear optical processes) for sum and difference frequency generation from lasers. Therefore NLO materials must display some nonlinear susceptibility (usually second or third-order susceptibility). In NLO borates like LBO and BBO the chemical bond is an ionic bond between the cation (Li, Ba) and an anion complex (B_3O_7 and B_3O_6). The anionic groups are considered to be the most basic structural units responsible for optical linearity, and their contributions can be summated to produce the bulk NLO properties [4].

Experimentally the electronic structure of borates has been studied by X-ray photoelectron spectroscopy. However the standard methods based on electron emission (resonant and nonresonant photoemission and Auger spectroscopies) suffer due to the strong charging effects in the wide band gap crystals. In case of the insulating materials it is timely to apply a charge neutral spectroscopic probe. Resonant inelastic x-ray scattering (RIXS) is a photon-only technique performed at soft x-ray absorption resonances making it atomic and orbital symmetry specific also bulk sensitive and thus complementary in many respects to electron spectroscopy.

Thus, we report resonant X-Ray inelastic scattering (RIXS) spectra of $Li_6YB_3O_9$ (LYBO) and $Li_6GdB_3O_9$ (LGBO). The experiments were performed at the beamline I511-3 in the synchrotron radiation facility MAX-Lab, Sweden.

The RIXS spectra excited in the vicinity of the B 1s core resonance show two principal features: the scattering on a valence excitation, which at higher excitation energies verges into the characteristic Kα emission, and a energy loss sideband to the elastic scattering peak. The energy loss shoulder appears to result from lattice relaxation in the absorption site.

References

[1] J. P. Chaminade, O. Viraphong, F. Guillen, C. Fouassier, and B. Czirr, *IEEE Trans. Nucl. Sci*. 48 (2001) 1158.

[2] J. B. Czirr, G. M. MacGillivray, R. R. MacGillivray, and P. J. Seddon, *Nuclear Instruments and Methods in Physics Research A* 424 (1999) 15.

[3] J. Sablayrolles, V. Jubera, F. Guillen, R. Decourt, M. Couzi, J. P. Chaminade, and A. Garcia, *Opt. comm.* 280 (2007) 103.

[4] R. H. French, J. W. Ling, F. S. Ohuchi, and C. T. Chen, *Phys. Rev. B* 44 (1991) 8496.

IONIC LIQUID-BASED SYNTHESIS AND ULTRAVIOLET EXCITATION SPECTROSCOPY OF LUMINESCENT NANOCRYSTALS

V. Pankratov[1], L. Shirmane[1], A. Kotlov[2], A. Kuzmanoski[3], C. Feldmann[3]

[1]*Institute of Solid State Physics, University of Latvia,* [2] *HASYLAB at DESY (Hamburg),*

[3]*Institute of Inorganic Chemistry, Karlsruhe Institute of Technology,*

e-mail of presenting author: vpankratovs@gmail.com

In present work we have summarized results for several types of luminescence nanoparticles (rare earth doped $LaPO_4$, $CaMoO_4$, CaF_2, etc.) having a high practical interest. All nanocrystals in the current study were produced by means of the microwave-assited synthesis in ionic liquids. This synthesis method allows the efficient control of nanoparticles size, their morphology and impurity level [1-3]. The luminescence emission and excitation measurements were carried out under pulsed synchrotron radiation (3.6 – 40 eV) emitted from DORIS III storage ring on the SUPERLUMI station of HASYLAB at DESY (Hamburg, Germany). Special attention was paid to the vacuum ultraviolet spectral range, which is not reachable in standard commercial spectrometers and “in house” equipment. Peculiarities in emission and excitation spectra of luminescent nanoparticles as well as the influence of surface states on luminescence properties of nanoparticle will be demonstrated and discussed.

References

1. G. Bühler, A. Zharkouskaya, C. Feldmann, *Solid State Sci.* **2008**, *10*, 461.
2. V. Pankratov, A.I. Popov, L. Shirmane, A. Kotlov, C. Feldmann, *J. Appl. Phys.* **2011**, *110*, 053522
3. V. Pankratov, A.I. Popov, A. Kotlov, C. Feldmann. *Opt. Mater.* **2011**, *33*, 1102.

ORIGINS OF ROOM TEMPERATURE FERROMAGNETISM AND PHOTOLUMINESCENCE IN CO-CONCENTRATED $CO_XZN_{1-X}O$ FILMS

W. Cao[1], V. Pankratov[1], M. Huttula[1], L. Shirmane[2], Y. R. Niu[3], F. Wang[4],

[1]*Department of Physics, University of Oulu,* [2]*Institute of solid State Physics, University of Latvia,*

[3]*MAX-lab, Lund University,* [4]*Physics and Information Engineering School, Quanzhou Normal University*

e-mail of presenting author: vpankratovs@gmail.com

Novel magnetic materials with possibilities to control both spin and charge simultaneously are strongly desired in the development of future spintronics devices. As one of the most probable candidates, ZnO-based dilute magnetic semiconductor (DMS) was predicted to have Curie temperatures *Tc* above room temperature. Experimental results proved that the room temperature ferromagnetism (RTFM) can be achieved by doping ZnO with the magnetic dopants of the 3*d* transition metal in proper ways. As the theoretically predicted and experimentally verified RTFM material, Co-doped ZnO compound has become a prototype of II-VI-based DMSs. However, origin of the RTFM is very debateful: the Co clustering was referred in earlier time; but recent studies showed RTFM only exists above a certain Co concentration and resulting from the extrinsic defects. In an attempt to get insight into magnetic and the luminescence properties of CoZnO compound, we studied the high Co content $Co_xZn_{1-x}O$ (x = 0.86, 0.92) thin films made through the radio frequency (RF) co-sputtering method. To understand experimental results, synchrotron radiation based photoemission electron microscope (PEEM) was employed to study the electronic structures and the phase-contrast microscopies of the samples. Phase-contrast microscopy was carried out at the energy filtered PEEM endstation located in I311 beamline of the MAX-Lab, (Lund Sweden).

Partial ionization of Co was observed through x-ray absorption spectra near Co *L*3-edge, and contrasts between Co and CoO in microscopies. The RTFM is attributed to Co clustering while photoluminesce caused by defect related centers of ZnO nanoclusters in Co-rich matrix. Present results show the potential of tuning the RTFM and luminescence properties of the metal-ZnO compounds by changing transition metal cluster concentrations and their ionization portions.

PROBING THE LOCAL STRUCTURE OF $ZrO_2:Yb^{3+},Er^{3+}$ UP-CONVERSION LUMINESCENCE MATERIALS BY X-RAY ABSORPTION SPECTROSCOPY

Tero Laihinen[1], Iko Hyppänen[1], Jorma Hölsä[1-3], Jouko Kankare[1], Mika Lastusaari[1,3], Luiz A.O. Nunes[4], Laura Pihlgren[1,5], and Tero Soukka[6]

[1]University of Turku, Department of Chemistry, Turku, Finland, [2]Universidade de São Paulo, Instituto de Química, São Paulo-SP, Brazil, [3]Turku University Centre for Materials and Surfaces (MatSurf), [4]Universidade de São Paulo, Instituto de Física de São Carlos, São Carlos-SP, Brazil, [5]Graduate School of Materials Research (GSMR), Turku, Finland, [6]University of Turku, Department of Biochemistry and Food Chemistry, Turku, Finland

e-mail of presenting author: telaih@utu.fi

$ZrO_2:Yb^{3+},Er^{3+}$ is one of the best up-converting materials providing red emission. Moreover, it shows measurable red afterglow, *i.e.* persistent up-conversion luminescence [1]. To probe the defects, the valences and surroundings of Yb^{3+} and Er^{3+} in $ZrO_2:Yb^{3+},Er^{3+}$ materials were studied with room temperature XANES and EXAFS measurements. The XANES results show only the trivalent form for both the Yb and Er dopants. This indicates that charge compensation must take place as the dopants enter a tetravalent Zr site. The distance distributions calculated from EXAFS (Fig.) indicate the rigidity of the structure but also the presence of oxygen vacancies around Er^{3+} and Yb^{3+} since the R-O distances are expected to shorten due to the decrease in coordination number around the R^{3+} ions owing to the presence of oxygen vacancies.

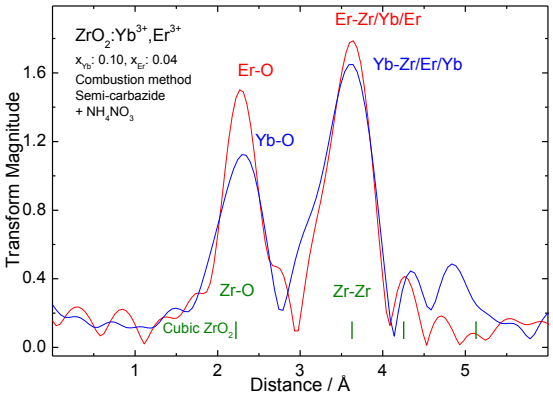

Fig. Distribution of interatomic distances in $ZrO_2:Yb^{3+},Er^{3+}$ as calculated from EXAFS data.

References

1. I. Hyppänen, J. Hölsä, J. Kankare, M. Lastusaari, M. Malkamäki, L. Pihlgren, *J. Lumin.*, 2009, **129**, 1739-1743.

SPECTROSCOPIC PROPERTIES OF Pr^{3+} -BASED POLYPHOSPHATES DOPED WITH Ce^{3+} IONS UPON VUV-UV AND X-RAY EXCITATION

Tetiana Shalapska[1], Gregory Stryganyuk[2], Pavlo Demchenko[3],
Anatoliy Voloshinovskii[3]

[1]*Institute of Physics, University of Tartu, Estonia,* [2]*Helmholtz Centre for Environment Research, Germany,*
[3]*Ivan Franko National University of Lviv, Ukraine*

e-mail of presenting author: tetiana.shalapska@ut.ee

Ce^{3+}-doped inorganic phosphates, owing to their high light yield, short decay time, and high stability, have promising characteristics for their application in scintillation detectors. It is well known that an effective way for the scintillation efficiency increase is to provide an optimal excitation energy transfer from the host lattice to the luminescence centers. In particular, in the case of Ce^{3+}-doped alkali gadolinium phosphates $MGdP_4O_{12}$ (M: Li^+, Na^+, Cs^+) it has been shown that an effective energy migration through the Gd^{3+} sub-lattice and the subsequent energy transfer from a Gd^{3+} ion towards an adjacent Ce^{3+} center lead to the significant increase of the Ce^{3+} luminescence [1,2].

The present work provides studies of the luminescence properties of Ce^{3+}-doped $MPrP_4O_{12}$ phosphates considering the Pr^{3+}-Ce^{3+} pair as a suitable candidate for the increase of the scintillation efficiency. The phosphates were prepared using melt solution technique, and their crystal structures were checked by the X-ray diffraction. The luminescence characteristics of $MPrP_4O_{12}$:Ce^{3+} were studied at 4.2-300 K upon excitation with high-energy quanta of the synchrotron radiation in the VUV-UV range. The analysis of the emission and excitation spectra of $MPrP_4O_{12}$:Ce^{3+} reveals the overlap of the spectral bands, arising from the Ce^{3+} $4f\leftrightarrow5d$ and Pr^{3+} $4f\leftrightarrow5d$ transitions which leads to an effective energy transfer between the Pr^{3+} and Ce^{3+} ions. The shortening of the decay time of the Pr^{3+} emission and the presence of the rise-up stage at the decay curve of the Ce^{3+} emission reflect the presence of the nonradiative $Pr^{3+}\rightarrow Ce^{3+}$ energy transfer in $MPrP_4O_{12}$:Ce^{3+}. The integral light yield of the Ce^{3+}-doped $MPrP_4O_{12}$ phosphates upon the X-ray excitation at RT is determined.

References

1. J. Zhong, H. Liang, Q. Su, J. Zhou, I.V. Khodyuk, P. Dorenbos, *Optic. Mater.*, 2009, 32, 378-381.

2. G. Stryganyuk, T. Shalapska, A. Voloshinovskii, A. Gektin, A. Krasnikov, S. Zazubovich, *J. Lumin.*, 2011, 131, 2027-2035.

VUV PHOTOLUMINESCENCE SPECTROSCOPY SETUP AT MAX III

Sebastian Vielhauer[1], Eduard Aleksanyan[1,2], Eduard Feldbach[1], Marco Kirm[1], Henri Mägi[1], Vitali Nagirnyi[1], Ergo Nõmmiste[1] and Sergey Omelkov[1]

[1]*Institute of Physics, University of Tartu, Tartu, Estonia*

[2]*A. Alikhanyan National Scientific Laboratory, Yerevan, Armenia*

e-mail: sebastian.vielhauer@ut.ee

With a circumference of 36 m and an electron energy of 700 MeV, the MAX III storage ring at MAX IV-lab (Lund, Sweden) is a perfect synchrotron source for VUV and XUV photon generation. The beamline I3 uses an undulator with adjustable gap and phase as a radiation source, and a 6.65 m off-plane Eagle type normal incidence monochromator (NIM) with vertical dispersion [1]. The NIM covers a photon range of ~ 4.5 to 50 eV with a maximum resolving power over 100 000. Two different branches for the monochromatized photon beam are available. The first beamline branch is permanently equipped with an angle and spin resolved photoelectron spectroscopy set-up for solids, whereas the second branch allows for installation of user-supplied end-stations of various kinds [2]. In the second FINEST branch developed by a consortium of Finnish and Estonian Universities, a toroidal mirror provides a focal spot of about 0.6 mm diameter.

For photoluminescence spectroscopy, a set-up consisting of a UHV chamber with a liquid Helium flow cryostat and attached 0.4 m Seya-Namioka monochromator for measurements in the UV and VUV range was developed by our group. To analyse photoluminescence in the UV to near IR range (200 to 1100 nm), a 0.3 m ARC spectrometer equipped with a CCD and PMT is coupled to an optical fibre, collecting emission from the sample. The reflected light can be recorded using luminescence from a sodium salicylate coated metal plate in a near-normal incidence angle. Options for time-resolved measurements are limited due to the time structure of the storage ring with small circumference (only ~10 ns between pulses).

The possibility of high-resolution excitation scanning and the option to change polarisation of the incident light by adjusting the undulator phase make this beamline very attractive for the field of luminescence studies under VUV excitation. Some first results from recent experiments will be shown to showcase the experimental possibilities and limits on wide gap materials.

References

1. T. Balasubramanian, B. N. Jensen, S. Urpelainen, et al., *AIP Conf. Proc*. 2010, **1234**, 661-664.

2. S. Urpelainen, M. Huttula, T. Balasubramanian, et al., *AIP Conf. Proc.* 2010, **1234**, 411 – 414.

Sustainable energetics

CRYSTAL STRUCTURE OF Cu-DEFICIENT PHASES IN THE $(1-x)Cu_2S$-xGa_2S_3 SYSTEM

A.L. Zhaludkevich[1], A.N. Salak[2], A.D. Lisenkov[2], M.L. Zheludkevich[2], M.G.S. Ferreira[2]

[1]*Scientific-Practical Materials Research Centre of NAS, Minsk, Belarus,* [2]*Department of Materials and Ceramic Engineering/CICECO, University of Aveiro, Portugal*

e-mail: salak@ua.pt

In ternary compounds based on CuBX_2 (B=Ga, In; X=Se, Te), formation of defect pairs ($2V_{Cu}^{1-}$+B_{Cu}^{2+}) has been found to be energetically favourable compared to the respective isolated defects in chalcopyrite structure. Such an effect causes appearance of so-called ordered defect compounds (ODCs) with decreasing ratio Cu/B: $Cu_3B_5X_9$, …, CuB_3X_5, CuB_5X_8 instead of continuous solid solutions. The tetragonal unit cell parameters a and c of ODCs depend linearly on m, which is a rate of the ($2V_{Cu}^{1-}$+B_{Cu}^{2+}) pairs per the formula unit CuBX_2. Among the phases which could be considered as ODCs in the $(1-x)Cu_2S$-xGa_2S_3 system, the tetragonal ($I\bar{4}2d$) chalcopyrite $CuGaS_2$ (m=0) as well as the cubic $CuGa_3S_5$ (m=1/5) and $CuGa_5S_8$ (m=1/4) with a zinc-blende structure ($F\bar{4}3m$) have only been reported so far. Besides, it is very likely that the last two compositions are actually solid solutions.

In this work, the phase diagram of the $(1-x)Cu_2S$-xGa_2S_3 system in the Cu-deficient range ($0.50<x<0.80$) was revised. It was found that a direct synthesis from elemental ingredients in a two-zone furnace results in an appearance of the regions with a different Cu/Ga ratio over the crystallization volume. Three particular phases with the crystal structure parameters dependent on x were distinguished. Along with the chalcopyrite phase with some Cu deficiency (up to x=0.55) and the zinc-blende one, a new tetragonal phase $I\bar{4}m2$ of the composition close to $Cu_5Ga_9S_{16}$ ($x\approx0.65$) and the crystal lattice parameters a = 3.7777(2) Å, c = 5.2483(4) Å has been revealed. On the basis of the obtained dependences of the crystal structure parameters on both m and x, it was concluded that, as opposed to the systems Cu-Ga-Se and Cu-Ga-Te, in the system based on sulphur, the ODC phenomenon is unlikely to occur. In this respect, the Cu_2S-Ga_2S_3 system is rather similar to the Ag_2Te-Ga_2Te_3 system, where the same sequence of the non-ODC phases ($I\bar{4}2d$ - $I\bar{4}m2$ - $F\bar{4}3m$) is observed. The likely reasons of the peculiarities of the defect phases derived from $CuGaS_2$ are discussed.

MODIFICATION OF NAFION® MEMBRANE WITH 2-HYDROXYETHYLAMMONIUM IONIC LIQUIDS

Valery Garaev[1], Sanita Pavlovica[1], Guntars Vaivars[1,2]
[1]*Department of Chemistry, University of Latvia, Latvia,*
[2]*Institute of Solid State Physics, University of Latvia, Latvia*
e-mail: valery.garaev@gmail.com

Fuel cells are one of the promising alternative sources of clean energy. Proton exchange membrane fuel cell (PEMFC) is currently selected from many different types of fuel cells for energy back-up systems. A key component of this type of fuel cell is proton exchange membrane (PEM). Nafion® membrane is the commonly used as PEM. High mechanical strength, excellent thermal and chemical stabilities are Nafion® membrane advantages over others PEM. However, Nafion® membrane has high cost and its proton conductivity is decreasing at high temperatures. Therefore, Nafion® membrane needs to be modified. Nowadays, there are many ways how membrane can be modified, e.g., incorporating titanium oxide [1], zirconium phosphate [2], etc. Last trend is to use ionic liquids (IL) due to their high conductivity, good thermal stability and wide electrochemical window.

In this work, 2-hydroxyethylammonium formate [HEA]F, acetate [HEA]A and lactate [HEA]L IL were used for the modification of Nafion® membrane. These IL are non-toxic and highly biodegradable [3]. Composites were prepared by incorporating membrane with IL.

Prepared composite membranes Nafion®/IL are characterized by mechanical testing, such as, tensile test and creep testing. It is found that IL decreases elastic modulus and increases plastic modulus, and it affects on membrane ductility and glass transition temperature. Also, composite membranes were studied by wide angle X-ray diffraction (XRD).

References

1. M. Satterfield, P.W. Majsztrik, H. Ota, J.B. Benziger, A.B. Bocarsly *J. Polymer Sci. B Polymer Phys*., 2006, No. 44, 2327-2345

2. J. Chabé, M. Bardet, G. Gébel *Solid States Ionics*, 2012, No. 229, 20-25

3. A. Zicmanis, S. Pavlovica, E. Gzibovska, P. Mekss, M. Klavins *Latv. J. Chem.*, 2010, No. 3, 269-277

$Cu_2ZnGeSe_4$ MONOGRAIN POWDER AS ABSORBER MATERIAL FOR SOLAR CELLS

Teoman Taskesen, Kristi Timmo, Jaan Raudoja, Inga Leinemann, Maarja Grossberg, Taavi Raadik, Marit Kauk-Kuusik, Tiit Varema, Mare Altosaar,

Institute of Materials Science, Tallinn University of Technology, Ehitajate tee 5, 19086, Estonia

e-mail: teomantaskesen@yahoo.com

In today's climate of growing energy needs and increasing enviromental concern, alternatives to the use of non-renewable and polluting fossil fuels have to be investigated. One such alternative is solar energy. Photovoltaic solar cells are one of the most promising devices to produce clean and renewable energy by converting sunlight directly to the electricity. Absorber materials in solar cells are the *p-type* semiconductors which absorb the sunlight and convert it to the electricity in the contact with an *n-type* semiconductor. One of the possibilities to produce absorber material in powder form with low production cost is monograin powder technology [1].

In this study, $Cu_2ZnGeSe_4$ monograin powder was synthesized from binary compounds in molten KI as a flux material in sealed quartz vacuum ampoules.The phase composition of the powder was determined by X-ray differaction and Raman methods. The bulk composition of powder crystals was determined by EDS. SEM was used to investigate the surface morphology of the monograins. The Raman spectra of the powder showed 3 main peaks at 92 cm^{-1}, 177 cm^{-1} and 204 cm^{-1}. The band gap energy of the absorber material 1.35 eV was determined from the quantum efficiency measurements of MGL solar cells made with the structure of graphite/$Cu_2ZnGeSe_4$/CdS/ZnO. Solar cells were characterized by *I-V* curve measurements. The efficiency of the solar cells was determined.

References :

1. E. Mellikov, M. Altosaar *et al.* Monograin materials for solar cells. *Solar Energy Materials & Solar Cells* 93 (2009) 65-68

CARBON MATERIALS FOR SUPERCAPACITOR APPLICATION BY HYDROTEHRMAL CARBONIZATION OF D-GLUCOSE

T. Tooming, T. Thomberg, T. Romann, R. Palm, A. Jänes and E. Lust

Institute of Chemistry, University of Tartu, 14A Ravila Street, Tartu 50411, Estonia

tauno.tooming@ut.ee

Synthesis of porous carbon materials with fine-tuned properties is essential for the improvement of EDLC technology [1]. Recently, intensive attention has been paid on the use of carbohydrates to synthesis of functional carbonaceous materials by hydrothermal carbonization (HTC) method. The HTC method is very attractive due to its simplicity, require of processing temperature (normally not higher than 300 °C), it is cheap and "green" in nature since it does not involve organic solvents, hazardous reactants or catalysts [2].

Hydrothermal carbonization of 1 M D-glucose solution was carried out in a stainless steel autoclave, which was introduced into a tube furnace and maintained at the temperature 260 ^{0}C for 24 hours for HTC reaction. After cooling down to room temperature, the carbonaceous materials were washed several times with Milli-Q+ water and dried in a vacuum oven overnight. Obtained carbonaceous materials were pyrolyzed and activated using some reagents to fine-tune the porosity of HTC carbons. X-ray diffraction, Raman spectroscopy and high-resolution transmission electron microscopy data revealed that synthesised carbon materials were mainly amorphous; scanning electron microscopy studies demonstrated that carbon materials were consisted of micrometer scale mainly spherically shaped particles maintaining their shape and structure throughout pyrolysis and activation processes. Based on the low-temperature N_2 sorption experiments the specific surface areas up to 1580 m^2 g^{-1} were measured for activated HTC. Various electrochemical methods were used to study influence of carbon materials physical characteristics on the EDLC electrochemical performance based on HTC carbon electrodes in 1 M $(C_2H_5)_3CH_3NBF_4$ in acetonitrile (AN) solution. Electrochemical characteristics obtained for synthesised electrodes show that cyclic voltammetry curves have a nearly rectangular shape up to scan rates ν = 200 mV s^{-1} demonstrating high capacitive values up to 109 F g^{-1}. HTC EDLCs retain about 50% of its initial capacitance even at scan rate ν = 1000 mV s^{-1}, showing excellent characteristics for applications as a high rate supercapacitor electrode materials.

References

1. R. Kötz, M. Carlen, *Electrochim. Acta*, (2000), 45, 2483-2498.

2. M.M. Titirici, A. Thomas, M. Antonietti, Adv. Funct. Mater., 2007), 17, 1010-1018.

COMPARATIVE STUDY OF CdS THIN FILM PROPERTIES ON GLASS AND ITO SUBSTRATES

Natalia Maticiuc, Jaan Hiie, Mart Kukk, Aleksandr Graf, Aleksei Gavrilov

Department of Material Science, Tallinn University of Technology, Estonia

e-mail: nataliamaticiuc@yahoo.com

This paper presents a comparative study of CdS film structural, optical and electrical properties on glass and ITO coated glass substrates (CdS/ITO) when annealed for 1 h in H_2, N_2 and H_2+N_2 atmospheres at 250 ^oC and 400 ^oC. The optically determined CdS film thickness on the glass and ITO coated glass was 405±10 nm and was not influenced by any annealing conditions.

By AFM and SEM was determined that CdS grains were columnar and grown in perpendicular direction to the base. The as deposited films on glass and ITO coated glass had similar one narrow diffraction peak of the (111) cubic plane at 2θ 26.70° and 26.75° respectively, which are near to the peak of the (002) hexagonal plane at 2θ 26.83°. Twice higher XRD peak for CdS/ITO than on glass indicates a more oriented CdS film; this is assigned to the strong influence of ITO unidirectional growth and to the higher density of nucleation centers on ITO compared to glass. The high density of nucleation centers generates denser CdS film on ITO and in the annealing process causes slower shift of the main cubic peak and lattice constant in the direction of pure zinc blend modification in comparision with CdS on glass.

Optical measurements showed approximately similar band gap and transparency (T) for as deposited CdS on both glass and ITO substrates. In the annealing process at 400 ^oC both structures remarkably decreased their T by 5% and 16% for glass and ITO substrates respectively. This phenomenon could be explained by the destruction of hydroxide group in the CdS lattice which resulted in creation of cadmium excess. At high temperature the Cd forms nano-precipitates and reduces SnO_2 to black SnO [1] in the ITO structure.

Strong reduction of T in H_2 annealing for CdS/ITO at 400 ^oC limits applicability of CBD CdS for superstrate configuration of solar cell. Anyway, the strong reduction of T can be minimized by annealing CdS/ITO in a mixture of H_2 + N_2.

References

1. M.S. Moreno, A. Varela, L.C. Otero-Diaz, *Phys. Rev. B*, **48** (1997) 5186.

SYNTHESIS OF Cu_2ZnSnS_4 MONOGRAIN POWDERS IN LIQUID PHASE OF CADMIUM IODIDE FOR PHOTOVOLTAIC APPLICATIONS

M. Pilvet, M. Kauk-Kuusik, J. Raudoja, M. Altosaar, M. Grossberg, K. Timmo, T.Varema, M. Danilson

Institute of Materials Science, Tallinn University of Technology,
Ehitajate tee 5, 19086, Tallinn, Estonia
Phone: +3726203362
maris.pilvet@mail.ee

Abstract

In this work, we investigated the synthesis of Cu_2ZnSnS_4 monograin powders starting from binary compounds and elemental S in the liquid phase of cadmium iodide in evacuated quartz ampoules at 615^{o}C. It is known that Cd from CdI_2 incorporates to the crystals of CZTS forming a solid solution of $Cu_2Cd_xZn_{1-x}SnS_4$ [1]. Use of CdI_2 flux allows us to study the impact of Cd to chemical and structural composition, to electronic properties and to the performance of solar cells based on the synthesized $Cu_2Cd_xZn_{1-x}SnS_4$ monograin powders. In order to study the effect of initial precursor mixtures on the final composition, the ratio of Cu/Sn was changed from 1.6 to 2.0 and the ratio of Zn/Sn was kept constant. The chemical composition of synthesized $Cu_2Cd_xZn_{1-x}SnS_4$ monograin powders was analyzed by energy dispersive X-ray spectroscopy. Compositional studies revealed that concentration of Cd in $Cu_2Cd_xZn_{1-x}SnS_4$ solid solutions depended on the Cu content in precursors. Decrease of the initial content of Cu in precursors increased the substitution of Zn by Cd atoms in the synthesized $Cu_2Cd_xZn_{1-x}SnS_4$ solid solutions from x=0.12 to x=0.21. In the same time, the Cu index in final product stayed almost constant deviating in the very narrow region from 1.91 to 1.93. Phase composition of the powders was determined by Raman spectroscopy. A linear shift of the A_1 Raman mode of $Cu_2Cd_xZn_{1-x}SnS_4$ towards lower wavenumbers with increasing cadmium concentration in powders was demonstrated. The band gap of materials was determined by solar cell quantum efficiency (QE) measurements. According to QE measurements, the band gap of $Cu_2Cd_xZn_{1-x}SnS_4$ solid solutions was shifting to the lower energy side with increasing Cd concentration in absorber material.

[1] Klavina, I. *et al.* Conference proceedings of the Conference of Young Scientists on Energy Issues, (2010), VII 345 - VII 353.

Symposium: E1.II Photovoltaics Processing and Devices

ACIDIC IONIC LIQUIDS AS COMPOSITE FORMING ADDITIVES FOR ION-CONDUCTING MATERIALS

Liga Lasmane, Elina Ausekle, Anda Priksane, Guntars Vaivars

University of Latvia, Department of Chemistry, Latvia

e-mail of presenting author: liga.lasmane91@gmail.com

Rising interest in field of ionic liquids during the last decades has resulted in a great deal of scientific information concerning characteristics of these compounds - covering research about their chemical, as well as physical properties [1].

As an addition to the research regarding electrochemical properties of ionic liquids, several AILs (Acidic Ionic Liquids (Fig.1.)) containing an alkane sulfonic acid group covalently bonded to pyridine and N–alkylimidazole–containing cations have been synthesized in two-step synthesis and examined in this work [2]. In addition three different anions have been introduced in the structure of ionic liquids to evaluate the impact of this factor on material conductivity. Structures of ionic liquids obtained in this work have been determined by ^{1}H NMR and water content by Karl Fischer method. Thermal stability of ionic liquids was controlled by thermogravimetry analysis. Conductivity of ionic liquids was obtained from impedance measurements using Autolab set-up in temperature range 20-120 ^{o}C.

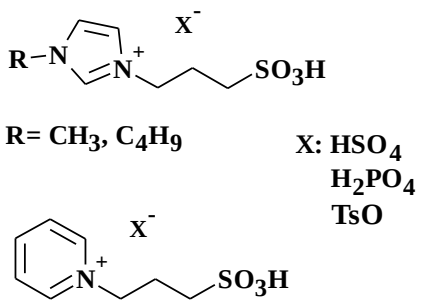

Fig.1 Structures of studied AILs.

References

1. J. P. Hallet, T. Welton, *Chem. Rev*. 2011, 111, 3508-3576.

2. A. C. Cole et. al., *J. Am. Chem. Soc*., 2002, 124, 5962-5963.

LUMINESCENT MATERIALS BASED ON NANOPARTICLES OF OXIDE SILICON FOR SOLAR CELLS

Nurakhmetov T.N., Kuterbekov K.A., [2]Schmedake, T. A., Zhanbotin A., Kainarbay A., Salihodja J.M., Zhunusbekov A.M., Pazylbek S., Bekmyrza K., Daurenbekov D., Baitemirova A.

L.N. Gumilyov Eurasian National University, [2]University of North Carolina at Charlotte, NC

e-mail of presenting author: kainarbay_azh@enu.kz

Conversion of solar emission into electrical energy is performed by semiconductor photovoltaic converter (PVC). Efficiency of conversion is about 25% in the laboratory and 10-15% in the production conditions, which is much inferior to conventional energy sources. Solar silicon cells are sensitive only to a certain spectral range of the continuous spectrum of solar radiation. This is 20-30% of the entire spectral range of the solar spectrum. The increase of efficiency based on silicon is carried out in two directions: - luminescent nanocrystalline films of various sizes are applied on the surface of silicon. The tension that occurs when excited by solar radiation can be removed from each film layer, i.e. electron-hole pairs occur with a different creation energy. This increases the overall efficiency of a PVC with a set of nanocluster films. - luminescent materials that convert ultraviolet and visible solar radiation into the red light, are placed on the silicon surface in the form of a film which is sensitive to the basic silicon PVC. This way the efficiency of PVC based on silicon can be increased. In this report, we discuss the luminescent mesoporous silica oxide particles of activated RE ions and lead sulfide nanocrystals of different sizes. Mesoporous silica particles were synthesized by sol-gel method. The element composition of a particle size of 300 ± 40 nm was identified. Using a scanning electron microscope JOEL-6460LU with the system of energy disperse analysis EDAX. Particle images were obtained using a field scanning electron microscope Raith 150. Additional light scattering method was used as an additional method for the determination of particle size. Brookhaven Corp. Zeta Poential Analyzer was used to measure the surface charge of the particles. Particles in solution were excited by near ultraviolet and visible light. The intensity of intrinsic emission was registered in range of 400-550 nm. Transmission of electron excitation energy of the matrix to the Eu^{3+} and Tb^{3+} was detected. Emission of Eu^{3+} and Tb^{3+} has been registered at 300K. It is assumed that the identical matrixes could work as converters of solar emission spectrum, to which some solar cells are sensitive. The possibility of converting by lead sulfide nanoclusters of solar radiation into the red-orange light has been discussed.

LASER CRYSTALLIZATION EFFECTS IN AMORPHOUS SILICON LAYERS FOR SOLAR CELLS

Julija Pervenecka, Guntis Marcins, Jelena Butikova, Boris Polyakov, Ivars Tale

Institute of Solid State Physics, University of Latvia

e-mail: j.kimmi@inbox.lv

Polycrystalline silicon thin films are popular and widely used in various electronic devices, especially solar cells. In order to improve the efficiency of thin film solar cells, laser crystallization have been studied [1].

In our experiments, silicon p-i-n structures were prepared by plasma-enhanced chemical vapour deposition (PECVD) technology on float glass substrates covered with ITO layer, and then crystallized with the 2nd harmonics of a Nd:YAG laser. The solar cells were characterized by standard current-voltage measurement procedure.

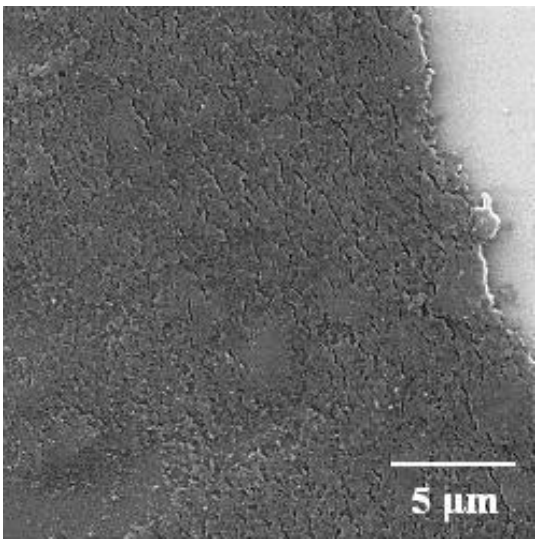

Fig.1. Lateral crystal growth after laser irradiation (532 nm) of the amorphous Si sample [2]

The chosen regime of laser irradiation allows crystallization of all the layers at once. Laser crystallization of the amorphous material leads to the super lateral crystal growth of the polysilicon grains, at the same time activating molecules of the dopants in p-i-n layer. As a result, conductivity increases with the charge carrier mobility, thus improving the performance of laser crystallized solar sells is higher in comparison to the non-crystallized ones.

J.P., J.B., B.P., I.T. are supported by the ERAF project Nr.2010/0252/2DP/2.1.1.1.0/10/APIA/VIAA/009

References

1. G. Schmidl et al., Material Letters **67**, 229 (2012)
2. J. Butikova et al., IOP Conf. Series: Materials Science and Engineering **38**, 012009 (2012)

PREPARATION AND CHARACTERIZATION OF NANOSTRUCTURED Fe-TiO_2 THIN FILMS

Ineta Liepina[1], Gunars Bajars[2], Andrejs Lusis[2], Martins Vanags[2]

[1]*Faculty of Chemistry, University of Latvia, Latvia*

[2]*Institute of Solid State Physics, University of Latvia, Latvia*

e-mail of presenting author: liepina.ineta@gmail.com

Titanium dioxide is a semiconductor photocatalyst that over the last years has been in great interest of study due to its low cost, durability and chemically inert properties. It has a wide range of practical application starting from electrochromic materials to gas sensing devices and solar cell technologies. The wide band gap (E_g = 3.2 eV) limits TiO_2 photocatalytic properties only in UV irradiation so modifications are necessary in order to gain photoactivity in visible light region of the spectrum (~ 40 % of solar radiation). One of options is doping with transition metals - in this case Fe^{3+} (0.64 Å) is a favourable choice since its radius is close to that of Ti^{4+} (0.68 Å). Furthermore iron ions act like hole-electron pair traps and reduce their recombination rate [1].

In this paper Fe-TiO_2 thin films were prepared with electrophoretic deposition (EPD) on titanium foil substrates using working potential ranges from 5 to 40 V. Among other traditional deposition methods (spin coating, spray pyrolysis, sputtering, chemical vapor deposition) EPD has the advantages of obtaining thin films with homogenous coating surface, high porosity and uniform thickness. As-deposited films were heated in 100 °C for 24 h and then annealed at 500 °C for 2 h. The phases and crystalline sizes of obtained Fe-TiO_2 films were determined by X-ray diffraction. X-ray fluorescence was used to establish iron content in thin films. Surface morphologies were analyzed using scanning electron microscopy. Open circuit potential and current density measurements were experimentally carried out as described [2]. Obtained Fe-TiO_2 thin films demonstrate photoactivity under visible light. Photoefficiency was calculated from open circuit potential and current density measurements.

Acknowledgments

Authors acknowledge ERAF projects No.2010/0243/2DP/2.1.1.1,0/10/APIA/VIAA/156 and No. 2010/0204/2DP/2.1.1.2.0/10/APIA/VIAA/010 for financial support.

References

1. X. Lu, Y. Ma, B. Tian, J. Zhang. *Solid State Sci.*, 2011, **13**, 625-629.
2. J. Linitis, A. Kalis, L. Grinberga, J. Kleperis. *IOP Conf. Ser.: Mater. Sci. Eng.*, 2011, **23**, 012010.

THE EFFECT OF THE PROPERTIES OF CARBON MATERIALS ON THE HYDROGEN UP-TAKE

H. Kurig[1], M. Russina[2], D. Wallacher[2], I. Tallo[1], M. Siebenbürger[2], E. Lust[1]

[1]Institute of Chemistry, University of Tartu, [2]Institute Soft Matter and Functional Materials, Helmholtz-Zentrum-Berlin

heisi.kurig@ut.ee

Hydrogen has the potential to replace conventional energy sources, in particular fossil fuels. Effective implementation of a hydrogen-based infrastructure requires major improvements in hydrogen storage technologies. Carbon nanomaterials have been considered as one of the hydrogen storage matrixes and several different types of micro/mesoporous carbons have been studied for this purpose [1]. However, more detailed information is needed to fully understand the effect of nanoporous carbon properties on the adsorption of hydrogen.

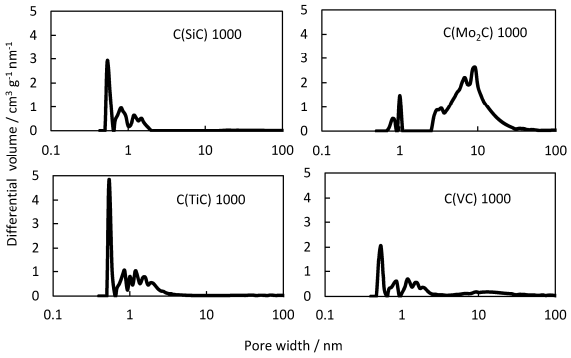

Fig.1 Pore size distributions calculated using non-local density functional theory

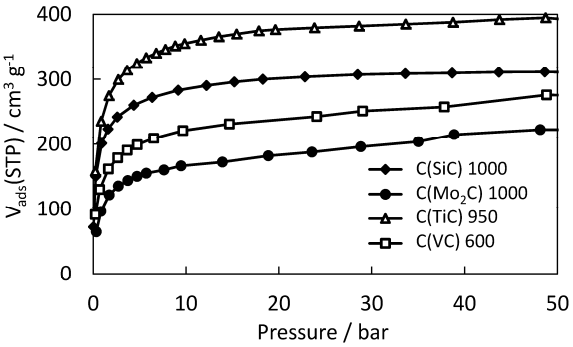

Fig.2 Hydrogen adsorption at 77 K for different carbon materials studied.

Due to the variety in their tuneable porosities and high purity [2], carbide derived carbons are ideal model systems to study the fundamental basics of gas and carbon interactions to gain full understanding of the effect of carbon properties on the H_2 up-take kinetics. For that purpose, four different carbide derived carbons, C(SiC) 1000, C(Mo_2C) 1000, C(TiC) 950 and C(VC) 600, with different pore size distributions have been chosen and fully characterized using gas adsorption, Raman spectroscopy, scanning electron microscopy etc. Also, small angle neutron scattering method has been used to characterize the structure of C(SiC) and C(Mo_2C) carbons. The results obtained have been compared with the H_2 up-take parameters for materials under discussion.

References

1. V. Jiménez, A. Ramírez-Lucas, P. Sánchez, J. L. Valverde, A. Romero, Appl. Surf. Sci. 258 (2012) 2498.

2. Y. Gogotsi (Ed.), Nanomaterials Handbook, CRC Press, (2006).

QUANTICATION OF IMPURITIES IN SOLAR SILICON

Gunita Kolosovska[1], Arturs Viksna[1], George Chikvaidze[2]

[1]*University of Latvia,* [2]*Institute of Solid State Physics University of Latvia*

e-mail: gunita.kolosovska@inbox.lv

About 95% of the current use of solar cell modules is derived from Silicon. Impurities in silicon significantly reduces the efficiency of solar modules. The aim of this work - development of reliable and sensitive method for the detection of impurities in silicon. In cooperation with "BioSan" the laminar flow thermostat-box was made with temperature regulation possibilities up to 50°C, which allows faster evaporation of the sample up to three times. In the thermostat there are two operation modes: a continuous exchange of air and adjustable exchange of air. This significantly reduces the contamination and losses volatile elements of samples during evaporation stage (Table 1).

Table 1. Effect of sample evaporation process on the analysis results for Solar Si samples

Element	In laminar flow thermostat-box		In fume cupboard	
	γ, μg g^{-1}	SD, μg g^{-1}	γ, μg g^{-1}	SD, μg g^{-1}
^{6}Li	0,0227	0,0018	0,016	0,008
^{10}B	1,9	0,2	1,4	0,9
^{31}P	14	2	20	6
^{48}Ti	6,2	0,5	25	9
^{52}Cr	0,015	0,008	0,03	0,02
^{63}Cu	0,043	0,012	0,20	0,10
^{75}As	0,055	0,005	0,013	0,009
^{204}Pb	0,82	0,03	0,5	0,4

Still quantification of impurities in solar Silicon is time consuming using wet chemistry mode. To avoid time consuming sample preparation LA-ICP-MS was used for the determination of impurities in Silicon samples. The obtained results are compared with the measurements obtained on ICP-MS and FTIR spectrometer Vertex 80v. Quantification problems are discused.

Acknowledgements

This work was supported by ERAF Project Nr.2010/0245/2DP/2.1.1.1.0/10/APIA/VIAA/114

PREPARATION AND ELECTROCHEMICAL PROPERTIES OF $LiFePO_4$/C/GRAPHENE NANOCOMPOSITE CATHODE FOR LITHIUM ION BATTERIES

Gints Kucinskis, Karina Bikova, Gunars Bajars, Janis Kleperis
Institute of solid State Physics, University of Latvia
e-mail of presenting author: karina.bikova@inbox.lv

As the worldwide production of lithium ion batteries continues to rise, there is an ever-increasing demand for high capacity, high rate capability lithium ion battery cathode materials. However, many of such materials suffer from low electron and lithium ion conductivity. This study attempts to increase the electron conductivity of $LiFePO_4$ cathode material with one of the best electron conductors available – graphene nanosheets.

$LiFePO_4$/C/graphene nanocomposite has been prepared via solution route by adding graphene oxide and reducing it simultaneously with the calcination of $LiFePO_4$/C precursor. The X-ray diffraction analysis reveals peaks corresponding to the olivine-type $LiFePO_4$ with no apparent maxima corresponding to graphite. Graphene content is determined to be approximately 5 wt. % via thermo gravimetric analysis. Graphene has thoroughly been mixed with the $LiFePO_4$, forming an effective electron-conducting network, as revealed by scanning electron microscopy. Electrochemical properties of $LiFePO_4$/C and $LiFePO_4$/C/graphene samples have been compared in order to determine if graphene can efficiently improve electrochemical characteristics of the $LiFePO_4$ cathode material. The analysis confirms that graphene additive has indeed efficiently improved the rate capability and decreased charge transfer resistance of the cathode. It can be concluded that the excellent electron-conducting properties of graphene have helped to improve the widely researched $LiFePO_4$ even further, suggesting graphene could be one of the most efficient electron-conducting additives for lithium ion battery cathode materials.

Acknowledgments

Authors acknowledge National Research Program in Material Science, Taiwan – Latvia – Lithuania cooperation project "Materials and processing development for advanced Li ion batteries" and European Regional Development Fund project No. 2010/0204/2DP/2.1.1.2.0/10/APIA/VIAA/010 for financial support.

COMPOSITE SPEEK POLYMER MEMBRANES WITH ACIDIC IONIC LIQUIDS FOR HIGH TEMPERATURE PEM FUEL CELLS

Einars Sprugis[1], Hongze Luo[2], Guntars Vaivars[1]

[1]*University of Latvia, Department of Chemistry, Latvia*

[2]*The Council for Scientific and Industrial Research, Pretoria, South Africa*

e-mail of presenting author: einars8@gmail.com

In alternative energy devices the high temperature polymer electrolyte membrane (PEM) fuel cells are of growing importance. It resulted in rising interest in field of ionic liquids as components for polymer membranes due to higher temperature and electrochemical stability [1].

Several AILs (Acidic Ionic Liquids) containing an alkane sulfonic acid group covalently bonded to pyridine and N–alkylimidazole–containing cations have been synthesized in two-step synthesis and used for composite with sulfonated poly(ether ether ketone) (SPEEK) membrane formation [2, 3]. Different approaches for membrane impregnation have been used (from ionic liquid solution in organic solvents, from melted ionic liquid). In addition three different anions have been introduced in the structure of ionic liquids. The effort was made to reduce the water content in membranes.

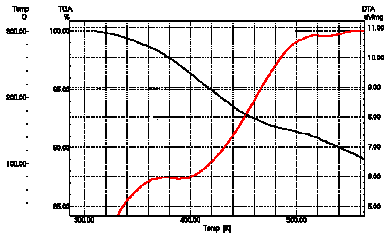

Fig.1. Thermal analysis of sulfonated poly(ether ether ketone) membrane with 1,2-bis-(3-methyl-imidazolium)ethane dibromide.

Composition of membranes obtained in this work have been determined by thermal analysis (Fig. 1) and water content by Karl Fischer method. The impact of ionic liquid on thermal stability of ionic liquids was controlled by thermogravimetry analysis. Conductivity of membrane was obtained from impedance measurements using Autolab set-up and 4-point method in temperature range 20-200 ^{o}C.

References

1. J. P. Hallet, T. Welton, *Chem. Rev*. 2011, 111, 3508-3576.

2. A. C. Cole et. al., *J. Am. Chem. Soc*., 2002, 124, 5962-5963.

3. A. Chandan et. al., *J. Power Sources*., 2013, 231, 264-278.

GLUCOSE OXIDASE AS A BIOCATALYTIC ENZYME-BASED BIO-FUEL CELL USING NAFION MEMBRANE LIMITING CROSSOVER

Sivapregasen Naidoo [1], Qiling Naidoo [2], Harro von Blottnitz [1], Guntars Vaivars [3]

[1] University of Cape Town, South Africa, [2] HySA/Catalysis Competence Center, University of Cape Town, South Africa, [3] Institute for Solid State Physics, Department of Chemistry, University of Latvia, Latvia

e-mail of presenting author: Guntars.Vaivars@cfi.lu.lv

A novel combination for an Enzyme-based Biofuel cell included a Nafion membrane as an ion transporter that maintained a working cell charge and inhibited membrane degradation. The prototype cell chamber used oxygen (O_2) in the cathode cell and glucose in the anode. The Nafion membrane stability studied here was evidently in the region of 0% loss of conductivity as the charge was constant and increased after the addition of glucose. The prototype cell chamber used NaCl in the cathode cell and glucose oxidase (GOx) in the anodic chamber was successfully studied for membrane stability showed in this study no evidence of poisoning from membrane leakage in a controlled pH environment. There was no crossover at the anaerobic operating ambient temperatures and under physiological pH 5 - 7 conditions. In this research we have successfully used a Nafion membrane together with GOx and under controlled conditions produced respectable power densities (30-250µW / cm^2). The acidic properties of Nafion are not conducive for biofuel cell performance due to enzyme inactivation at low pH's; however, the use of NH_4OH to neutralize the sulphonic acids while maintaining the optimum pH of approximately 6.5 was able to ensure longer periods of operation (Fig.1).

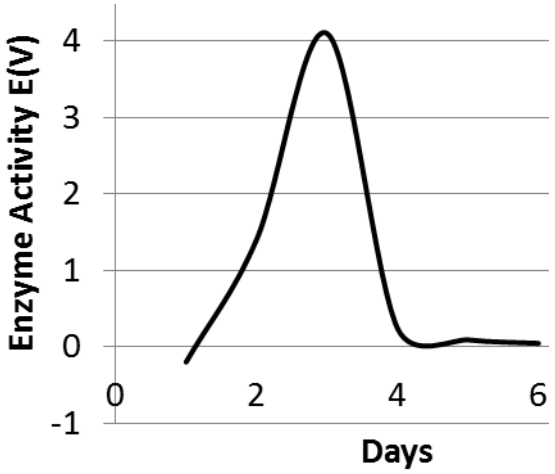

Fig.1 Enzyme activity determined over a period of 6 days.

.

OPTICAL, STRUCTURAL AND PHOTOELECTRIC PROPERTIES OF MULTILAYER TIO2/COFE2O4 THIN FILMS

A.Knoks, J. Kleperis

Institute of solid State Physics, University of Latvia,

e-mail: ainars.knoks@gmail.com

Conventional crystalline silicon solar photovoltaic panels today in the World is the most common, but it is difficult to lower their price due energy-intensive production process of monocrystalline silicon. The second generation of photovoltaic solar cell is based on thin multi-layer system from amorphous silicon or other semiconductor materials with a thickness less than few microns. Thin film solar cells obtained on the metal foil is flexible and can be mounted on different surfaces with large areas - roofs, facades, windows. Typically thin films solar panels are with lower efficiency, faster aging than crystalline silicon panels, therefore it is important to study more different material thin films, their characteristics, multi-layer systems.

Our work is focusing on cobalt ferrite and titanium dioxide thin films, both individually and multilayer coatings (structure, optical and photoelectrical properties). Thin films are obtained by spray pyrolysis, using solutions of cobalt nitrate and ortho-butyl-titanate with various concentrations. Optical properties of obtained films are determined by measuring the absorption spectrum in the near-ultraviolet and visible light ranges and absorption edge is determinate in dependence from the composition of film and multi-layer systems. The structure and elemental composition of obtained films is investigated using XRD and EDAX methods. Photoelectrical properties are measured by recording the open circuit potential change in the presence of ultraviolet and visible light.

Acknowledgement: Authors thanks financial support from National Research Program LATENERGI

Table of contents

Preface		1
International Steering Committee		2
Program comittee		3
Local organizing comittee		3
FM&NT-2013 program		4

Invited talks

Andris Sternberg	Latvian national instruments for material science and nanotechnologies within a framework of Baltic cooperation	12
Anne Kahru	Bio-nano interactions: benefits *versus* environmental and health risks	14
Robert Evarestov	First-principles calculations of single-walled nanotubes in sulfides AS_2 (A = Ti, Zr)	16
Vladimir Makhov	VUV luminescence of wide band-gap solids studied by timeresolved spectroscopy using synchrotron radiation	18
A. Suchocki	Multicenter structure of cerium ions in garnet crystals studied by infrared absorption and high-pressure spectroscopies	20
Miroslav D. Dramićanin	Rare earth doped sequioxide luminescent down- and up-conversion nanopowders prepared by polymer complex solution method	22
Juris Purans	Synchrotron radiation X-ray absorption studies of local structure with femtometer accuracy	24
Alexander Föhlisch	Direct observation of chemical dynamics: photodissociation and surface catalysis	26
Peter V. Sushko	Revealing the character of optical absorption in complex oxides	28
Vitaly V. Mikhailin	Synchrotron radiation in scintillator investigations	30
Suzy Lidström	This is the way it is	32
K. Schwartz	Ion tracks and nanotechnology	34
Marina Popova	Far infrared studies of multiferroic iron borates	36
Vladimir Trepakov	Heavily manganese doped strontium titanate nanoparticles: synthesis, structure and properties	38

Oral talks

Dmitry Spassky	Optical spectroscopy of $Gd_3(Al_xGa_{1-x})_5O_{12}:Ce^{3+}$ epitaxial films	42
Yurii Orlovskii	Fluorescence quenching in the Nd^{3+} doped Y_2O_3 nanoparticles of monoclinic phase	43
Uldis Rogulis	Advances in oxyfluoride glass-ceramics	44
Janis Teteris	Optical field-induced surface patterning of soft materials	45
Andris Ozols	Effect of holographic grating period on its relaxation in amolecular glassy film	46
A.N. Salak	A surface ldh structure grown on Zn-Al alloy	47
Alexander Chaykin	Microscopic crystal field effects in $CsCdBr_3:Ni^{2+}$ crystals	48
Veera Krasnenko	Cubic monocarbides XC (X=Ti, V, Cr, Nb, Mo, Hf) as explored by ab initio calculations	49
A.I. Popov	Photostimulable storage phosphors and image-plate development for neutron imaging	50
A. Belsky	Non-proportionality of luminescence excitated in XUV photon energy range	51
Alexei Kuzmin	EXAFS spectroscopy and first-principles study of $SnWO_4$	52
Janis Timoshenko	Analysis of exafs data from copper tungstate by reverse monte carlo method	53
Andris Anspoks	Local structure studies of $SrTi^{16}O_3$ and $SrTi^{18}O_3$	54
Jaanus Kruusma	Electrochemical *in-situ* xps studies of negatively polarized micromesoporous molybdenium carbide derived carbon double layer capacitor electrode	55
Ilya A. Gofman	Electronic structure and inner shell excited luminescence in gadolinium molybdate crystals	56
R. Drunka	Synthesis and photocatalytic properties of sulfur modified TiO_2 nanopores and nanotubes	57
Urmas Joost	Synthesis of nanoparticles using wet chemistry methods	58
Mikk Antsov	Static friction of CuO nanowires on substrates with varying roughness	59
Mikhail G. Brik	Ab-initio studies of the structural, electronic, optical and elastic properties oF $ZnWO_4$ and $CdWO_4$ single crystals	60
C.-G. Ma	A hybrid computational-experimental spectroscopic analysis of Eu^{3+} ions doped in hexagonal wurtzite ZnS	61

V. Hizhnyakov	Theory and md simulations of intrinsic localized modes and defect formation in solids	62
Anatolijs Sarakovskis	Oxygen related defects and their impact on upconversion processes in $NaLaF_4:Er^{3+}$	63
Eduard Aleksanyan	Luminescence properties of hafnia and zirconia nanopowders prepared by solution combustion synthesis	64
Maido Merisalu	Development of effective atomic layer deposited corrosion resistant coatings for Al 2024-T3	65
Vambola Kisand	Heat treatment effects in case of metal containing titania sol-gel films	66
Yuri Shunin	Electromagnetic properties of interconnects in nanodevices based on CNT, GNR and graphene aerogels	67
G. Zvejnieks	Cellular automata modelling of void latice selforganization in CaF_2 under irradiation	68
Urmas Nagel	Terahertz spectroscopy of the cycloid in multiferroic $BiFeO_3$ in high magnetic fields	69
Toomas Rõõm	Spin waves and directional dichroism in the multiferroic $Ba_2CoGe_2O_7$ probed by THz spectroscopy	70
Boris Hudec	Resistive switching vs. charge trapping in TiO_2-based metal-insulator-metal structures with Al_2O_3 barrier	71
Liga Grinberga	Gravimetric and spectroscopic studies on reversible hydrogen adsorption on nanoporous clinoptilolite	72
Yuri F. Zhukovskii	Modeling of Y-O precipitation in α-Fe and γ-Fe lattices	73
E.A. Kotomin	Prediction of structural stability of complex perovskites for solid oxide fuel cells from first principles	74
Gunnar Nurk	Redox behaviour of sulphur at Ni/GDC SOFC anode at midand low-range temperatures: S K-edge XANES study	75
L. Ardaravicius	High frequency noise in epitaxial graphene on SiC	76
Mikhail Shuba	The influence of finite-size effect on the electromagnetic response of carbon nanotubes	77
Polina Kuzhir	Multi-layerd graphene in microwaves	78
Andris Sutka	Photocatalytic activity of $ZnFe_2O_4$ nanoparticle clusters under visble light irradiation	79
E. D. Politova	Dielectric relaxation in bismuth-containing ceramics	80

Kelli Hanschmidt	Structure and properties of nanocolloidal SnO_2 watersols applied in preparation of optical quality micro- and nanospheres	81
Eriks Klotins	Electron-phonon interactions: spatial localization	82
Mikhail G. Brik	Ab-initio analysis of the (001) surface in cubic $CaZrO_3$	83
Maarja Grossberg	Photoluminescence studies of solar cell absorber material Cu_2ZnSnS_4	84
Marit Kauk-Kuusik	Investigation of quaternary compounds for monograin layer solar cells	85
Teolan Tomson	Formal and technological solar resource in Estonia	86

Commercial

RaithGmbH	Raith	88
Xradia	4D X-ray microscopy(XRM), *in situ* imaging of practical volume samples	89
Park Systems	Polymer Pen Lithography: Massive parallel fabrication of repetitive nanostructures	91
SIA Armgate	Introduction to free liquid surface technology as developed by Elmarco s.r.o.	92
Bruker Baltic	Bruker	93
FM&NT-2013 poster session program		95

Poster Session: Nanomaterials

A. Zhyshkovych	The luminescence of $CaF_2:Eu^{3+}$ nanoparticles	106
Vladimir I. Kondratiev	Sol-gel technics for processing transparent and conductive Al-doped zinc oxide films	107
Viesturs Sints	Nanoparticle transfer under magnetic field in a nonisothermal porous layer saturated with a ferrofluid	108
Vera Serga	Catalytic activity of novel ceria supported nano-sized platinum catalyst synthesized by extractive-pyrolytic method for low-temperature WGS reaction	109
Vera Serga	Production of mono- and bimetallic nanoparticles of noble metals by pyrolysis of organic extracts on silicon dioxide	110
Valdis Kampars	Synthesis and thermal deoxygenation of graphite oxide	111
Veera Krasnenko	Conjoined structures of carbon nanotubes and graphene ribbons	112
Triinu Taaber	Novel anti-wear lubricant based on nanoparticles/ionic liquid combination	113
Jana Grigorjeva	Spectral characterization of AlGaN nanomaterials with tunable bandgap	114
Toomas Plank	Technet_nano – the cooperation network of clean rooms in baltic sea region	115

Tõnis Arroval	Atomic layer deposition of nanostructural TiO_2 films on Si, α-Al_2O_3 and RuO_2	116
Tauno Kahro	Temperature induced reversal of oxygen response in CVD graphene on SiO_2	117
Tatjana Dedova	Growth of zinc oxide nanostructured layers on SnO_2 electrodes by spray pyrolysis	118
Tatjana Dedova	Nanostructured layers of zinc sulfide obtained by spray pyrolysis	119
Tanel Käämbre	Iron oxide nanoparticles by precipitation from ferrous source: structural phase transformation dependence on synthesis parameters and annealing	120
Taivo Jõgiaas	Atomic layer deposition of aluminium oxide on silicon carbide nanopowder	121
Svetlana Vihodceva	Improvement of UV protection properties of the textile from natural fibres by the sol-gel method	122
Silver Leinberg	Aligning nano-wires for anisotropic spectral properties	123
Siim Heinsalu	Core-shell silica-gold nanoparticles for control of fluorescence in the sol-gel films activated by rare earth	124
Sergey Tsarenko	Generation of metal nanoparticles in cathode spots of pulsed discharges	125
Sergey Plotnikov	Segregation on the surface of titanium steel 12Cr18Ni10Ti exposed electron beam	126
Šarunas Svirskas	Dielectric and ultrasonic investigations on polyurea elastomers with embedded inorganic nanotubes	127
Šarunas Svirskas	Broadband dielectric spectroscopy of PVDF polymers embedded with ferrite nanoparticles	128
Santa Stepina	Ethylene vinylacetate copolymer and nanographite composite as chemical vapour sensor	129
Sanja Ćulubrk	Synthesis of Eu and Sm doped Y_2O_3 nanophosphors by room temperature self-propagating reaction	130
R. Zabels	Structural and micromechanical changes in MgO after high-dose irradiation with swift heavy ions	131
Raul Rammula	Atomic layer deposition of aluminum oxide films on graphene	132
Rainer Pärna	Influence of iodine doping and annealing on the properties of sol-gel prepared thin titania films	133
R. Mackevičiūtė	Dielectric properties of nanograin BSPT caramics	134
Pavel Merzlyakov	Statistical analysis of void lattice formation in CaF_2	135
Olga Malyshkina	Conoscopic study of strontium-barium niobate single crystals	136
O.M. Morozov	Deuterium desorption temperature from Mg-Ti composites prepared by method of atom-by-atom mixing of components	137
Nina Mironova-Ulmane	Neutron scattering study of structural and magnetic size effects in NiO	138
Nadzeya Valynets	Exfoliated graphite composites: microwave applications	139

Mikk Vahtrus	Two point electrical measurements of 1D nanostructures	140
Meeri Visnapuu	Dissolution-dependent antibacterial effects of silver nanowires	141
Maksim S. Shashkov	Examination of dielectric dispersion of complex oxides on the basis of bismuth-containing titanates	142
Madis Umalas	Elaboration of alumina nanofibers reinforced yttria stabilized zirconia nanocomposites by sol-gel method	143
Madis Paalo	Preparation and characterization of electrically conductive metal oxide CNT-composites by sol-gel method	144
Lauri Aarik	Titanium dioxide thin films grown from titanium chloride and ozone by atomic layer deposition	145
Larisa Grigorjeva	Characterization of hydroxiapatite by time-resolved luminescence and FTIR spectroscopy	146
L.Kuznecova	Spark plasma sintering (SPS) of nanosized zirconia powders, obtained by azeotopic distillation	147
Krisjanis Smits	Rare earth doped zirconia nanostructured transparent ceramics	148
Konstantins Dubencovs	Novel fine-disperse bimetallic Pt-Pd/Al_2O_3 catalysts for glycerol oxidation with molecular oxygen	149
Kaspar Roosalu	Investigation of Ti doping effect on stabilization of R'-plane oriented epitaxial Cr_2O_3 thin films on R-plane sapphire	150
Kaido Siimon	Development of nanofibrous 3D collagen/polyaniline composites as tissue engineering scaffolds	151
Kaarel Piip	Influence of He/ D_2 plasma fluxes on tungsten coatings morphology and crystallinity	152
Juris Katkevics	Impedance and admittance characteristics of Bi_2S_3 nanowire arrays	153
Jekaterina Kozlova	Characterization of graphene prepared by chemical vapour deposition on nickel	154
Janis Timoshenko	Two limits of electron capture in a dynamic quantum dot	155
Janis Maniks	Structure, micromechanical and magnetic properties of polycarbonate nanocomposites	156
Janis Maniks	Modification of LiF structure by irradiation with swift heavy ions under oblique incidence	157
Janis Kleperis	Electrodeposition of nanoporous nickel layers using inductive voltage pulses	158
J.Kalnacs	Chemical vapor deposited graphene adsorbtion ability	159
Janis Grabis	Characteristics of stabilizied zirconia nanoparticles prepared by molten salts and microwave synthesis	160
Jan Macutkevic	Electrical percoliation in onion like carbon composites	161
Jan Macutkevic	Influence of preparation technology on the dielectric properties of carbon nanotubes polymer composites	162
Ivan Zakharchuk	Magnetic moment of single vortices in YBCO nanosuperconducting particles: eilenberger approach	163
Ivan Netšipailo	Corrosion protection of metals using multilayer thin films based on TiO_2 and Al_2O_3 grown by ALD	164

Indrek Tallo	Hydrogen chloride as a possible reactant for synthesis of titanium carbide derived carbon powders for high-technology devices	165
Ieva Kranauskaite	Dielectric spectroscopy of graphite loaded epoxy resin composites	166
Guntis Japins	Manufacturing, structure and properties of recycled polyethylene terepthalate/liquid crystal/montmorillonite clay nanocomposites	167
Erkki Lähderanta	Transport properties of indium antimonide with magnetic nanoprecipitates	168
Dziugas Jablonskas	Dielectric and ultrasonic investigations of composites of poly(ε-caprolactone) and $Mo_6S_3I_6$ nanowires	169
Dmitry Kuruch	Nanotubes folded from cubic and orthorhombic $SrZrO_3$: first-principles study	170
Dmitry Zablotsky	Numerical investigation of arrays of concentration microstructures in dispersions of magnetic nanoparticles	171
Daulet Sergeyev	The influence of external weak magnetic field on anharmonic nanocontacts of Josephson type	172
A. Vīksna	Preparation of short range ordered nanodot arrays and analysis of particle optical properties	173
Andrei Bandura	Force-field choice for the simulation of TiO_2- and ZrO_2-based nanotubes	174
Anastasija Ivanova	Near-infrared sensitive organic solar cell	175
Alexandr Popov	Spectroscopy of the $5d^1$-$4f^1$ transitions of Ce^{3+} in nanocrystalline xenotime- and rhabdophane-type yttrium phosphates	176
Alexander Vanetsev	Microwave-hydrothermal synthesis of nanocrystalline xenotime- and rhabdophane-type yttrium phosphates doped with Ce^{3+} ions	177
Alar Jänes	Surface analysis of supercapacitor electrodes after long-lasting constant current tests	178
Aile Tamm	Atomic layer deposition of hafnium and zirconium oxides on carbon nanoparticles	179
Agnese Grigalovica	Explotitation and structural properties of modified polyacetal nanocomposites	180
A.I. Popov	Cathodoluminescence study of Al-doped ZnO nanofilms	181
Patrick Martin	Femtosecond excitonic dynamic and relaxation in solid ZnO: dependence of the luminescence decay time on nano particles size and excitation mode	182

Poster Session: Multifunctional materials

A.M. Pashaev	On the Possibilities for Improving the Efficiency of Radiation in Heterostructures Based on the IV-VI Semiconductors	184
Włodzimierz Śmiga	Investigation of Mechanical and Electrical Properties of Li Doped Sodium Niobate Ceramic System	185
Vladimir Lisitsin	Dielectric and Pyroelectric Properties of Calcium-Barium Niobate Single Crystals	186
Vladimir Ivanov	Luminescence of $LaBr_3$:Ce,Hf Scintillation Crystals under UV-VUV-XUV and X-Ray Excitation	187
Virginija Liepina	Investigation of Luminescence Mechanism of Persistent Strontium Aluminate Phosphor	188
V.Dimza	The Effect of Cu Admixture on Relaxor Properties of The PLT8/65/35 Electrooptical Ceramics	189
Vera Skvortsova	Optical Properties of Natural Topaz	190
V.S. Levushkina	Luminescent Properties and Energy Transfer in $Y_xLu_{1-x}PO_4:Re^{3+}$ (Re = Eu, Ce) Solid Solutions	191
Ugis Gertners	Optical-Field Induced Surface-Relief Formation Phenomenon in Thin Films of Vitreous Chalcogenide Semiconducors	192
Triin Kangur	Cell Growth on Patterned Surfaces Prepared by a Novel Sol-Gel Phase Separation Method	193
Svetlana Zazubovich	Electron and Hole Centers in X-Ray- or UV-Irradiated Oxyorthosilicate Crystals	194
Sergey Nikoghosyan	The Effect of Aging on the Superconducting Transition Temperature And Resistivity Of Y-Ba-Cu-O Ceramics After High Temperature Treatment	195
Santa Popova	Optical and Electroluminescence Properties of Tercbutil Group Containing Piraniliden Derivatives	196
Rimas Janeliukstis	Improvement of CdS Film Optical Properties by Laser Radiation for Application in Solar Cells	197
Reinis Ignatans	Structure and Dielectric Properties of $Na_{1/2}Bi_{1/2}TiO_3$-$BaTiO_3$ Solid Solutions in the Phase Transition Region	198
Raul Välbe	Modification of Carbon Nanotubes and Cellulose Cotton Fibers Using Hybrid Ionic Liquid – Sol-Gel Approach	199
Raul Laasner	Band Tail Absorption Saturation In $CdWO_4$ with 80-fs Laser Pulses	200
Rasmus Talviste	Atmospheric Pressure Plasma Jet in Microtubes	201
R.M. Grechishkin	Laser Conoscopy of Large-Sized Optical Crystals	202
R. Mackevičiūtė	Dielectric and Impedance Spectroscopy of Fe Doped $0.94(Na_{0.5}Bi_{0.5}TiO_3)$-$0.06BaTiO_3$ Ceramics	203
R. Mackevičiūtė	High-Frequency Dielectric Properties of $Pb(Fe_{1/2}Nb_{1/2})O_3$ Ceramics and Single Crystal	204
Peet Konsin	Semi-Microscopic Vibronic Theory of Quantum Paraelectricity and Ferroelectricity	205
Nurgul Zhanturina	The Influence of Elastic Stress on the Surface of Adiabatic Potential of KI Crystal at Fixed Temperatures	206

Nikolajs Ponomarenko	The Study of Correlation Between Microstructure of Ferrites and their Complex Permeability Spectra	207
Gunta Kizane	Tritium retention studies in W coated JET divertor CFC tiles	208
M.Narels	Influence of Temperature on Photoisomerisation Process of Polymer Films Doped by Azobenzene Derivatives	209
Marko Part	ZrO_2 Microtubes As Substrates in ALD Processes	210
Maris Springis	Green Luminescence Decay Kinetics Analysis in $NaLaF_4:Er^{3+}$	211
Marija Dunce	Phase Transitions and Physical Properties in Ca Modified $Na_{1/2}Bi_{1/2}TiO_3$-$SrTiO_3$-$PbTiO_3$ Solid Solutions	212
Margarita Baitimirova	Characterization of Functional Groups of Airborne Particulate Matter	213
M. Reinfelde	Influence of Grating Period on Surface Relief Hologram Recording Efficiency in Amorphous AS_2S_3 and $AS_{40}S_{15}SE_{45}$ films	214
Maksims Polakovs	Influence of Radiation on EPR and Optical Spectroscopy of Human Blood	215
M. Zubkins	Hall-Effect Studies in Doped ZnO Thin Films	216
M. Kinka	Dielectric Properties of $Ba_2NdFeNb_{3,7}Ta_{0,3}O_{15}$ Solid Solution	217
Liga Freivalde	Hemp Fiber Non-Wovens Properties Analysis	218
Liga Avotina	Analysis of Fullerene C_{60} Possible Formed in the Divertor Area of a Tokamak Like Devices	219
Laurits Puust	Afterglow and Thermoluminescence of ZrO_2 Nanopowders	220
Kuanyshbek Shunkeyev	Exciton-Phonon Interaction in Alkali Halide Crystals at Low Temperature Uniaxial Elastic Stress	221
Kuanyshbek Shunkeyev	Specificity of Stabilization of H^- Centers in Crystal KBr at Low Temperature Deformation	222
Kristel Möldre	Real-Time Optical Characterization of Atomic Layer Deposition of Dielectrics on Graphene	223
K. Klismeta	Photoinduced Mass Transport in Azo-Benzene Containing Compounds	224
Kirils Surovovs	Modelling of Crust Thickness for Silicon Purifying Process with Electron Beam	225
Kaspars Traskovskis	Triphenylpentane Substituents Containing Molecular Glasses with Nonlinear Optical Activity	226
Kaspars Pudzs	Charge Carrier Mobility in Thin Films of Glass Forming Low Molecular Organic Compounds	227
Kaiva Luse	Reflectance and Multispectral Evaluation of Color Vision Asessment Plates	228
Kairi Otto	Effect of Titanium(IV)Isopropoxide and Acetylacetone Molar Ratio in the Solution on Spray Deposited TiO_2 Films	229

K.Konieczny	Influence of Compressive Stress on Dielectric and Ferroelectric Properties of the $(Na_{0.5}Bi_{0.5})_{0.7}Sr_{0.3}TiO_3$ Ceramic	230
K. Chernenko	The Effect of Annealing on Spectra and Decay Time of X-Ray Luminescence of Zinc Oxide Powders	231
K. Bormanis	Photorefractive Light Scattering In $LiNbO_3$:B, $LiNbO_3$:Y, $LiNbO_3$:Y:Mg, and $LiNbO_3$:Ta:Mg Crystals	232
K. Bormanis	Ferroelectric Lead Nickel-Niobium Titanate Ceramics: Phase Transition Studies	233
M. Antonova	Effects of Illumination on the Dielectric Response of Barium-Strontium Niobate Ceramics	234
Jurgis Grube	Up-Conversion Luminescence of $NaLaF_4$ Doped With Tm^{3+} And Yb^{3+}	235
Janis Latvels	Photoelectrical Properties of DMAB Derivatives as Materials For Solar Cells	236
Jakob Jõgi	Role of Diffusion in Formation and Properties of Sol-gel Micro-Structures	237
J.Gabrusenoks	Lattice dynamics of $CdWO_4$	238
Ivo Romet	Thermally and optically stimulated luminescence in $Li_2B_4O_7$ doped with metal ions	239
Ingars Reinholds	The effect of radiation modification on properties of poly(ethylene-1-octene) magnetic nanocomposites	240
Ieva Kranauskaitė	Broadband dielectric investigation of $(Sr_{1-1.5x}Bi_x)TiO$ (x=0.15, 0.1, 0.05)	241
Irina Kudryavtseva	Electronic excitations and self-trapping of electrons in $CaSO_4$	242
I. Smeltere	Features of lithium niobate single crystals modified by rare earth admixtures	243
Harijs Cerins	Improvement of sol-gel deposited ZnO:Al thin films by laser radiation	244
Guna Doke	Synthesis and photoluminescence in Eu^{3+} doped $NaLaF_4$ material	245
George Chikvaidze	Raman scattering analyses of defects in SiC	246
Galyna Dovbeshko	Strong secondary emission of opal-based photonic crystal: light localization and defect luminescence	247
Fatima U. Abuova	First-principles calculations of defects in MgF_2	248
Elina Potanina	Photo-induced formation of surface relief in amorphous AS_2S_3 films	249
Edvins Dauksta	Improvement of CdZnTe detector properties by laser	250
E.V. Barabanova	Effect of porosity on the electrical properties of PZT ceramics	251
Dorota Sitko	Dielectric properties of $BaTiO_3$ based materials with addition of transition metal ions with variable valence	252
Dmitry V. Azamat	Fourier transform-EPR spectroscopy of transition metal ions in ZnO	253
Barbara Garbarz-Glos	Structural, microstructural and dielectric spectroscopy study of functional ferroelectric ceramic materials based on barium titanate	254

Aurimas Sakanas	Broadband dielectric investigation of barium titanate and nickel-zinc ferrite composite ceramics	255
Arturs Zarins	Influence of Li_2TiO_3 on chemical reactivity of Li_4SiO_4 pebbles	256
Ansis Mezulis	Application of sedimentation experiments with suspended nanoparticles	257
Annika Pille	Investigation of iodine implanted C12A7 ceramics	258
Anna Putnina	Multifunctional materials from hemp fibers treated with steam explosion technology	259
Andris Lescinskis	Experimental setup for analysis of sorption and desorption of tritium in liquid lithium under different external conditions	260
Andrejs Lusis	Investigation of carbonized layer on surface of NaAlSi glass fibers	261
Andrejs Gerbreders	Photosensitive properties of composite films based on copper chloride in polymer matrix	262
R. Kassymkanova	Pecularities of defect creation in LiF-WO_3, LiF- TiO_2 and LiF-Fe_2O_3 crystals under pulsed electron irradiation	263
A. Zolotarjovs	TSL equipment development and application for crystalline silicon dioxide study	264
Jelena Aleksejeva	Surface relief grating recording in AZO polymer films	265
Aleksandr Pishtshev	A comparative DFT study of structural energetics and chemical bonding features in crystalline lithium borates	266
Aivars Vembris	Energy structure and photoelectrical properties of glass forming pyranyliden derivatives in thin films	267
A. Usseinov	First principles calculations of ZnO crystals doped with hydrogen	268
A. V. Sorokine	First-principles calculations of electronic structure and phonon properties of Al- and H-doped ZnO	269
A.S. Kuprin	Nanocrystalline tin films after deuterium ions irradiation	270
A.I. Ivanova	Engineering aspects of multilayer piezoceramic actuators	271
A. N.Trukhin	Luminescence of stishovite	272
Andrius Dziaugys	Dielectric and electric properties of $CuFeP_2S_6$ crystal	273
Dmiri Azamat	Pulse-EPR studies of transition metal impurities in $SrTiO_3$	274

Poster Session: Synchrotron radiation

A.I. Popov	VUV synchrotron radiation spectroscopy of PLZT ceramics	276
Eduard Aleksanyan	X-ray excited emission of YAG and YAG:Nd^{3+} single crystals	277
N.R. Krutyak	Temperature dependence of energy transfer to the luminescence centers in $ZnWO_4$ and $ZnWO_4$:Mo	278
Mika Lastusaari	Local structures and valences of dopants in persistent luminescence materials	279

Marek Oja	Luminescence studies of ultra-porous alumina nanopowders	280
Lucas C.V. Rodrigues	Persistent luminescence of cadmium silicates	281
Ivar Kuusik	X-ray spectroscopy of $Li_6YB_3O_9$ and $Li_6GdB_3O_9$ single crystals	282
V. Pankratov	Ionic liquid-based synthesis and ultraviolet excitation spectroscopy of luminescent nanocrystals	283
V. Pankratov	Origins of room temperature ferromagnetism and photoluminescence in co-concentrated $CO_XZn_{1-X}O$ films	284
Tero Laihinen	Probing the local structure of ZrO_2:Yb^{3+},Er^{3+} up-conversion luminescence materials by X-ray absorption spectroscopy	285
Tetiana Shalapska	Spectroscopic properties of Pr^{3+} -based polyphosphates doped with Ce^{3+} ions upon VUV-UV and X-ray excitation	286
Sebastian Vielhauer	VUV photoluminescence spectroscopy setup at MAX III	287

Poster Session: Sustainable Energetics

A.N. Salak	Crystal structure of Cu-deficient phases in the$(1-x)Cu_2S$-xGa_2S_3 system	290
Valery Garaev	Modification of nafion® membrane with 2-hydroxyethylammonium ionic liquids	291
Teoman Taskesen	$Cu_2ZnGeSe_4$ monograin powder as absorber material for solar cells	292
Tauno Tooming	Carbon materials for supercapacitor application by hydrotehrmal carbonization of D-glucose	293
Natalia Maticiuc	Comparative study of CdS thin film properties on glass and ITO substrates	294
Maris Pilvet	Synthesis of Cu_2ZnSnS_4 monograin powders in liquid phase of cadmium iodide for photovoltaic applications	295
Liga Lasmane	Acidic ionic liquids as composite forming additives for ion-conducting materials	296
A. Kainarbay	Luminescent materials based on nanoparticles of oxide silicon for solar cells	297
Julija Pervenecka	Laser crystallization effects in amorphous silicon layers for solar cells	298
Ineta Liepina	Preparation and characterization of nanostructured Fe-TiO_2 thin films	299
Heisi Kurig	The effect of the properties of carbon materials on the hydrogen up-take	300
Gunita Kolosovska	Quantication of impurities in solar silicon	301
Karina Bikova	Preparation and electrochemical properties of $LiFePO_4$/C/graphene nanocomposite cathode for lithium ion batteries	302
Einars Sprugis	Composite speek polymer membranes with acidic ionic liquids for high temperature pem fuel cells	303

Guntars Vaivars	Glucose oxidase as a biocatalytic enzyme-based biofuel cell using nafion membrane limiting crossover	304
Ainars Knoks	Optical, structural and photoelectric properties of multilayer $TiO_2/CoFe_2O_4$ thin films	305
Table of contents		306
Index		319

Index

A

Aarik, J 116, 117, 132, 145, 150, 179, 223
Aarik, L 65, 117, 132, 145, 164, 179
Abdrakhmetova 263
Aboltins 215
Abuova 248
Adamson 223
Aints 152
Akhvledian 184
Akilbekov 248, 263, 268
Albino 217
Aleksanyan 42, 64, 277, 287
Aleksejeva 265
Algueró 134
Alles 117, 132, 154
Altosaar 85, 292, 295
Amamra 280
Amorín 134
Ansone 219
Anspoks 52, 53, 54
Antal 70
Antonova 189, 198, 212, 230, 234, 254, 276
Antsov 59, 140
Apsīte 173
Ardaravicius 76
Aronzon 168
Arroval 116, 145
Asari 65
Azamat 253, 274
Azens 216
Augustovs 46
Ausekle 296
Auzina 244
Avotina 208, 219

B

Badalyan 253, 274
Bagdzevičius 241
Baghdasaryan 195
Baitemirova 297
Baitimirova 213
Bajars 158, 261, 299, 302
Bąk 252, 254

Bakis 213
Balagurov 138
Balčiūnas 134
Bandura 16, 170, 174
Banys 127, 128, 134, 161, 162, 166, 169, 203, 204, 217, 241, 255, 273
Barabanova 142, 251
Barmina 222
Batakliev 109
Batrakov 78
Baumane 219
Bekmyrza 297
Bekris 208
Bellucci 67, 139, 166
Belova 163
Belsky 51, 182, 278
Bensalah 250
Berezovska 197
Bergfelds 225
Bergs 173
Berkowski 20
Berzina, B 114
Berzina, R 167
Bikova 302
Bilalov 233
Birks 198, 212
Blinova 14
Blottnitz 304
Blumberga 236
Blums 108, 257
Bobrikov 138
Bocharov 54
Boiko 247
Boltrushko 112
Bordacs 70
Borjanovic 161
Bormanis 232, 233, 234, 241, 243
Borodavka 38
Braun 75
Brice 44
Brik 20, 48, 49, 60, 61, 83
Brito 279, 281
Bučinskas 203
Budziak 252, 254
Bulanovs 262
Burkhanov 234
Burlutskaya 67

Buscaglia 255
Butikova 298
Bychkova 184
Bystrov 152

C

Cao 284
Carlson 279
Carvalho 281
Castro 134
Celzard 139, 166
Cerins 244
Chaykin 48
Chen, Kuei-Hsien 114
Chen, Li-Chyong 114
Cheong 69
Chernenko 231
Chikvaidze 190, 225, 246, 301
Chornaja 110, 149
Corradi 239
Ćulubrk 130
Cvetkov 110, 149

D

Dabrowska 181
Daineko 251
Danilkin 239
Danilson 295
Dauksta 197, 244, 250
Dauletbekova 157, 263
Daurenbekov 297
Davarashvili 184
Dec 136, 186
Dedova 118, 119
Dejneka 38, 54, 253, 274
Demchenko 286
Demko 70
Denks 258
Dérer 71
Diéguez 197, 250
Dimza 189, 276
Dmitruk 197
Dobročka 71
Doke 63, 235, 245
Dolgov 124, 247

Dorogin 59, 140
Dovbeshko 247
Drahokoupil 38
Dramićanin 22, 61, 130
Drunka 57
Dzagania 184
Dziaugys 273
Dubencovs 110, 149
Dubovik 278
Dujardin 51
Dumergue 182
Dunce 198, 212
Dyuzheva 272

E

Eastman 76
Ecis 216
Elsts 44
Engelkamp 69, 70
Enukashvili 184
Erts 153, 173
Eskusson 178
Evarestov 16, 170, 174

F

Faszczowy 230
Fedorenko 43
Fedorov 200
Fedotovs 44
Feher 70
Feldbach 64, 258, 280, 287
Feldmann 283
Felinto 281
Ferreira 47, 290
Fesenko 247
Floren 117
Fomins 228
Freivalde 218
Fröhlich 71, 116
Fuks 74
Furukawa 70
Föhlisch 26

G

Gabayn 232
Gabrielaitis 217
Gabrusenoks 238, 261
Gaitko 176, 177
Galashev 278
Galitskiy 137
Garaev 291
Garbarz-Glos 185, 252, 254
Gavrilov 294
Gektin 51, 106
Gelb 89
Georgiev 109
Gerbreders, A 262
Gerbreders, V 262
Gerst 117, 154
Gertners 192
Giglia 51
Gofman 56
Goian 204
Golovnin 271
Gopejenko, V 67
Gopejenko, A 73
Gorelik 247
Gorokhova 231
Grabis 57, 160, 180
Graf 294
Grants 131, 157
Gravitis 259
Grechishkin 136, 202, 271
Grehov 159
Grigalaitis 203, 217, 255
Grigalovica 180, 240
Grigorjeva, L 146, 148, 188
Grigorjeva, J 114
Grīnberga 12, 72, 79
Gromõko 118, 119
Grossberg 84, 85, 292, 295
Grzibovskis 236, 267
Grube 63, 211, 235, 245
Gryaznov 269
Guizard 200

H

Haas 62
Hakola 152
Halitovs 208
Hallén 258
Hanschmidt 81, 144, 237
Harutunyan 195, 277
Heinsalu 124
Hens 161
Hiie 294
Hizhnyakov 62, 112
Holmes 153
Hoop 199
Huczko 181
Hudec 71, 116
Hussainov 144
Hussainova 121, 143
Hušekova 116
Huthwelker 75
Huttula 284
Hölsä 279, 281, 285
Hyppänen 285

I

Ignat`ev 187
Ignatans 198
Izvolski 93
Itoh 54
Ivanov, M 134, 203, 241
Ivanov, V 187, 282
Ivanova, A.I. 202, 251, 271
Ivanova, An. 175
Ivanova, T 167, 180
Ivask 14, 141

J

Jaaniso 117
Jablonskas 169
Jakovlevs 120, 138, 207
Jaks 193
Janeliukstis 197
Janichev 232
Jankoviča 146, 148, 160, 188
Jankovskis 207
Janossy 70

Japins 167
Jarasiunas 114
Jastrabik 38, 253, 274
Jastrzębsk 20
JET-EFDA contributors 208
Joost 58, 66, 133, 141
Josse 217
Jovanović 61
Juganson 141
Jõgi I 152, 201
Jõgi J 237
Jõgiaas 121
Jäger 38
Jänes 165, 178, 293
Järvekülg 151, 193, 237

K

Kahro 117, 132, 154, 223
Kahru 14
Kainarbay 297
Kajtoch 252
Kalda 237
Kalendarev 52, 216
Kaleva 80
Kalinko 52, 53
Kalkis 167, 240
Kallaev 233
Kalnacs 159, 219
Kalvane 233, 252
Kamba 204
Kamenskikh 191
Kamińska 20
Kampars 111, 149
Kanaev 280
Kangur 193
Kania 204
Kankare 285
Kaplas 78
Kaplunov 271
Kaplunova 202
Karpierz 185, 230
Kasemets 14
Kashcheyevs 155
Kasikov 117, 132, 154
Kassymkanova 263

Katkevics 153, 213
Katuwal 69
Kauk-Kuusik 85, 292, 295
Kaulachs 175
Kelp 81
Kerikmäe 239
Kezsmarki 70
Khakhalin 42
Kida 70
Kidiraliyeva 263
Kiisk 220, 247
Kikas 55, 120, 282
Kink 59, 66, 107, 113, 133, 140, 144
Kinka 217
Kirchner 88
Kirm 60, 64, 200, 258, 280, 287
Kisand 58, 66, 120, 123, 133, 141
Kizane 208, 219, 256, 260
Kleperis 72, 79, 120, 158, 302, 305
Klimkowski 230
Klimova 231
Klismeta 224
Klopov 62, 112, 242, 266
Klotins 82
Knite 129
Knitter 256
Knoks 305
Kochura 168
Kodols 110
Kodu 115
Kokars 46, 226
Kolb 256
Kolesnikov 136, 202
Kollo 121, 143
Kolobanov 42
Kolodiy 137
Kolosovska 301
Kondratiev 107
Konieczny 230
Konsin 205
Korolyova 142
Korsaks 114
Kozlova 65, 117, 121, 132, 152, 154, 179, 210
Kotlov 239, 276, 283
Kotomin 68, 73, 74, 135, 248, 268, 269
Kranauskaitė 166, 241

Kranaviciute 162
Krasnenko 49, 83, 112
Krasnikov 162
Krauze 225
Kravalis 260
Kronkalns 108
Krsmanović 61
Kruk 232
Krumina 110
Krunks 118, 119, 229
Krustok 84
Krutyak 278
Kruusma 55
Kucinskis 302
Kudryavtseva 242
Kukk 294
Kukle 122, 218, 259
Kukli 121, 179, 210
Kuklja 74
Kulikova 109, 110, 149
Kulish 137
Kunakova 153
Kundzina 189
Kundzins, K 189
Kundzins, M 189, 212
Kuprevičiūtė 169
Kuprin 137, 270
Kurig 300
Kuruch 170
Kurvet 141
Kuzhir 78, 139, 162
Kuzmanoski 283
Kuzmin 52, 53, 138, 147
Kuznecova 147
Kuznetsov, M 56
Kuznetsov, V 161, 162
Kuzovkov 68, 135
Kuterbekov 297
Kuusik 120, 282
Käämbre 120, 282
Künnis-Beres 141

L

Laamanen 279
Laan 152, 201
Laasner 200

Lagzdina 120
Laguta 194
Laidmäe 151
Laihinen 285
Laizane 209
Lanceros-Mendez 128
Lancok 253, 274
Lander 89
Lange 176
Lashkul 168
Lasmane 296
Lastusaari 279, 281, 285
Lazdoviča 111
Latvels 236
Lau 89
Leinberg 123
Leinemann 292
Lembinen 133
Lescinskis 260
Lesnicenoks 72
Lewczuk 230
Levushkina 191
Leys 256
Liberis 76
Lidström 32
Lielausis 260
Liepina, I 299
Liepina, V 188
Likonen 152, 208
Lisenkov 47, 290
Lisitsin 186
Lissovski 125, 152
Lisunov 168
Lityagina 272
Livinsh 185, 189, 276
Lobanova-Shunina 67
Lobjakas 144
Lojpur 130
Lomino 137
Lu 179
Ludwig 75
Łukasiewicz 136, 186
Luo 303
Luse 228
Lushchik, A 242
Lushchik, Ch 242

Lusis 261, 299
Lust 55, 75, 165, 178, 293, 300
Lõhmus, A 143, 144, 199, 237
Lõhmus, R 59, 81, 113, 123, 140, 143
Lähderanta 163, 168

M

Ma 20, 61, 83, 176
Maaroos 64
Mackevičiūtė 134, 203, 204
Macutkevic 139, 161, 162, 166
Maderniece 236
Maglione 217
Maier 74
Maiorov 108, 120, 138, 257
Makarova 38
Makhov 18, 200, 277
Maksimenko 78, 162
Maļinovskis 173
Māliņš 111
Malnieks 79
Malta 281
Malyshkin 136
Malyshkina 136, 142, 186, 251
Mamykin 124
Manika 131, 157
Maniks 131, 156, 157
Marcins 298
Markov 200
Markova 149
Martin 182
Martins 128
Masenelli 182
Mastrikov 73, 74
Mazov 162
Maticiuc 294
Matisen 65
Matulionis 76
McIntyre 50
McNally 169
Mednikov 234
Medvied 197, 244, 250
Mélinon 182
Mellikov 85
Melnikov 77
Meltchakov 51

Mere 118, 119, 229
Merijs-Meri 156, 167, 180, 240
Merisalu 65
Merzlyakov 68, 135
Mezinskis 79, 120, 244
Mezzenga 127
Mezulis 171, 257
Mikhailin 30, 191, 278
Mikli 118, 119, 229
Millers 146, 148, 188, 264
Mirme 125
Mironova- Ulmane 138, 190, 207, 215, 246
Mishnov 212
Mitarov 233
Mitina 106
Mitoseriu 255
Miyahara 70
Molchanov 202
Monty 148
Moretti 51
Morozov 137, 270
Moseenkov 161
Mosunov 80
Mughnetsyan 195
Muiznieks 225
Murakawa 70
Murashov 159
Museur 280
Muska 85
Mäeorg 81, 113, 144, 199
Mägi 287
Mändar 64, 81, 116, 145, 150, 152, 179, 210
Möldre 116, 223
Möslang 73
Myasnikova 221
Mychko 250

N

Nagel 69, 70
Nagirnyi 60, 64, 200, 239, 287
Naidoo, Q 304
Naidoo, S 304
Nanaronne 51
Nanni 255
Narels 209
Natali 81

Neklyudov 137
Nemcevs 158
Netšipailo 164
Nhan 234
Niilisk 116, 117, 132, 154, 223
Nikl 194
Nikoghosyan 195
Nikolić 130
Niu 284
Nunes 285
Nurakhmetov 297
Nurk 75
Nurmis 193
Nuzhnyy 204
Nõmmiste 55, 123, 287

O

Oja, M 280
Oja Acik 229
Omarov 233
Omelkov 287
Onose 70
Onufrijevs 197
Oras 59
Orlovskaya 176, 177
Orlovskii 43, 176, 177
Ozolinsh 228
Ozols 46
Otto 229
Ovcharenko 137, 270

P

Paalo 140, 144
Paddubskaya 78, 162
Palatnikov 232, 243
Palm 293
Pankratov 276, 283, 284
Paris 152
Part 201, 210, 237
Pashaev 184
Paskaleva 71
Pazylbek 297
Pathak 181
Patmalnieks 57
Pavlovica 291

Peikolainen 179
Pękala 230
Penc 70
Pentjuss 261
Persson 81
Pervenecka 298
Piekarczyk 185
Pihlgren 285
Piip 152
Pikker 81, 124
Pille 258
Pilvet 85, 295
Pishtshev 62, 242, 266
Piskunov 248
Piyr 142
Plank 115
Plaza 197
Platacis 260
Plate 225
Plaude 189, 198, 246
Plotnichenko 42
Plotnikov 126
Pohl 143
Polakovs 215
Politova 80
Polyakov 59, 140, 298
Ponomarenko 207
Popļausks 173
Popov, Al 43, 176, 177
Popov, A.I 50, 181, 276
Popova, M 36
Popova, S 196
Posadova 251
Potanina 249
Priksane 296
Prikulis 173
Progolaieva 137
Przybylińska 20
Pudzs 227, 267
Puķina 146
Pungas 150
Purans 24, 54, 181, 216, 268, 269
Pustovarov 56, 187, 282
Putnina 259
Puust 220
Põhako-Esko 113

Pärna 55, 66, 120, 133

R

Raadik 84, 292
Rakovsky 109
Rammula 115, 132, 145
Randoshkin 42
Razumov 187
Raud 201
Raudoja 84, 85, 292, 295
Reedo 143, 199
Reemann 193
Reinfelde 214
Reinholds 167, 240
Reshetnyak 270
Rocca 54
Rodnyi 231
Rodrigues 279, 281
Rogulis 44
Romanchuks 260
Romann 293
Romanov 107, 237
Romet 239
Romhanyi 70
Roosalu 150, 179
Rosová 71
Roze 175
Rozhin 81
Rubio 197
Rusakova 157
Russell 218
Russina 300
Rutkis 12, 226
Rõõm 69, 70
Rödel 203

S

Saal 113, 123
Saar 58
Sadykov 233
Safonchik 163
Saharov 46
Sakale 129
Sakanas 255
Salak 47, 290

Salihodja 297
Salu 84
Salundi 237
Sammelselg 65, 117, 145, 154, 164
Samulionis 127, 169, 217
Sanchez-Ferrer 127
Sandler 243
Sapper 203
Sarakovskis 44, 54, 63, 211, 235, 245
Sarkisyan 195
Savchyn 181
Schmedake 297
Schwartz 34, 131, 157
Seeman 239
Segalla 80
Serga 109, 110, 149
Sergeev 246
Sergeyev 172
Shakhov 168
Shalapska 106, 286
Sharia 74
Shashkov 142
Shelkan 62
Shenderova 161
Shimano 70
Shipkovs 175
Shirmane 276, 283, 284
Shivaraman 76
Shlegel 278
Shlihta 175
Shuba 77
Shulga 125
Shunin 67
Shunkeyev, K 172, 206, 221, 222
Shunkeyev, S 222
Sidorov 232, 243
Siebenbürger 300
Siimon 151
Sildos 43, 119, 124, 176, 177, 215, 220, 247
Sints 108
Sitko 252
Sivars 72
Skvortsova 190
Sledevskis 262
Smeltere 243
Śmiga 185

Smits 146, 148, 188, 264, 272
Sokolov 42
Sokolova 160
Sorkin 205
Sorokine 268, 269
Soukka 285
Spassky 42, 191, 278
Spencer 76
Springis 63, 211, 235, 245
Sproge 110, 149
Sprugis 303
Szaller 70
Szczepkowski 20
Stan-Sion 208
Stepina 129
Sternberg 12, 212, 230
Struis 75
Stryganyuk 286
Stupakov 38
Subedi 181
Suchanicz 230
Suchocki 20
Supe 256
Surovovs 225
Sushko 28
Sutka 79, 120
Svirko 78
Svirskas 127, 128, 169
Sybilski 20
Syuy 232

Š

Šeputis 128
Šteins 160

T

Taaber 113
Talbayev 69
Tale 298
Tallo 165, 300
Talviste 201
Tamm A 121, 179, 210
Tamm E 125
Ťapajna 71
Tarkanovskaja 199

Tarre 116, 150, 223
Taskesen 292
Teil 174
Temmerman 152
Teteris 45, 192, 214, 224, 249, 262, 265
Thomberg 165, 293
Timmo 85, 292, 295
Timoshenko 52, 53, 155
Timusk 123
Tkachenko 206
Tokmakovs 226
Tokura 70
Tolmachova 270
Tomson 86
Tooming 293
Traito 163
Traskovskis 46, 226
Trepakov 38, 54, 253, 274
Treshchalov 125
Tretiakov 202
Tretyakova 191
Trinkler 114, 190
Trukhin 264, 272
Tsarenko 125
Tupitsyna 200, 278
Turovska 267
Tõldsepp 258
Tõnisoo 55, 154
Tätte 81, 144, 201, 210, 237

U

Uin 125
Umalas 143
Usseinov 268
Utt 58, 119, 124, 220

V

Vahtrus 59, 140
Vaivars 291, 296, 303, 304
Wallacher 300
Valynets 78, 139
Vanags 158, 299
Vanetsev 176, 177
Vardanjan 92
Varema 85, 292, 295

Vasil’ev 51, 200, 278
Vasil’eva 42
Vembris 196, 209, 227, 267
Vezenkova 244
Vielhauer 42, 200, 287
Vihodceva 122
Vīksna 153, 173, 213, 301
Vilkens 159
Vilnis 216
Visnapuu 133, 141
Vistovskyy 106
Vitins 260
Vladimirov 73
Vlassov 59, 140
Volobujeva 85, 118, 119
Voloshinovskii 106, 286
Voronovich 78
Vorontsova 202
Voss 245
Välbe 199
Värva 133
Vyprintsev 187
Vysochanskii 273

W

Wang 284
Wittlin 20
Welter 279

Y

Yerdibayeva 126
Yi 69

Z

Zabels 131, 156, 157
Zablotsky 171
Zaborovskiy 251
Zadneprovski 191
Zaichenko 106
Zakharchuk 163
Zargaryan 195
Zarins 256
Zazubovich 194
Zdorovets 157
Zhaludkevich 290

Zhanbotin 297
Zhanturina 172, 206, 221
Zheludkevich 47, 290
Zhukovskii 67, 73, 268
Zhunusbekov 297
Zhurba 137
Zhyshkovych 106
Zicans 156, 167, 180, 240
Zimmermann 276
Zoetemelk 91
Zolotarjovs 264
Zorenko 20
Zubkins 216
Zvejnieks 68, 82, 135